WindLogics®

Final Report -
2006 Minnesota Wind Integration Study
Volume II - Characterizing the Minnesota Wind Resource

Prepared for:
The Minnesota Public Utilities Commission
c/o Mr. Ken Wolf
Reliability Administrator
121 7th Place E.
Suite 350
Saint Paul, MN 55101-2147

Prepared by:
WindLogics, Inc.
1217 Bandana Blvd. N.
St. Paul, MN 55108
Tel: (651) 556-4200
FAX: (651) 556-4210
www.windlogics.com

November 30, 2006

Table of Contents

Characterization of the Minnesota Wind Resource and Wind Power Technology

Description

In this study three levels of wind penetration were modeled, characterized and then analyzed at 15%, 20%, and 25% of projected Minnesota retail electric energy sales (ranging up to 6,000 MW of wind generation in the year 2020).

A review and characterization of current and projected wind turbine technology including cost of energy (as a function of wind resource quality), maintenance costs, reliability, and interconnection and power system impacts (capabilities and requirements; e.g. reactive power control, and low voltage ride through) was conducted. The technical characteristics of distributed / dispersed / distribution connected utility scale wind generation including technical benefits and technical challenges were also reviewed and described.

The wind generation resource and resulting relative economics of wind generation for each County in Minnesota were assessed, and the wind speeds at hub height were quantified using GIS techniques. The input data used was the October 2005 Minnesota Department of Commerce high resolution (500 meters) state-wide wind maps and associated GIS files.

The regional wind generation resources were identified (representing community, corporate, and utility developed projects) in the amounts outlined above based on: existing projects, contracted projects, wind resource quality, interconnection queues, proposed projects, and proximity to load.

The appropriate time series wind plant output profiles were developed and validated for use in the 5-minute and hourly time frames for the wind generation in the study, including 80 and 100-meter hub heights. Modeling was performed at 4 km and 5- minute resolution for 3 years. The extent of wind generation variability that the power system should experience was analyzed, including the effects of projected wind turbine technology. The effects of geographic diversity were also quantified.

The diurnal, monthly, and inter-annual Midwest wind patterns and resulting wind generation patterns and variability were characterized.

The wind generation forecast accuracy on an hour and day-ahead basis was quantified, and the implications on the degree of certainty that is included in the forecast were assessed.

Introduction and Modeling Overview

Recent studies have shown that a high-fidelity, chronological representation of wind generation is perhaps the most critical element of this type of study. For large wind generation development scenarios, it is very important that the effects of spatial and geographic diversity be neither under- or over-estimated. The approach for this task has

been used by EnerNex and WindLogics in at least six wind integration studies, including the southern Minnesota study completed in 2004 for the Minnesota Department of Commerce with funding from the Xcel Renewable Development Fund. The base data for both the wind resource characterization and the production of wind speed and power time series were generated from the MM5 mesoscale model (Grell et al. 1995). This prognostic regional atmospheric model is capable of resolving mesoscale meteorological features that are not well represented in coarser-grid simulations from the standard weather prediction models run by the National Centers for Environmental Prediction (NCEP). The MM5 was run in a configuration utilizing two grids as shown in Figure 1. This “telescoping” two-way nested grid configuration allowed for the greatest resolution in the area of interest with coarser grid spacing employed where the resolution of small mesoscale meteorological phenomena were not as important. This methodology was computationally efficient while still providing the necessary resolution for accurate representation of the meteorological scales of interest within the inner grid.

More specifically, the 4 km innermost grid spacing was deemed necessary to capture topographic influences on boundary layer flow and to resolve mesoscale meteorological phenomena such as thunderstorm outflows. The 12 and 4 km grid spacing utilized in grids 1 and 2, respectively, yield the physical grid sizes of 2400 x 2400 km for grid 1, and 760 x 760 km for grid 2.

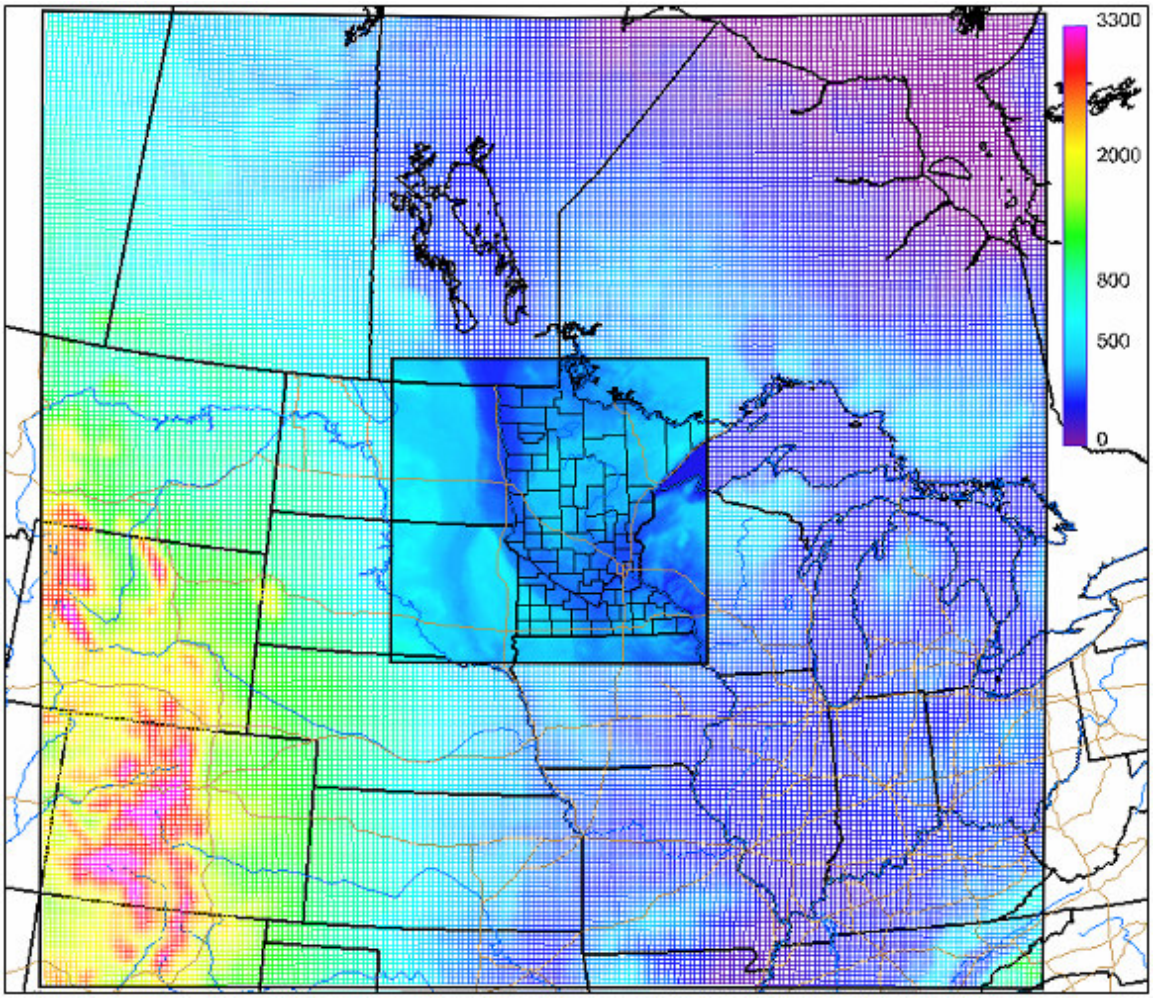

Figure 1: MM5 nested grid configuration utilized for study domain. The two-grid run includes an inner nested grid to optimize the simulation resolution in the area of greatest interest. The grid spacing is 12 and 4 km for the outer and inner grids, respectively. The colors represent the surface elevation.

To provide an accurate assessment of the character and variability of the wind resource for Minnesota and the eastern Dakotas, three full years of MM5 simulations were completed. To initialize the model, the WindLogics archive of NCEP Rapid Update Cycle (RUC) model analysis data was utilized. The years selected for simulation were 2003, 2004 and 2005. The RUC analysis data were used both for model initialization and for updating the model boundary conditions every 3 hours. This RUC data had a horizontal grid spacing of 20 km for all three years.

Wind Generation Technology Assessment

Commercial wind turbine technology has been evolving rapidly over the past decade, and this trend will almost certainly continue. As the wind energy industry matures, lessons learned from existing wind generation facilities are driving improvements to successive generations of wind turbine equipment and wind

plant designs. Efforts to reduce the levelized cost of energy have always been, and continue to be, a major driver of technological advancement.

In this subtask, a characterization of wind generation technology was developed for the period commencing at the present and extending to the year 2020. Recent developments in grid interconnection standards and codes were summarized, along with wind turbine and plant design features that improve grid compatibility. Projections of other performance parameters , such a levelized cost of energy for new wind turbine concepts and designs, were developed from NREL research and other published reports.
Much of the focus of previous integration studies has been on, at least implicitly, large facilities connected to the transmission network. In some regions of the country there has been a parallel path for development in which small groups of turbines are connected to a public distribution system.

Wind turbines as distributed generation resources may have benefits over and above the electrical energy produced. Transmission losses may be reduced as the amount of generation increases to match the local load, and since most or all of the energy would be consumed locally, capital-intensive transmission network or substation upgrades can sometimes be deferred or eliminated. When local generation exceeds load, power would flow from distribution substations into higher voltage grid. Connection of distributed generation to a public distribution network raises some technical questions, especially as the aggregate capacity of the distributed generation becomes significant with respect to the rating of the distribution feeder. Done on a large scale for wind generation, the challenges for forecasting and interoperability with other power system control functions can also be much more difficult.

The advantages and disadvantages of transmission-connected bulk wind generation vs. small distributed plants were analyzed in this subtask. The project team drew upon its significant experience in distributed generation to compile this summary report that specifically analyzes wind generation as a distributed resource.

Electrical Aspects of Wind Turbine Technology

Almost all of the wind turbines deployed in large wind generation facilities in the U.S. over the past decade can be generally described by one of the following configurations:

- Stall-regulated (fixed-pitch) blades connected to a hub, which is coupled via a gearbox to a conventional squirrel-cage induction generator. The generator is directly connected to the line, and may have automatically switched shunt capacitors for reactive power compensation and possibly a soft-start mechanism which is bypassed after the machine has been energized. The speed range

of the turbine is fixed by the torque vs. speed characteristics of the induction generator.

- A wound rotor induction generator with a mechanism for controlling the magnitude of the rotor current through adjustable external rotor circuit resistors, and pitch regulation of the turbine blades to assist in controlling speed. The speed range of the turbine is widened because of the external resistors.
- A wound rotor induction generator where the rotor circuit is coupled to the line terminals through a four-quadrant power converter. The converter provides for vector (magnitude and phase angle) control of the rotor circuit current, even under dynamic conditions, and substantially widens the operating speed range of the turbine. Turbine speed is primarily controlled by actively adjusting the pitch of the turbine blades.

While not represented in the present fleet of commercial turbines for application in the United States, the variable-speed wind turbine with a full-rated power converter between the electrical generator and the grid deserves mention here. The first utility-scale variable-speed turbine in the U.S. employed this topology, and many see this configuration reemerging for future large wind turbines. The power converter provides substantial decoupling of the electrical generator dynamics from the grid, such that the portion of the converter connected directly to the electrical system defines most of the characteristics and behavior important for power system studies.

Overview of Operation

A generalized wind turbine model is shown in Figure 2, and illustrates the major subsystems and control hierarchy that may influence the behavior of a single wind turbine in the time horizon of interest for large power system studies.
A wind turbine converts kinetic energy in a moving air stream to electric energy. Mechanical torque created by aerodynamic lift from the turbine blades is applied to a rotating shaft. An electrical generator on the same rotating shaft produces an opposing electromagnetic torque. In steady operation, the magnitude of the mechanical torque is equal to that of the electromagnetic torque, so the rotational speed remains constant, real power (the product of rotational speed and torque) is delivered to the grid. Since the wind speed is not constant, a variety of control mechanisms are employed to manage the conversion process and protect the mechanical and electrical equipment from conditions that would result in failure or destruction.

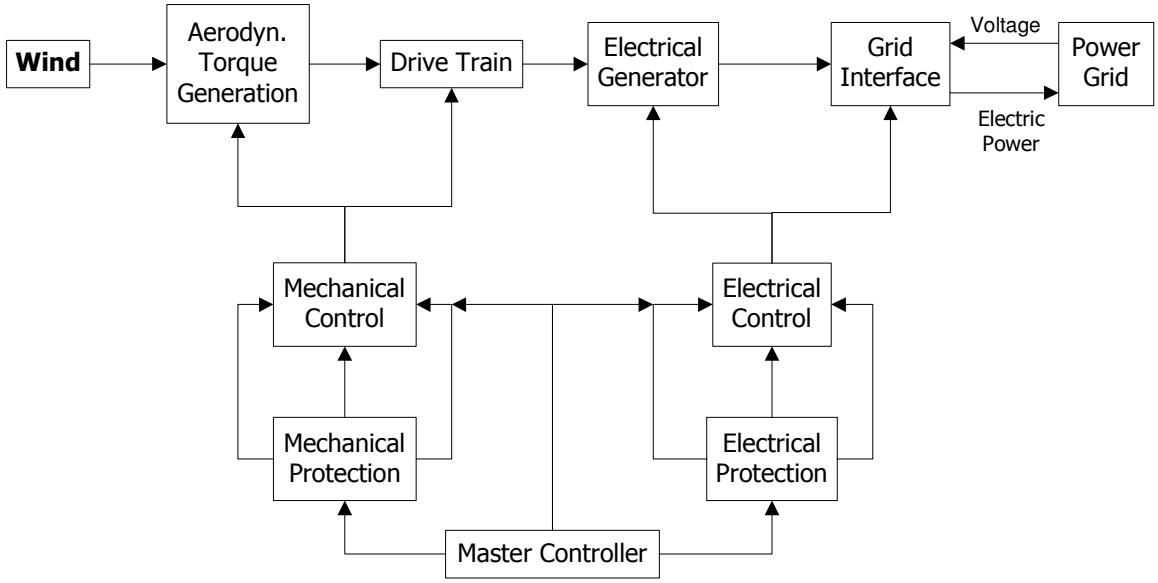

Figure 2: Generalized wind turbine model with control elements and hierarchy.

Mechanical Systems and Control

Mechanically, the turbine must be protected from rotational speeds above some value that could lead to catastrophic failure. Mechanical brakes are provided for stopping the turbine in emergency conditions, but are not used in normal operations. Controlling the power (and hence, torque) extracted from the moving air stream is the primary means for protecting the turbine from over-speed under all but emergency shutdown conditions.

In fairly steady conditions, the power extracted from the air stream by blades can be characterized by Equation 1:

$$P = \frac{1}{2} \cdot \rho \cdot \pi \cdot R^2 \cdot \upsilon^3 \cdot C_p$$

where

ρ = air density (nominally 1.22 kg/m^3)
R = radius of area swept by the turbine blades
υ = speed of moving air stream
C_p = "coefficient of performance" for the composite airfoil (rotating blades)

C_p itself is not a constant for a given airfoil, but rather is dependent on a parameter λ, called the tip-speed ratio, which is the ratio of the speed of the tip of the blade to the speed of the moving air stream.

Since wind speed and air density cannot be controlled, and the radius of the blades is fixed, the performance coefficient is the only means for torque control. In some wind turbines, blades are designed so that C_p falls dramatically at high wind speeds. This method of aerodynamic torque control is known as *stall regulation*, and is limited to preventing turbine over-speed during extreme gust

conditions and limiting maximum shaft power in winds at or above the rated value.

Large wind turbines employ a more sophisticated method of aerodynamic torque regulation that has benefits in addition to preventing mechanical over-speed. The performance coefficient can also be changed by adjusting the "angle of attack" of the blades, as is done on some modern propeller-driven aircraft.

Figure 3 shows C_p as a function of λ for a modern wind turbine. Blade pitch adjustment allows the energy capture to be optimized over a wide range of wind speeds (even if the rotational speed of the shaft is relatively constant), while still providing for over-speed protection through large adjustments in pitch angle.

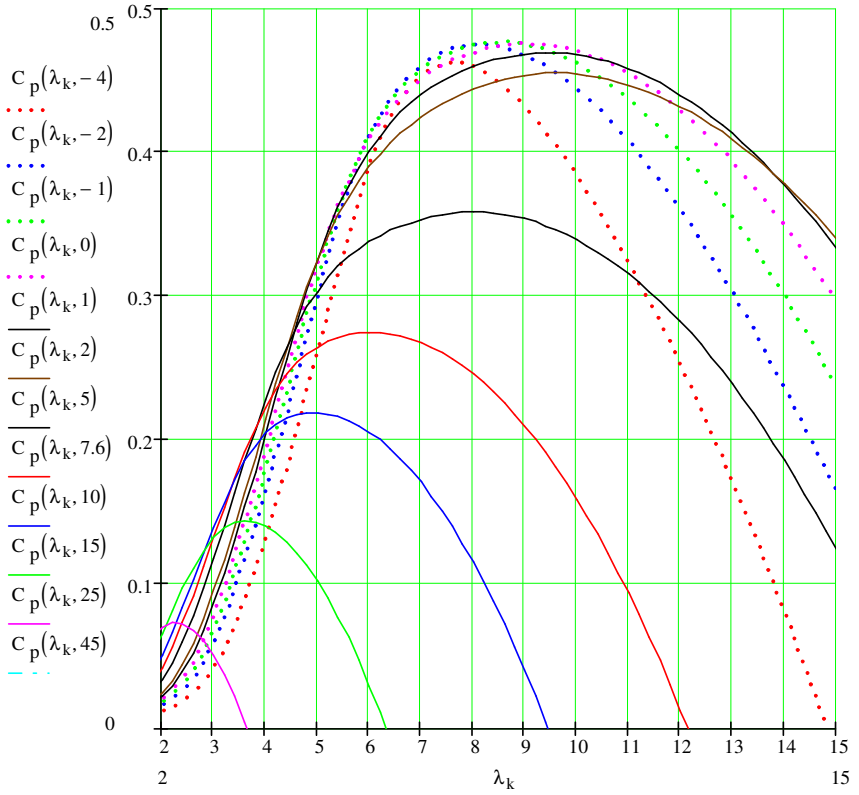

Figure 3: Coefficient of performance (C_p) for a modern wind turbine blade assembly as a function of tip-speed ratio (λ) and blade pitch (β, in degrees).

The pitch of the turbine blades is controlled by an actuator in the hub that rotates each blade about a longitudinal axis. The inertia of the blade about this axis and the forces opposing such a rotation of the blades are not negligible. Pitching of the blades, therefore, does not happen instantaneously, with the dynamics governed by the longitudinal inertia of the blades, forces acting on the blade (which can be wind speed and pitch dependent), and the torque capability of the pitch actuator mechanism.

The characteristic shown in Figure 3 is a "quasi-static" depiction of the blade performance, in that is does not account for turbulence effects, blade vibration with respect to the average speed of rotation, or other asymmetries such as tower shadowing. It does, however, provide a much simpler means of

incorporating the otherwise very complex details of the aerodynamic conversion process into models for electrical-side studies of the turbine.

The overall conversion of wind energy to electric power is normally described by a turbine “power curve”, which shows turbine electrical output as a function of steady wind speed (Figure 4). Such a representation is accurate only for steady-state operation, since the inherent dynamics of the mechanical and electrical systems along with all possible control functionality is neglected.

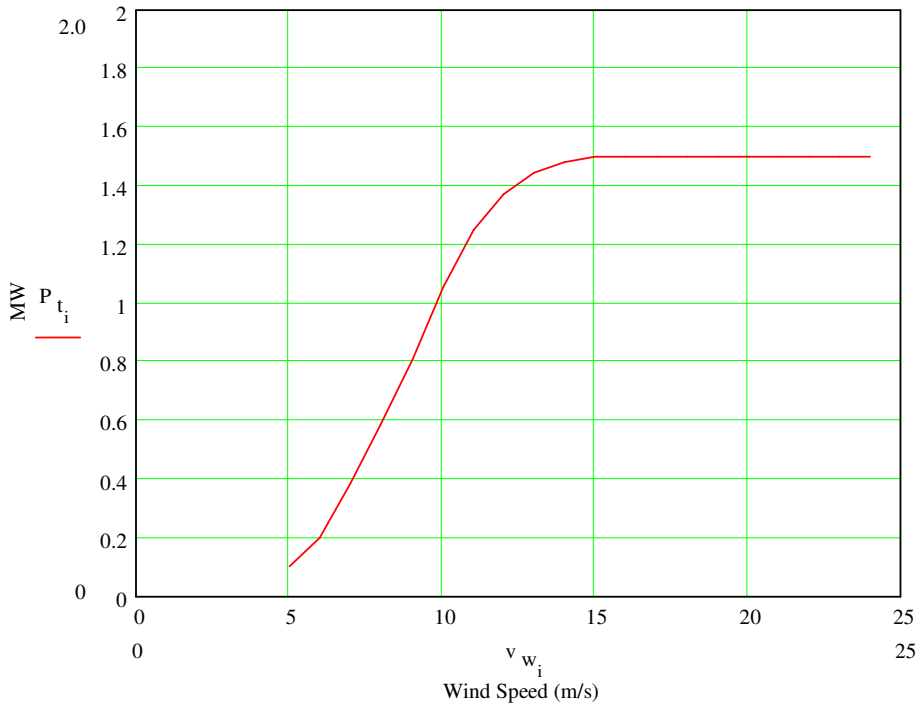

Figure 4: Power curve for a variable-speed, pitch-controlled wind turbine. Note “flatness” of output for wind speeds at or above rated value.

Rotational speeds of large wind turbines are partly limited by maximum blade tip speed, and so for megawatt-class turbines with long blades are relatively low, in the 15 to 30 rpm range. With conventional electrical generators, a gearbox is necessary to match the generator speed to the blade speed. The resulting mechanical system, then, has low-speed and high-speed sections, with a gearbox in between, as shown in Figure 5 (top). An even simpler representation is shown at the bottom of Figure 5, where the gearbox inertia is added to the inertia of the generator, and all components are referred to the high-speed shaft by the square of the gear ratio.

For megawatt-scale turbines, the mechanical inertia is relatively large, with typical inertia constants (H) of 3.0 seconds or larger (the inertia constant for the generator only will typically be about 0.5 s). The mechanical inertia is an important factor in the dynamic behavior of the turbine, because the large inertia implies relatively slow changes in mechanical speed for both normal variations in wind speed and disturbances on the grid. In addition, the various control systems in the turbine may utilize turbine speed as an input or disturbance signal, so that large inertia will then govern the response time.

With a two-mass mechanical model, there will be one oscillatory mode. With relatively flexible drive shafts in large wind turbines, the natural frequency of this primary mode of oscillation will be in the range of 1 to 2 Hz.

Electrical Systems and Control

Induction machines are the energy conversion devices of choice in commercial wind turbine design. In addition to their robustness and reliability, they provide a "softer" coupling between the grid and the mechanical system of the turbine. Wind turbine manufacturers have also moved beyond the basic induction generator systems with technologies for improving control and overall efficiencies. These technologies have a definite impact on the electrical and dynamic performance of wind turbines, even to the extent of masking or overriding the dynamic characteristics that would normally be associated with rotating machinery. The four major types of generator technologies used in today's commercial wind turbines are discussed in the following sections.
.

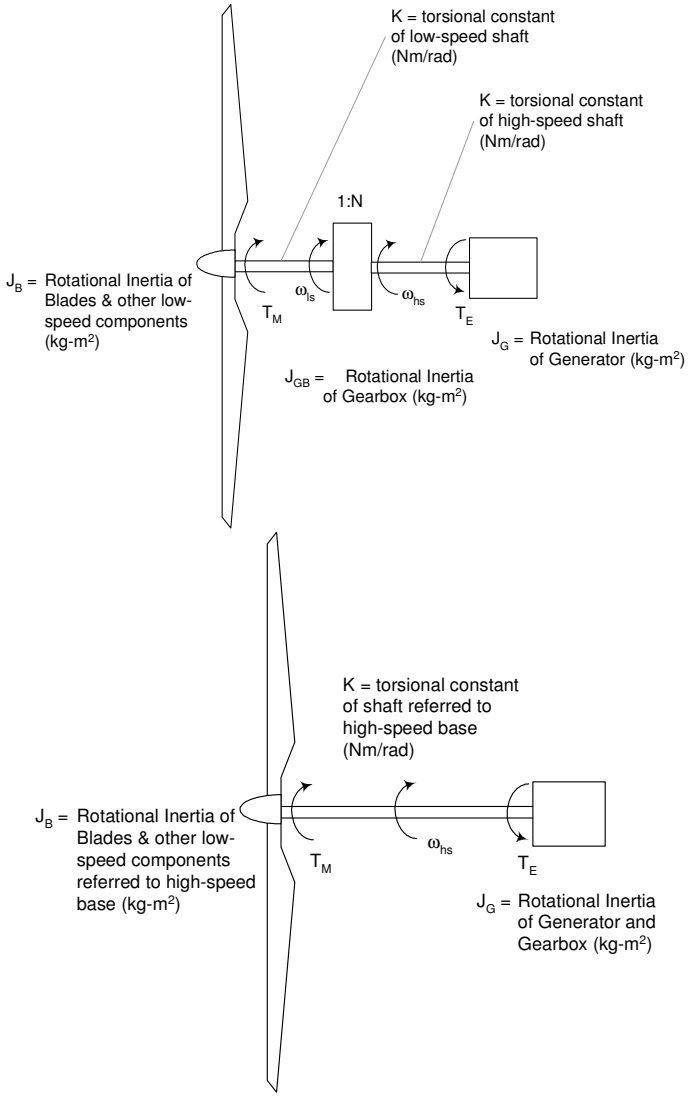

Figure 5: Simplified model of wind turbine mechanical system. Two mass model with gearbox (top) and model with equivalent gearbox inertia and reference of all components to high-speed shaft (bottom).

Direct-Connected Induction Generators

Wind turbines with squirrel-cage induction generators connected directly to the line are the simplest electrically. While for purposes of aerodynamic efficiency they operate at nearly constant speed, the slight variation of speed with torque (and power) can significantly reduce mechanical torque transients associated with gusts of wind and grid-side disturbances.

The speed range of the turbine is dictated by the torque vs. speed characteristic of the induction generator (Figure 6). For large generators in today's commercial turbines, slip at rated torque is less than 1%, which results in very little speed variation over the operating range of the turbine. For a given wind speed, the operating speed of the turbine under steady conditions is a nearly linear function of torque, as illustrated by the torque vs. speed characteristic of Figure 6. For

sudden changes in wind speed, the mechanical inertia of the drive train will limit the rate of change in electrical output.
Because the induction generator derives its magnetic excitation from the grid, the response of the turbine during a grid disturbance will be influenced by the extent to which the excitation is disrupted

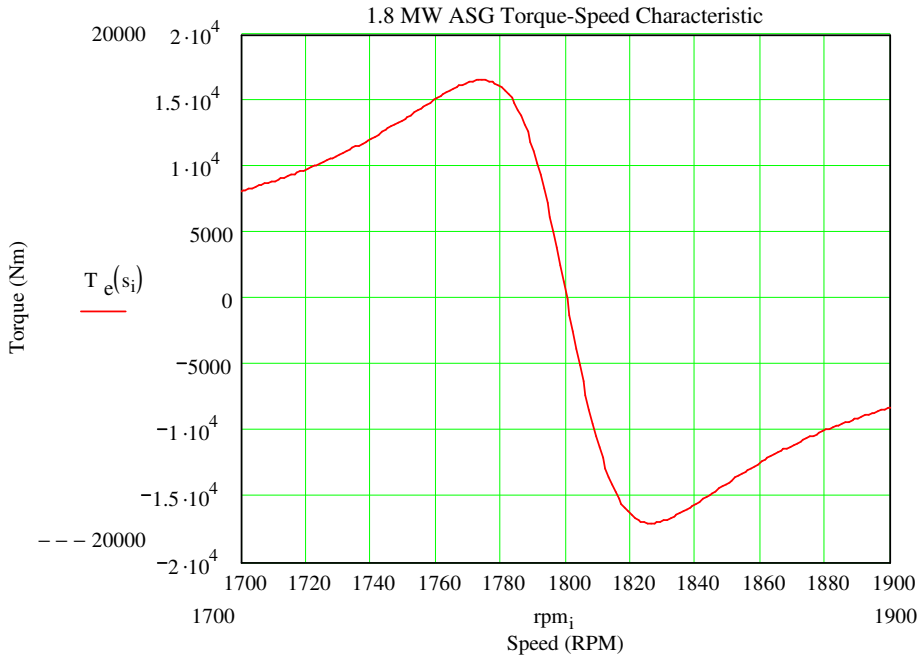

Figure 6: Torque vs. Speed characteristic for an induction machine used in a commercial wind turbine.

Wound-Rotor Induction Generator with Scalar Control of Rotor Current

In a squirrel-cage induction generator, the rotor “circuits” are fictitious and not accessible external to the machine, and the induced currents responsible for torque generation are strictly a function of the slip speed. The turbine shown in Figure 7 utilizes a wound-rotor induction machine, where each of the three discrete rotor winding assemblies is electrically accessible via slip rings on the machine shaft. This provides for modification of the rotor circuit quantities and manipulation of the rotor currents, and therefore the electromagnetic torque production. The Vestas turbines for domestic application (e.g. V47 and V80) utilize a patented system for controlling the magnitude of the rotor currents in the induction generator over the operating speed range of the turbine. The system (Vestas Rotor Current Controller, or VRCC) consists of an external resistor network and a power electronics module that modulates the voltage across the resistors to maintain a commanded rotor current magnitude. The operation of the VRCC is quite fast, such that it is capable of holding the turbine output power constant for even gusting winds above rated wind speed, and significantly influences the dynamic response of the turbine to disturbances on the grid.

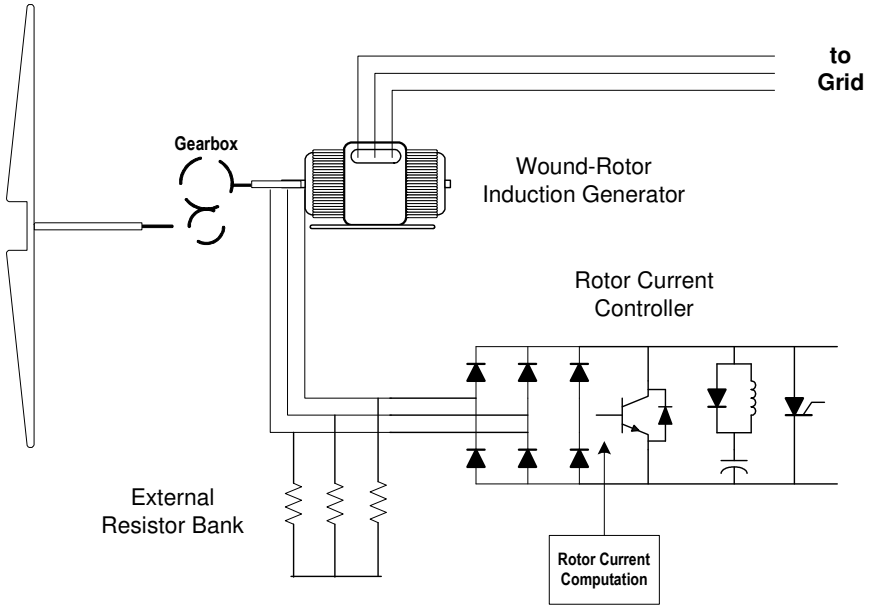

Figure 7: Configuration of a Vestas turbine for domestic application. Diagram illustrates major control blocks and Vestas Rotor Current Controller (VRCC).

The 750 kW and 1.5 MW turbines (and the 3.6 MW prototype for offshore applications) from GE Wind Energy Systems employ an even more sophisticated rotor current control scheme with a wound-rotor induction generator (Figure 8). Here, the rotor circuits are supplied by a four-quadrant power converter (capable of real and reactive power flow in either direction) that exerts near-instantaneous control (e.g. magnitude and phase) over the rotor circuit currents. This "vector" control of the rotor currents provides for fast dynamic adjustment of electromagnetic torque in the machine. In addition, the reactive power at the stator terminals of the machine can also be controlled via the power converter. Field-oriented or vector control of induction machines is a well-known technique used in high-performance industrial drive systems, and its application to wind turbines brings similar advantages. In an earlier version of this turbine, the torque command (and therefore the magnitude of the rotor current component responsible for torque production) was linked to the speed of the machine via a "look-up" table. The field-orientation algorithm effectively creates an algebraic relationship between rotor current and torque, and removes the dynamics normally associated with an induction machine. The response of the power converter and control is fast enough to maintain proper alignment of the torque-producing component of the rotor current with the rotor flux so that the machine remains under relative control even during significant grid disturbances.

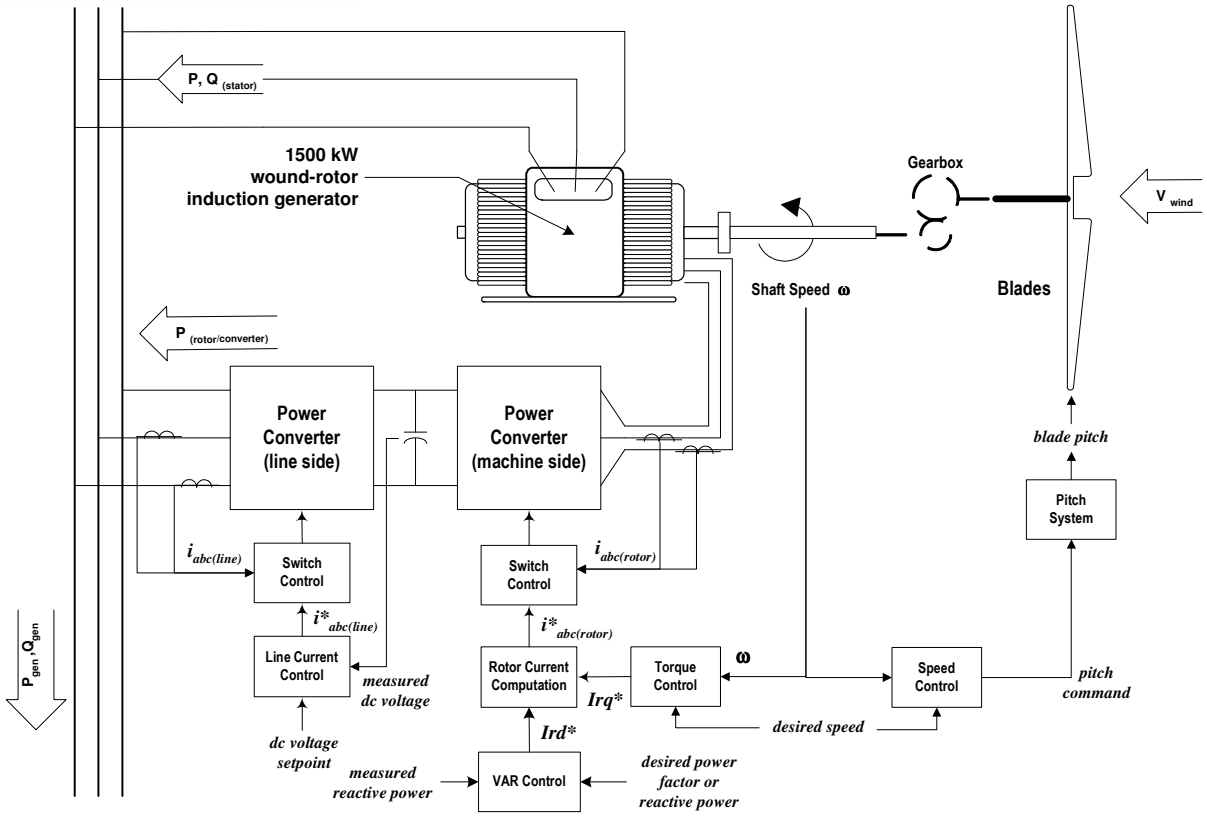

Figure 8: Configuration of GE with four-quadrant power converter supplying rotor circuit of a wound-rotor induction generator. Control blocks for torque control also shown.

Static Interface

The Kenetech 33 MVS, introduced commercially in the early 1990's, was the first utility-scale (i.e. large) variable-speed wind turbine in the U.S. The turbine employed a squirrel-cage induction generator with the stator winding supplied by a four-quadrant power converter (Figure 9). Because all of the power from the turbine is processed by the static power converter, the dynamics of the induction generator are effectively isolated from the power grid.

A modern static power converter utilizes power semiconductor devices (i.e. switches) that are capable of both controlled turn-on as well as turn-off. Further, the device characteristics enable switch transitions to occur very rapidly relative to a single cycle of 60 Hz voltage – nominal switching frequencies of a couple to several kHz are typical. This rapid switching speed, in combination with very powerful and inexpensive digital control, provides several advantages for distributed generation interface applications:

- Low waveform distortion with little passive filtering
- High-performance regulating capability
- High conversion efficiency

- Fast response to abnormal conditions, including disturbances, such as short-circuits on the power system
- Capability for reactive power control

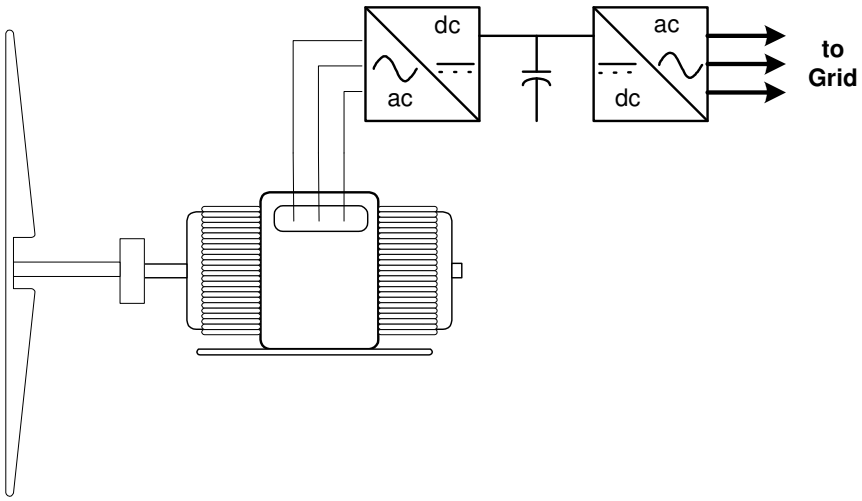

Figure 9: Variable-speed wind turbine with static power converter grid interface.

Because the effective switching speed of the power semiconductor switches is quite fast relative to the 60 Hz power system frequency, it is possible to synthesize voltage and current waveforms with very little lower-order harmonic distortion. Most modern converters easily meet limits on these harmonics found in the IEEE 519 standard.

Figure 10 depicts a simplified control schematic for a static power converter in grid-parallel operation. Since an individual wind turbine is likely small in rating relative to the short-circuit capability of the system to which it is connected, the voltage magnitude at this point will only be slightly influenced by the operation of the turbine. The control scheme, therefore, is designed to directly regulate the currents to be injected into this “stiff” voltage source.

The ac line voltages, dc link voltage, and two of the three ac line currents – for a three-wire connection - are measured and provided to the main controller. The ac voltage and line currents are measured at a high resolution relative to 60 Hz, so that the controller is working with instantaneous values. By comparing the measured dc voltage to the desired value, the controller determines if the real power delivered to the ac system should be increased, decreased, or held at the present value. Such a simple regulation scheme works because there is no electric energy storage in the converter (except for that in the dc filter capacitor), so the energy flowing into the dc side of the converter must be matched at all times to that injected into the ac line. If these quantities do not match, the dc link voltage will either rise or fall, depending on the algebraic sign of the mismatch.

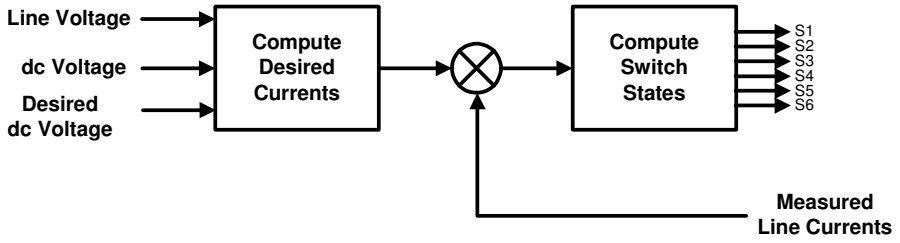

Figure 10: Simple output current control stage for a static power converter in a grid-tied DG application.

The error in the dc voltage is fed into a PI (proportional-integral) regulator to generate a value representing the desired rms magnitude of the ac line currents. Another section of the control is processing the instantaneous value of the ac line voltage to serve as a reference or "template" for the currents to be produced by the converter. The desired instantaneous value of the line current is computed by multiplying the desired rms current magnitude by the present value from the template waveform. In the next stage of the control, often times called the "modulator" section, the desired instantaneous value of line current is compared to the measure value (in each phase). The modulator then determines the desired state of the six switches in the matrix based on the instantaneous current error in each phase of the line currents. The states are transmitted to the IGBT gate drivers, which then implement the state of each IGBT in the matrix as commanded by the controller. The process is then repeated at the next digital sampling interval of the overall control.

The process is repeated thousands of times per single cycle of 60 Hz voltage. By using the line voltage as a template for the shape of the currents to be synthesized, synchronism is assured. Additionally, if there is no intentional phase shift introduced in the control calculations, the currents will be almost precisely – save for small delays introduced by the control itself - in phase with the line voltages, for unity power factor operation.

Figure 11 depicts the output of a current-regulation scheme that might be employed in a grid interface converter in a wind turbine. Here, the modulator will only change the state of the switches if the absolute value of the difference between the desired and actual line currents exceeds a certain value. The small errors that are continually corrected by the action of the converter control are clearly visible. Because of the high switching speed, however, the distortion of the current waveform is very low, well within IEEE 519 limits.

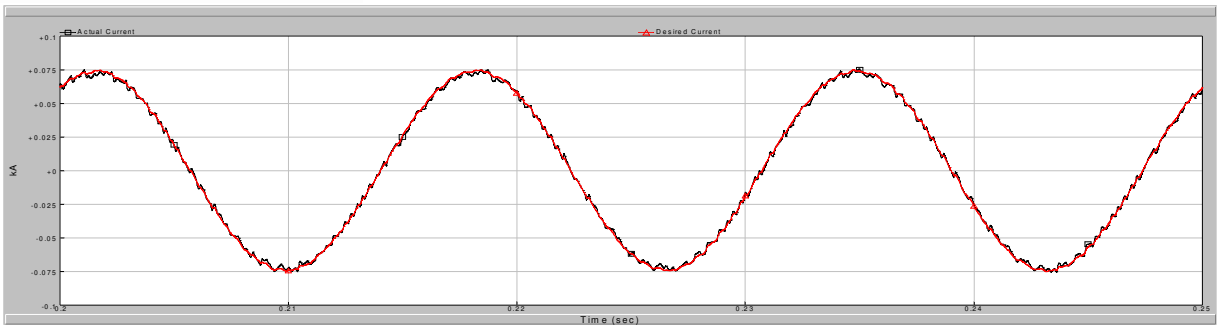

Figure 11: Static power converter output current showing reference (desired) current and actual current.

By modifying the control scheme just described to incorporate a commanded "shift" in the reference or template waveforms, reactive power flow to or from the line may also be controlled. Since the net energy flow from the reactive currents is zero (apart from very small conductive and switching losses), the dc voltage will be unaffected. Reactive power may be adjusted independently of real power flow up to the thermal limits of the switches and passive components in the converter. Reactive power generation with zero real power is also possible.
The significance of the previous discussion from the modeling perspective is that, unlike rotating machinery whose behavior is bound by fairly well-know physical principles, the response of the wind turbine static power converter equipment to events on the power system is almost entirely dictated by the embedded control algorithms. How a static power converter contributes to short-circuits, for example, cannot be deduced from the topology or values of passive elements such as tie inductors or dc link capacitors.

Grid Interface

Commercial wind turbines use low-voltage generators (<1000 V), and connect to the medium voltage public distribution feeder or wind plant collector system through a three-phase transformer. The transformer connection is usually wye on the low-voltage side to serve turbine loads. The medium-voltage side may be either wye or delta. The transformer may be supplied by the turbine vendor, and in some cases can be located "up tower" – in the nacelle of the turbine to reduce cabling losses. Pad-mount transformers near the base of the turbine tower are also common.
All commercial wind turbines have either power factor correction or some type of power factor control. Direct-connected induction generators and those with scalar rotor current control use staged/switched shunt capacitors to correct power factor across the operational range of the turbine.
Advanced machines are capable of power factor control via the advanced rotor power converter. The converter itself may have a small L-C network on its terminals for filtering noise resulting from the fast operation of the semiconductor switches.

Protection Systems

Commercial wind turbines incorporate sophisticated systems for protection of electrical and mechanical components. These turbine-based systems respond to local conditions, detecting grid or mechanical anomalies that indicate system trouble or potentially damaging conditions for the turbine. Some are computer-based, as with those associated with the high-performance static power converter, or run as algorithms in the master turbine controller, and therefore can respond almost instantaneously to mechanical speed, vibration, voltages, or currents outside of defined tolerances.
In addition, conventional multi-function relays for electric machine protection are also provided to detect a wide variety of grid disturbances and abnormal conditions within the machine.

Wind Plant Design and Configuration

Wind turbines are just one (albeit an important) component of bulk wind plants. With individual turbine sizes now exceeding 1 MW, nameplate ratings for single wind plants of many tens to hundreds of MW are common. The geographic extent of the wind plant must be large enough to not only accommodate the dozens to a hundred or more turbines, but also allow optimal spacing and utilization of local terrain features that will maximize energy production. The infrastructure for connecting a large number of widely distributed turbines to a single point of interconnection with the transmission system has important influence over the electrical characteristics of the wind plant.
The installed and proposed utility-scale wind plants in the U.S. have some common design characteristics that offer potential simplifications for constructing aggregated models for transmission system studies. These commonalities stem from practicalities and optimizations regarding the local wind regime, micro-siting of individual turbines, electric system design, and operations and maintenance economies. The result is that, from the power system modeling perspective, large wind plants have the following features in common:

- **A single turbine type** – Since wind turbines are complex machines that require preventative, predictive, and on-demand maintenance to achieve the highest availability, it is better from a maintenance and operations perspective to utilize the same turbine throughout the wind plant and have a maintenance and operations staff that specializes in all aspects of this single turbine design.
- **Medium voltage collector systems and interconnect equipment** – The electrical infrastructure which “collects” power generated by each turbine in the plant and delivers it to the transmission system utilizes standard overhead and underground medium voltage (15 to 35 kV) equipment and design practices. Some variations from standard utility practice for medium voltage design are necessary, however, as the operation of wind

turbines varies significantly from the distributed end-use loads for which the utility practice is optimized. For example, voltage regulation and protection schemes must be modified to account for generation, rather than load, distributed along the collector lines. The collector lines are an integral part of the wind plant; i.e. they are not utilized to serve non-wind plant load or other electric utility customers.

- **Reactive compensation** – Maintaining voltages within tolerances at individual turbines within a wind plant while at the same time meeting power factor or voltage regulation requirements at the point of interconnection with the transmission system requires careful management of reactive power. Typical locations for reactive power compensation within a wind plant are 1) at each individual turbine, dependent on the reactive power requirements and characteristics of the rotating machinery in the turbine; 2) at the interconnect substation in the form of switched shunt capacitor banks; and 3) at locations along the medium voltage collector lines depending on the layout of the plant. Some plants have the ability to dynamically control reactive power from each turbine, which offers the possibility of reactive power management for transmission system considerations to be accomplished by the turbines themselves. Terminal voltages at individual turbines, however, may be a constraint on the amount of reactive power that can be delivered to the interconnect substation during periods of high wind generation. In addition, when reactive power is required at the point of interconnection to the transmission network to support voltage, substantial reactive power may be "lost" in the medium voltage collector system between individual wind turbines and the interconnect substation.
- **SCADA and Plant Control** – Large wind plants typically have fairly extensive means for remote operation of individual turbines and collection of high-resolution operating data. Interfaces to power system operations centers are also being implemented, allowing automated implementation of control area operator commands during certain system conditions – e.g. automatic curtailment.

The most important influence of the wind plant infrastructure on the interconnection bus bar characteristics of the wind plant is on the net reactive power capability of the wind plant. Voltage profiles along the collector lines are an internal issue. For purposes of characterizing the plant for transmission studies, the static, dynamic, and load-dependent effects of the collector system on the net reactive power at the interconnection substation must be characterized. Figure 12 illustrates this influence with an example from an operating wind plant. Wind plant generation and net reactive power requirements are shown as functions of wind speed. In the figure, the net reactive power is entirely a function of reactive losses in the lengthy overhead collector lines, since the turbines are assumed to be operating at unity power factor. The stepped line shows how staged shunt capacitor banks on the collector lines might be deployed to account for this load-dependent reactive

loss. Not shown on the diagram is how such a scheme would contribute to the dynamic nature of the plant. As wind speed and power output vary, so will the net reactive requirements. Details of the capacitor switching scheme are critical here, since there will be time delays and hysterisis associated with the capacitor bank controls. These parameters must be selected with some knowledge of the time variation of wind generation on the collector line to prevent unnecessary capacitor switching operations and potentially associated voltage flicker.

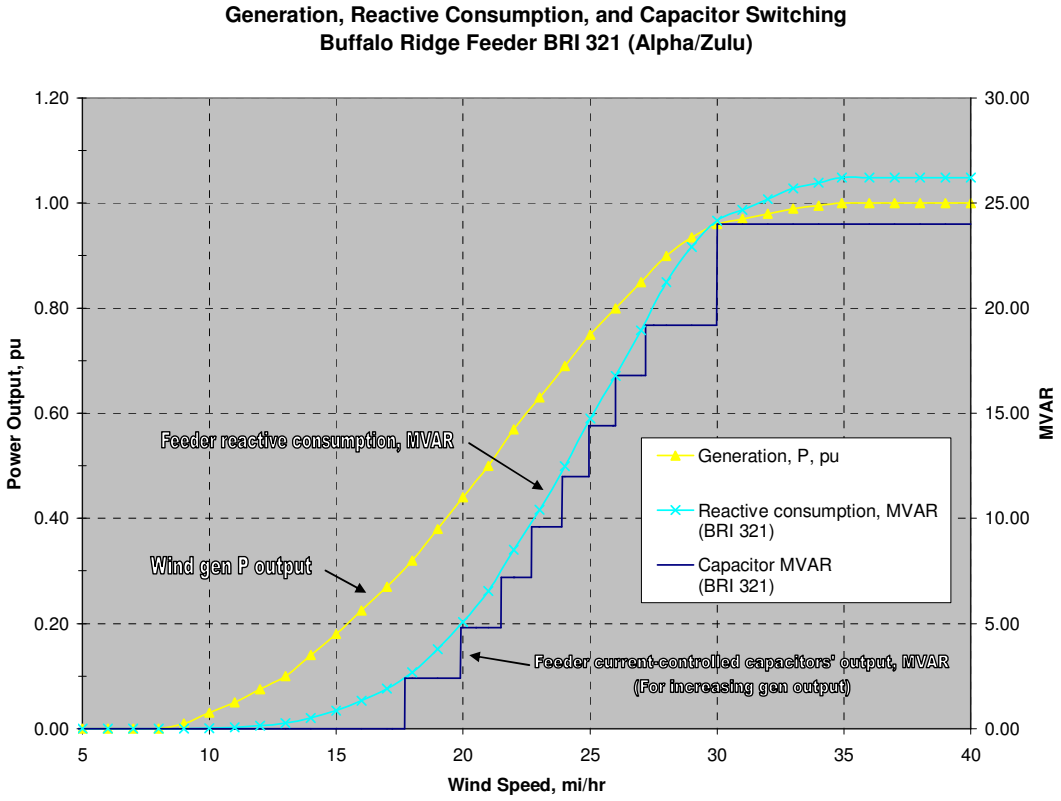

Figure 12: Illustration of the impact of collector line reactive losses on the net reactive power capability of a large wind plant.

Wind Generation Technology and Application Trends

The turbine types described previously have served the U.S. wind industry from the beginning of the explosive growth in the mid 1990's. Newer, bigger turbine models have been introduced along the way, but the technological improvements and modifications in the new commercial introductions have not changed the basic electrical behavior of the turbines.

Reducing the cost of energy is still today the primary driver for ongoing developments in wind turbine technology. Increases in the price of natural gas over the last few years have put made wind generation in good wind resource areas cost competitive with natural gas fired generation. While the cost of wind energy has actually increased over the past few years due to rising steel prices and currency exchange issues, further reductions in cost are still being projected going forward due to incremental improvements in technology. Many of these

increments can be found in the low wind speed turbine research program at the National Renewable Energy Laboratory (NREL). The desired outcome of this significant research effort is wind turbine technology capable of producing competitively-priced energy in sites with lower average annual wind speeds. These sites tend to be much closer to major electric load centers, which would easethe transmission issues faced by wind plants in more favorable but remote wind resource locations.

Technological advances from this research will also contribute to further cost reductions from plants in higher wind speed regimes. NREL projections for wind energy costs under a generating company ownership assumptions are shown in Figure 13.

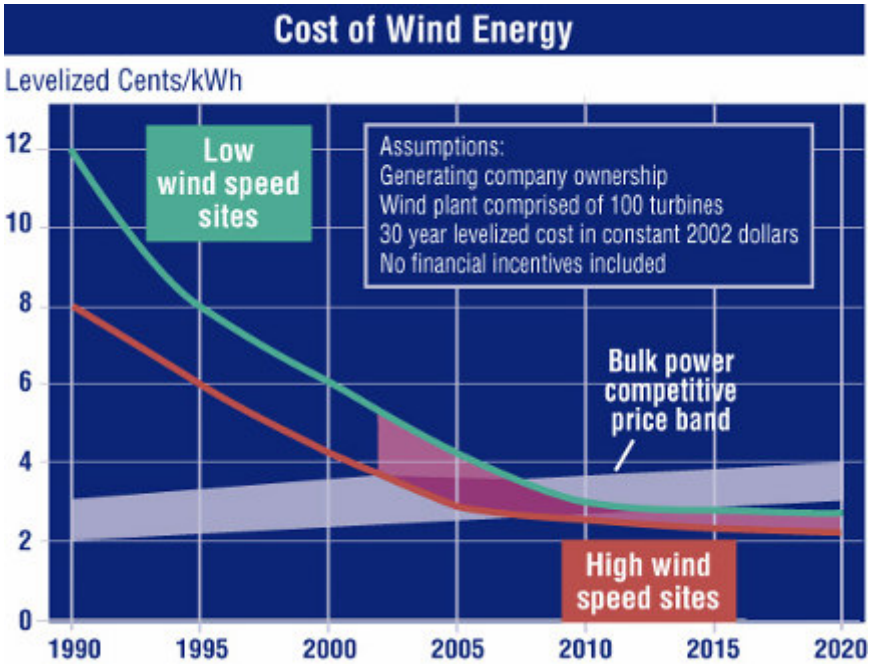

Figure 13: Projected wind energy costs with low wind-speed turbine technology. (Source: NREL National Wind Technology Center)

Experiences from large wind projects are also influencing wind turbine developments, and are expected to have even more impact going forward. Wind turbine vendors now recognize that some features and enhancements to the electrical performance of their products are or will be demanded by customers and are critical for further expanding the overall market potential for wind generation in the U.S.

Wind plant design is undergoing some evolution. Plant operators and project developers are gaining important experience from the first generations of large wind plants developed since the mid-1990's. Awareness is growing of the importance of the portion of the wind plant between the turbines and the interconnection point to the transmission network to plant availability, turbine performance, and successful operation with the grid.

Finally, with wind generation becoming a visible fraction of the generating assets in some control areas, transmission service providers are beginning a push for more stringent wind plant performance requirements and interconnection standards.

These influences will have a positive impact on the characteristics of wind generation facilities as viewed from the transmission network over the coming years. This section describes technological changes that will lead to new wind plant features and capabilities over the coming years that will affect electrical performance and integration with the grid.

Wind Turbine Technology Trends

The value of variable speed technology for large wind turbines has been proven in the marketplace over the past decade, and will be the predominate technology going forward. Variable speed operation has benefits in terms of managing mechanical loads on the turbine blades, drive train, and structure. The grid-side benefits are also significant, and include dynamic reactive power control, increased dynamic control over electric power generation, and opportunities for further enhancement of grid-integration features of the turbine.

Electrical Topology

At present, the doubly-fed induction machine topology is favored both in the U.S. and globally. As the size of individual turbines continues to grow, there is an emerging consensus that future turbines will likely employ machines other than induction generators, possibly advanced synchronous or permanent magnet designs. For variable speed operations, these new machines will require that all of the electrical output flow through some type of power converter. This converter would almost completely define how the turbine “looks” to the power system, offering some new opportunities for improving interconnection and integration.

Electrical Robustness

Wind turbine vendors are now well aware of the need for improving turbine electric robustness, especially in terms of the ability to ride-through faults on the transmission system. Enhanced low-voltage ride through is already an option for several commercial turbines, and will likely be a standard feature in the coming few years. Farther down the road, it is expected that wind turbines will be no more sensitive in terms of tripping for transmission system faults than conventional generators, and will provide flexibility with respect to “programming” their shutdown modes for grid events.

Since it first emerged as an important issue for the electric power and wind generation industries just a few years ago, the performance of wind turbines during network disturbances and their ability to ride-through low voltage events been the subject of extensive discussion and debate.

After extensive discussions and debated involving the Federal Energy Regulatory Commission (FERC), the American Wind Energy Association (AWEA), and the North American Electric Reliability Council (NERC), an agreement on requirements and language concerning LVRT for wind plants was reached, and published in FERC Order 661a. The Order stated that:

1. Wind generating plants are required to remain in-service during three-phase faults with normal clearing (which is a time period of approximately 4 – 9 cycles) and single line to ground faults with delayed clearing, and subsequent post-fault voltage recovery to pre-fault voltage unless clearing the fault effectively disconnects the generator from the system. The clearing time requirement for a three-phase fault will be specific to the wind generating plant substation location, as determined by and documented by the transmission provider. The maximum clearing time the wind generating plant shall be required to withstand for a three- phase fault shall be 9 cycles after which, if the fault remains following the location-specific normal clearing time for three-phase faults, the wind generating plant may disconnect from the transmission system. A wind generating plant shall remain interconnected during such a fault on the transmission system for a voltage level as low as zero volts, as measured at the high voltage side of the wind GSU. (generator step-up transformer; for wind plants in this context, the transformer at the interconnection substation is considered to be the GSU)
2. This requirement does not apply to faults that would occur between the wind generator terminals and the high side of the GSU.
3. Wind generating plants may be tripped after the fault period if this action is intended as part of a special protection system.
4. Wind generating plants may meet the LVRT requirements of this standard by the performance of the generators or by installing additional equipment (e.g., Static VAr Compensator) within the wind generating plant or by a combination of generator performance and additional equipment.
5. Existing individual generator units that are, or have been, interconnected to the network at the same location at the effective date of the Appendix G LVRT Standard are exempt from meeting the Appendix G LVRT Standard for the remaining life of the existing generation equipment. Existing individual generator units that are replaced are required to meet the Appendix G LVRT Standard.

It was recommended that the standard be effective as of January 1, 2007. For a transition period which includes turbines purchased under a contract executed prior to December 31, 2005 for delivery through 2007, or turbines purchased for projects with interconnection agreements singed prior to December 31, 2006, a requirement in line with the WECC standard would apply. Notable in this recommendation is there is no specification of LVRT requirements after the fault,

only the mandate that the plant and turbines not trip during the dynamic period is which the voltage is recovering to nominal.

In the negotiations with AWEA, NERC agreed that exceptions to this LVRT requirement should only be considered if they are made on an *interconnection-wide* basis. There are three interconnections in the U.S. and Canada: Western (WECC), ERCOT (Texas) and Eastern (everything else).

The agreement and subsequent FERC order does not restrict individual transmission providers from implement a more stringent standard. However, to do so, it must make a case in a formal filing to FERC that such a deviation is necessary for system reliability. FERC will then consider the filing and solicit comments from the public. Such a process effectively prevents individual transmission providers from implementing a technically unnecessary requirement for the purpose of discriminating against wind generation.

LVRT requirements as agreed to in the NERC/AWEA negotiations will likely become the the basis for future standards in the U.S. and Canada. In meeting this requirement, wind plants will be adhering to the same standard as for all other types of large generation installations.

The non-quantitative performance specified for the post fault period (must not trip) places additional emphasis on other plant design factors, especially in terms of reactive power compensation. The optimal reactive compensation for a wind plant will be quite specific to the type of turbine, plant layout, and grid characteristics. When the strength of the grid interconnection relative to the plant rating is adequate, the issues for reactive compensation will generally be less difficult. A grid short-circuit capacity to plant size ratio of 10 or more would characterize these situations. When the short circuit ratio falls below ten, reactive compensation issues for both steady state operations and response to grid events will become more acute. Such weak interconnections are not unheard of in the wind generation industry, as many good wind resource areas are remote from load centers where the grid capacity would tend to be higher. The Lamar, Colorado plant, for example, may be one of the weakest wind plant interconnections to date. The short-circuit ratio at the point of interconnection for this plant is less than 3.

Reactive Power Control

Managing reactive power in the electric power network critical for maintaining voltage profiles and stability. Most elements of the power system – loads, transformers, lines, motors, etc. - absorb some amount of reactive power during normal operation. To maintain proper voltage, this reactive power must be supplied by generators, shunt capacitors, or some other type of compensation. In addition, reactive power supplies must be adjustable as reactive power requirements will vary as loads and flows in lines change.

Dynamic reactive power control allows the compensation to be adjusted continuously very quickly, and provides the wind plant designer with an additional tool for managing collector line voltage profiles within the plant and the overall

reactive power characteristics of the plant. It should be recognized, however, that turbine-based reactive power control is not a "magic bullet", especially in cases where reactive power is required to support the transmission system, since in this situation the reactive power is being produced as far away as possible from where it is needed. The fast dynamic response of turbine-based reactive compensation may be very important, however, for assisting with system voltage recovery following faults.
To realize the full value for dynamic reactive power control, future wind turbines should be able to make reactive power available even when not generating. If not available when the wind plant is not producing, the value to the transmission network would be significantly discounted.

Because of the fast pace at which the wind industry has emerged and grown over the last decade, the reactive power characteristics of a wind plant are more often than not an "outcome" rather than a design requirement. With more stringent interconnection requirements, more attention and analysis will be given to this topic for plants built over even the next few years. The required reactive power capability of a wind plant will be determined from the results of the interconnection study, and will drive the overall wind plant design, possibly impacting even turbine selection.
Where the transmission system interconnection is weak or vulnerable, there will be more use of auxiliary equipment such as static var compensators. As design experience accumulates, the ability of the wind plant to provide for the needs of the transmission system at the point of interconnection will be much improved.

Real Power Control

At present, commercial wind turbines generally operate to maximize energy production. When winds are at or above the rated speed, electrical output is "capped" at the nameplate rating. In light to moderate winds, however, the turbine is operated to capture as much energy as possible, such that the output will fluctuate when wind speed fluctuates.
These fluctuations are not optimal from the perspective of the grid, as they can lead to voltage variations and potentially increase the regulation burden at the control area level. In future generations of wind turbines, it will be possible to "smooth" these fluctuations to a greater degree than is achieved now with mechanical inertia alone. More sophisticated pitch regulation schemes, improved blade aerodynamic designs, and wider operating speed ranges will provide means for limiting the short-term changes in turbine output while at the same time minimizing the loss of production. Such a feature could be enabled only where and when it has economic value in excess of the lost production.
Extending this type of control would allow wind turbines to participate in Automatic Generation Control (AGC). In this mode, the turbine would have to operate at a level somewhat below the maximum available from the wind to provide room for "ramping up" in response to EMS commands. Again, the value of providing this service would have to be evaluated against the cost in terms of

lower production as well as the cost of procuring this service from a different source. Technically, though, such operation is possible even with some of the present commercial wind turbine and wind plant technology.

Dynamic Performance

The dynamic characteristics of the more advanced commercial turbine technologies are complicated functions of the overall turbine design and control schemes. Little consideration has been given thus far to what would constitute desirable dynamic behavior from the perspective of the power system. Much of the attention to date in this area has been focused on the ride-through question. Once that matter is resolved, there may be opportunities to fine-tune the dynamic response of the turbine to transmission network faults so that it provides maximum support for system recovery and enhances overall stability.
Given the sophistication inherent in the topology and control schemes of future wind turbines, it should be possible to program the response to a degree to achieve such stability benefits. Such a feature would allow a wind turbine / wind plant to participate in a wide-area Remedial Action Scheme (RAS) or Special Protective System (SPS) as is sometimes done now with HVDC converter terminals and emerging FACTS devices.

Wind Plant Design and Operation

Realizing the benefits of enhanced capabilities of wind turbines will depend in large part on the overall wind plant design, since the actions of a large number of relatively small wind turbines must be coordinated to have positive impacts on the overall power system.

Communications and Control

The communications and control infrastructure of even present-day wind plants can be sophisticated, with high-speed SCADA to each turbine and other critical devices or points within the collector system. This sophisticated infrastructure has yet to be exploited for purposes of improving the interconnection performance and integration of the wind plant with the power system; mostly it has been used for maximizing plant production and availability.
In the future, this infrastructure will be the foundation upon which many of the advanced features and capabilities will be based. The interface between the wind plant control center and power system control area operations will also be developed to a much higher degree. Advanced wind plant performance such as AGC participation will likely be accomplished by the control area EMS interacting with the wind plant control center, rather than from EMS to individual wind turbines. Such an interface would also facilitate other plant capabilities that could benefit power system security and reliability, such as automatic full- or partial-curtailment of wind generation under severe system contingencies.

Bulk Wind Plants vs. Distributed Wind Generation

Most of the current installed wind generation capacity in the U.S. is comprised by collections of turbines operating as a single plant with direct connection to a high-voltage transmission network. While much smaller in terms of installed capacity, individual or small numbers of turbines connected to a public distribution network are common sights in some regions of the country, especially in the upper Midwest. Much of current installed wind generation in Germany consists of small turbine clusters connected to the public distribution system.
From an electrical perspective, the important distinction between the bulk vs. distributed application lies in the nature of the electric power system to which the facility is connected. Transmission systems are physically networked, which generally means that the system can continue operations after the loss of a single line. Such is not the case for radial distribution systems. Consequently requirements for the physical interconnection and performance can be markedly different between these applications.

In some parts of the country, there is potentially a “middle ground” between true distributed plants and bulk facilities. The mostly likely example would involve a small wind generation facility connected to what is commonly referred to as the “sub-transmission” system. These facilities operate at voltages below the lowest networked system voltage (again, usually 115 kV in Minnesota) and above distribution voltages. Facilities at 69 kV or even 34.5 kV are found in this class. Sub-transmission lines are sometimes connected in a radial fashion between a transmission substation and remote distribution substations. The radial configuration can have implications for how a generating facility would be interconnected.

The size of the wind plant will usually determine the required interconnection voltage level. Beyond that, the nature of the system at the point of interconnection (networked transmission vs. radial distribution) will govern the requirements for interconnection and operation, regardless of the size of the plant.

Bulk wind generation facilities appear to power system operators and dispatchers as conventional power plants, albeit with unique operational characteristics. Energy produced by individual turbines is gathered by the low and medium voltage plant infrastructure, transformed to a higher voltage, and injected into the transmission network. From there it makes its way to bulk energy delivery points both near and far, where it is then stepped down to lower voltages and distributed to end users. Adequate transportation and delivery capacity must be made available all along the way for the energy to be utilized.
Distributed generation, on the other hand, provides a “short cut” between the supply and utilization of electric energy. Energy is produced and consumed locally, eliminating the need for transformation to and from higher voltages and the transmission capacity to move the energy relatively long distances. Reduced

losses and capital investment in the transmission infrastructure are two of the potential benefits of distributed generation. The earliest power systems were all based on this principle.

While simple in concept, there are some technical challenges related to distributed generation, with most of them related to the inherent limitations of electric distribution networks. A great majority of electrical distribution lines ("feeders"), and almost all of them in rural areas, were designed to connect end users with a single source of electric supply in a radial manner. This notion permeates all aspects of distribution system design and operation, from physical characteristics (e.g. conductor size) to over-current and over-voltage protection systems to equipment for managing and maintaining proper voltage at all points along the line. Most modern distribution systems are not very "smart". Distributed generation violates the underlying principle since it constitutes a second source of electric supply. However, it has been demonstrated many times that certain amounts of distributed generation can be accommodated by even the most unsophisticated distribution feeders without compromising performance, safety, or reliability. Interest in distributed generation has increased in recent years with the emergence of attractive technologies for small-scale power generation. Focus on the technical barriers to and solutions for accommodating larger amounts of distributed generation in public distribution systems has also grown. IEEE Standard 1547 is an early outcome of this technical focus, and represents a consensus view on how and to what extent distribution generation can be applied in existing distribution systems.

As the amount of distributed generation relative to the distribution feeder capacity or peak load increases, the technical challenges for maintaining performance and safety become more severe. In addition, some of the aforementioned benefits of distributed generation, such as loss reduction, may be lost. Technical solutions that become necessary require significant capital investment, and have the effect of transforming the "dumb' distribution feeder into something with much more flexibility, intelligence, reliability, and power quality. While certainly possible from the technical perspective, this capital investment can be cost prohibitive.

Wind generation as a distributed energy resource brings some unique challenges. The first is that the scale of modern commercial wind turbines is an order of magnitude or more beyond other common distributed generation technologies (note: While there are smaller commercial wind turbines (10 to 50 kW) available and in operation today, the focus of this report is on the wind development scenarios that are part of this study. Because of the large installed capacity under consideration, the distributed wind generation application of interest here would likely consist of the larger commercial turbines.) The addition of just a couple of wind turbines to a rural distribution feeder can bring the "penetration level" (ratio of installed DG capacity to feeder rating or peak load) to a point where existing protective systems can be challenged. Secondly, variability in turbine output due to changing wind speeds can stress the equipment and systems for regulating feeder voltage. Finally, the uncontrollable nature of wind energy production leaves some important benefits of distributed generation on the table, namely those associated with peak load shaving and

capacity deferral. During periods of minimal wind energy production, the distribution infrastructure must still be able to serve the connected load,

Smaller transmission-connected wind generation facilities may have some advantages with regard to transmission capacity questions. Wind energy injected at points of bulk power delivery could reduce loading on transmission lines (though not transformers) depending the size of the wind plants relative to the load at that delivery point. Wind energy delivery in excess of load at the injection point would flow into the transmission network. Quantification of the benefits of this type of arrangement in terms of loss reduction or capital investment deferral is not necessarily straightforward, but could be accomplished through a detailed transmission planning study.

Wind Generation Resource Assessment by County

WindLogics used the 2005 Minnesota Department of Commerce high-resolution state wind map to assess the wind generation resource and relative economics of wind generation for each county in Minnesota. WindLogics used GIS techniques that delineated annual mean wind speeds and net capacity factors for each county. The nominal, peak, and potentials by wind class were delineated. Spatial analysis was used to break down the areal coverage within each county that falls within a spectrum of wind energy production limits.

The source data for these maps was the Minnesota Department of Commerce State Wind Maps. These maps have a resolution of 500 meters. High-resolution county polygon data from the U.S Census was used to define the county borders for the State of Minnesota. In ArcGIS, the polygon data was overlaid on the wind raster data. Using the spatial analyst extension, zonal statistics were calculated. Zonal statistics were calculated by defining which county polygon each raster cell belongs in. The raster cells for each zone were tallied, summed and averaged to arrive at a statistical value for each county. A table was generated based on this process for both average wind speed and average capacity factor. Net capacity factor was calculated by assuming 14% losses from the original gross value with the calculation: gross * 0.86 = net. These losses include electrical losses, turbine availability losses, turbine interaction losses, and other losses. Electrical losses include cabling losses (0-1%), pad-mount transformer losses (.5-.7%), and substation interconnect losses (1-1.5%). Electrical losses at the wind plant level typically amount to roughly 3%. Turbine availability losses are based on scheduled and unscheduled outages for maintenance at the individual turbine level. Turbine availability losses can be as high as 5%, but a 2-3% availability loss is more typical. Turbine interaction losses occur when turbines are operating directly downwind from the wakes of other turbines in the array. Turbine interaction losses (2%) and other losses such as blade icing (1-3%), blade fouling from dirt and insects (.5-1%), and high wind turbine cut-out periods (1%) can total up to 7% at the wind plant level.

For the purposes of this study it is appropriate to assume that electrical losses, turbine interaction losses, and other losses total 10% of gross energy and turbine availability losses total 3% of gross energy production. In order to calculate net energy beyond the point of interconnect a deduction of 13% from gross energy would be appropriate and 14% was used as a more conservative estimate.

These tables were then joined with the original county polygon data for mapping purposes. The map polygons were categorized for display using the natural breaks method. The natural breaks categorization divides the data into any number of categories, in this case seven, based on “natural breaks” in the data. This method of categorization is advantageous for map display as it very effectively gives the data a high amount of geographical contrast on the map regardless of the range and standard deviation of the data.

Lincoln, Lyon, Pipestone, Murray, Cottonwood, Nobles, and Jackson Counties in southwestern Minnesota were classified in the highest mean annual wind speed bin of 7.93-8.51 m/s at 80 m. Lincoln, Pipestone, Murray, Cottonwood, and Nobles Counties in southwestern Minnesota were classified in the highest mean annual net capacity factor bin of 42%-43%.

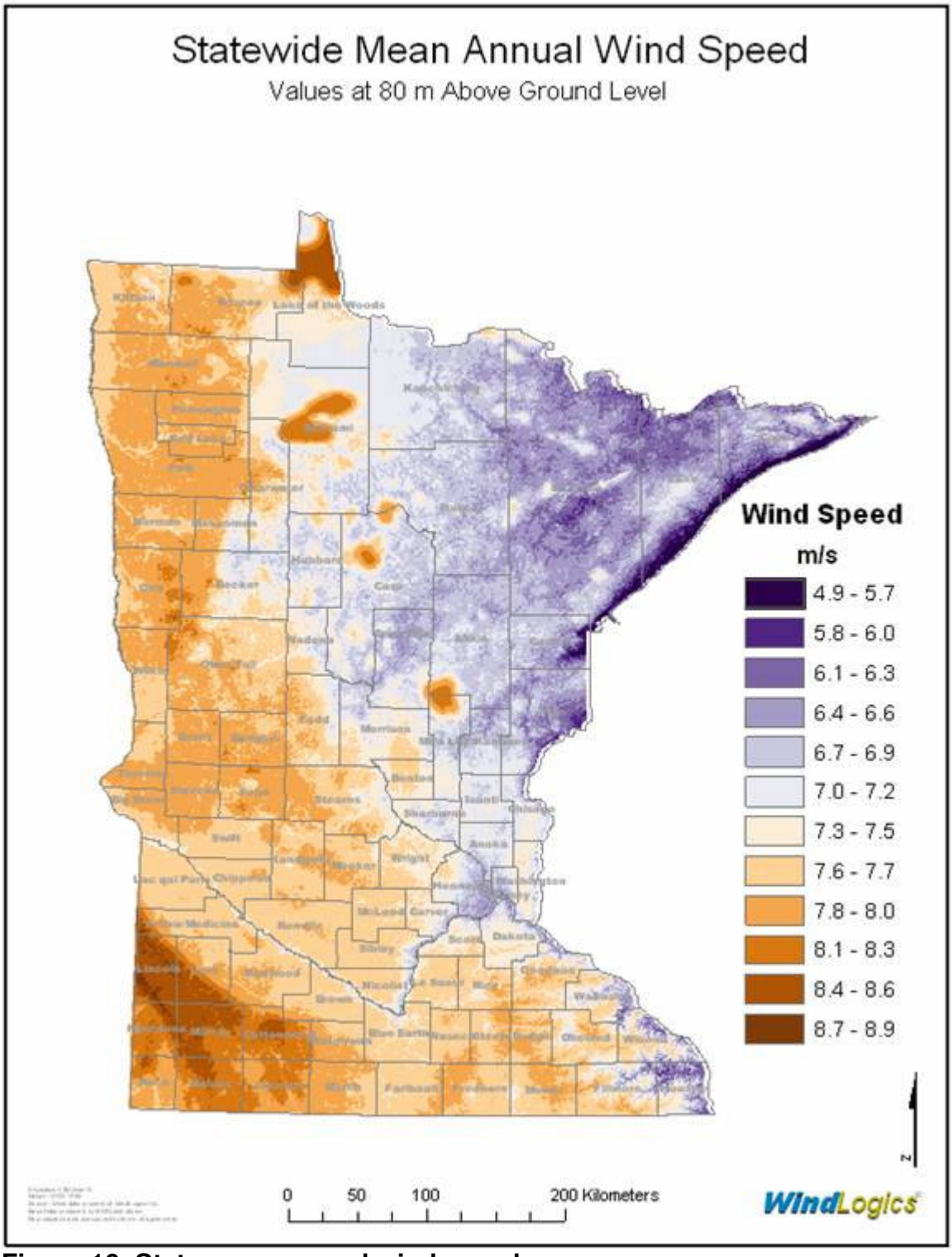

Figure 16: State mean annual wind speeds.

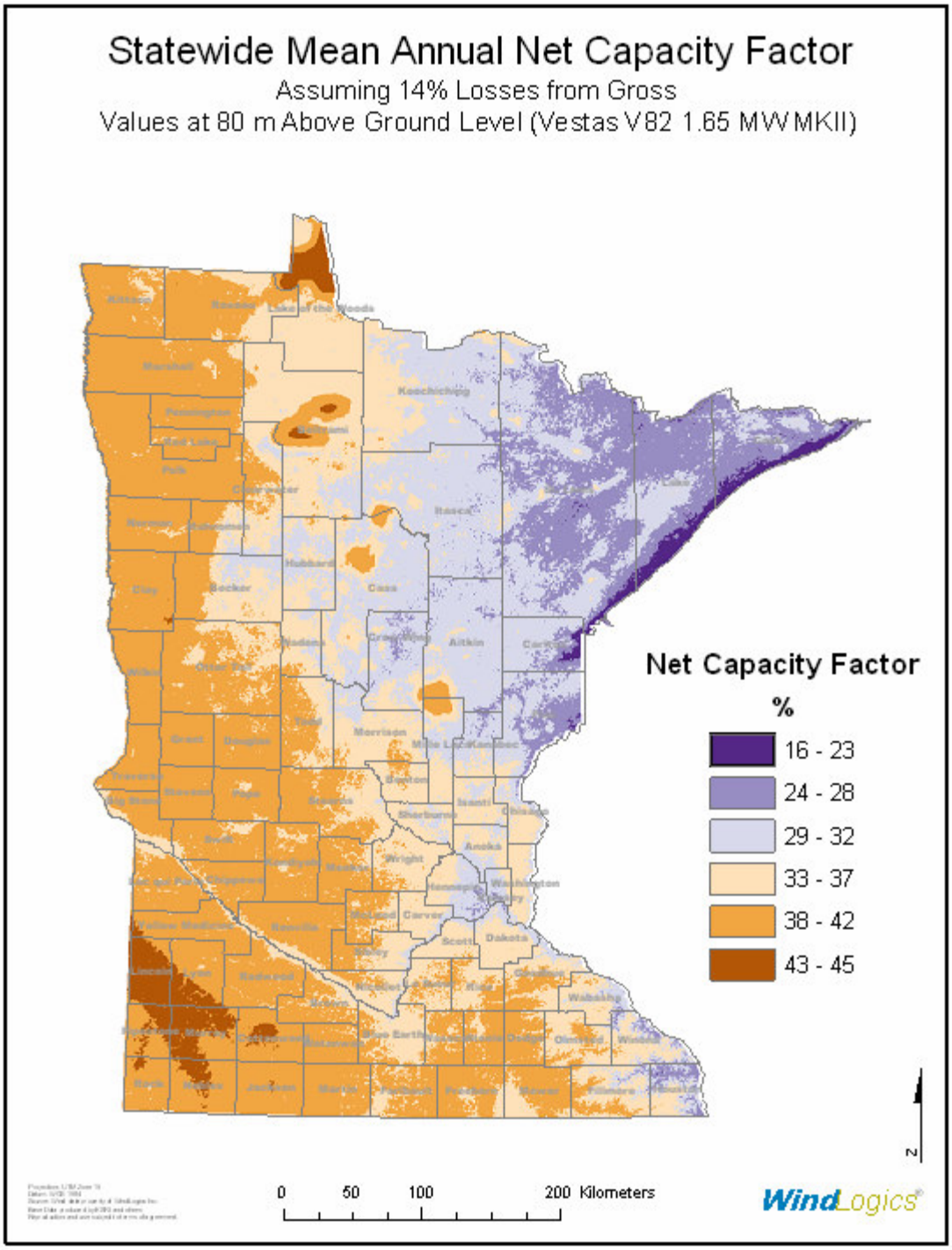

Figure 17: State mean annual capacity factors.

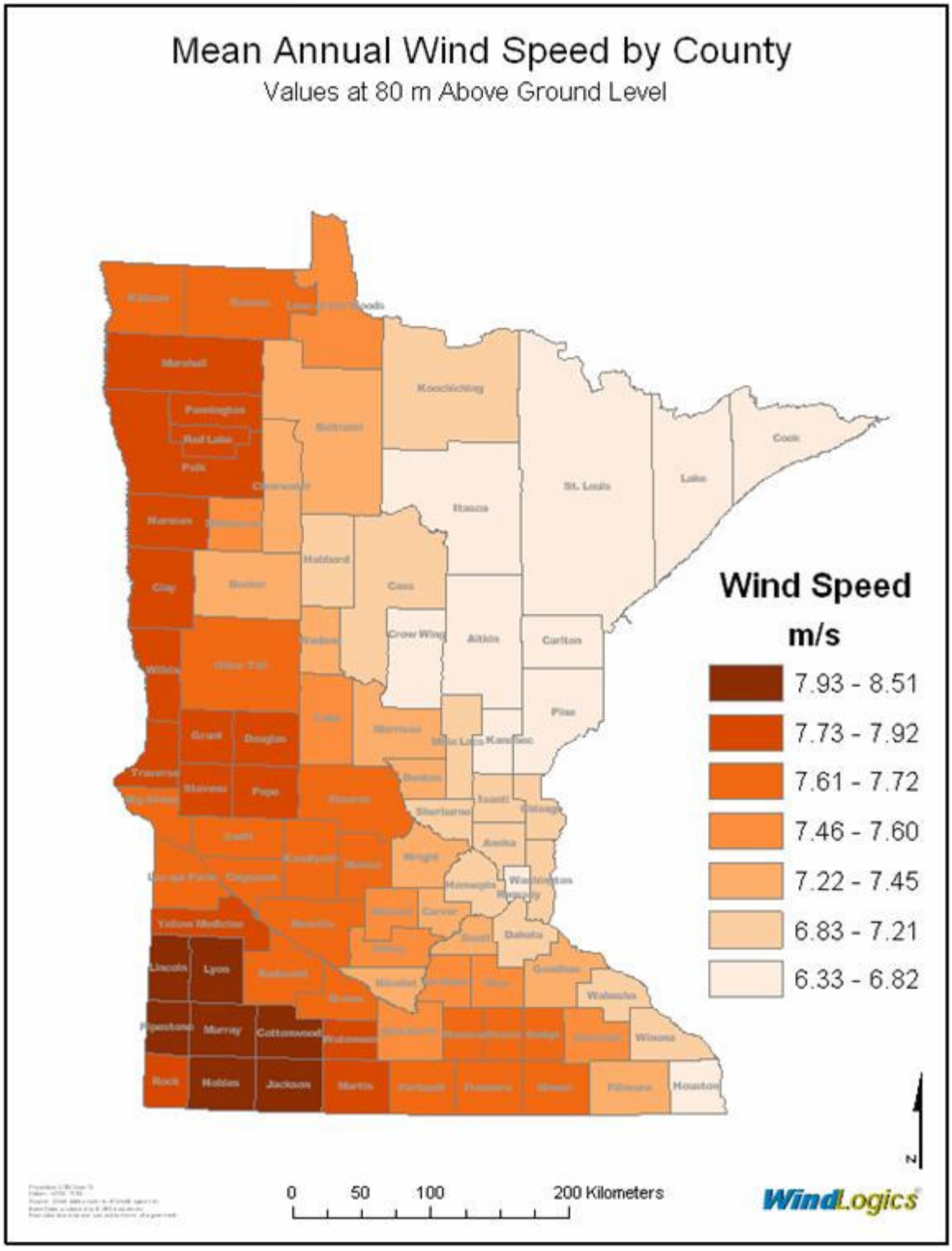

Figure 18: State mean annual wind speeds by county.

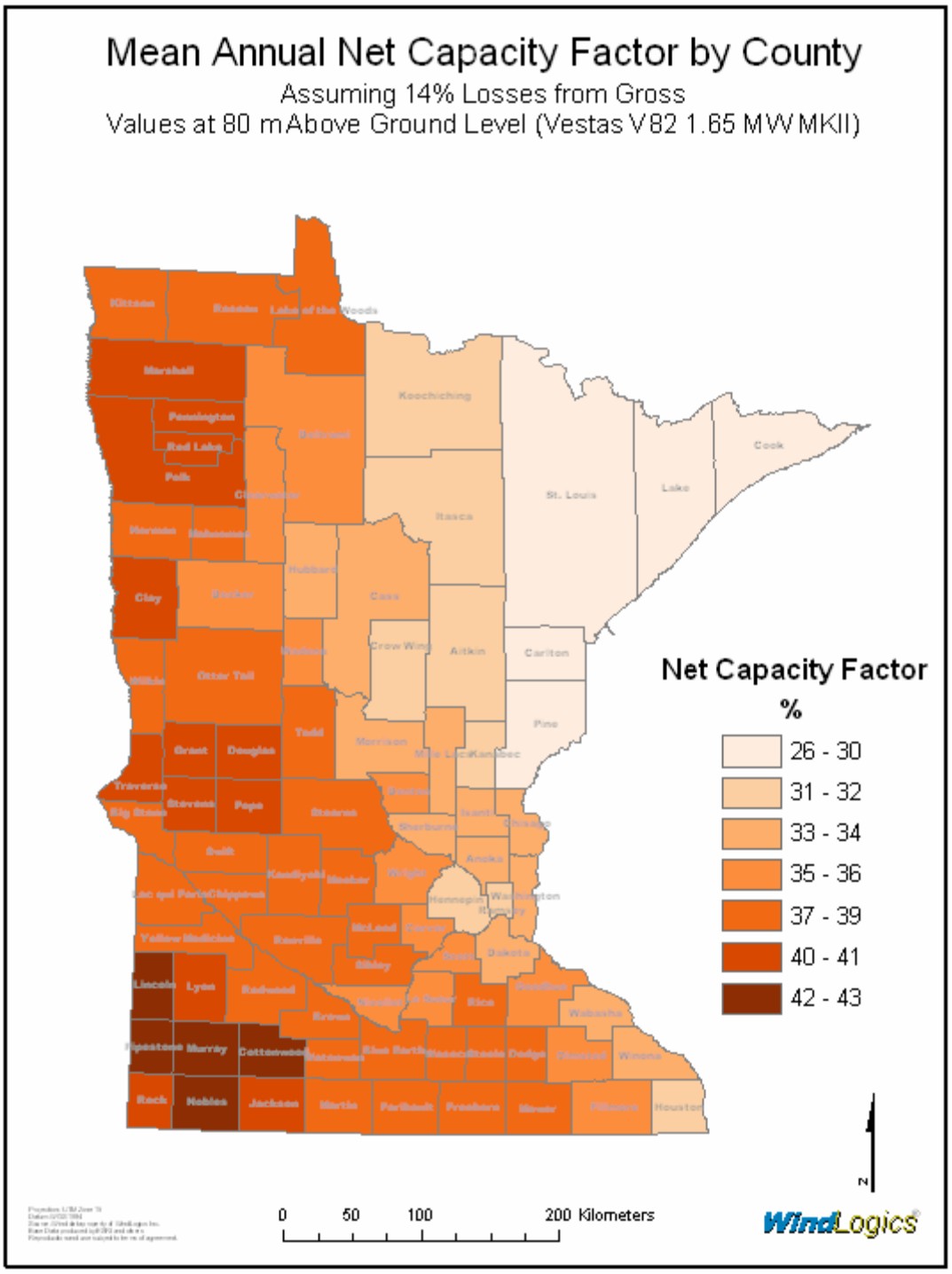

Figure 19: State mean annual net capacity factors by county.

Regional Wind Generation Resource

Based on existing projects, contracted projects, wind resource quality, interconnection queues, proposed projects, and proximity to load, WindLogics and EnerNex created wind generation scenarios consistent with the RFP cited 15%, 20%, and 25% penetration levels. In collaboration with participating utility and other technical review partners, 152 wind generation proxy locations were selected throughout the study area in Minnesota, North Dakota, and South Dakota. See figure 20 for the Proxy Tower locations.

Wind Generation Time Series

Develop Wind Speed and Power Time Series

To support the development of the system integration wind model, data at 152 grid points (proxy towers) in the inner model nest were extracted every 5 min as the simulation progressed. This process ensured that an analysis of the character and variability of the wind resource over several time scales could be performed at geographically dispersed locations. Figure 20 depicts the MM5 innermost grid with selected locations for high time-resolution data extraction. The sites were selected in coordination with the utility and government stakeholders represented on the Technical Review Committee to correspond to 1) existing wind plant locations such as those along the Buffalo Ridge and other regions of southern Minnesota, 2) proposed locations for near-future wind plant development or 3) favorable locations for future wind production with emphasis given to a distribution of wind energy plants that would provide beneficial geographic dispersion. The 2005 Minnesota Department of Commerce high-resolution state wind map was used, in part, for guidance in assessing favorable development areas. Overall, 152 sites were located in 62 counties in the three state domain at locations within the county with an expected favorable county-relative wind resource. Consideration was also given to the existence of nearby transmission and substations. Model data extracted at each site included wind direction and speed, temperature and pressure at 80 and 100 m hub heights. The non-wind variables were extracted to calculate air density that is used along with the wind speed in turbine power calculations. With this data, WindLogics developed time series of 80 and 100 m wind speed and power at 5 minute and 1 hour time increments for use by EnerNex in system modeling efforts described in Tasks 2 and 3.

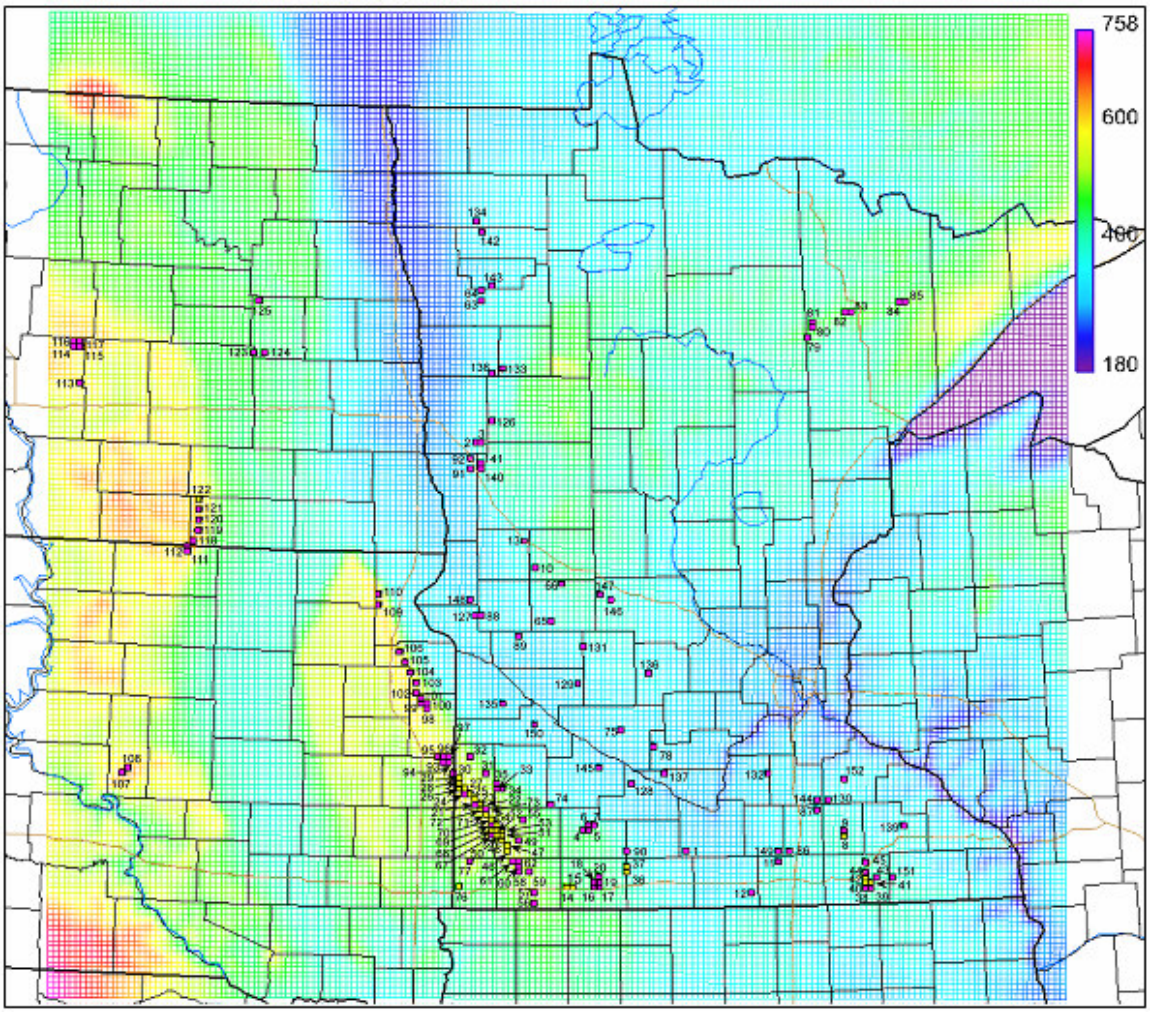

Figure 20: Inner model grid with 152 proxy MM5 tower (data extraction) locations. The color spectrum represents surface elevation. Yellow boxes indicate MM5 extraction sites that are collocated with existing wind production.

Model Validation

To ensure that the MM5 simulations were accurately representing the wind resource, WindLogics conducted a validation test using the Minnesota Department of Commerce administered meteorological tower at Breckenridge in Wilkin County of western Minnesota. This tower was selected due to its height (70 m) and due to its favorable design that featured sufficient sensor boom lengths that mitigate detrimental tower shadowing and over-speeding effects. The results from this validation analysis are presented in Table 1. Annual wind speeds from the model were compared to the tower for the year 2004 at three levels (50, 60, and 70 m AGL). The model compared very favorably with the tower, with only small biases in the annual wind speeds of ≤ 5.3% and mean monthly absolute errors (MAE) of 4.1 to 5.7 percent. At the critical near-hub

height level of 70 m, only a 3.2 percent annual bias was realized along with a monthly MAE of just 4.5%.

Table 1. MM5 Validation with the Breckenridge Tall Tower

Level (m)	Tower - Annual Wind Speed (m/s)	MM5 – Annual Wind Speed (m/s)	Bias	Monthly Average MAE
50	6.76	6.40	-5.3%	5.7%
60	6.81	6.72	-1.3%	4.1%
70	7.27	7.04	-3.2%	4.5%

Frequency Distribution of Power Generation Including Geographic Dispersion

An analysis of power generation was conducted for four levels of geographic dispersion employing all hours of the three-year dataset. Given the nature of this analysis and the objective of demonstrating the attributes of geographic dispersion, a single extraction point tower was analyzed for three representative regions of Minnesota and one region in North Dakota. Specifically, the objective of this research is to utilize the annual and seasonal expected wind power generation at a control location in southwest Minnesota, and incrementally examine the influence geographic dispersion has on the percentage occurrence of specific hourly capacity factor values. The four levels of geographic dispersion are 1) Minnesota Southwest (Buffalo Ridge), 2) Minnesota Southwest + Minnesota Southeast (Mower County), 3) Minnesota Southwest +Minnesota Southeast + Minnesota Northeast (Iron Range), 4) Minnesota Southwest +Minnesota Southeast + Minnesota Northeast + North Dakota Central. The MM5 proxy towers selected to represent each of these areas are Towers 71 (Minnesota Southwest), 41 (Minnesota Southeast), 82 (Minnesota Northeast) and 115 (North Dakota Central). See Figure 21 for the locations of Towers 71, 41, 82, and 115. In light of the idealized objectives of this investigation, gross capacity factors were utilized in the analysis.

Note that since a single model proxy tower was used to represent each region, the influence of local and intra-regional geographic dispersion is not accounted for. Specifically, when considering hourly statistics, the expected benefit from geographic dispersion over the limited area of a wind farm of approximately 40 MW is negligible. Thus, using one turbine site to represent a 40 MW wind farm would reasonably approximate the mean per turbine gross generation of the 24 units of 1.65 MW rated capacity. The idealized methodology of using one production site to represent a region does underplay the beneficial aspects of intra-regional geographic dispersion when the specific region is large. For instance, considering wind production over the entire Minnesota and South Dakota extent of the Buffalo Ridge (approximately 300 km), using a single centralized production point (Tower 71) neglects the beneficial aspects of

regional geographic dispersion of production. In a prior wind integration study for southern Minnesota (Minnesota Department of Commerce 2004), analysis of regional geographic dispersion using a 104 km section of the Minnesota portion of the Buffalo Ridge showed small but non-negligible beneficial aspects.

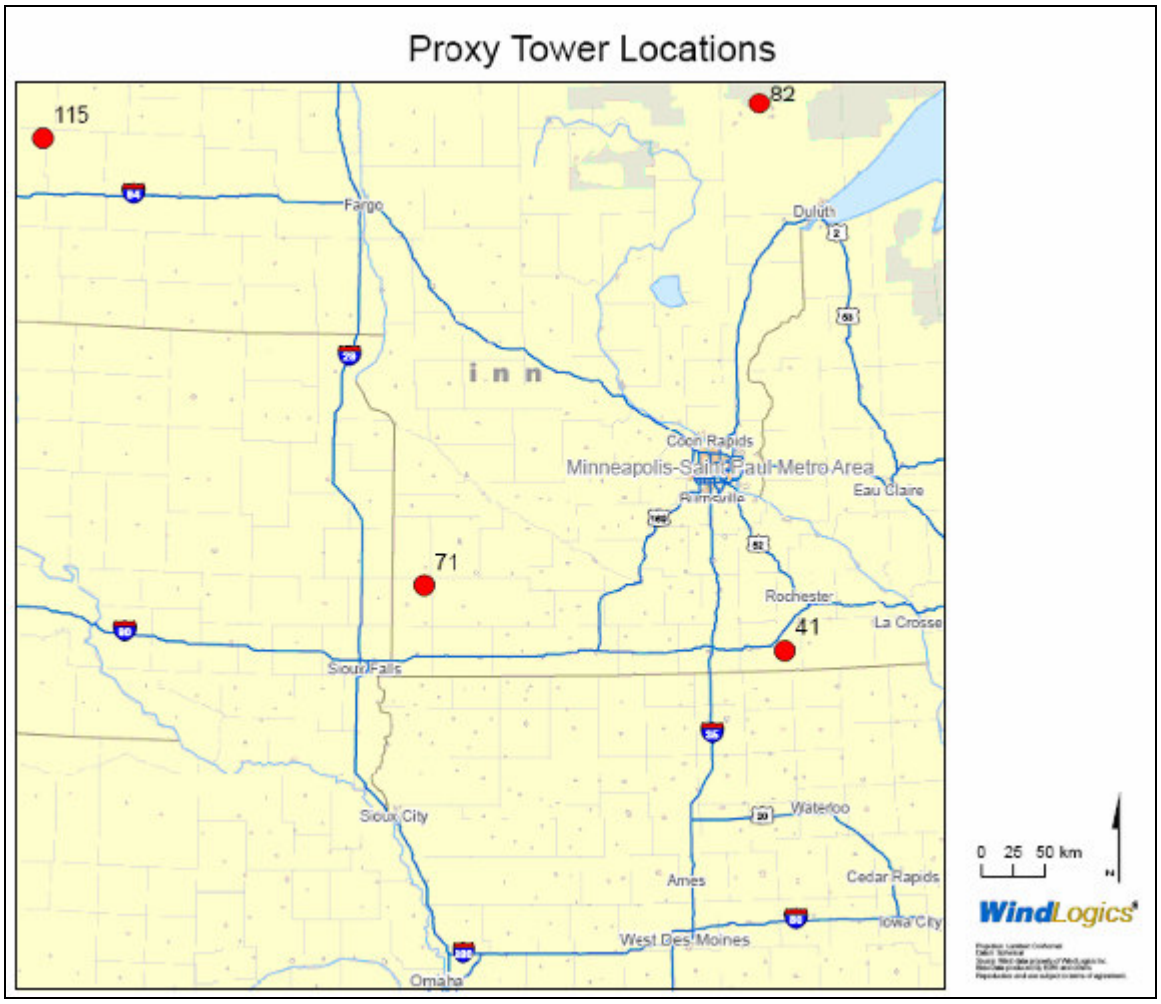

Figure 21: Locations for proxy towers 71, 41, 82, and 115.

As shown in the annual and seasonal frequency histograms in Figs. 22-24, the Minnesota Southwest (MN_SW) site has a distribution both annually and seasonally that is characterized by frequent occurrence of either winds too weak to produce much power (the 0-5 % capacity factor bin) or strong enough to reach (or nearly reach) the top of the power curve for the Vestas V82 1.65 MW turbine (95-100 % capacity factor bin). The distribution of occurrence percentages of hourly capacity factor over the other 5% bins is of similar magnitude, and represents the cumulative majority of all occurrences. Note that the bin extremes at either end of the distribution are synthetically pronounced due to just one tower representing Minnesota Southwest. An inter-seasonal comparison of the first and last bins reveals a much more favorable wind climatology for fall and

winter, and to a lesser extent, spring, than that realized for summer. The increased incidence of “top of power curve” production and decreased frequency of light wind conditions can be explained by recognizing the stronger synoptic meteorological forcing of the wind resource in the winter and transition seasons.

Of much interest in Figures 22-24 is the effect of increasing geographic dispersion on the occurrence percentage distributions of hourly capacity factors. While gradual increases in geographic dispersion reduce the occurrence percentage of maximum or near maximum capacity, a considerable benefit is realized both at the extreme lower end of the distributions and in a broad middle range of the distributions. For instance, when just the first increment of geographic dispersion is incorporated, the drop in the annual occurrence percentage of lowest production (0-5% capacity factor bin) is about 7%. As the levels of geographic dispersion increase, the occurrence percentage in this lowest bin drops to just 4% (from nearly 18%). The dramatic effect of geographic dispersion is even larger in the summer season as shown in Figure 23. In this season of weakest wind resource, the occurrence percentage of 0-5% capacity factor drops from nearly 26% for just the Minnesota Southwest site to just under 4% for the broadest geographic dispersion scenario. As may be seen in Figure 22, benefit is also realized with increasing levels of geographic dispersion spanning the approximate range from the 20-25% capacity factor bin to the 75-80% capacity factor bin. These beneficial attributes of geographic dispersion may be seen in all seasonal capacity factor distributions.

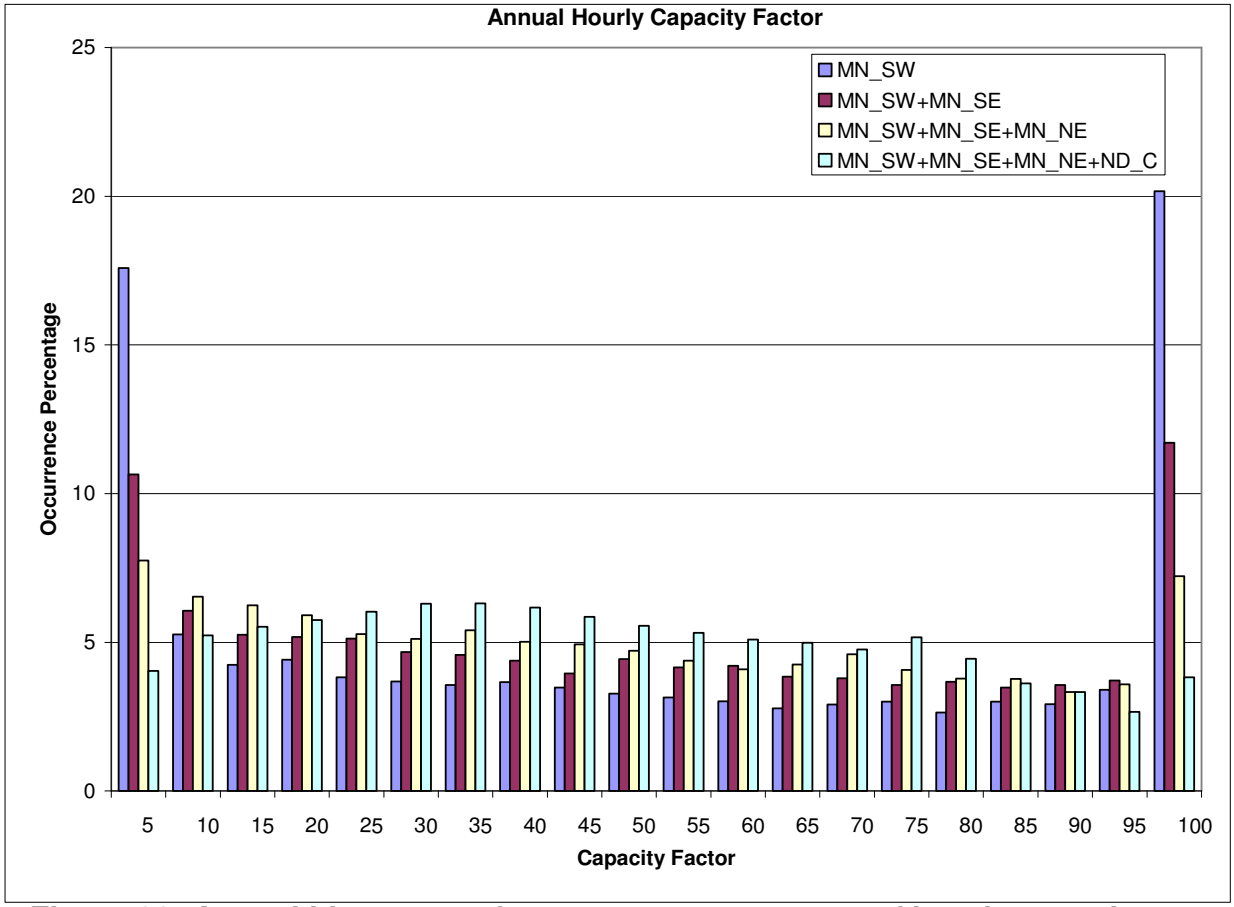

Figure 22: Annual histogram of occurrence percentage of hourly capacity factor for four levels of geographic dispersion. Data is based on hourly performance for the Vestas V82 1.65 MW turbine and reflects gross capacity factors. See legend for specific geographic dispersion scenario. Note: MN_SW = Minnesota Southwest, MN_SE = Minnesota Southeast, MN_NE = Minnesota Northeast, and ND_C = North Dakota Central.

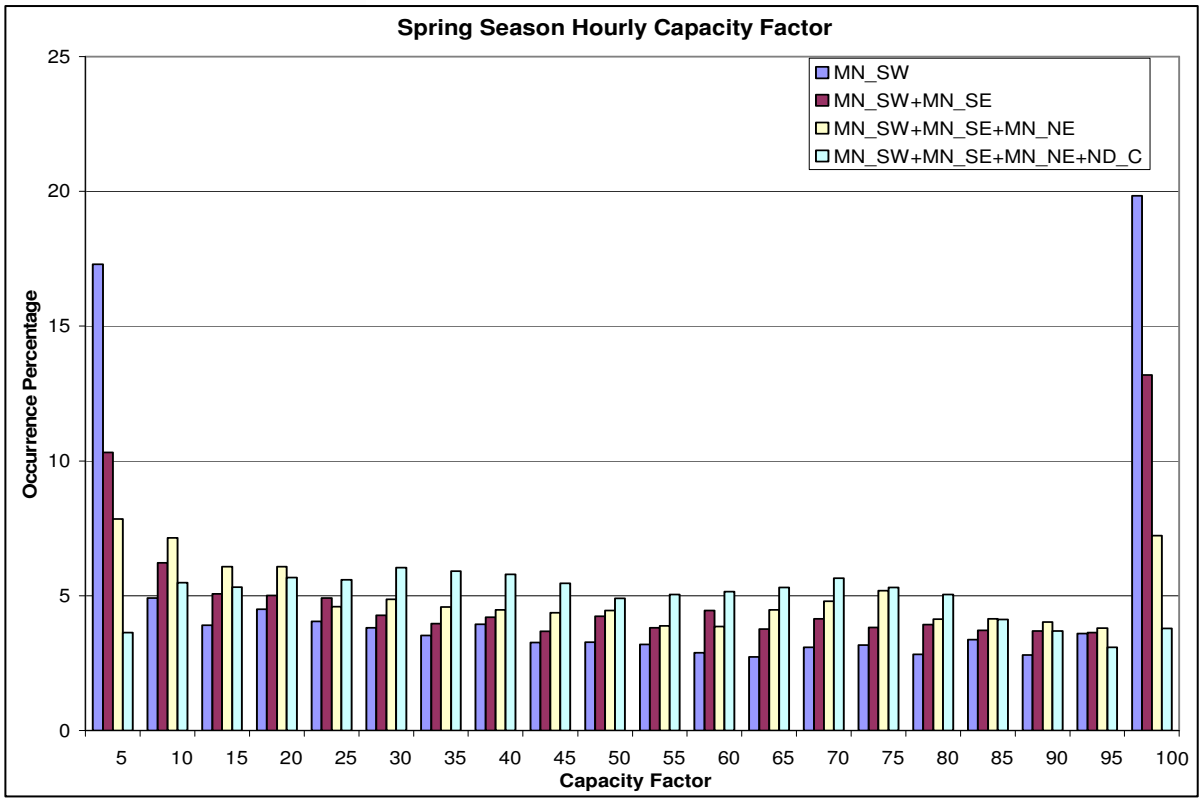

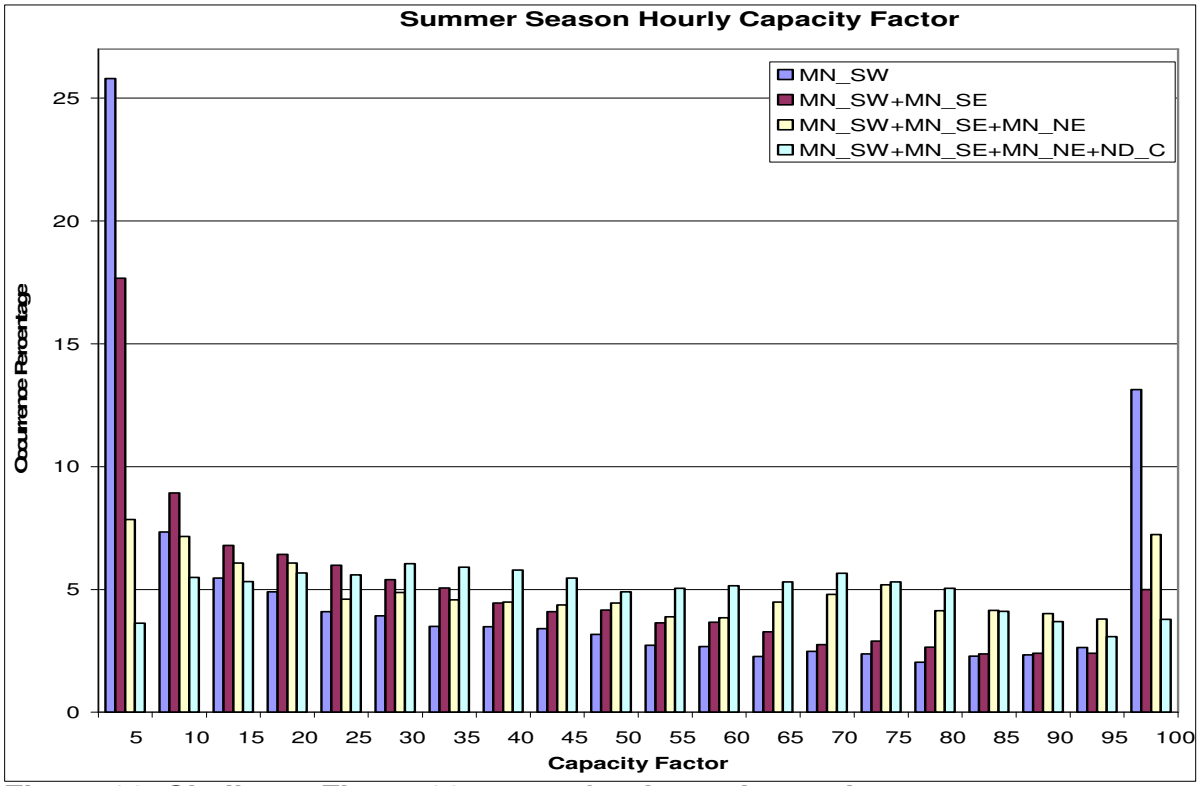

Figure 23: Similar to Figure 22 except for the spring and summer seasons.

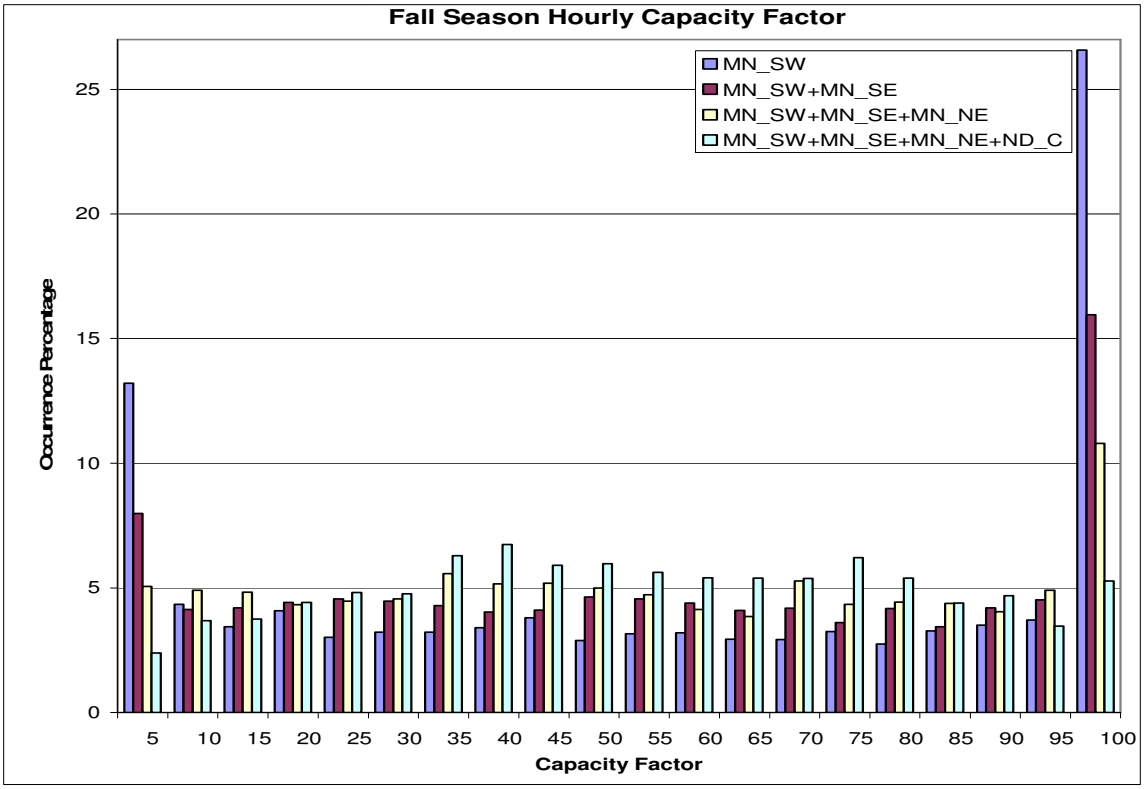

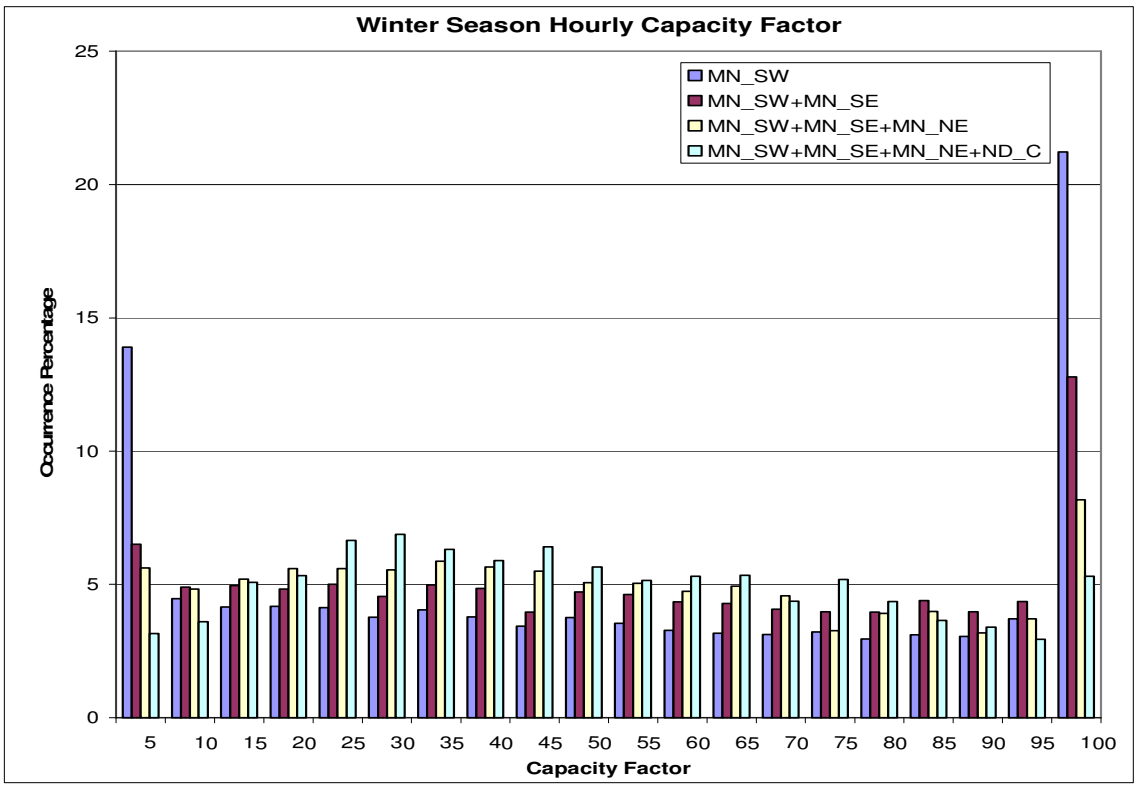

Figure 24. Similar to Figure 22 except for the fall and winter seasons.

Power Production Hourly Ramp Rate Analysis with Geographic Dispersion

Using a similar set of wind production scenarios as described in the previous section, an analysis was undertaken of the hourly power changes utilizing all hours in the three-year dataset. Figures 25-27 show frequency histograms of hourly power changes for annual and seasonal datasets. The annual and seasonal distribution profiles are similar; however, important seasonal differences exist. The most important of these differences lie in the incidence of very large hourly power changes observed on the far wings of the distributions. Examining Figures 25-27 for Minnesota Southwest reveals that summer, and to a lesser extent spring, stand out as having an enhanced risk of experiencing very large hourly power changes (i.e, those exceeding 31% of rated capacity). This may be explained by the dominant meteorological factors influencing short-term wind variability in these months. Thunderstorms and their associated outflow boundaries exert a strong influence on local wind speed variability during these seasons. In contrast, in the fall and winter seasons deep convection is a much rarer occurrence, with larger scale synoptic weather systems providing the primary atmospheric forcing for the wind resource and variability.

As may be seen in Figures 25-27, as the wind power production geographic diversity increases, a steady improvement in reducing the number of large hourly power changes is realized. In general, beyond approximately two standard deviations from the center point of the distributions (i.e., outside of the approximate 9-11% bin in hourly power change) the benefits of geographic dispersion are readily apparent. Examining the annual power change graph in Figure 11 reveals that the occurrence percentage of very large hourly power changes (≥ ±31 % of rated capacity) for Minnesota Southwest is 2.5%. With the addition of greater degrees of geographic dispersion, this percentage drops to 0.8%, 0.2% and 0.1% by cumulatively adding production from Minnesota Southeast, Minnesota Northeast, and North Dakota central, respectively. Stated another way, the incidence rate for these large hourly power changes is 25 times larger for the single site generation scenario versus the full geographically dispersed scenario. Thus, based on the incidence statistics, large hourly power changes are rare for the intra-Minnesota tri-region generation scenario and very rare for the fully dispersed generation scenario including central North Dakota generation.

The benefits of geographic dispersion in mitigating very large hourly ramp rates are most dramatic in the summer season as seen in Figure 26. As noted previously, the summer season has the greatest percentage of these large hourly power changes. The Minnesota Southwest summer frequency of very large ramp rates (≥ ±31% of rated capacity) was 4. %. With the addition of greater degrees of geographic dispersion, this percentage dramatically drops to 1.5%, 0.5% and 0.1% by cumulatively adding production from Minnesota Southeast, Minnesota Northeast and North Dakota central, respectively. Thus, even in the worst season for large hourly ramp rate changes, the implementation of various degrees of

geographic dispersion can greatly mitigate the adverse impacts caused by mesoscale meteorological phenomena.

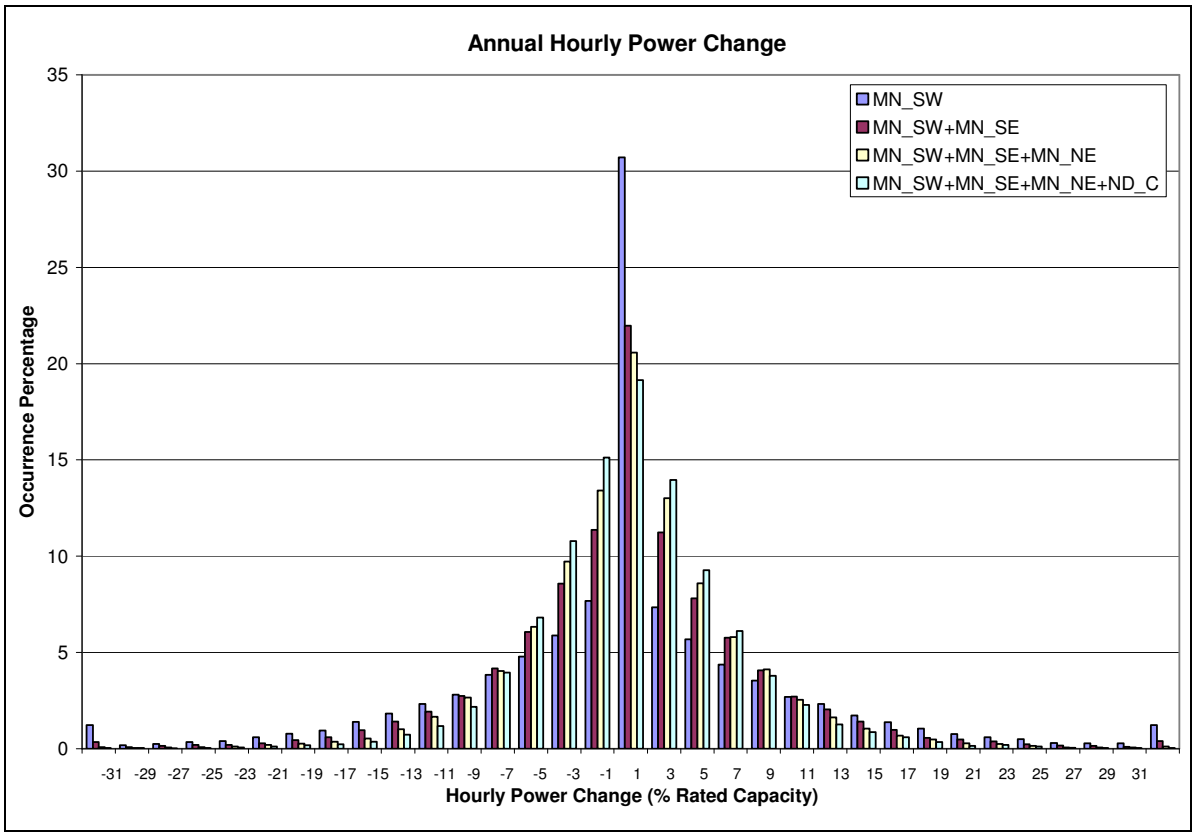

Figure 25: Annual frequency distribution of hourly power change (as a percent of rated capacity) for four levels of geographic dispersion. Data based on Vestas V82 1.65 MW turbine performance. Legend designations as in Figure 22.

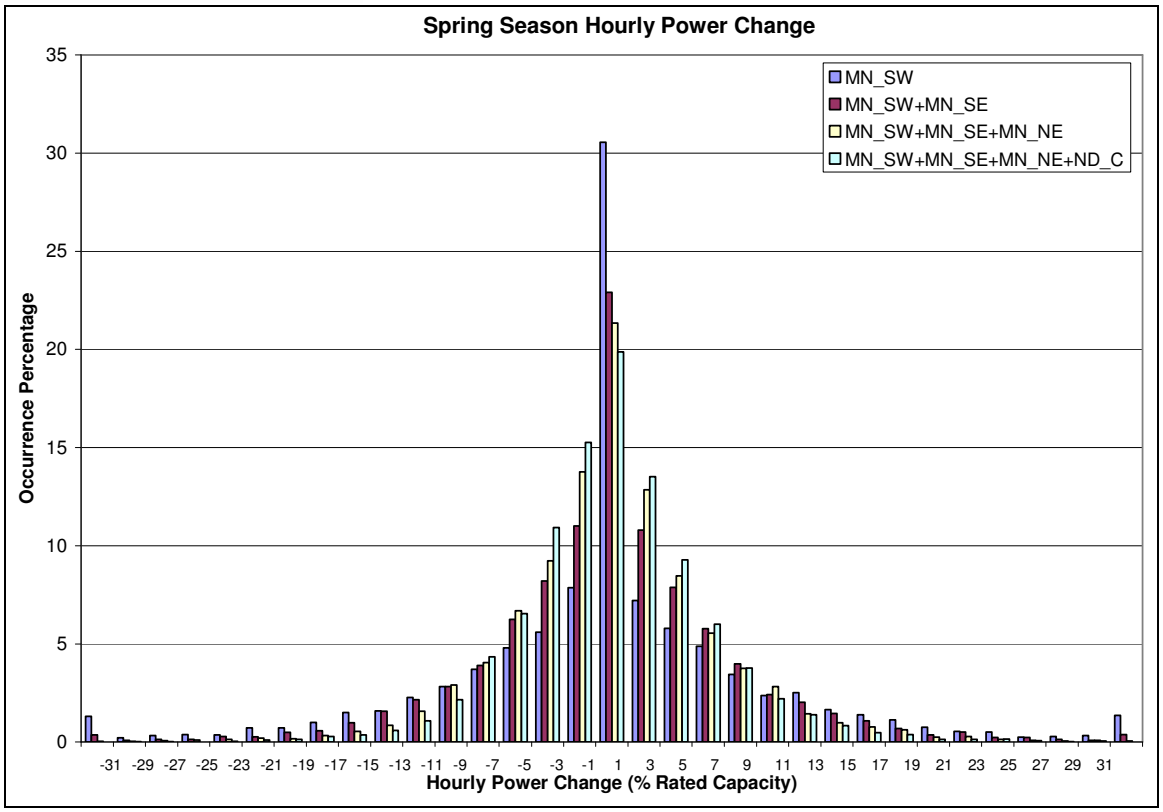

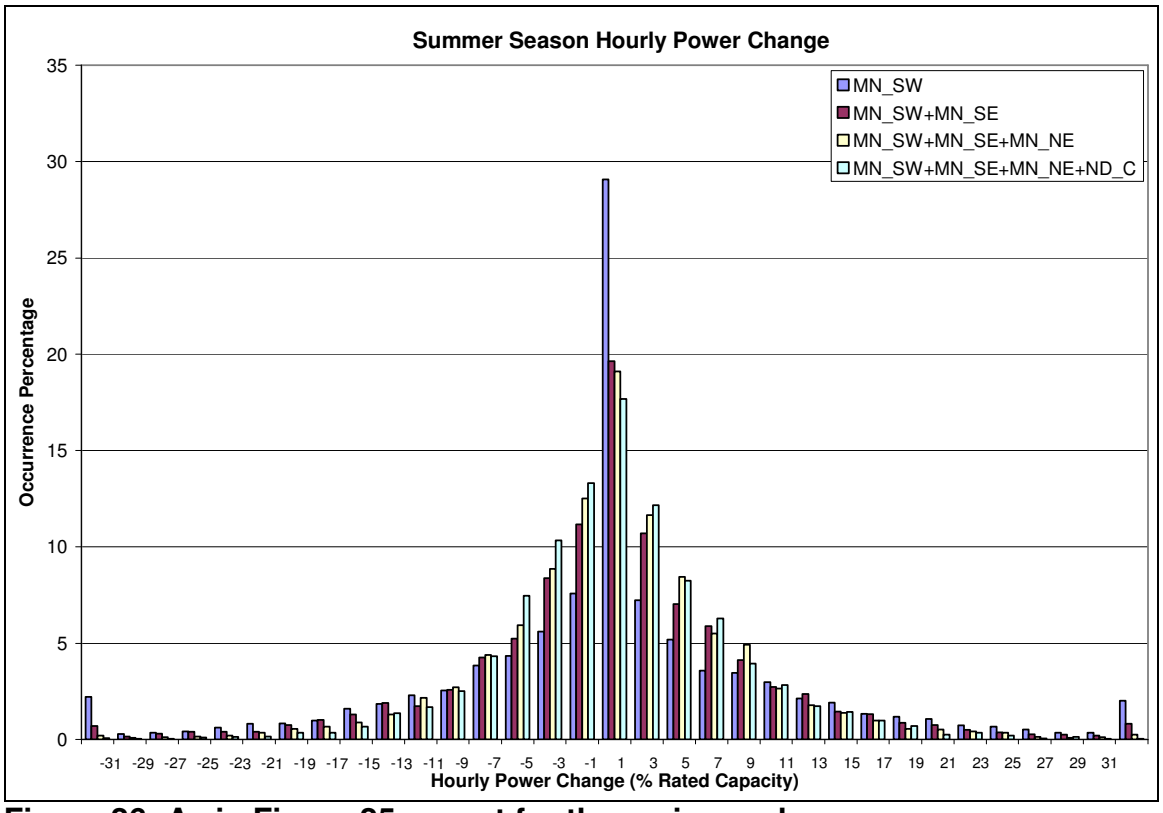

Figure 26: As in Figure 25 except for the spring and summer seasons.

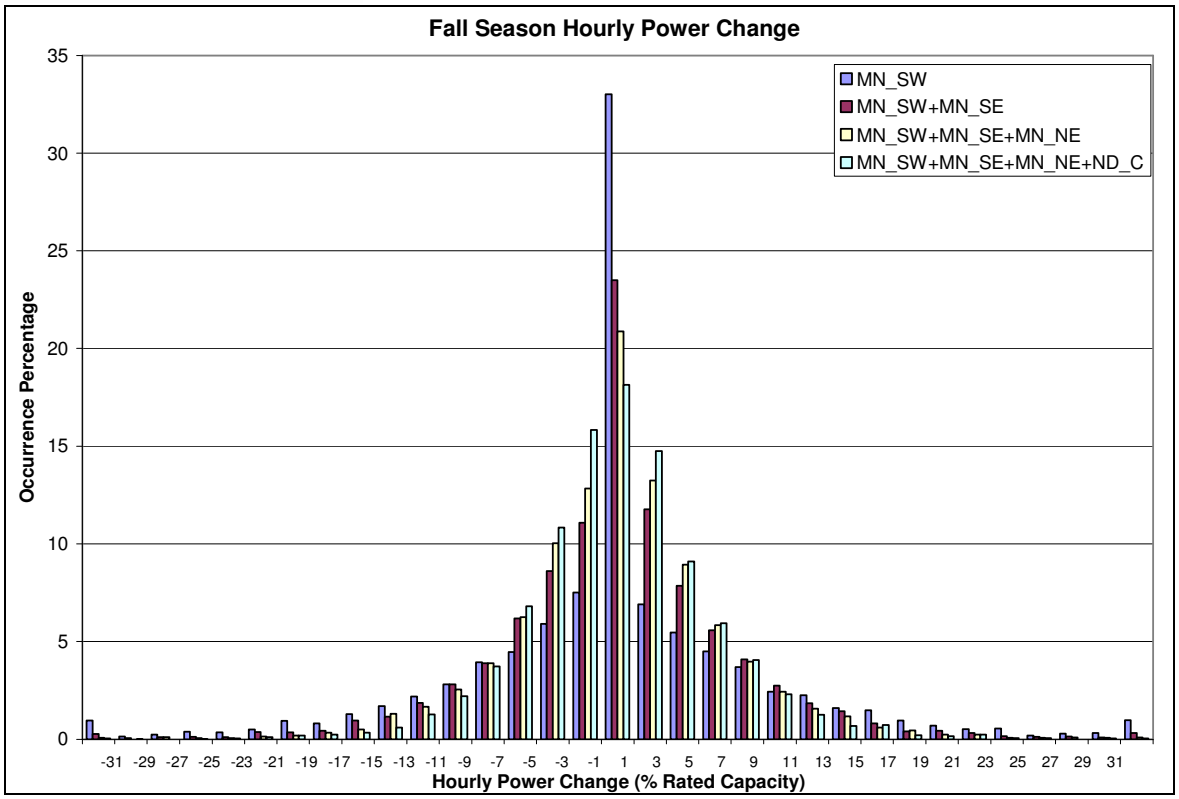

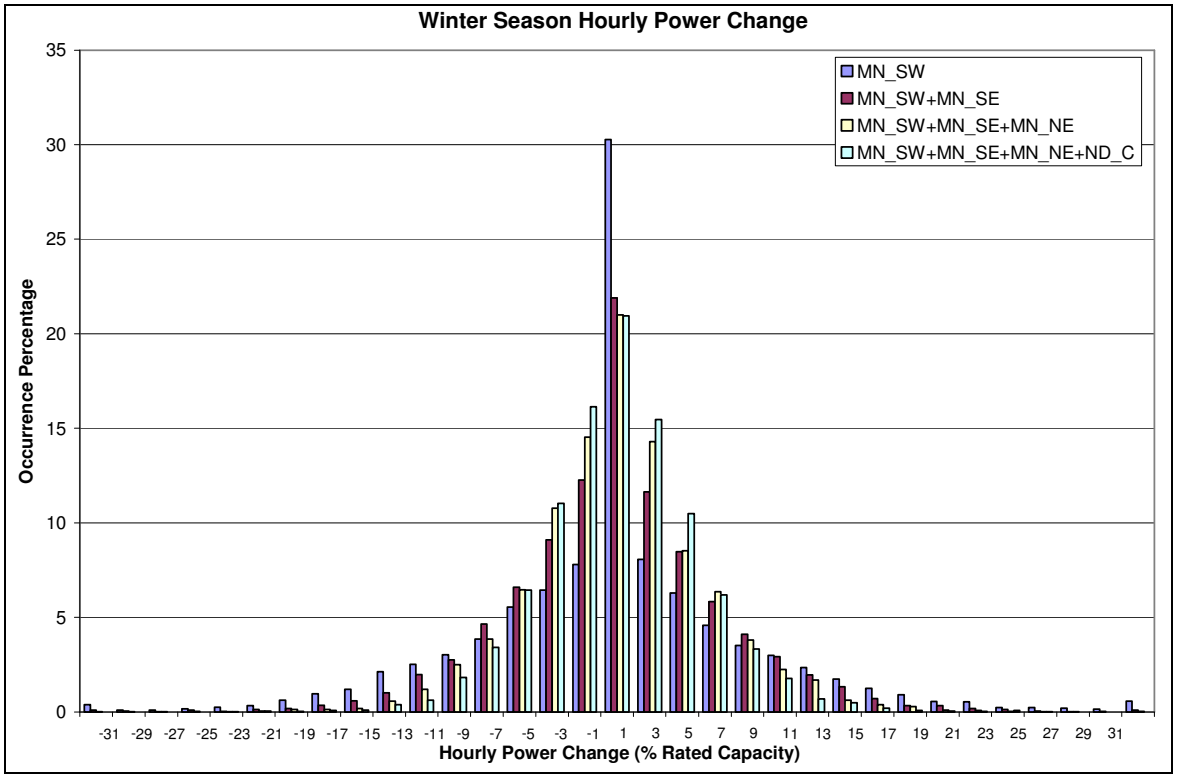

Figure 27: As in Figure 25 except for the fall and winter seasons.

Annual and Seasonal Capacity Factors for Regional Wind Generation Sites and Various Levels of Geographic Dispersion

To assess and compare the wind power production and its seasonal and spatial variability at the four regional representative sites, a capacity factor analysis for annual and seasonal time periods was undertaken. A similar analysis was also completed for the cumulative geographic dispersion scenarios. Shown in Table 2 are gross and estimated net capacity factors for the Vestas V82 1.65 MW turbine derived from the MM5 proxy tower time series at 80 m for 2003, 2004 and 2005. The net capacity factors assume a 14% reduction from gross values due to losses.

Table 2. Capacity Factors (Gross/Net) for Regional Sites* and Geographic Dispersion Scenarios (in %)

Location	Annual	Spring	Summer	Fall	Winter
MN_SW (Tow 71)	48.8/42.0	49.2/42.3	38.5/33.1	55.9/48.1	51.9/44.6
MN_SE (Tow 41)	46.3/39.8	49.0/42.1	33.5/28.8	51.1/43.9	51.6/44.4
MN_NE (Tow 82)	42.2/36.3	42.3/36.4	36.1/31.0	49.6/42.7	41.0/35.3
ND_C (Tow 115)	47.2/40.6	49.8/42.8	40.7/35.0	50.6/43.5	47.9/41.2
MN_SW + MN_SE	47.6/40.9	49.1/42.2	36.0/31.0	53.5/46.0	51.8/44.5
MN_SW + MN_SE + MN_NE	45.8/39.4	46.8/40.2	36.0/31.0	52.2/44.9	48.2/41.5
MN_SW + MN_SE MN_NE + ND_C	46.1/39.6	47.6/40.9	37.2/32.0	51.8/44.5	48.1/41.4

* See Figure 21 caption for regional site descriptors

Apparent in Table 2 is the seasonality of the wind resource in the Upper Midwest. Only at the North Dakota Central location do gross capacity factors stay above 40% in all seasons. The Minnesota Southwest site along the Buffalo Ridge realizes the next highest summer gross capacity factor (38.5%). In general, an excellent wind resource exists at North Dakota Central, Minnesota Southwest and Minnesota Southeast. Of these three, the wind resource is broadly comparable with the notable exception of the Minnesota Southeast site in the summer season, where the winds fall off to a much greater extent. In fact, even the generally slower Minnesota Northeast site realizes a better wind resource in the summer season than Minnesota Southeast. The annual and seasonal capacity factors for the various geographic dispersion scenarios reflect the generally favorable wind resource of their component sites. While adding Minnesota Northeast to the other Minnesota sites usually reduces the collective capacity factor (except in the summer season when compared to Minnesota Southwest + Minnesota Southeast), the advantages of adding this geographically dispersed region to create a Minnesota tri-regional generation scenario as discussed in sections 1D.3 and 1D.4 argue strongly for its value in establishing an optimal geographically dispersed resource.

Power Generation Correlation Analysis For Regional Wind Generation Sites

To understand the time dependent relationship of the wind resource between the four regions used in the geographic dispersion analysis, a correlation analysis was completed by using Tower 71 (representing Minnesota Southwest) as the control point, and finding the correlation of wind power production at the three other representative sites (Towers 41 – Minnesota Southeast, 82 – Minnesota Northeast, and 115 – North Dakota Central) with Tower 71. This analysis was performed using hourly capacity factor data and using 24-hour capacity factor running means. One would expect *a priori* that on the time scale of seconds to tens of seconds (unresolvable with the model configuration employed), that the regional sites would be relatively uncorrelated. As the representative sampling time period increases and the distance between sites decreases, one would expect increasing correlations. As shown in Table 3, this expectation is realized. All site combinations show a correlation increase for the longer time period sample of 24 hours, since on this time scale the influence of synoptic systems on the entire region is dominant. Mesoscale meteorological influences (like thunderstorm outflows or frontal passages) would tend to lower the correlation based only on hourly data. In general, as the tower pairings get farther apart, the correlation decreases with the caveat that the distance between Towers 71 and 82 and the distance between Towers 71 and 115 are nearly identical (466 km).

Table 3. Correlation Coefficient (r) For Power Generation Between Geographically Dispersed Regional Sites

Regional Site Combination	Correlation – Hourly	Correlation – 24 Hour
Towers 71 and 41	0.57	0.72
Towers 71 and 82	0.44	0.61
Towers 71 and 115	0.38	0.52

An analysis of covariance between the site pairs using both the hourly and 24 hr power generation data revealed the highest values for the closest site pairing (Towers 71 and 41, 289 km) with decreasing covariance values for tower pairing 71 and 82 and the lowest values for tower pairing 71 and 115.

Upper Midwest Wind Patterns and Variability

Controlling Meteorology for the Upper Midwest

The climatology of wind in the Upper Midwest exhibits significant seasonal variability. The essential meteorology driving the wind resource is largely controlled by the position and strength of the upper-level jet stream and disturbances (jet streaks) within the jet stream. As shown in Figure 28, the jet stream position in the winter season is both farther south and stronger than in the summer. In the transition seasons of spring and fall, the mean jet stream position generally lies between these locations. The main factor controlling both the jet stream position and speed is the magnitude and location of the tropospheric meridional (north-south) temperature gradient. A larger (smaller) temperature gradient exists in the winter (summer) and corresponds to a stronger (weaker) jet stream. Note that although Figure 28 indicates a mean ridge axis over western North American and trough axis over eastern North American, at any particular time (e.g., day, week, or even several week period), the jet stream orientation and strength could be very different from that indicated in Figure 28.

The jet stream position can be thought of as the “storm track”. In this context, “storm track” means the track of mid-latitude cyclones and anticyclones (i.e., low and high pressure systems of one to several thousand kilometer horizontal dimension) seen on a meteorological surface pressure and geopotential height analysis maps. Weather phenomena of this size are called *synoptic*-scale systems. In general, the stronger the jet stream and jet streaks, the more intense the lower-tropospheric pressure systems due to the dynamic link between the upper and lower troposphere. The key factor driving the wind resource in the lowest 100 m of the atmosphere is the horizontal pressure gradient. Large pressure gradients are associated with the transient cyclones and anticyclones, thus, if a region is co-located near the storm track, that region will generally realize higher mean wind speeds than a region farther away from the storm track. Figure 29 provides a schematic of typical cyclone tracks that influence the Upper Midwest. The northwest-southeast track represents the most frequent storm track in all seasons. The southwest- northeast track, although less common and usually relegated to transition and winter seasons, can correspond to large and intense cyclones.

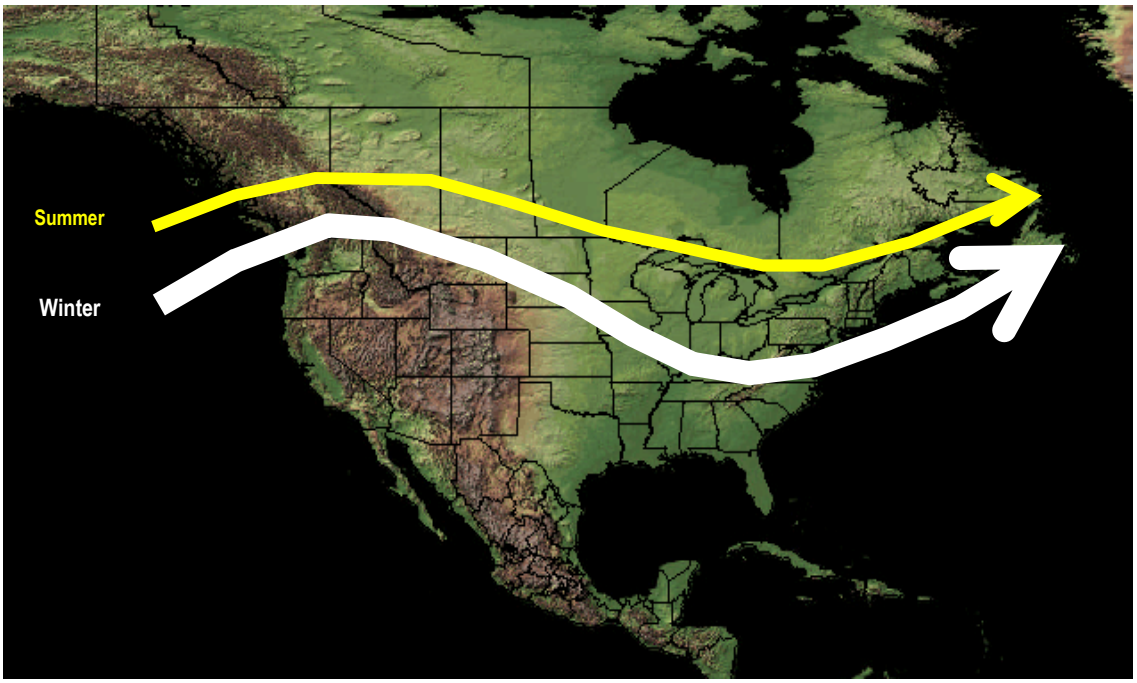

Figure 28: Approximate mean winter and summer positions of the upper-tropospheric jet stream. Line width is indicative of jet stream wind speed.

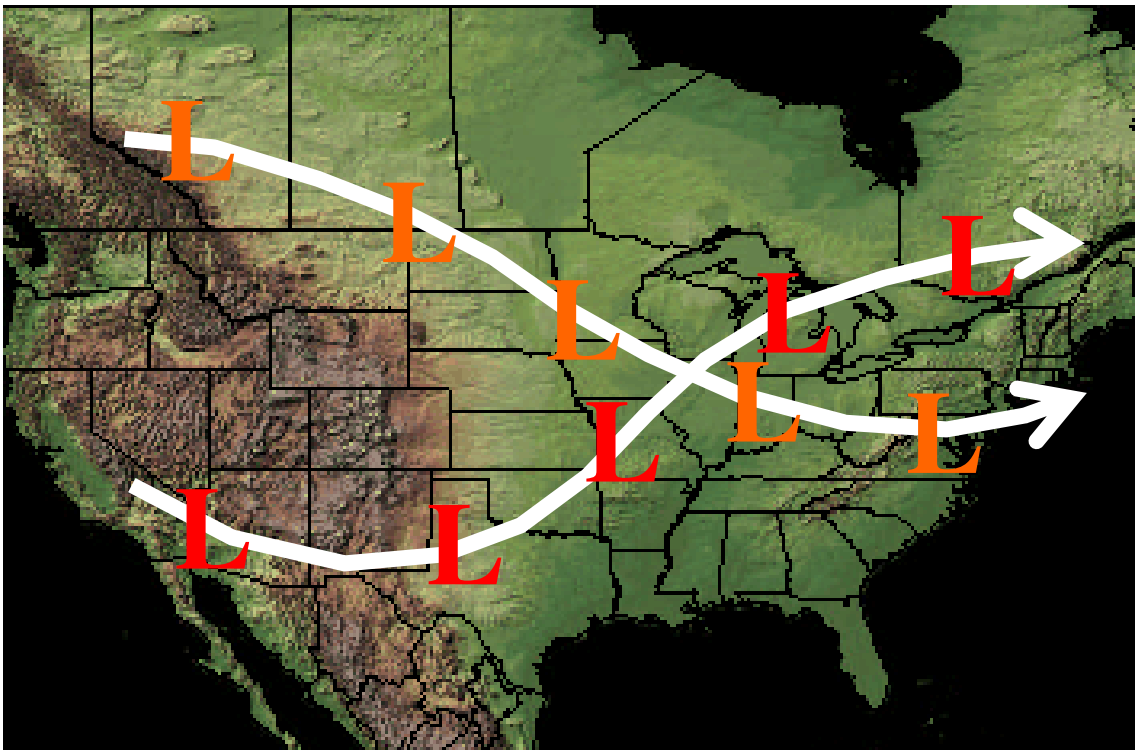

Figure 29: Typical "storm tracks" that influence the wind resource of the Upper Midwest. The bold L's represent surface cyclone positions as they move along the track.

Another important aspect of the wind resource over the western portion of the project domain involves the summer season nocturnal low-level jet climatology (Bonner 1968). Affecting the eastern Dakotas and southwest and west central Minnesota, the low-level jet is responsible for a considerable enhancement of the wind resource at a time when locations farther east see a large drop in wind speeds. This may readily be seen in Table 2 by comparing Minnesota Southwest or North Dakota Central with Minnesota Southeast. The pressure system distribution responsible for the southerly winds and associated low-level jet is depicted in Figure 30. Over the eastern and particularly southeastern United States, the summer pattern is dominated by a pressure system called the Bermuda High. At the same time, an area of predominantly low pressure, called a thermal low, sets up over the southwestern and intermountain western United States. The juxtaposition of high pressure to the east and low pressure to the west establishes generally southerly flow in the transitional zone between these two features. As a result, a corridor of reasonably energetic southerly summertime winds exits from west Texas to the Dakotas. The low-level jet is most manifest at night when low-momentum near-surface air no longer mixes vertically due to the development of the shallow nocturnal inversion. While the lowest levels may experience their weakest wind speeds of the day during nocturnal hours, layers just above the surface layer (> ~50 m) will often realize their highest diurnal wind speeds.

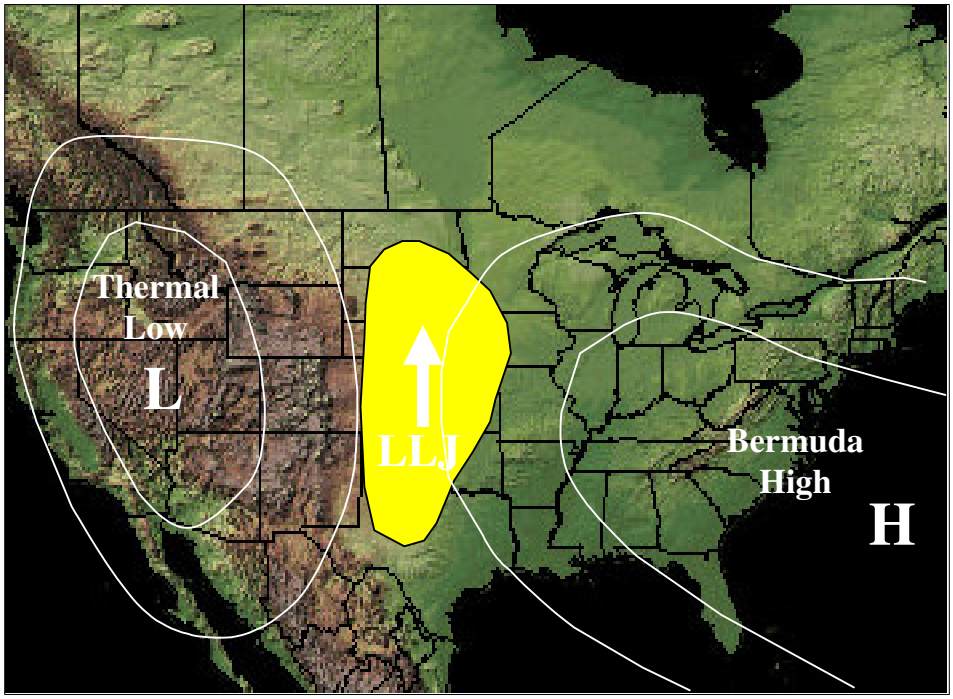

Figure 30. Schematic of the summer season pressure system distribution leading to the development of the low-level jet climatology over the Great Plains of the United States. In summary, the seasonal wind resource is largely controlled by the jet stream position and frequency of associated cyclone and anticyclone passages over the region. The best wind resource for the Upper Midwest is expected with the stronger low-level pressure gradients of the winter and transition seasons while the weaker pressure systems of summer yield a reduced wind resource. The presence of the climatologic low-level jet over the western portion of the project domain mitigates to some degree the weakness of the summer season wind climatology.

Wind speed variability on time scales ranging from days to seconds is directly associated with the intrinsic time scale of the meteorological features influencing a particular location. For instance, on the time scale of one day to several days, the passage of discrete synoptic systems controls the overall wind resource. On time scales of a day to several hours, fronts attendant to the transient cyclones have a large influence on wind variability. On the shorter time scale of several hours to tens of minutes, wind variability is frequently influenced by thunderstorm outflow boundaries during the convective season (late spring through early fall). These outflow boundaries can range in size from only a few kilometers to hundreds of kilometers in horizontal extent. Outflow strength and size are usually dependent on the degree of organization of the convective system and the thermodynamic environment that the thunderstorms develop in. The very small time scale wind speed variability (10's of seconds to one second) is controlled by boundary layer turbulence. The climatology of wind speed also has a prominent diurnal variability that is tied to the daily insolation cycle. On this diurnal time

scale, low-level wind speed variability is highly influenced by the vertical transport of momentum that is dictated by thermal stability and boundary layer evolution.

In addition to the mesoscale meteorological phenomena noted above, there are region-specific mesoscale influences on the wind resource and its variability that are tied to topographic characteristics. For example, the Buffalo Ridge which extends from southwest Minnesota through northeast South Dakota appears to excite buoyancy waves (gravity waves) under stable thermodynamic conditions when the ridge-relative flow has a large orthogonal component to the ridge axis. Model evidence indicates this flow regime extends the excellent wind resource northeast of the top of the ridge. As another example, Lake Superior exerts a marked effect on the climate of northeast Minnesota by the inland penetration of air possessing characteristics of Superior's marine boundary layer.

Mapping of Mean Quantities

WindLogics conducted a quantitative wind resource analysis characterizing annual and mean monthly patterns using atmospheric data at 80 m from the three years of modeling. These mean quantities were normalized to represent the long-term wind resource. Further, diurnal wind patterns are presented below for several geographic locations within Minnesota and North Dakota. Proxy tower locations 41, 71, 82, and 115 were chosen for diurnal wind analysis. Each parameter map series is followed by a summary analysis.

Normalization of Model Wind Data with Long-Term Reanalysis Database

To more accurately characterize the historic wind resource over the project domain, the MM5 wind speed data was normalized with the WindLogics archive of the National Center for Atmospheric Research/NCEP Reanalysis Database (RNL). This RNL database represents 40 years of atmospheric data that has been processed through a modeling assimilation cycle to ensure dynamic consistency. This RNL database is the best objective long-term atmospheric dataset available and was created for purposes such as climate research investigations. By comparing applicable RNL grid points for a given month and year to the long-term average at those points, ratios are created that are applied to the MM5 wind data. This process normalizes the model data to better represent the historic character of the wind resource.

Mean Annual and Monthly Wind Speed – Normalized to 40-Year Climatic Mean

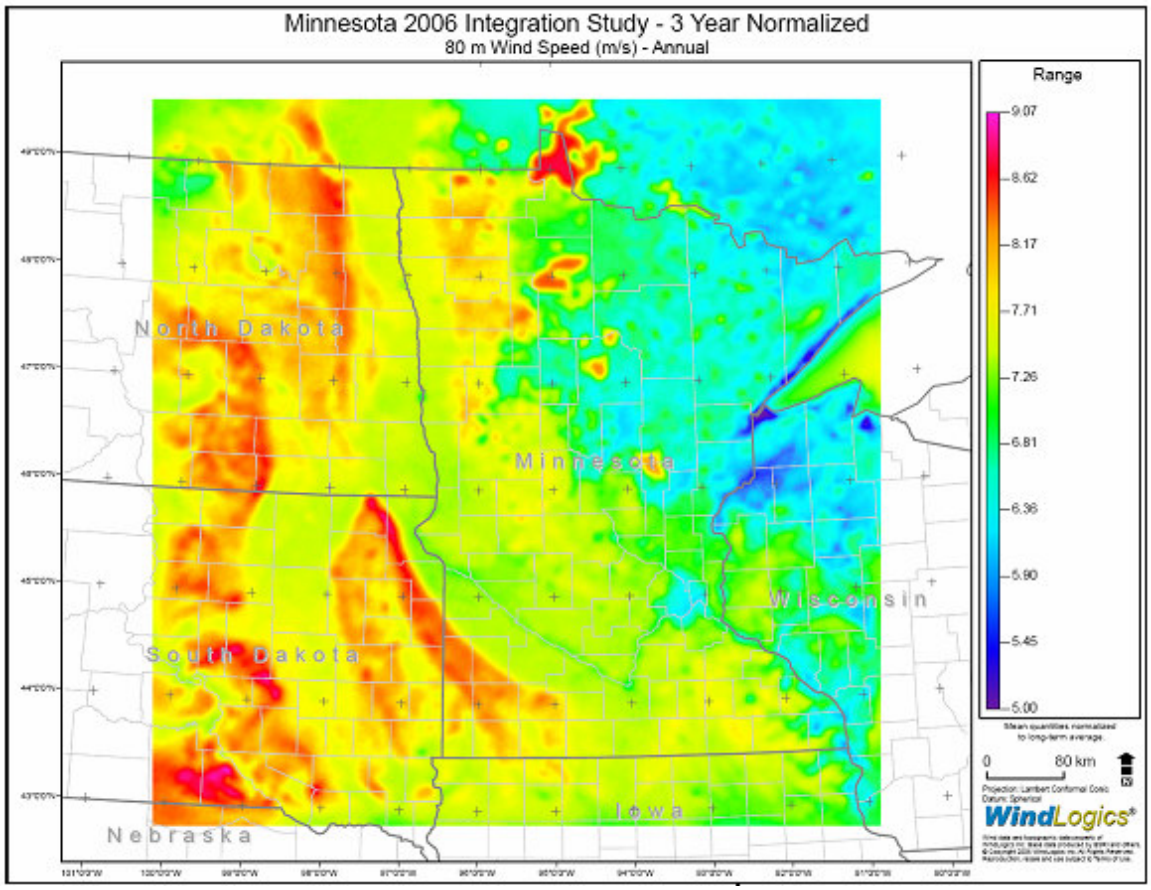

Figure 31: Mean annual 80 m wind speed in m/s.

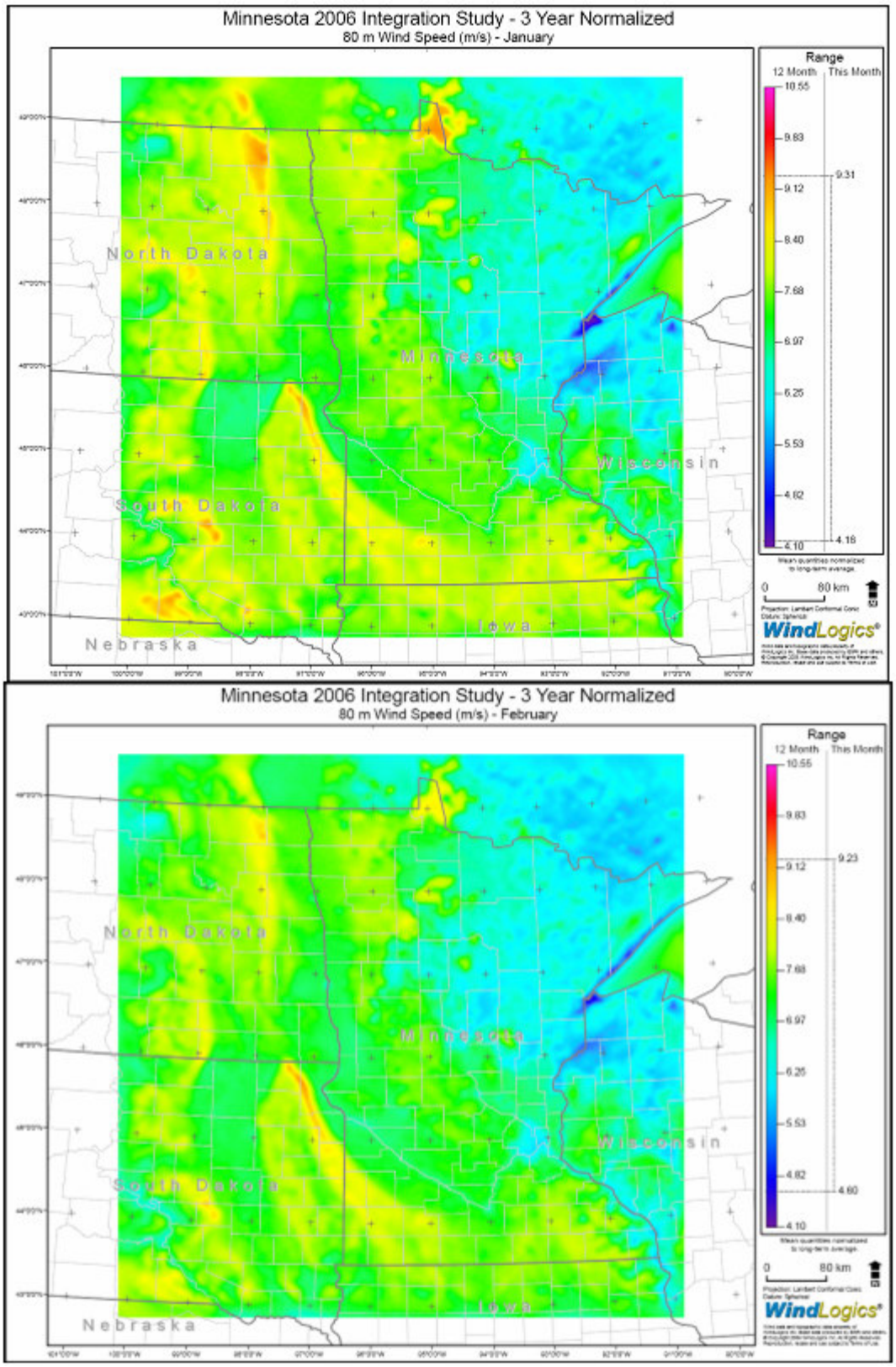

Figure 32: Mean January and February 80 m wind speed in m/s.

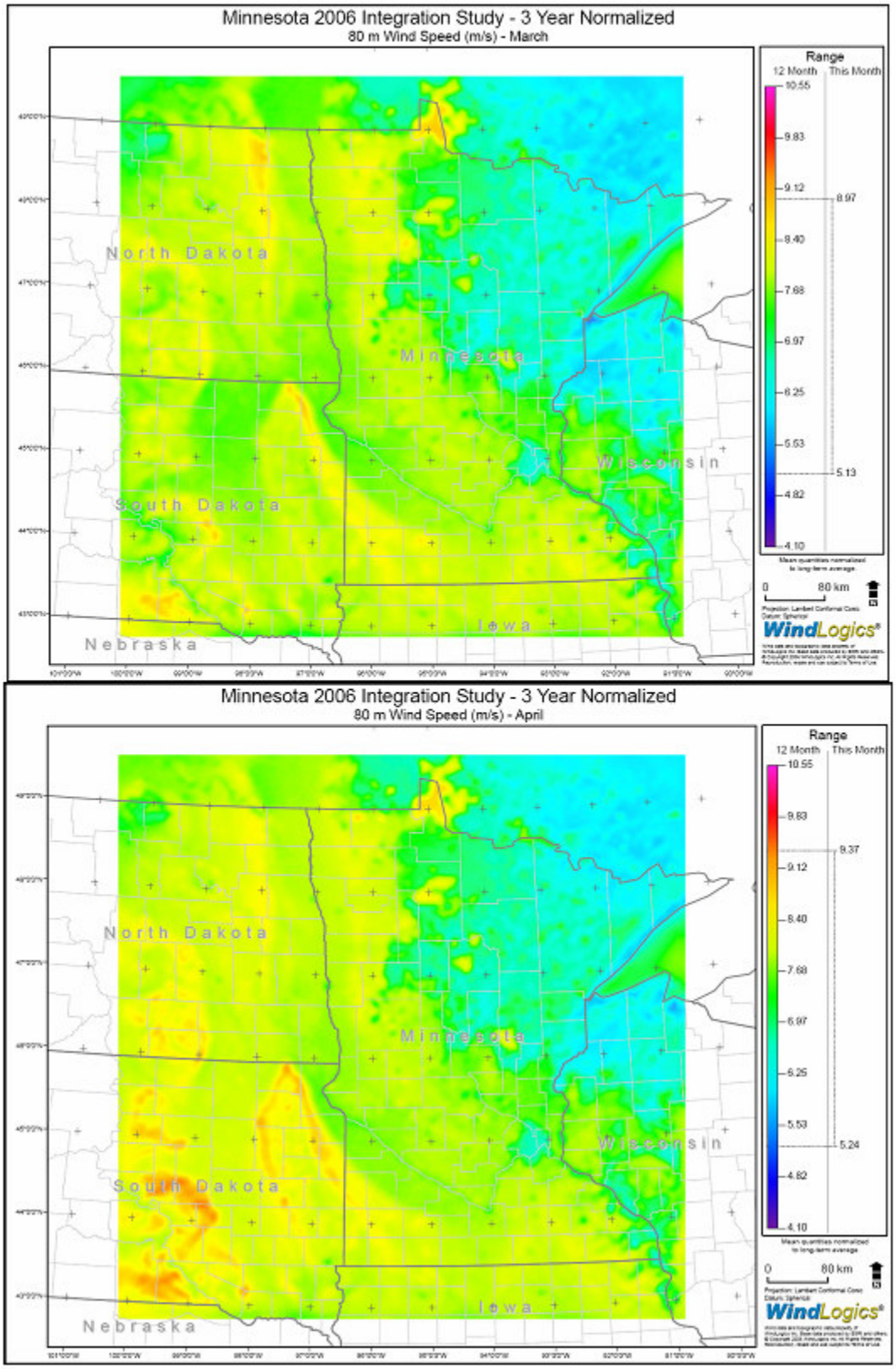

Figure 33: Mean March and April 80 m wind speed in m/s.

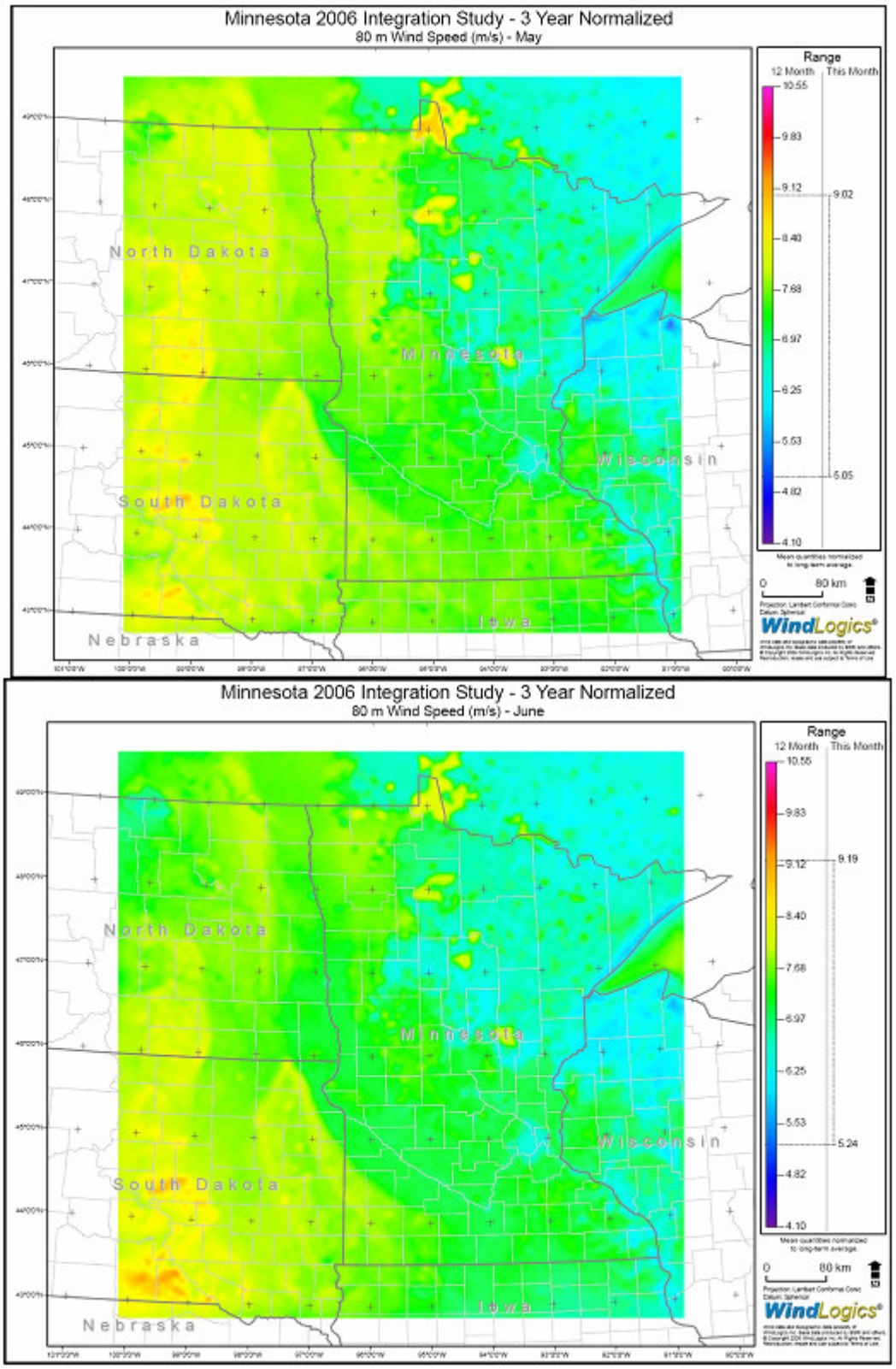

Figure 34: Mean May and June 80 m wind speed in m/s.

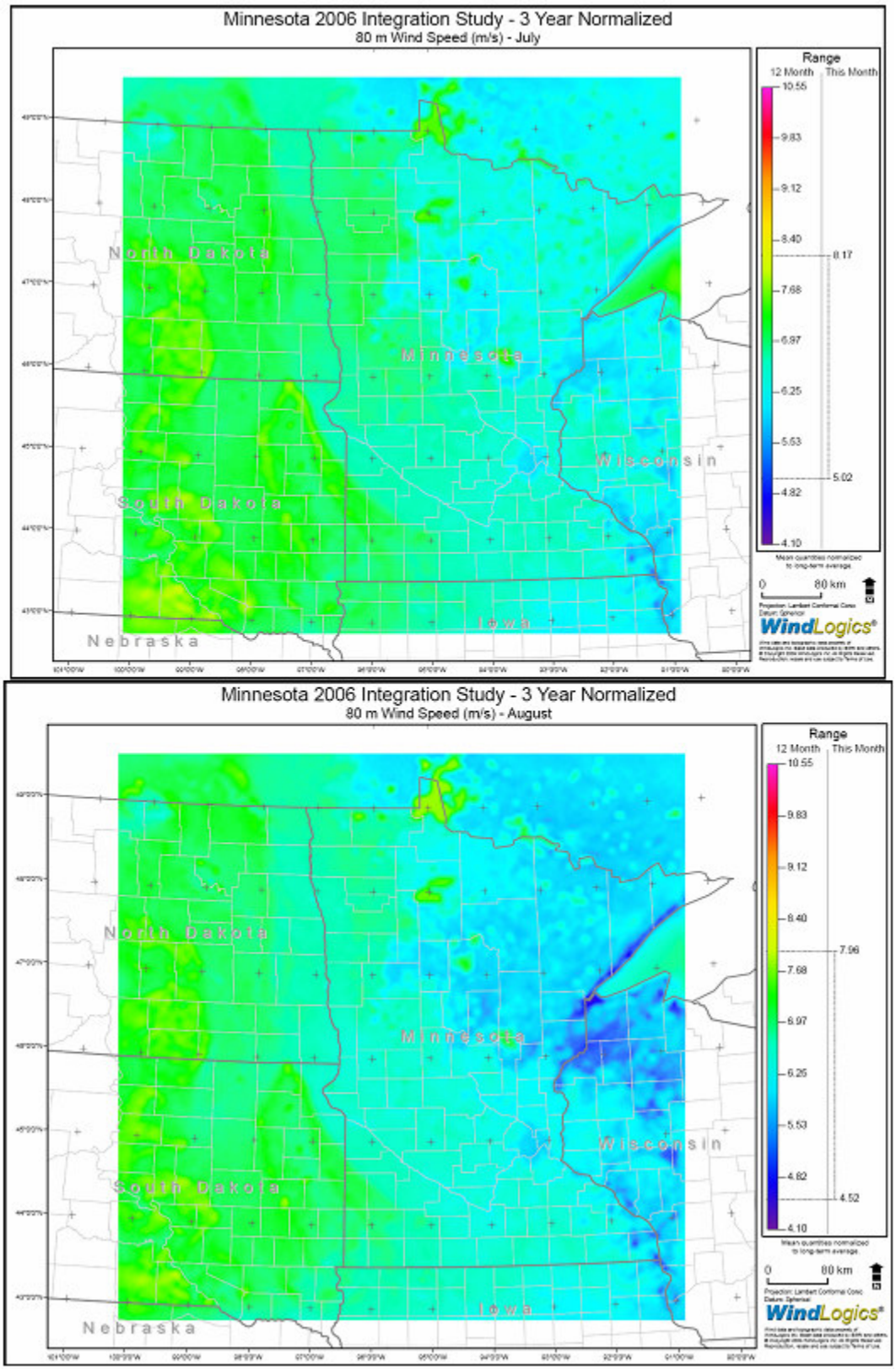

Figure 35: Mean July and August 80 m wind speed in m/s.

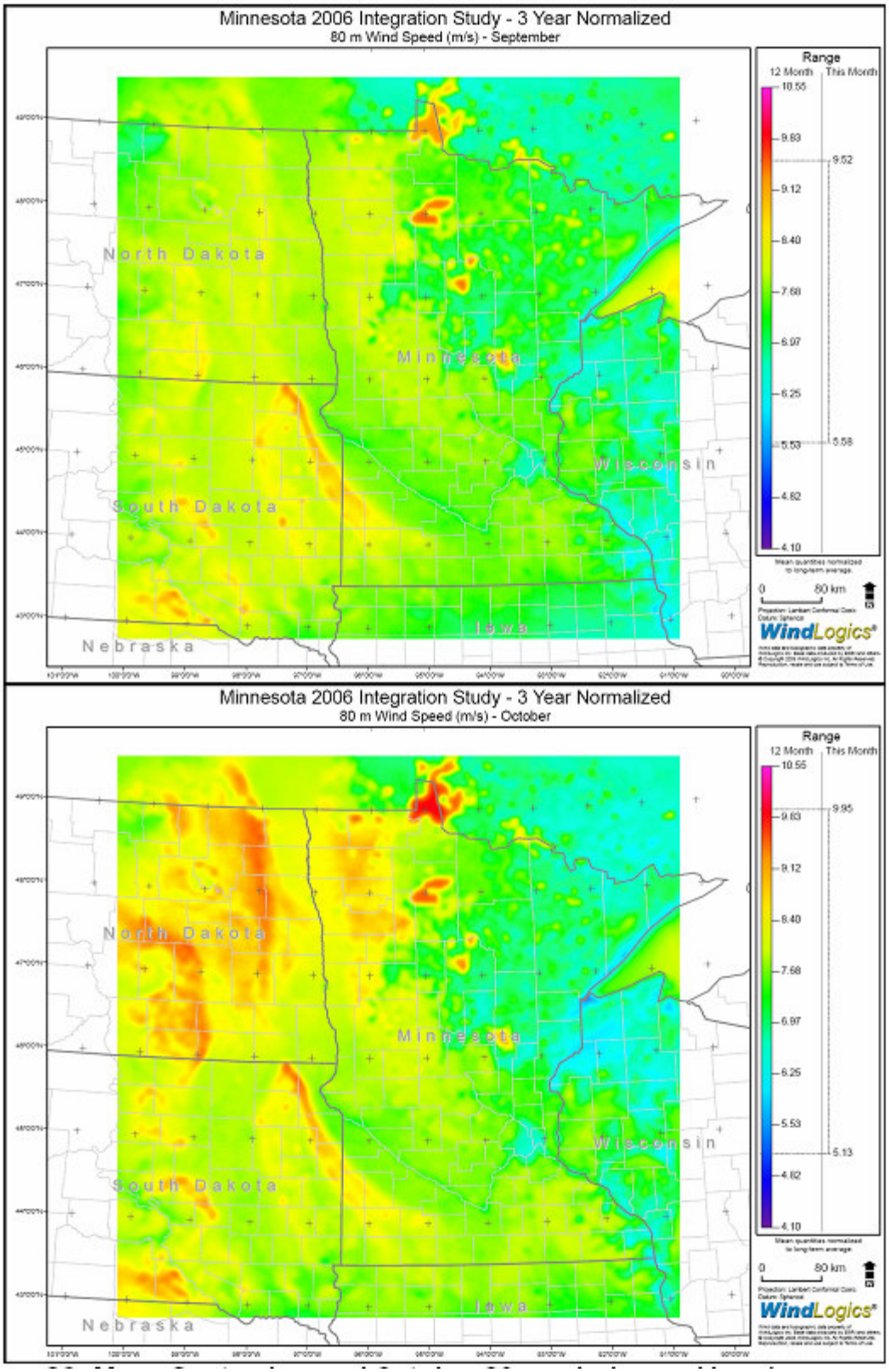

Figure 36: Mean September and October 80 m wind speed in m/s.

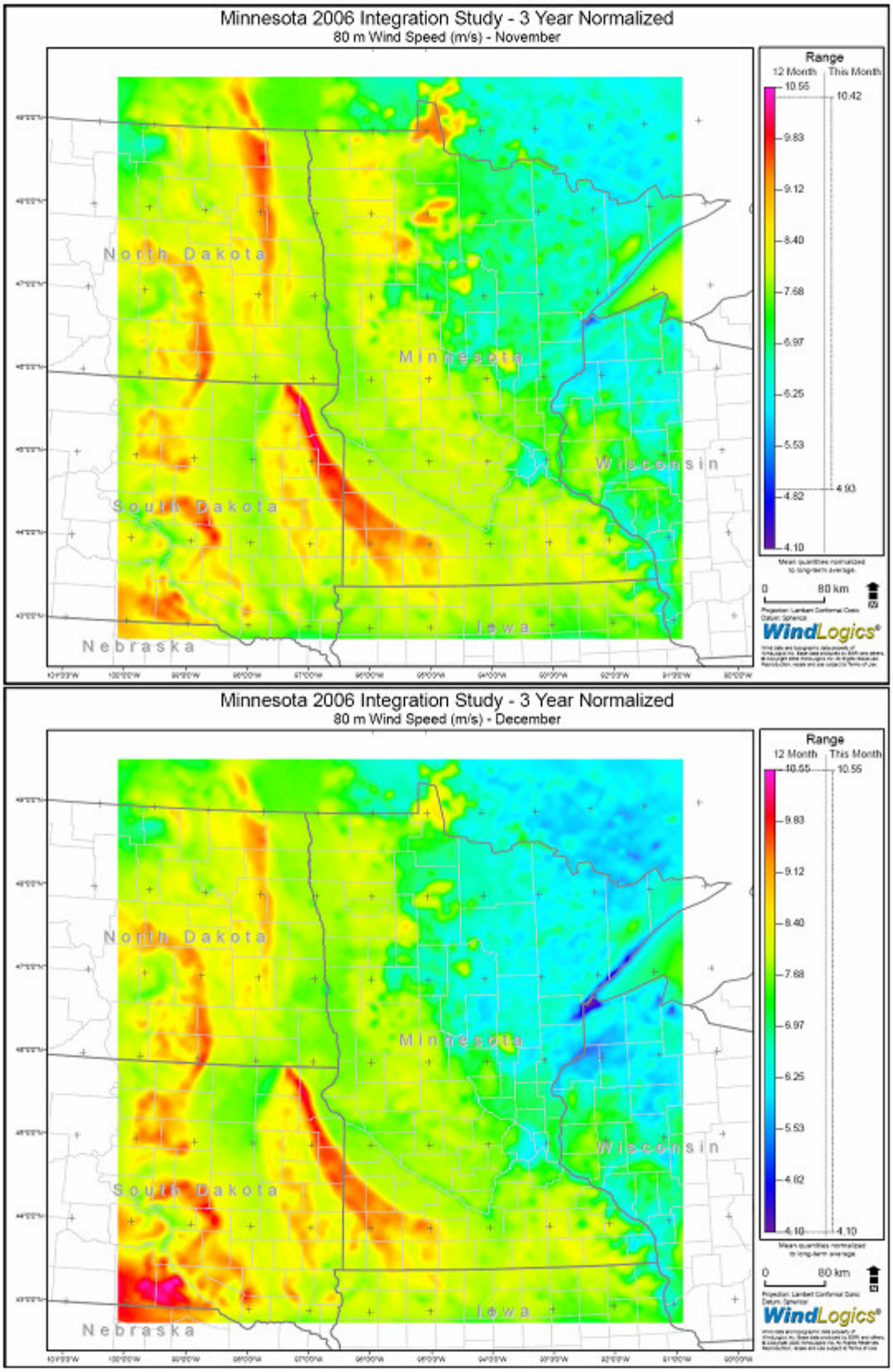

Figure 37: Mean November and December 80 m wind speed in m/s.

Summary of 3-year averages of annual and monthly wind speed.

The 3-year annual and monthly normalized wind speed averages portray marked geographic and seasonal signals. As shown in Figures 31 through 37, the considerable wind resource of the topographic ridges of the eastern Dakotas and Buffalo Ridge are conspicuous features of the wind speed mapping on an annual and monthly basis. The agricultural and prairie region of northwest Minnesota, and to a lesser extent Mower County in southeast Minnesota, are notable secondary resource areas. Not surprisingly, due to their low surface friction, the big lakes of central and northern Minnesota stand out as having an excellent wind resource, especially Lake of the Woods along the Minnesota-Canada border. The seasonality of the wind resource of the Upper Midwest is a prominent feature of the map series. The best wind resource exists in the climatologic winter and transition seasons with a wind resource minimum in July and August. This meteorological characteristic of more vigorous flow in the winter and transition seasons is fundamentally related to the jet stream position and corresponding synoptic weather system pattern as described in section 1E.1. The weaker pressure gradient in the summer months is responsible for the slower mean wind speeds. Notable in the summer month wind speed analysis are the considerably greater relative wind speeds maintained on the eastern Dakotas' topographic ridges and the Buffalo Ridge. The presence of the climatologic low-level jet discussed in section 1E.1 is largely responsible for the enhanced summer wind resource in these regions.

Another aspect of the wind resource mapping that affirmed the beneficial aspects of running more than a single year for this wind integration study involved the sometimes considerable year-to-year variation in monthly wind speed and year-to-year variation in annual wind speed. As a case in point, the 80 m November non-normalized wind speeds for the years 2004 and 2005 are substantially different as shown in Figure 38. A study utilizing single year data would be relegated to using the only month available; however, the three years of data in this investigation allows for more realistic year-to-year variations in the representative monthly winds. Similarly, annual wind speeds for certain regions show distinct yearly variability. As may be seen in Figure 39, mean annual wind speed differences from 2004 and 2005 are readily apparent near the regions of maximum wind speed in the Dakotas and Buffalo Ridge, as well as in northwest Minnesota and over Lake of the Woods. While budgetary limitations restrict the number of modeling years in some wind integration studies, the benefits of modeling three years are significant.

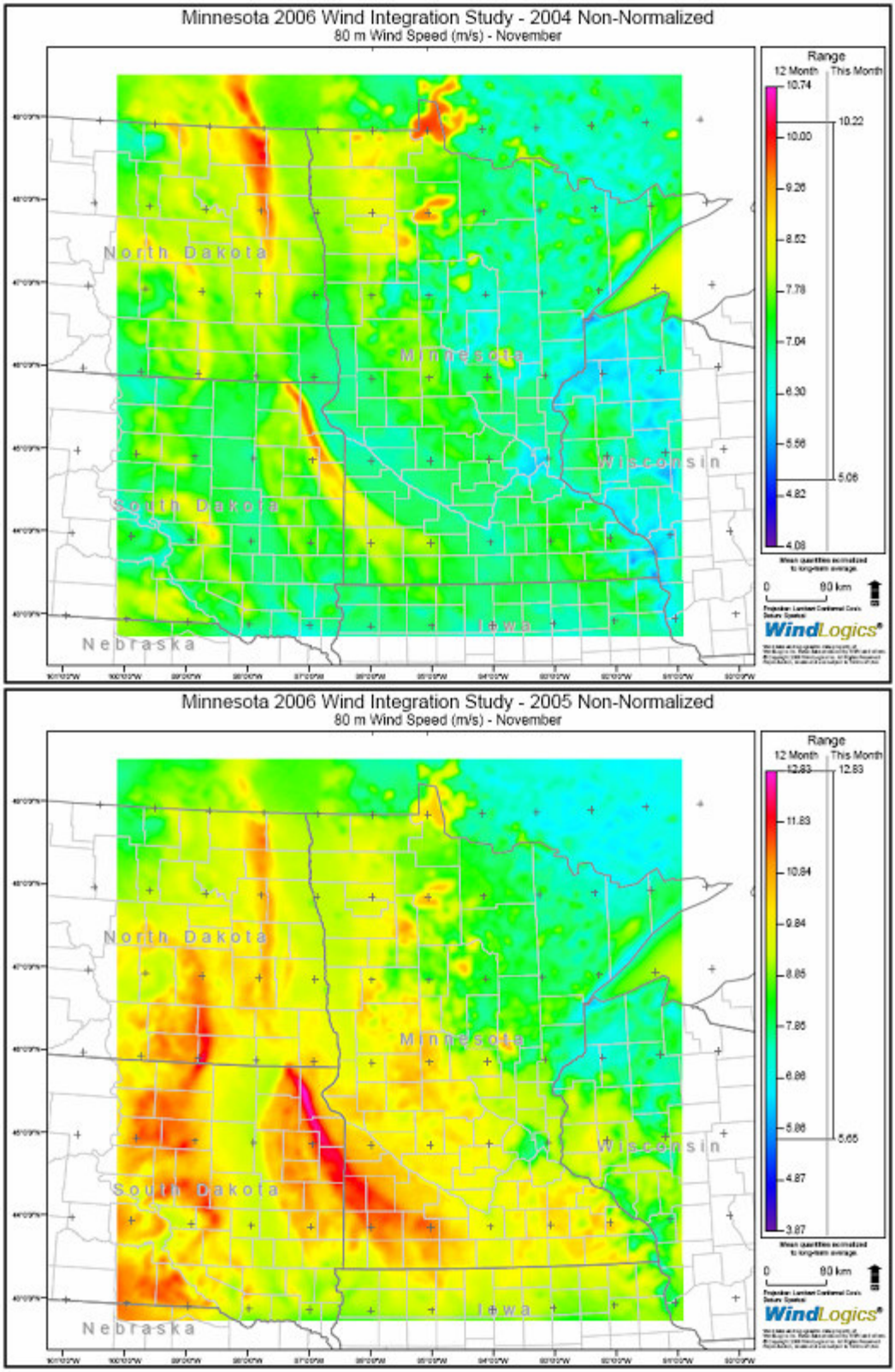

Figure 38: Mean November non-normalized 80 m wind speed for 2004 and 2005 in m/s.

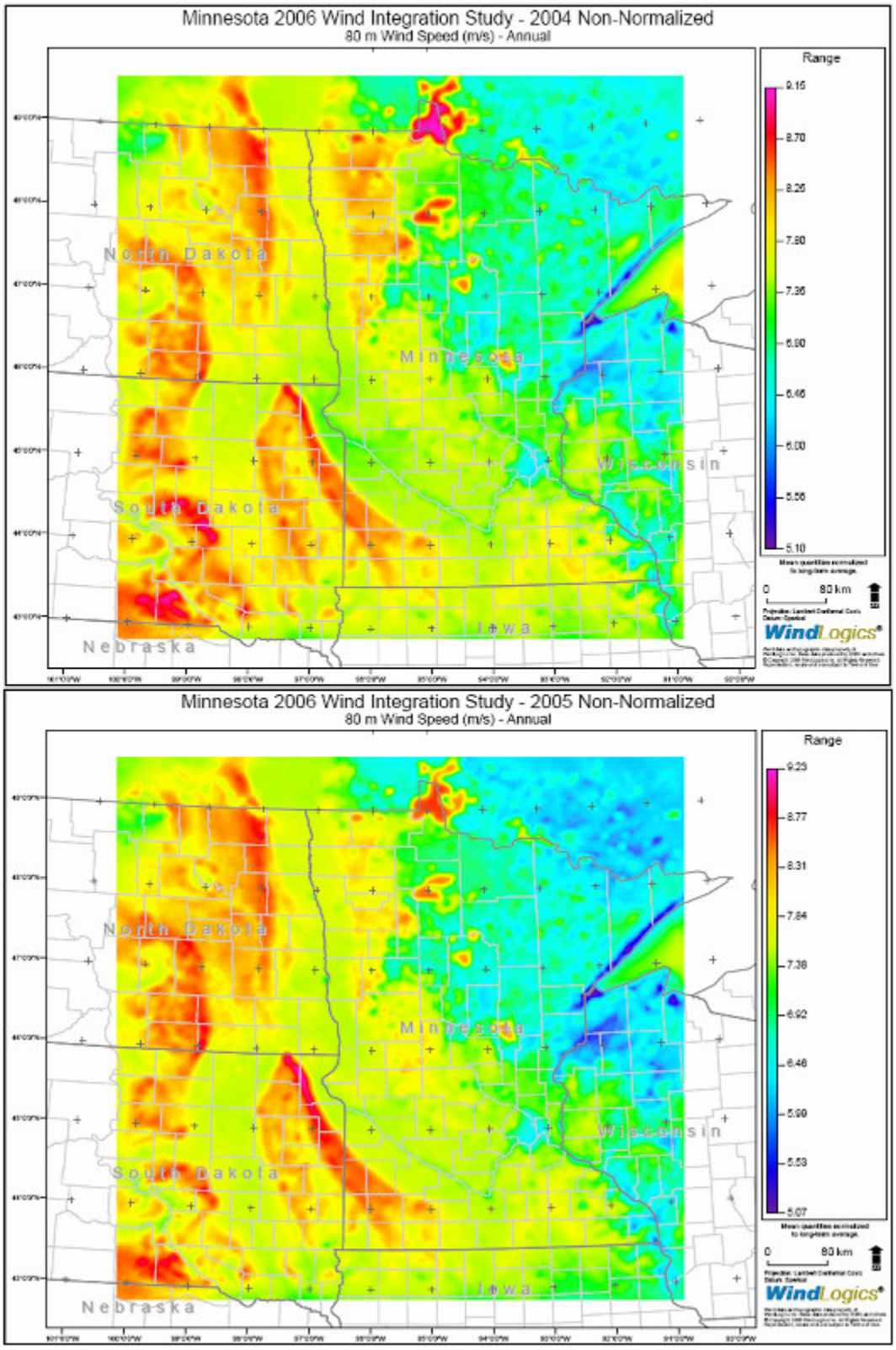

Figure 39: Mean annual non-normalized 80 m wind speed for 2004 and 2005 in m/s.

Mean Annual and Monthly Power Density

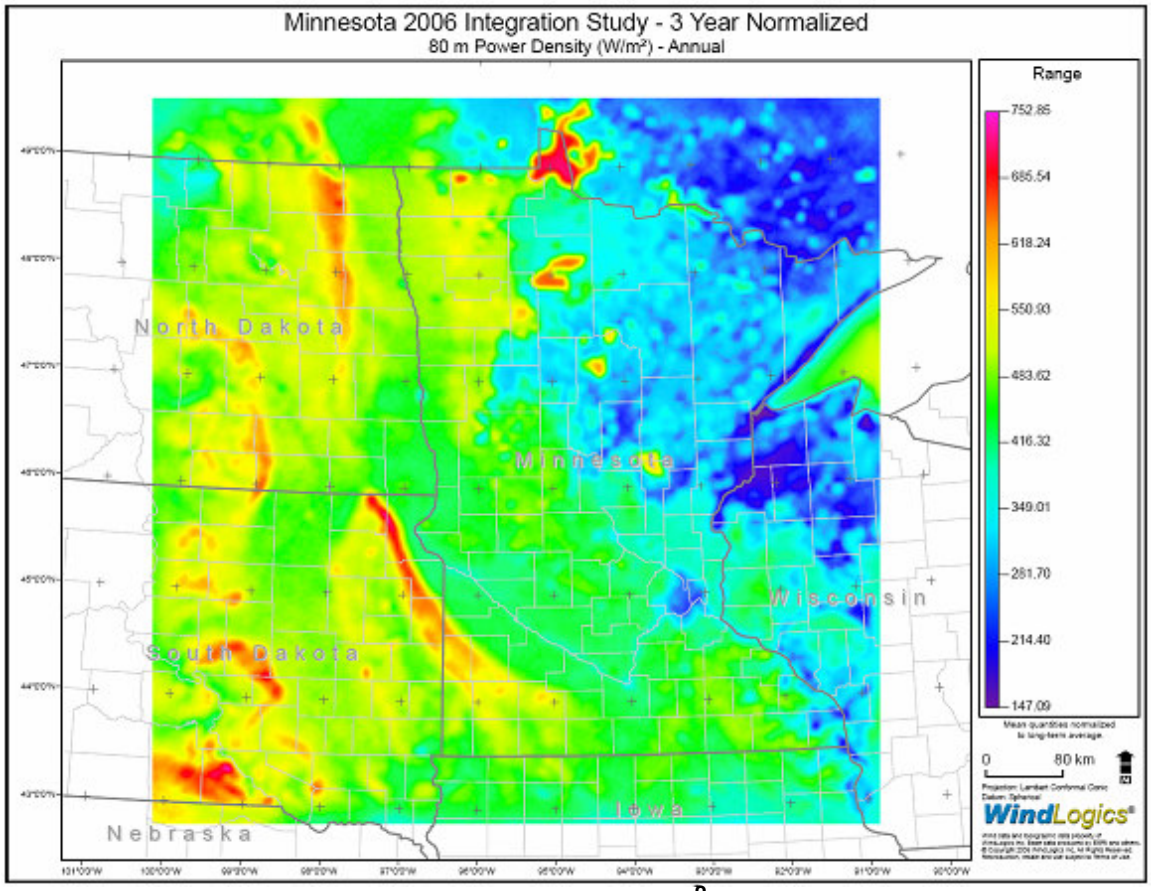

Figure 40: Mean annual power density in W/m^2.

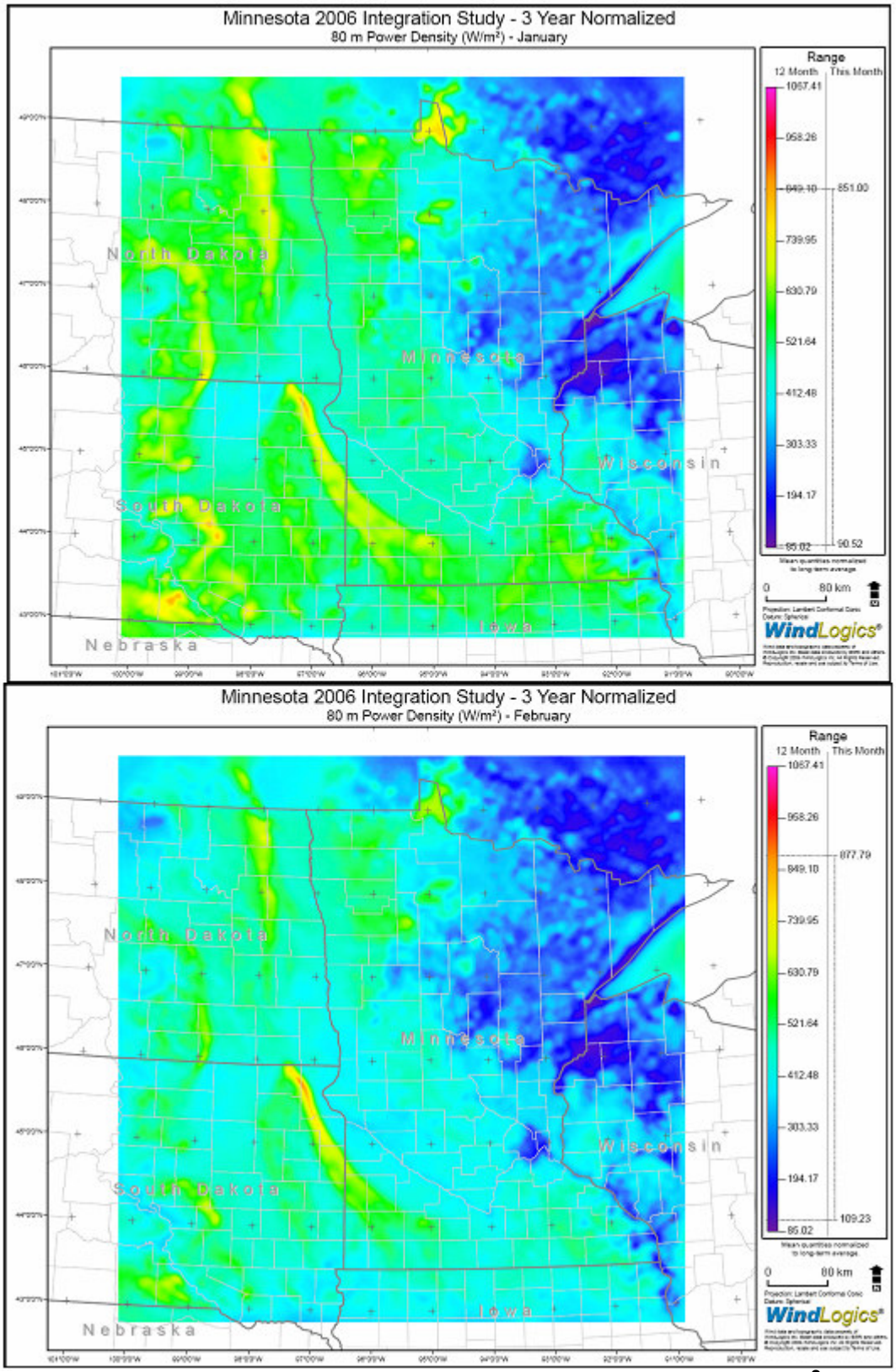

Figure 41: Mean January and February 80 m power density in W/m^2.

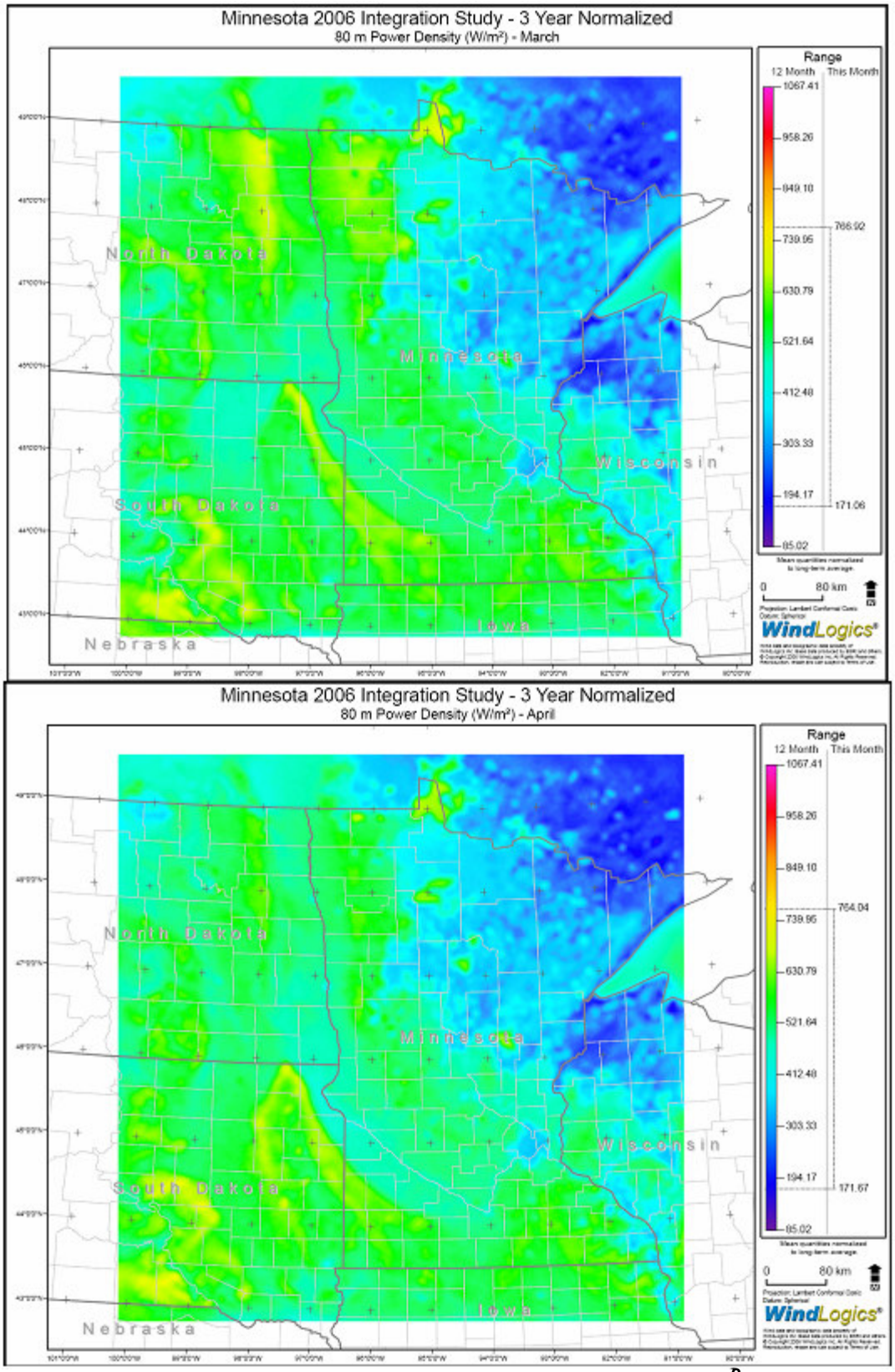

Figure 42: Mean March and April 80 m power density in W/m^2.

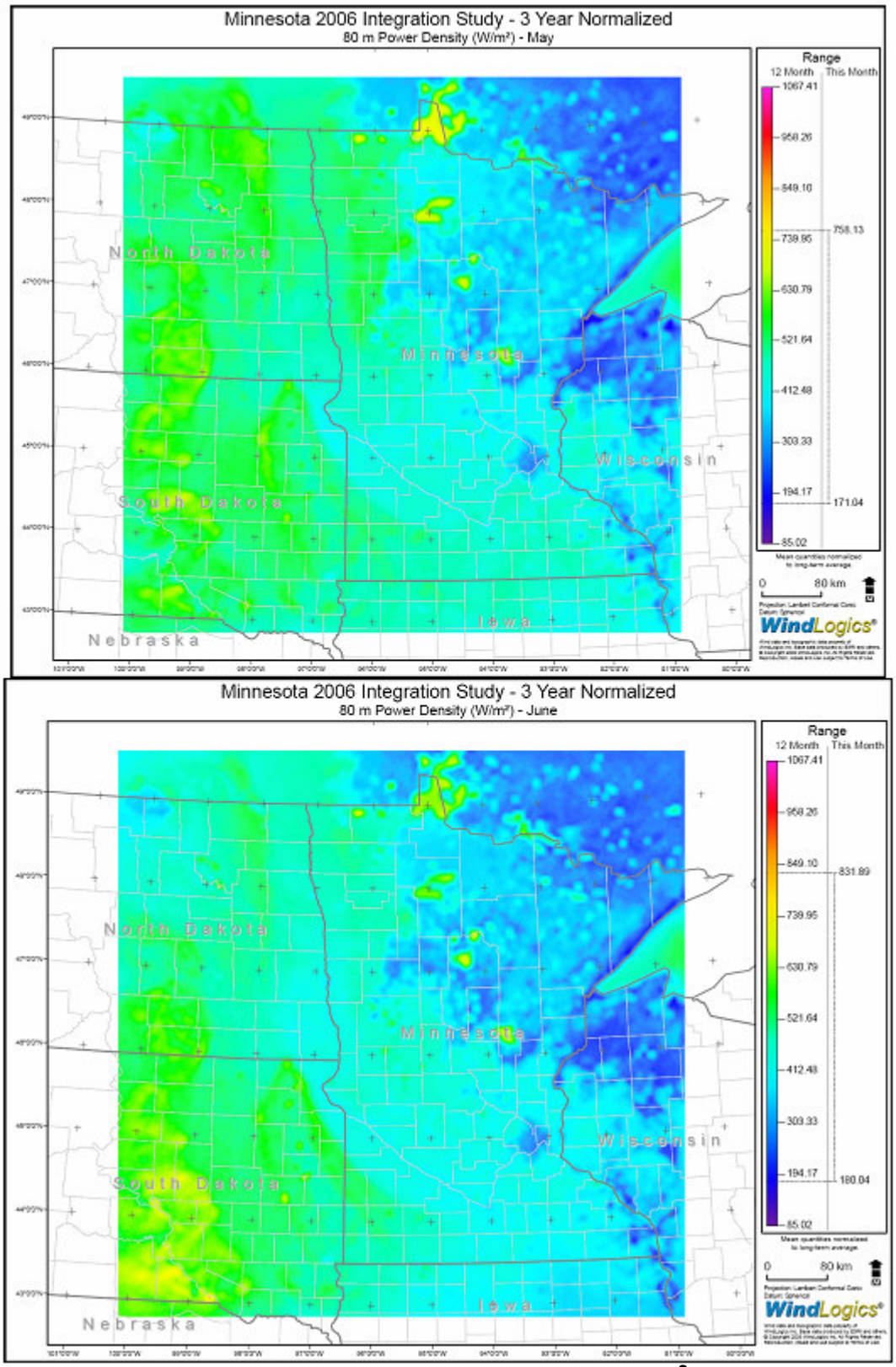

Figure 43: Mean May and June 80 m power density W/m^2.

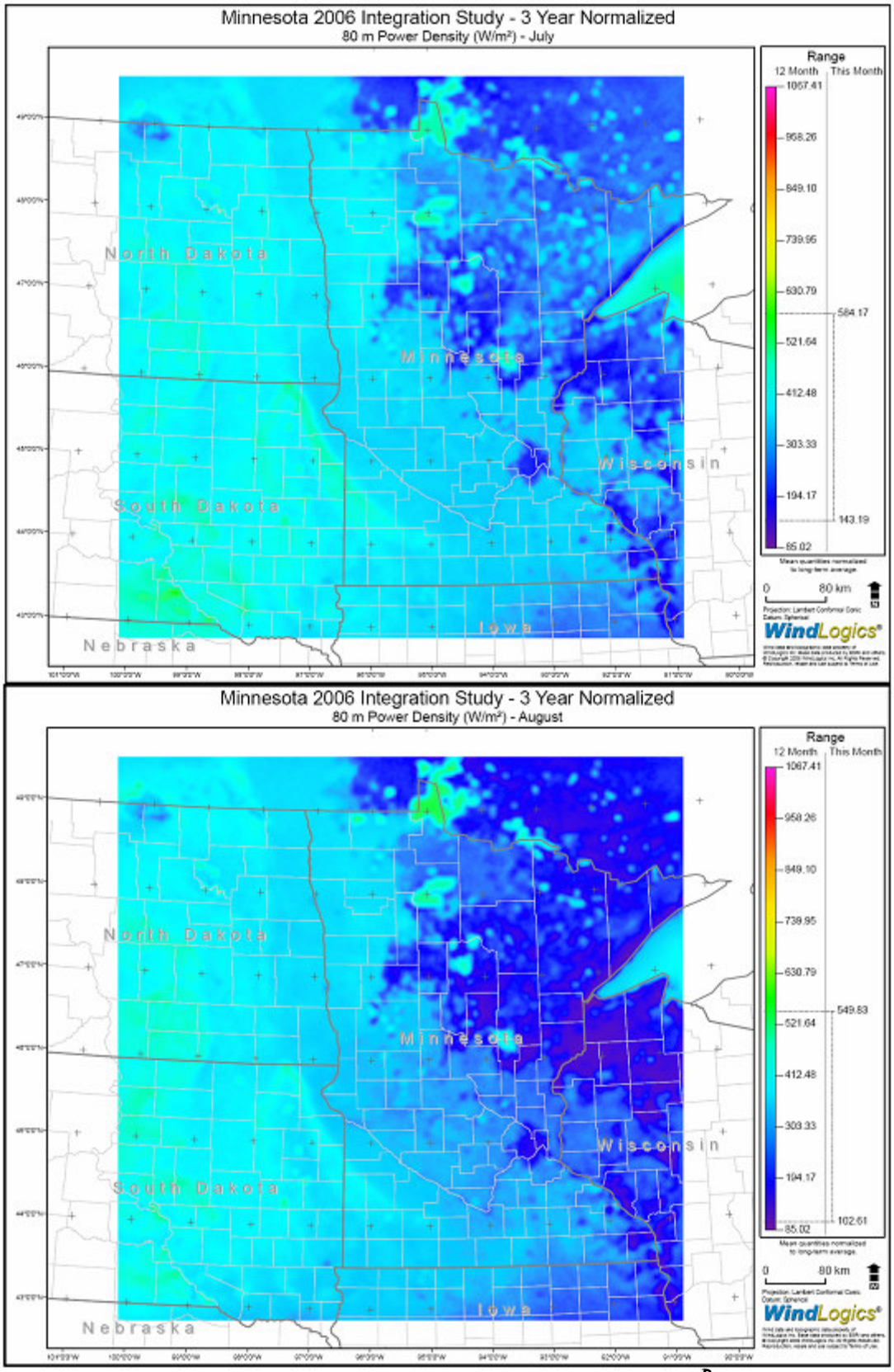

Figure 44: Mean July and August 80 m power density W/m^2.

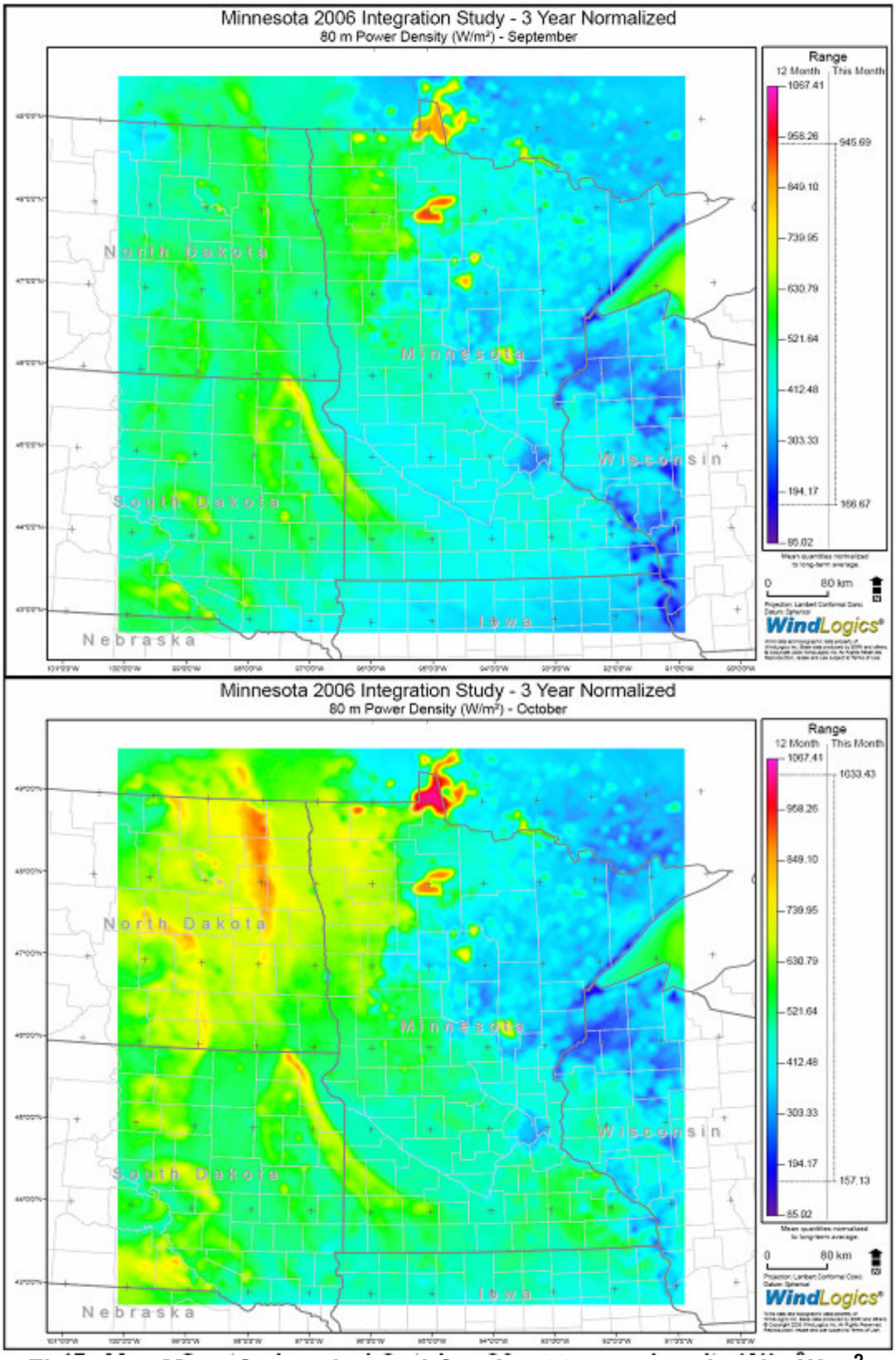

Figure 45: Mean September and October 80 m power density W/m^2.

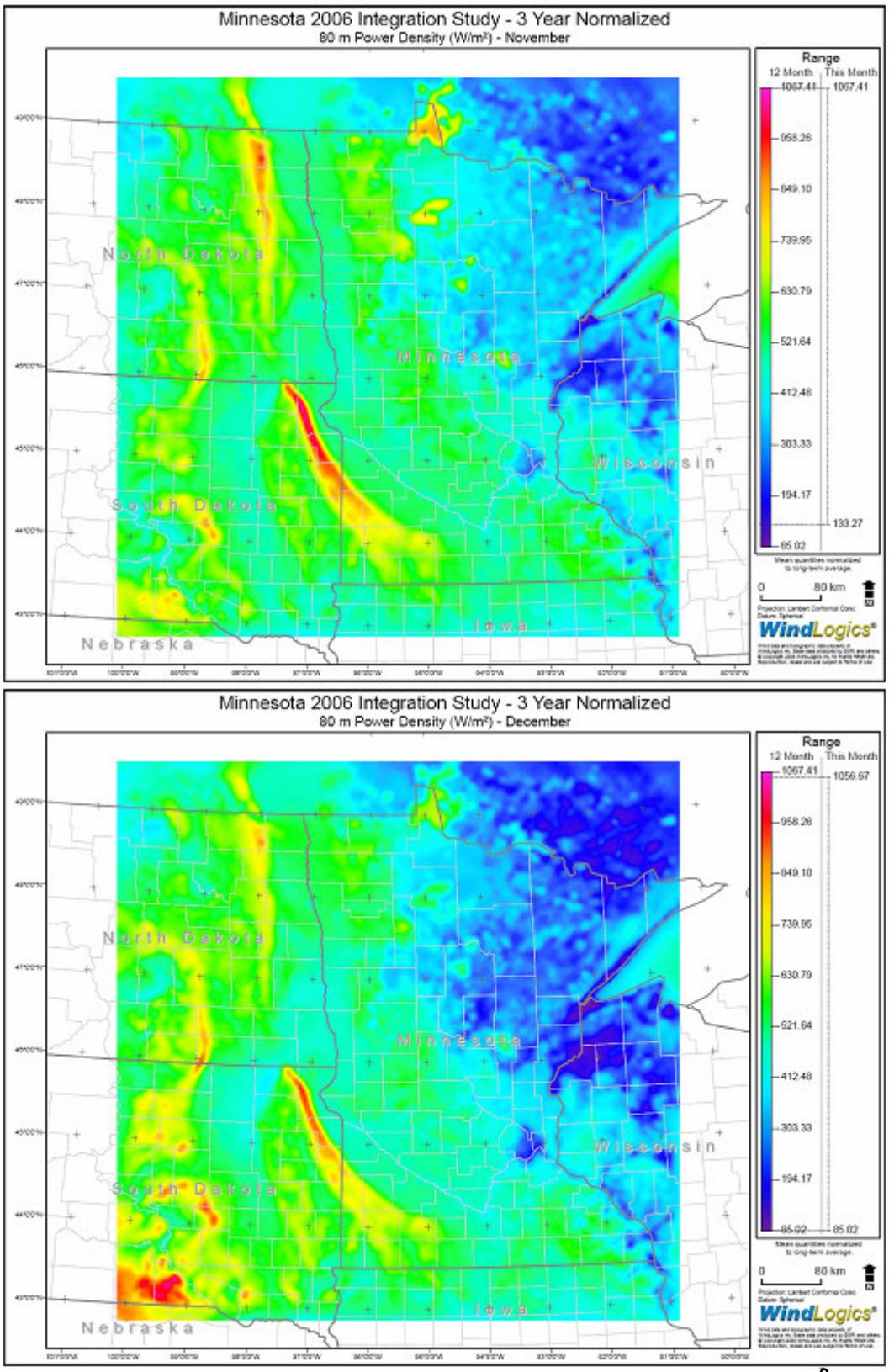

Figure 46: Mean November and December 80 m power density W/m^2.

Summary of 3-year averages of annual and monthly power density

The mean annual geographic distribution of normalized power density is dominated by the annual distribution of wind speed (note the pattern correspondence with Figure 31). As shown in Figures 40 - 46, the topographic ridges of the eastern Dakotas, the Buffalo Ridge and the big lakes of central and northern Minnesota exhibit a maximum in power density throughout the year. Even though the eastern Dakotas' topographic ridges and Buffalo Ridge have generally lower air density due to their elevation than locations farther east, the greater wind speeds occurring in these areas dominate the power density calculation. The secondary northwestern Minnesota and Mower County wind resource areas may also be seen; however, the Mower County feature is less distinguishable in the summer months. The monthly power density variations correspond to the monthly wind climatology.

Mean Annual and Monthly Capacity Factors

Mean annual capacity factor calculations were completed using time dependent air density and normalized 80 m wind speed data from the model and utilizing the Vestas V82 1.65 MW turbine power curve. The values plotted are gross capacity factor.

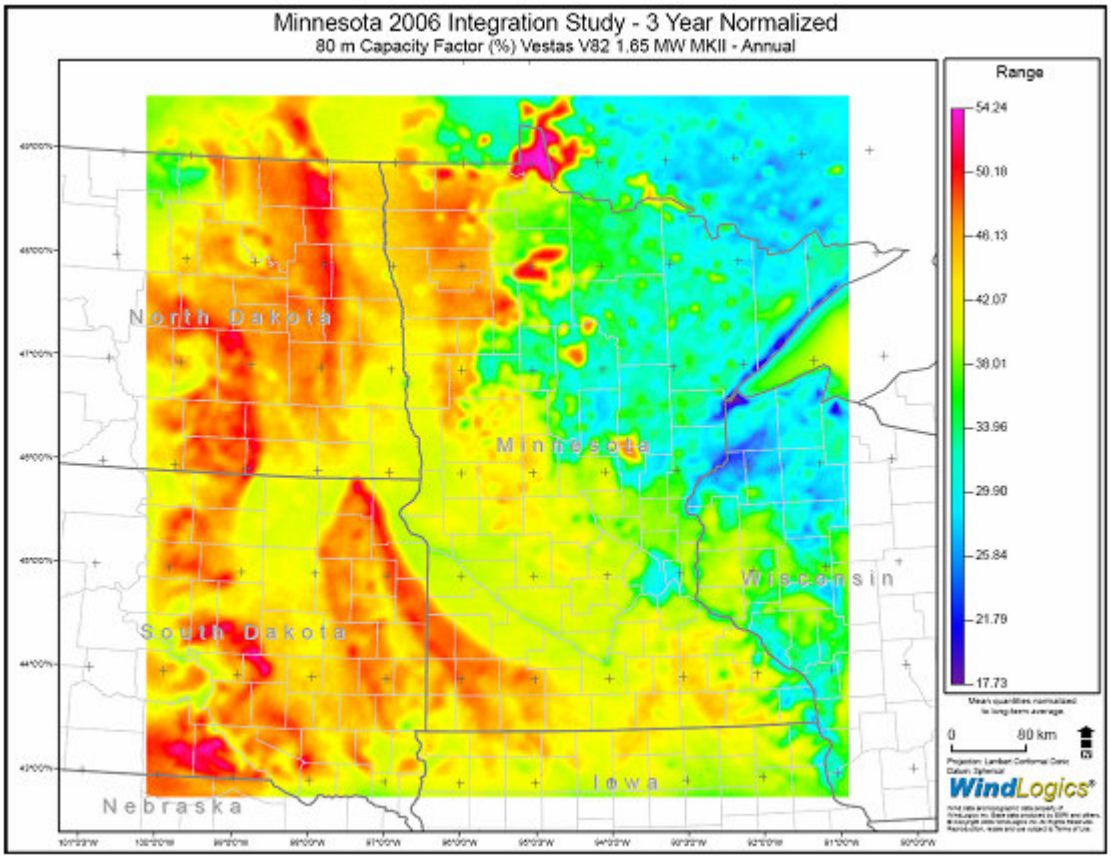

Figure 47: Mean annual capacity factor at 80 m for the Vestas V82 1.65 MW turbine.

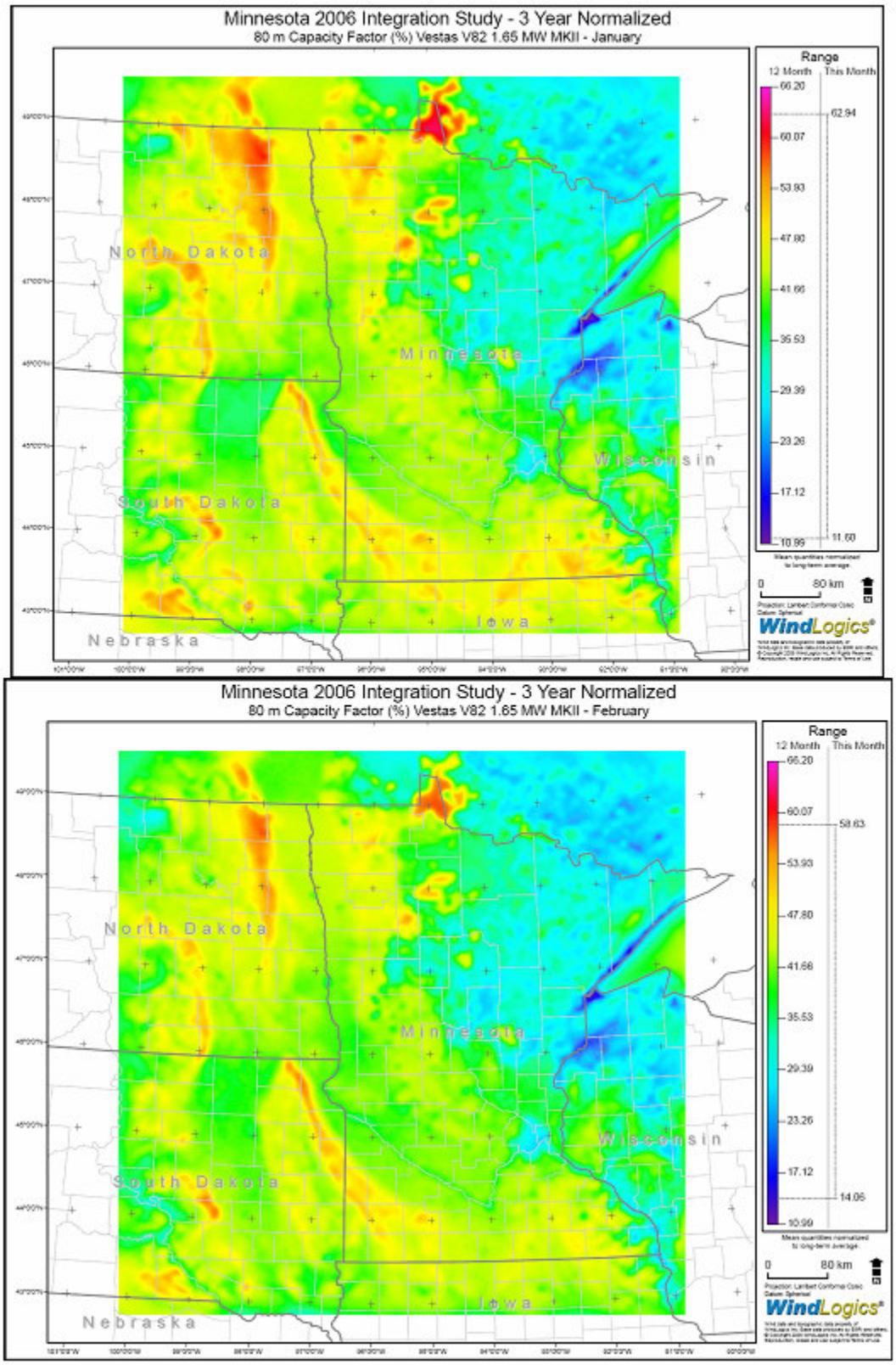

Figure 48: Mean January and February capacity factor at 80 m for the Vestas V82 1.65 MW turbine.

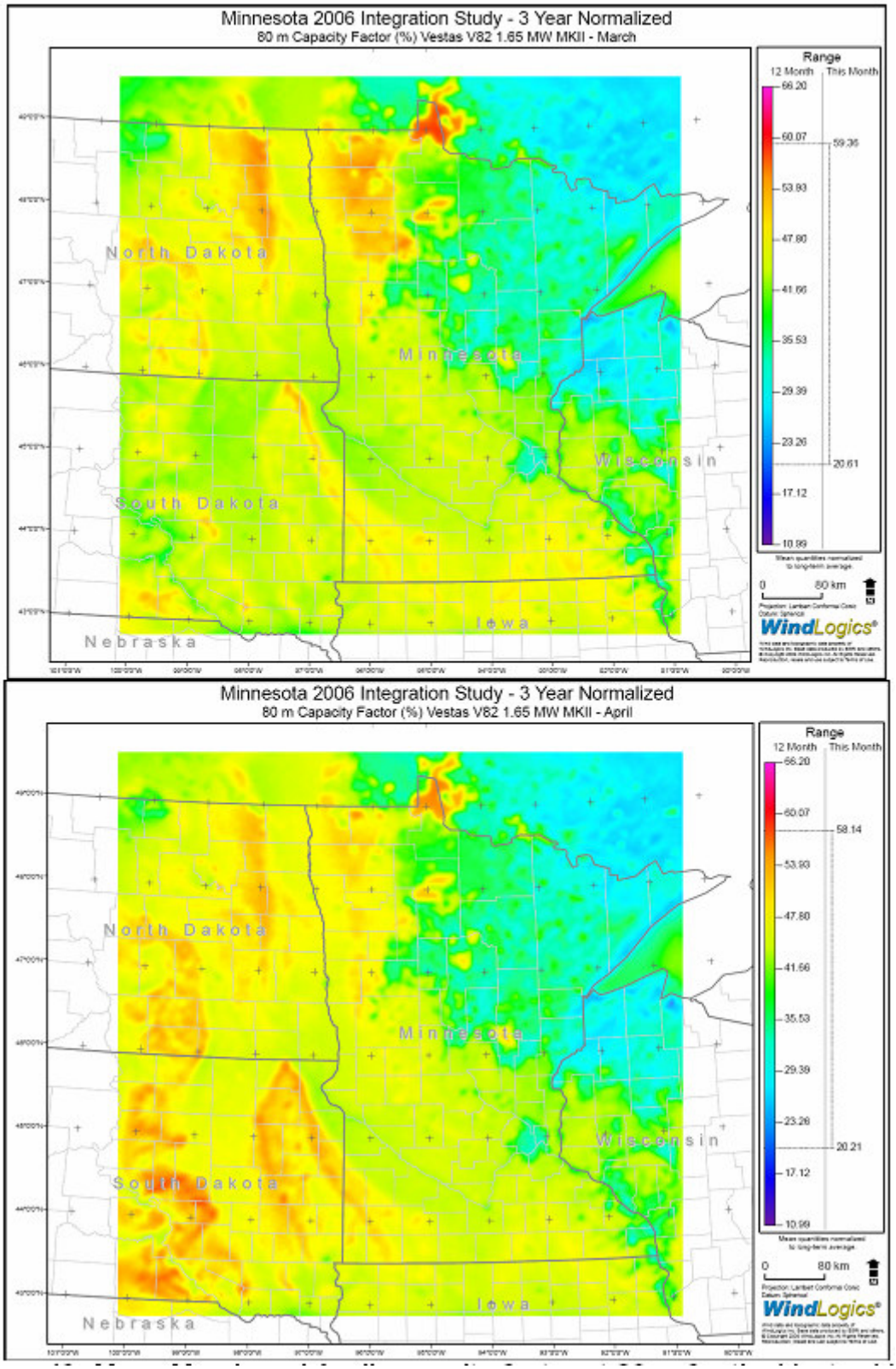

Figure 49: Mean March and April capacity factor at 80 m for the Vestas V82 1.65 MW turbine.

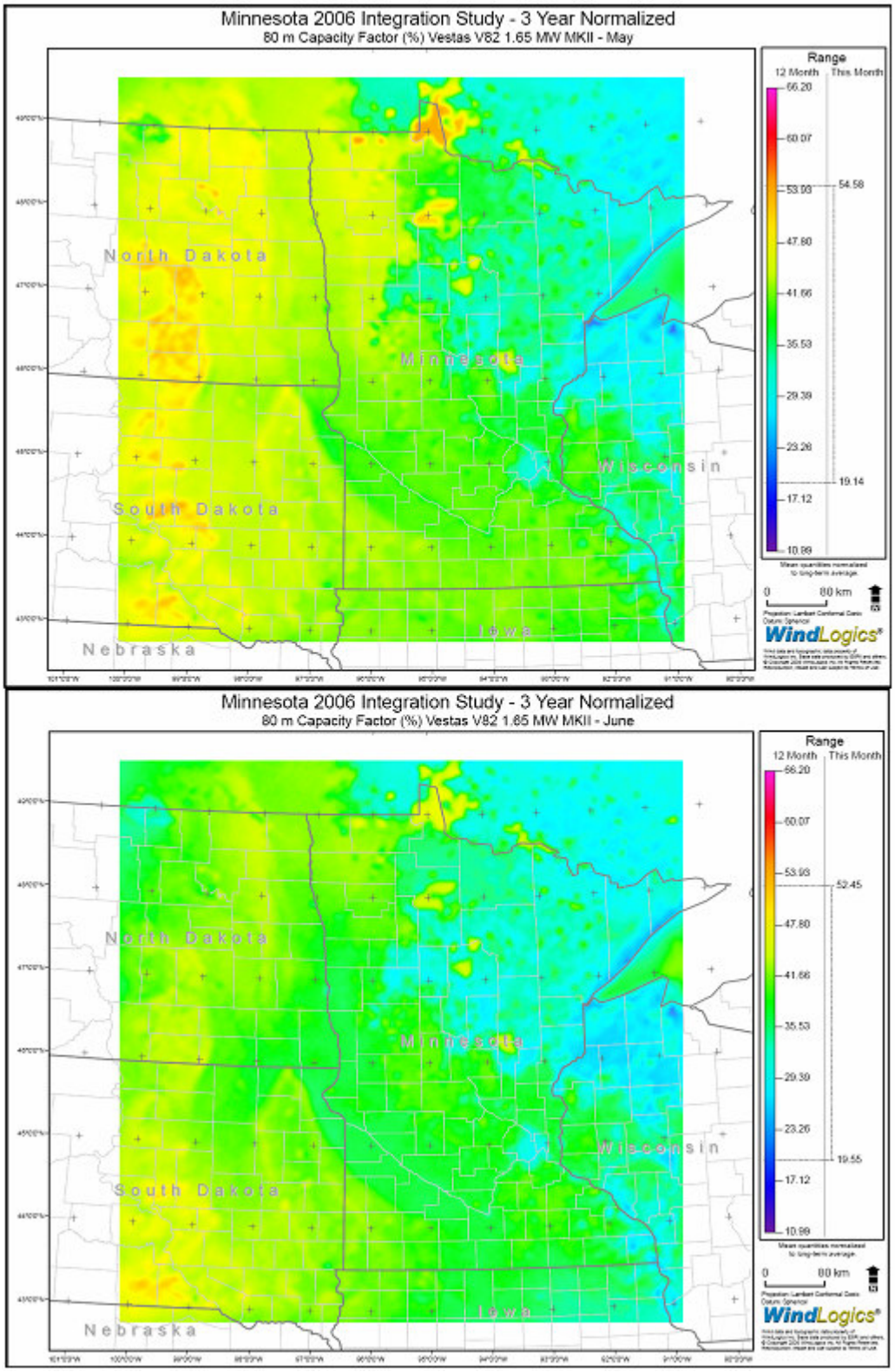

Figure 50: Mean May and June capacity factor at 80 m for the Vestas V82 1.65 MW turbine.

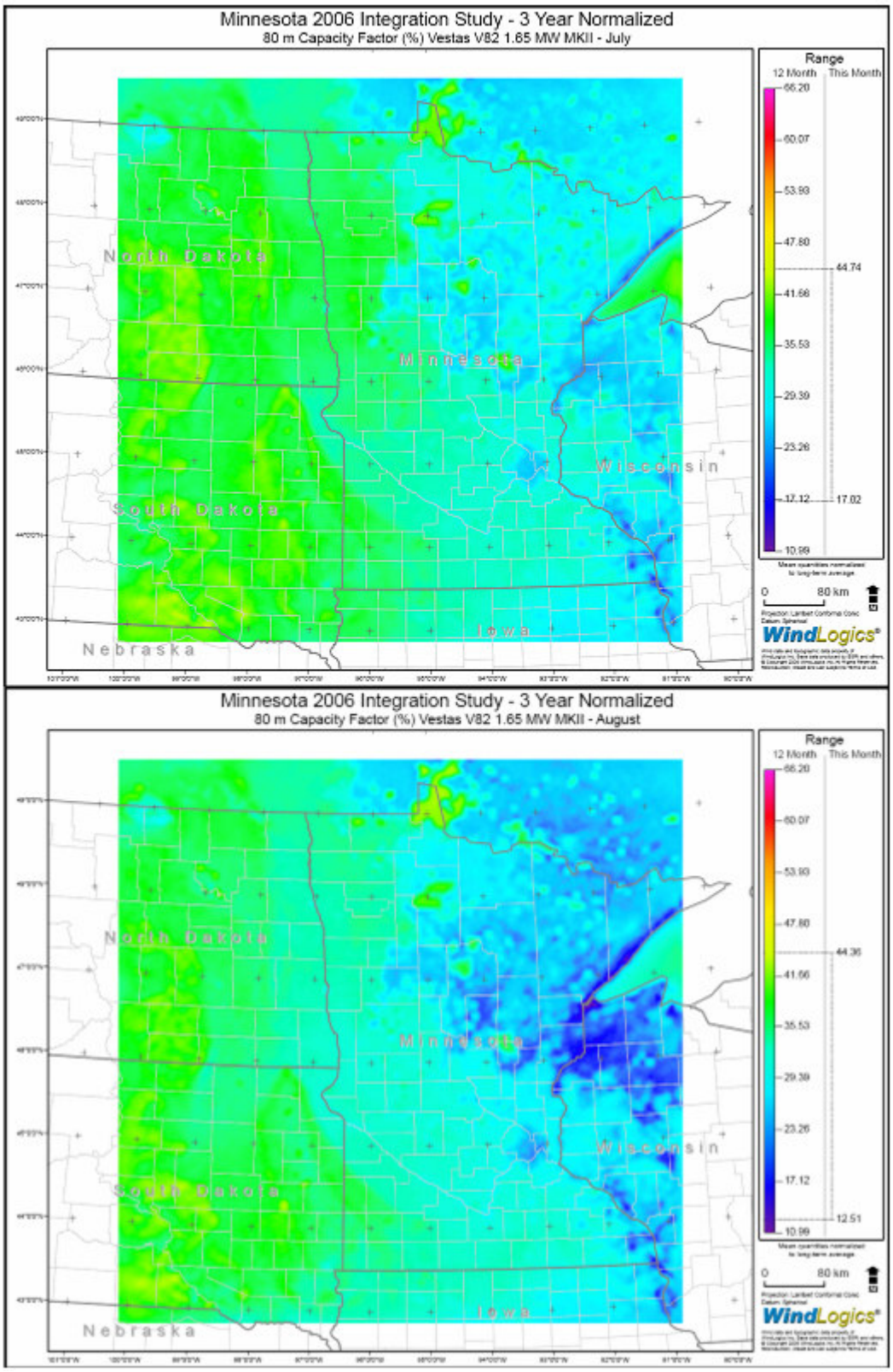

Figure 51: Mean July and August capacity factor at 80 m for the Vestas V82 1.65 MW turbine.

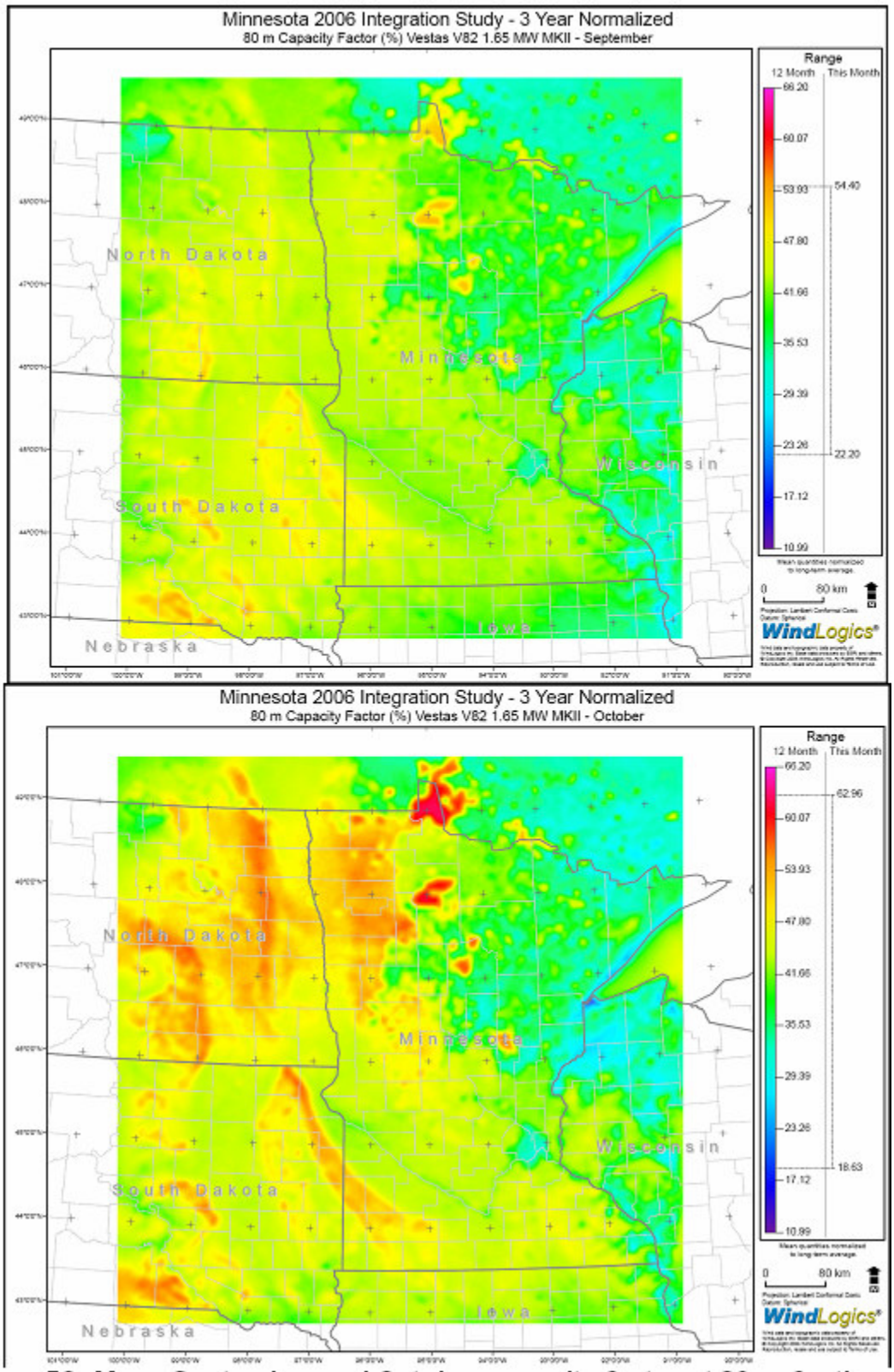

Figure 52: Mean September and October capacity factor at 80 m for the Vestas V82 1.65 MW turbine.

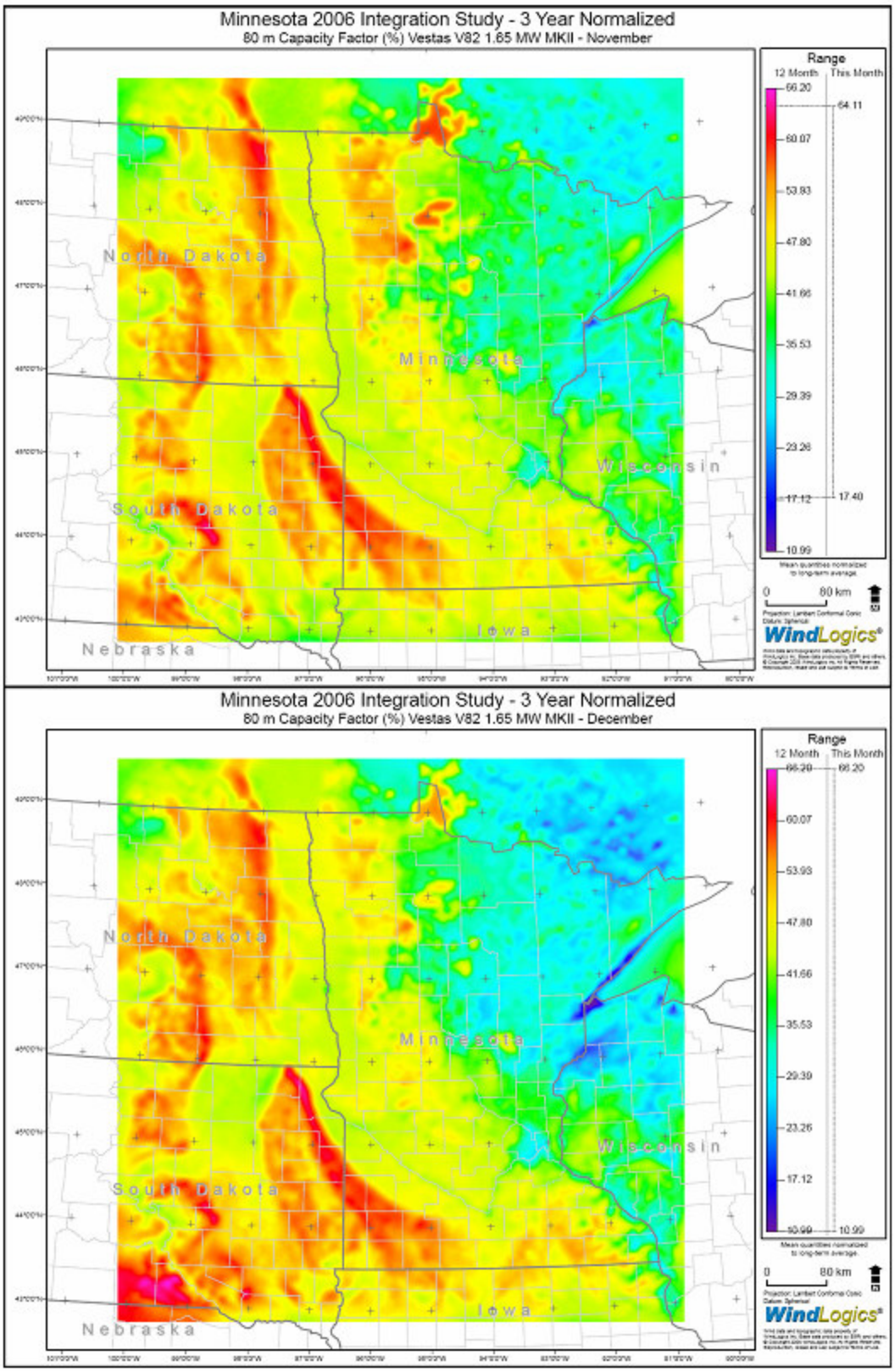

Figure 53: Mean November and December capacity factor at 80 m for the Vestas V82 1.65 MW turbine.

Summary of 3-year averages of annual and monthly capacity factor

The normalized 3-year annual and monthly mean capacity factor maps clearly delineate geographic regions of the Upper Midwest possessing a good to excellent wind resource. As shown in Figures 47 - 53, the considerable wind resource of the topographic ridges of the eastern Dakotas and Buffalo Ridge are prominent features of the capacity factor mapping on an annual and monthly basis. The agricultural and prairie region of northwest Minnesota, and to a lesser extent Mower County in southeast Minnesota, are notable secondary resource areas. As previously noted, the big lakes of central and northern Minnesota stand out as having excellent capacity factors. In fact, Lake of the Woods along the Minnesota-Canada border has the highest capacity factor of any area on an annual basis. The seasonality of the mean capacity factors are consistent with the climatology of regional wind speed described previously. Of note are the summer season capacity factors of the topographic ridges of the Dakotas and the Buffalo Ridge that remain substantial from a wind energy perspective. While lower, the summer season regional capacity factor in northwest Minnesota fares much better than most land areas of the state outside the Buffalo Ridge. The Vestas V82 1.65 MW turbine appears to be well-suited to the wind resource climatology of the Upper Midwest.

Mean Annual and Monthly Energy Production

Mean annual and monthly energy production calculations were completed using time dependent air density and normalized 80 m wind speed data from the model and utilizing the Vestas V82 1.65 MW turbine power curve. The values plotted are gross energy production.

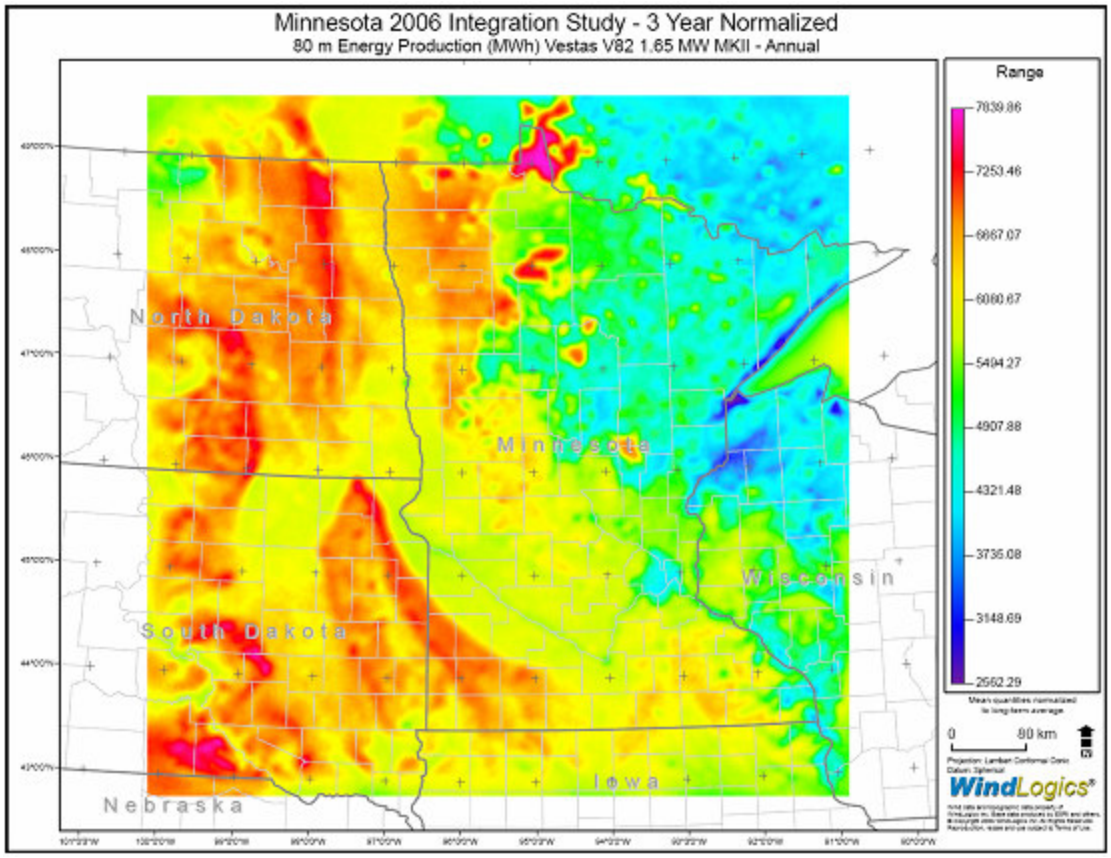

Figure 54: Annual energy production at 80 m for the Vestas V82 1.65 MW turbine in MWh.

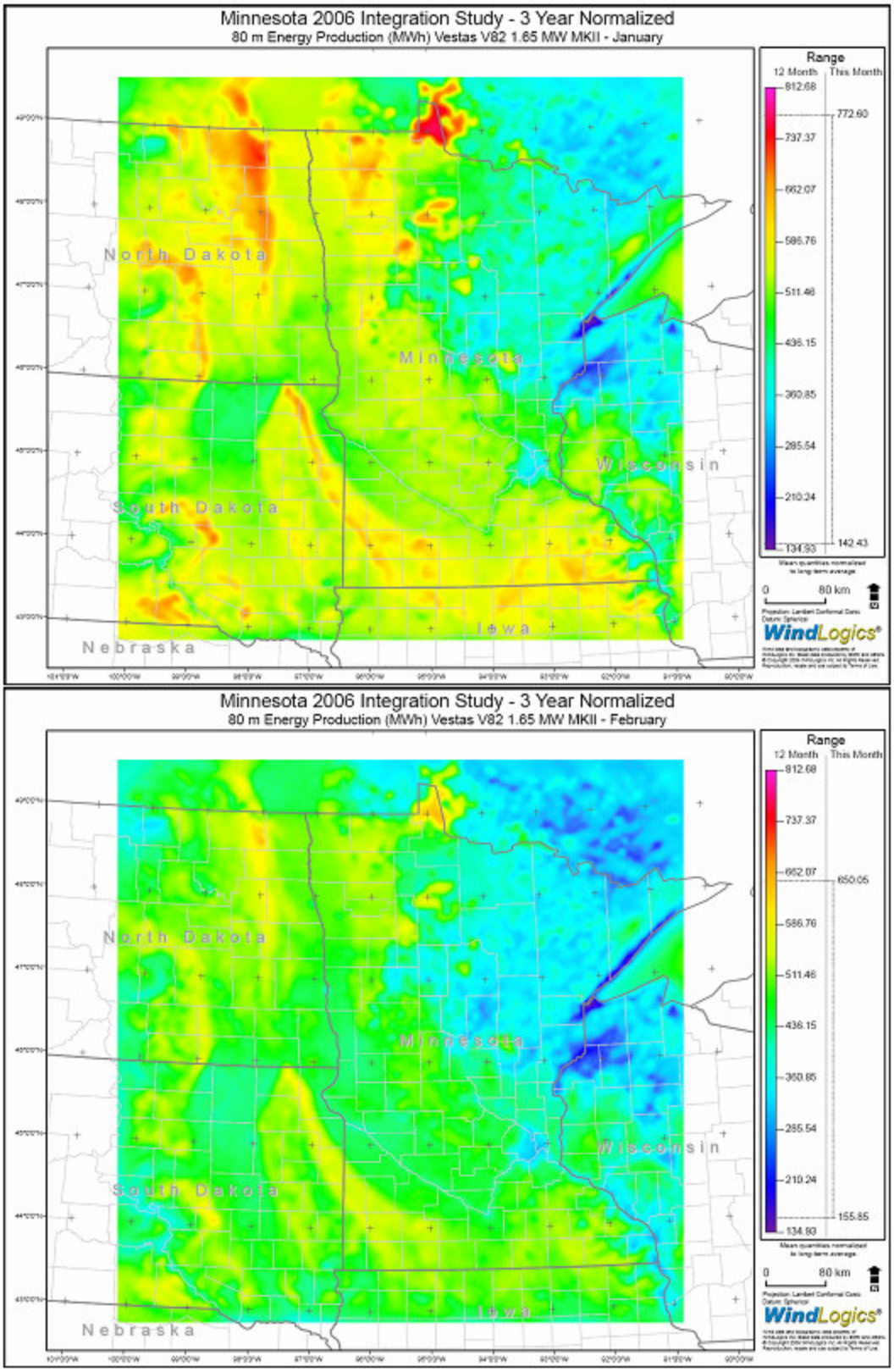

Figure 55: January and February energy production at 80 m for the Vestas V82 1.65 MW turbine in MWh.

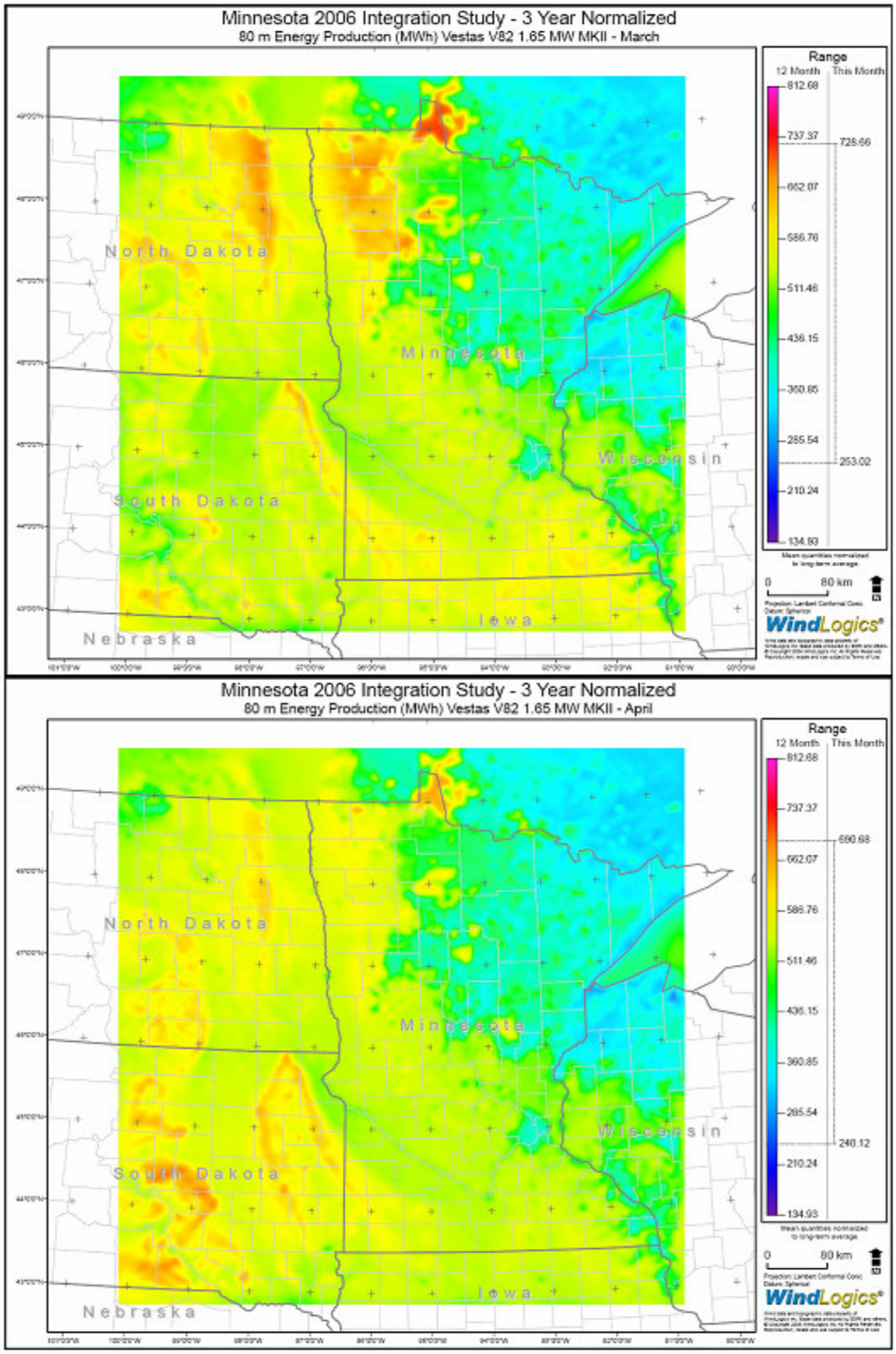

Figure 56: March and April energy production at 80 m for the Vestas V82 1.65 MW turbine in MWh.

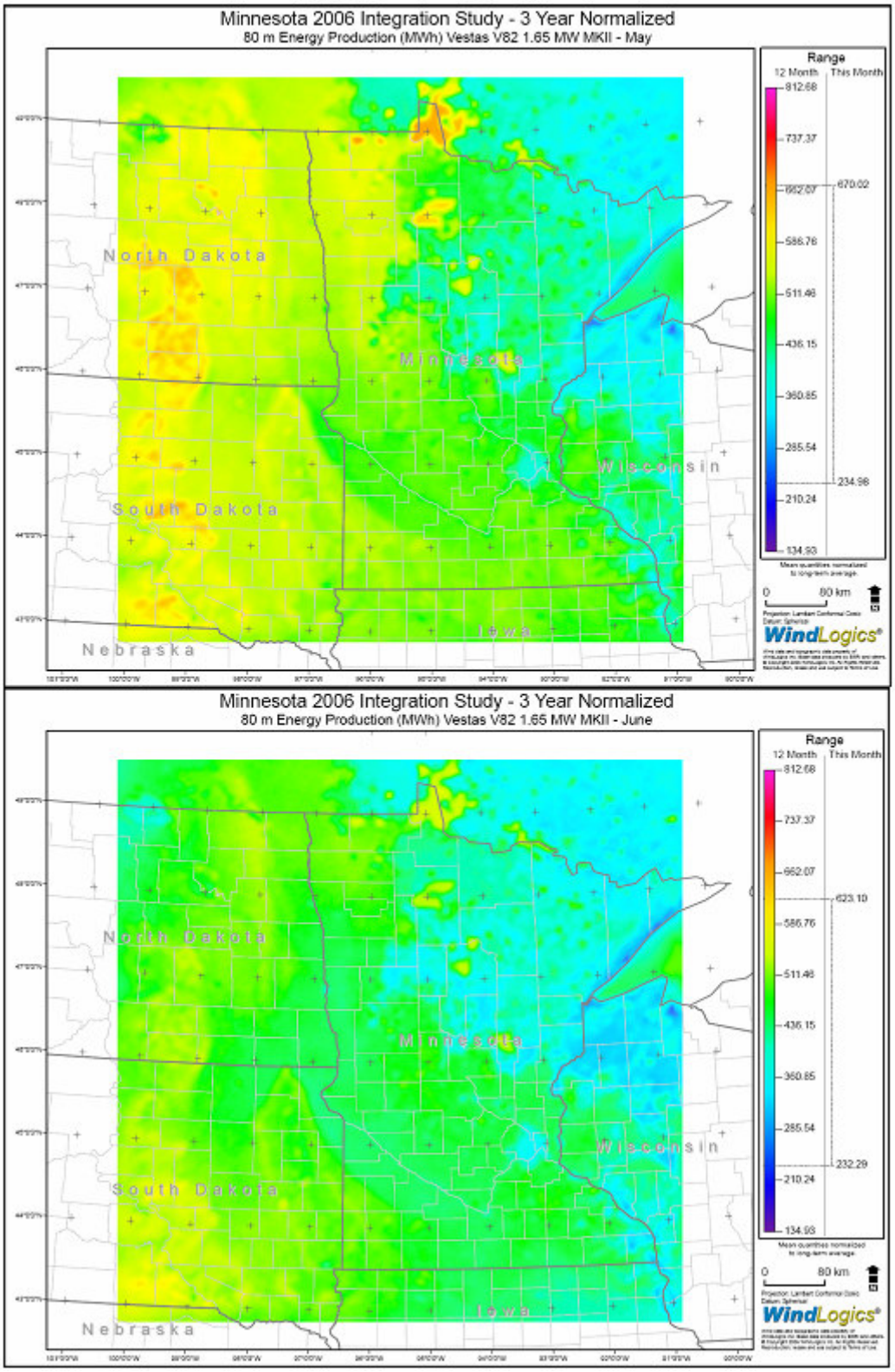

Figure 57: May and June energy production at 80 m for the Vestas V82 1.65 MW turbine in MWh.

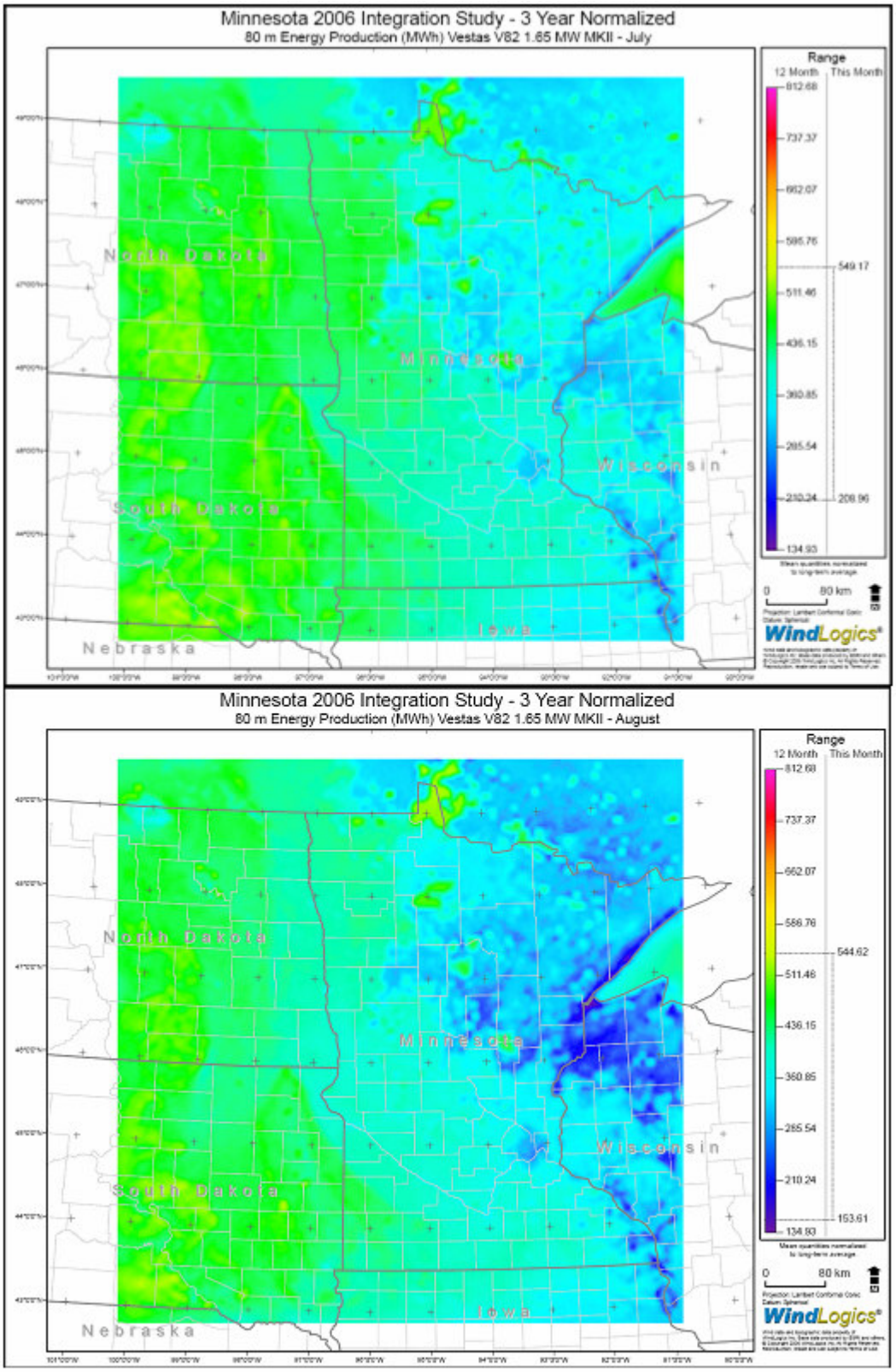

Figure 58: July and August energy production at 80 m for the Vestas V82 1.65 MW Turbine in MWh.

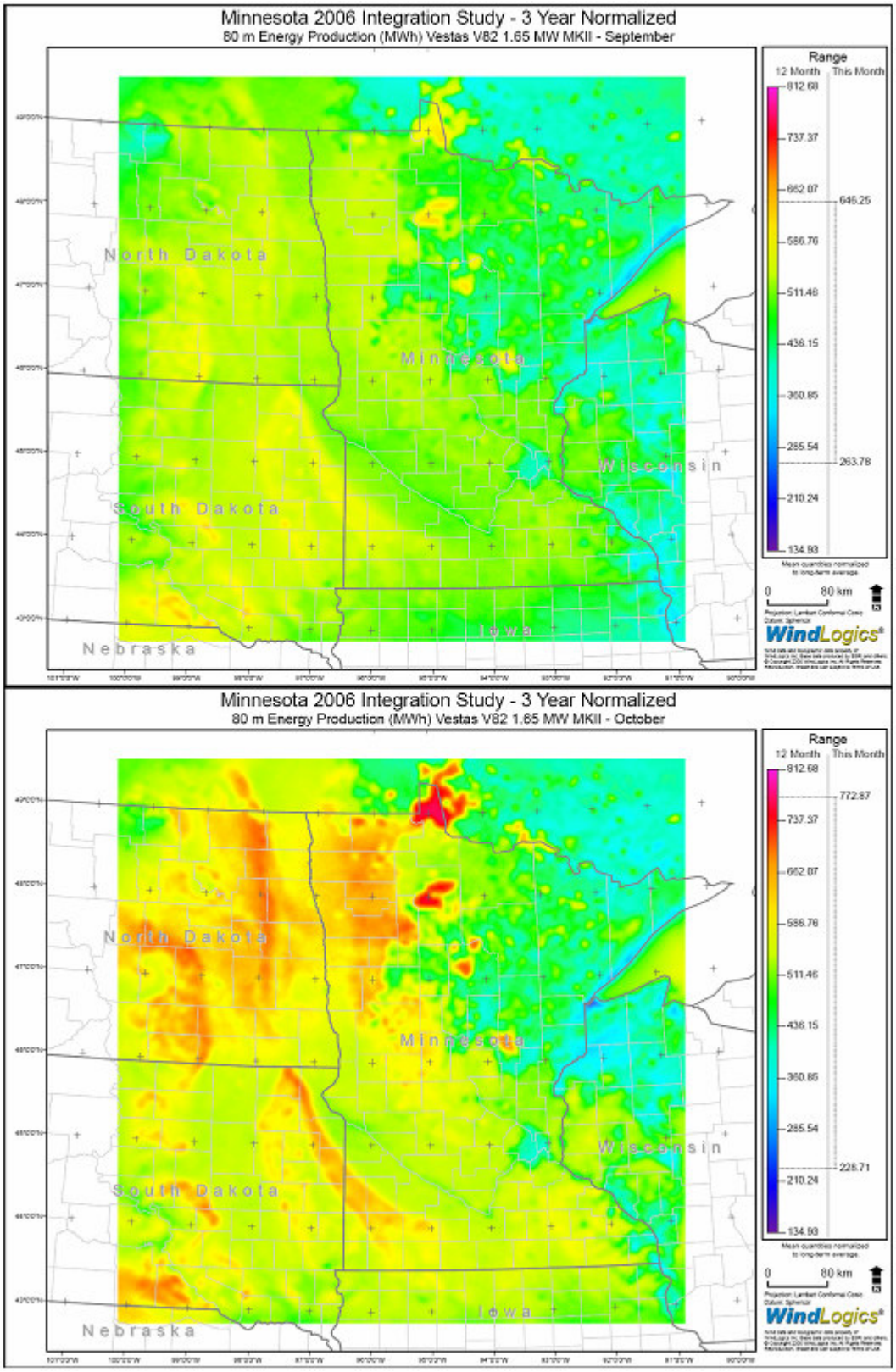

Figure 59: September and October energy production at 80 m for the Vestas V82 1.65 MW turbine in MWh.

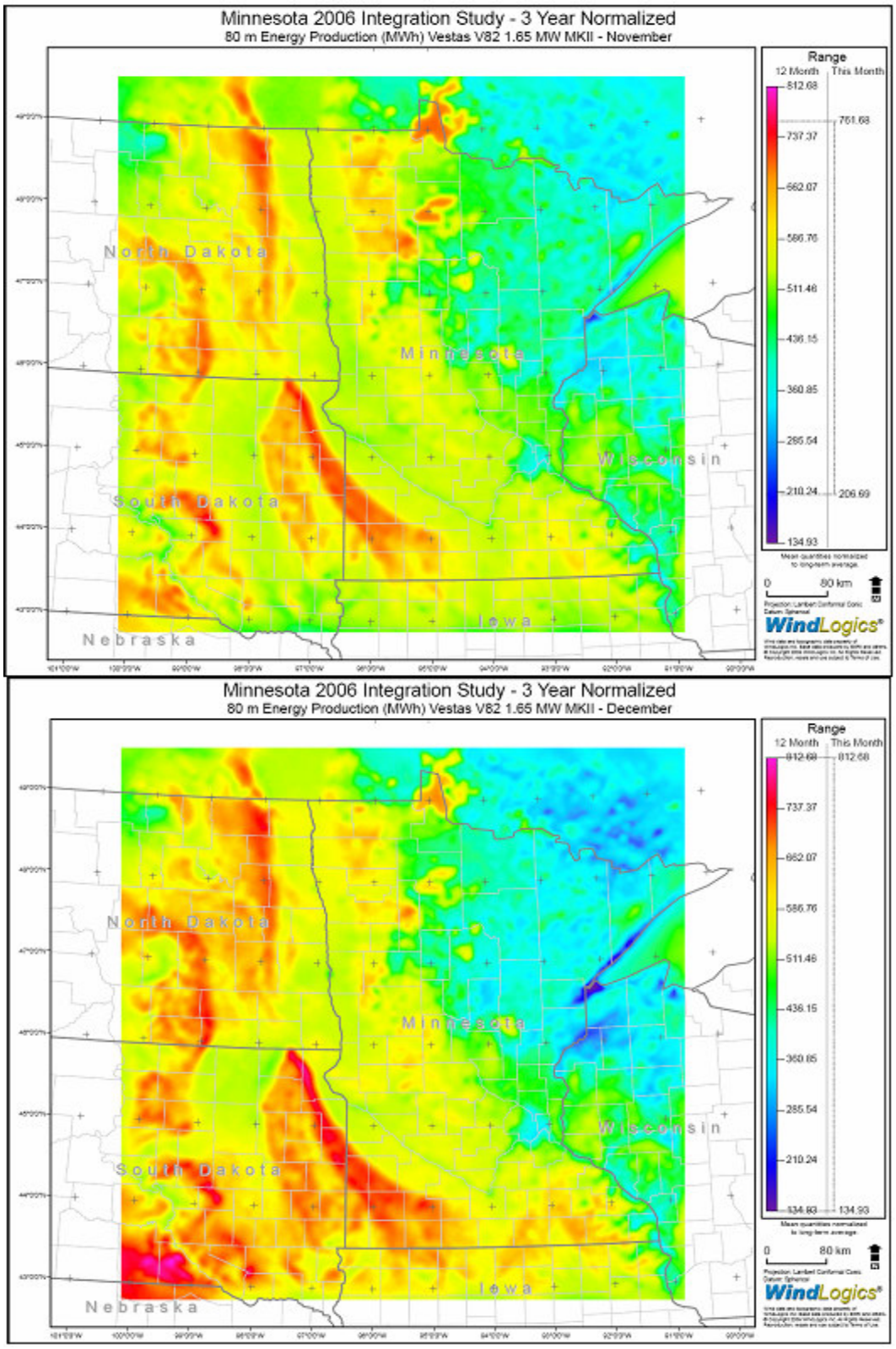

Figure 60. November and December energy production at 80 m for the Vestas V82 1.65 MW turbine in MWh.

Summary of 3-year averages of annual and monthly energy production

Consistent with the previously displayed wind resource quantities, the three-year normalized mean annual and monthly energy production maps clearly portray the geographic regions of the Upper Midwest possessing good-excellent wind resource. As shown in Figure 54 through 60, the considerable wind resource of the topographic ridges of the eastern Dakotas and Buffalo Ridge are prominent features of the energy production mapping on an annual and monthly basis. It is noteworthy that some of the topographic ridges of the eastern Dakotas and Lake of the Woods maintain monthly energy production values near or above 500 MWh even throughout the weakest wind speed period of summer (July and August).

Regional Characteristics of Diurnal Wind Speed Variability

To document the diurnal wind speed and spatial differences of the diurnal winds across the project domain, mean annual and monthly diurnal time series have been created from the MM5 80 m wind speeds using all three simulation years. The same regional representative sites that were utilized in section 1D for the geographic dispersion scenarios are used here. The MM5 proxy towers selected to represent each of these areas are Towers 71 (Minnesota Southwest), 41 (Minnesota Southeast), 82 (Minnesota Northeast) and 115 (North Dakota Central).

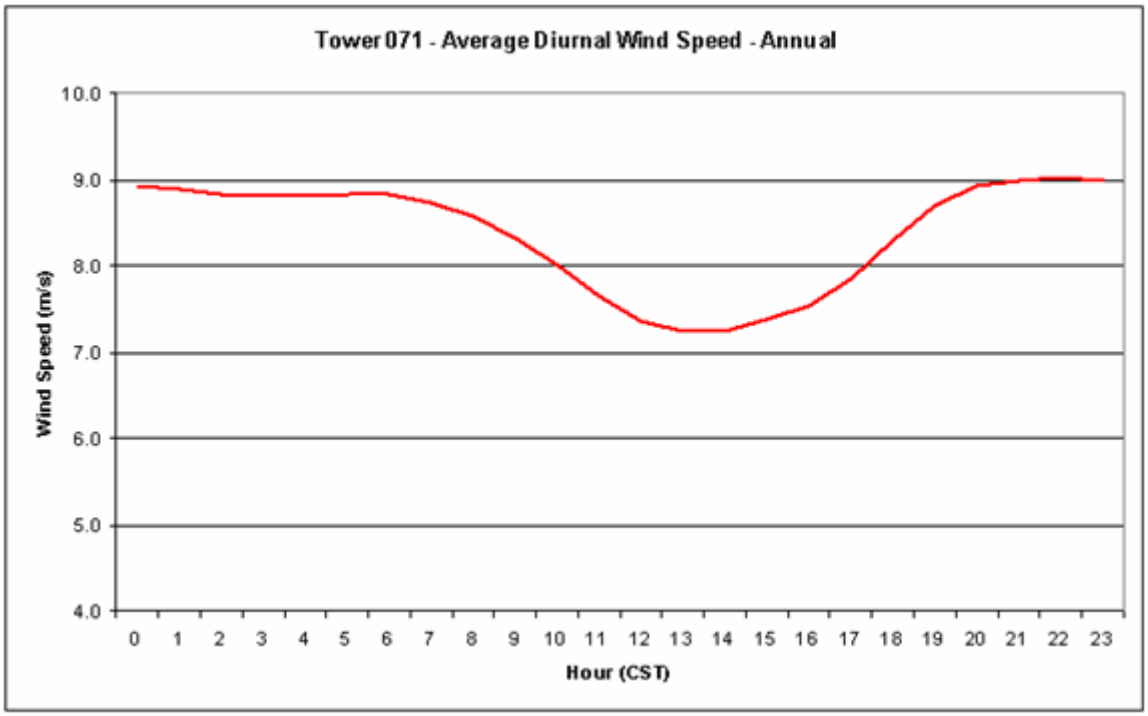

Figure 61: Average annual 80 m diurnal wind speed at Tower 71 in m/s.

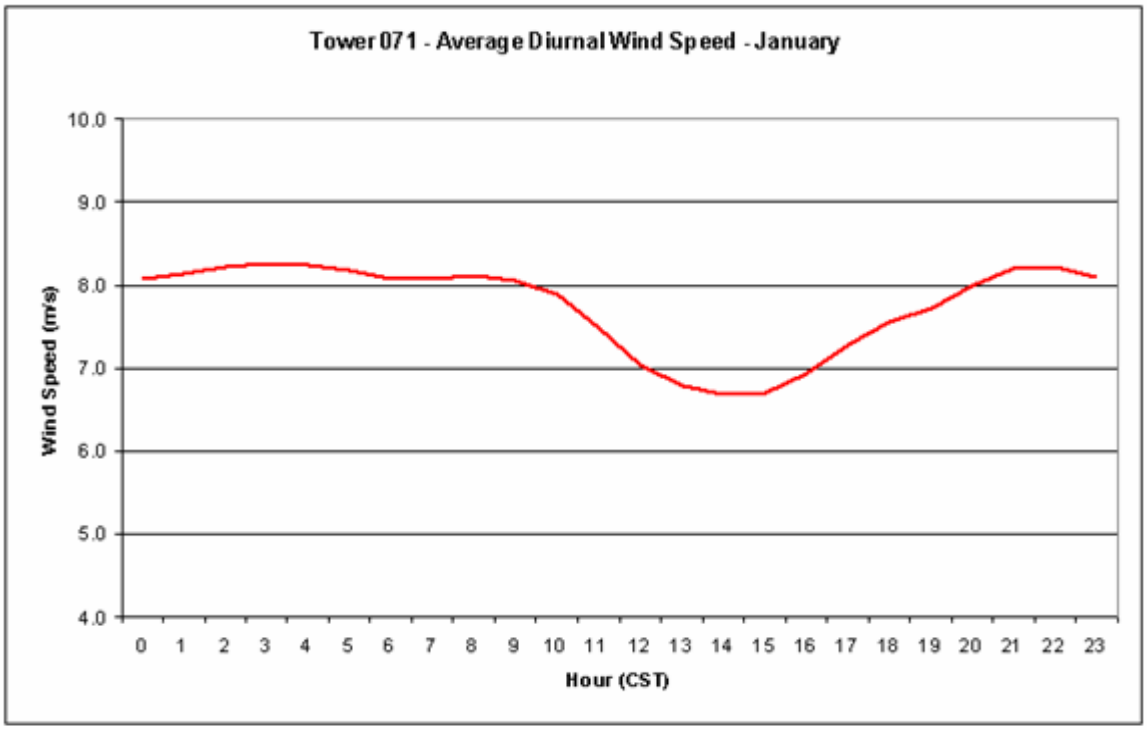

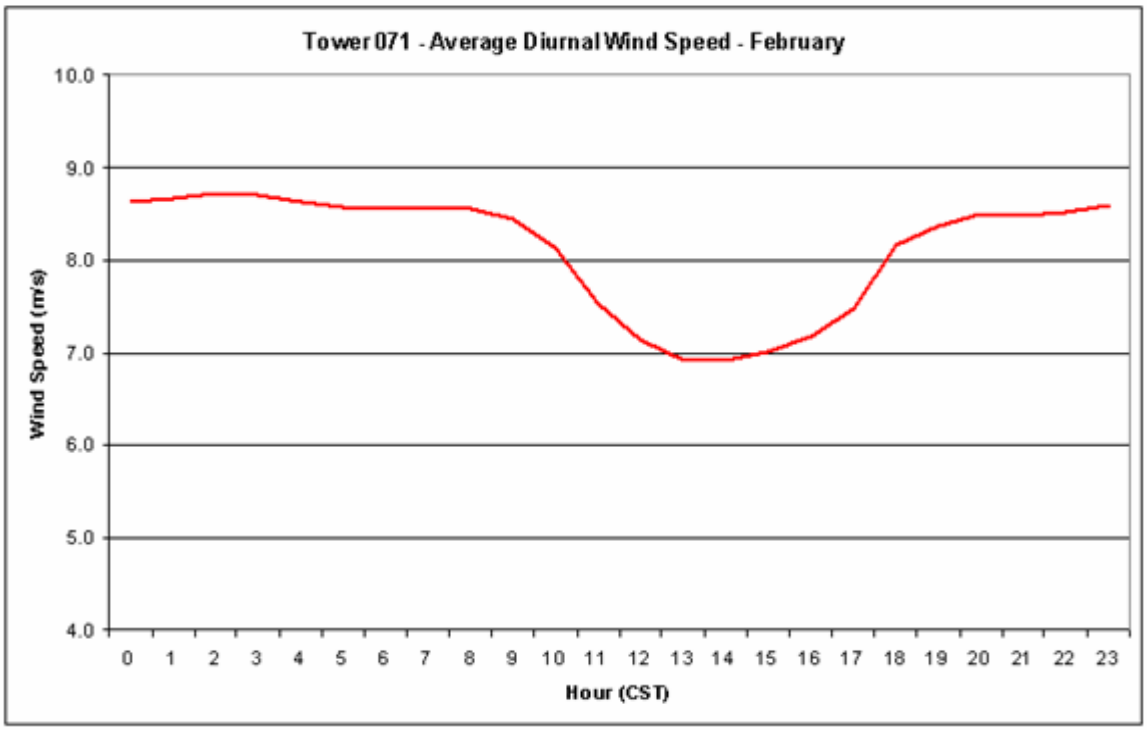

Figure 62: Average January and February 80 m diurnal wind speed at Tower 71 in m/s.

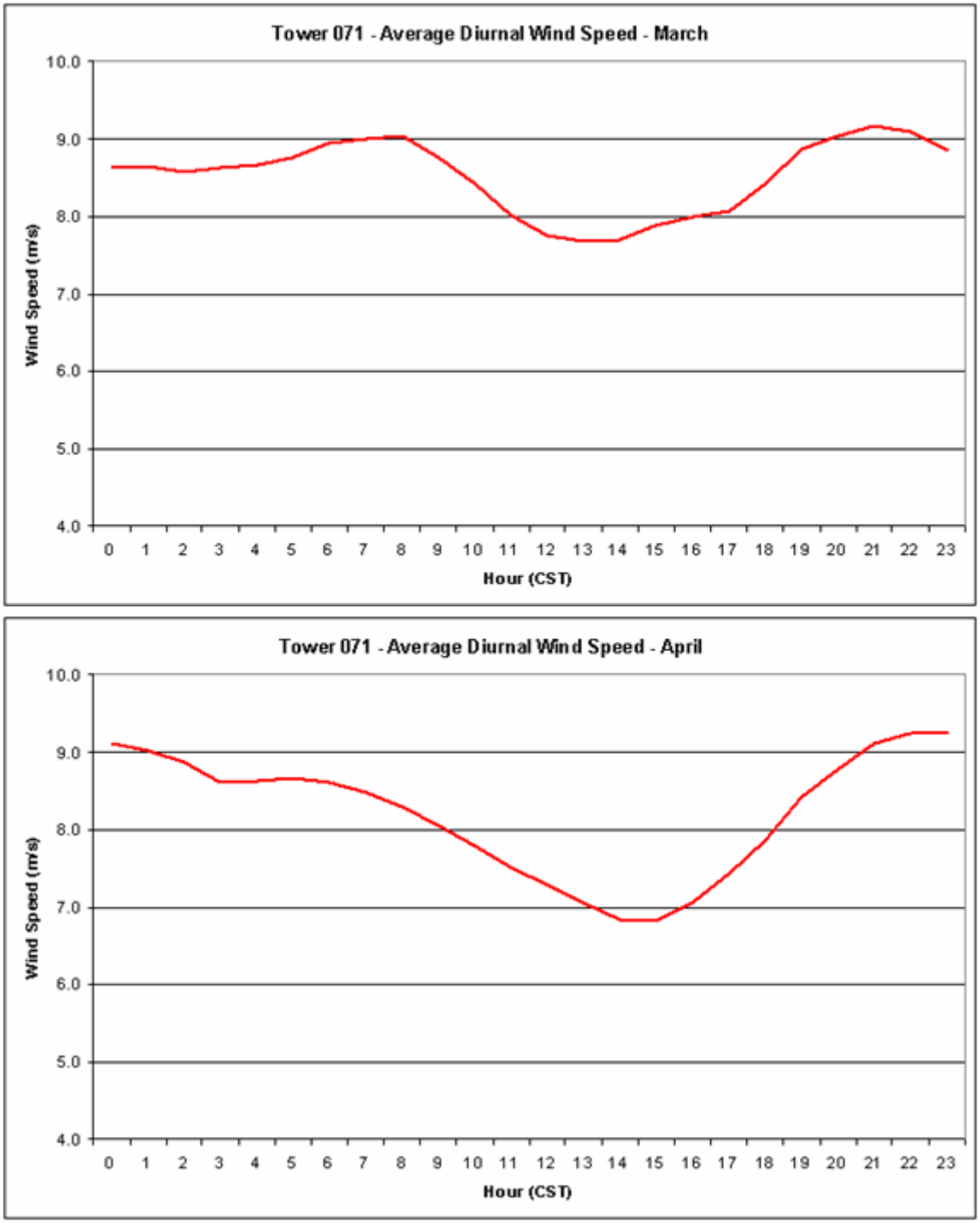

Figure 63: Average March and April 80 m diurnal wind speed at Tower 71 in m/s.

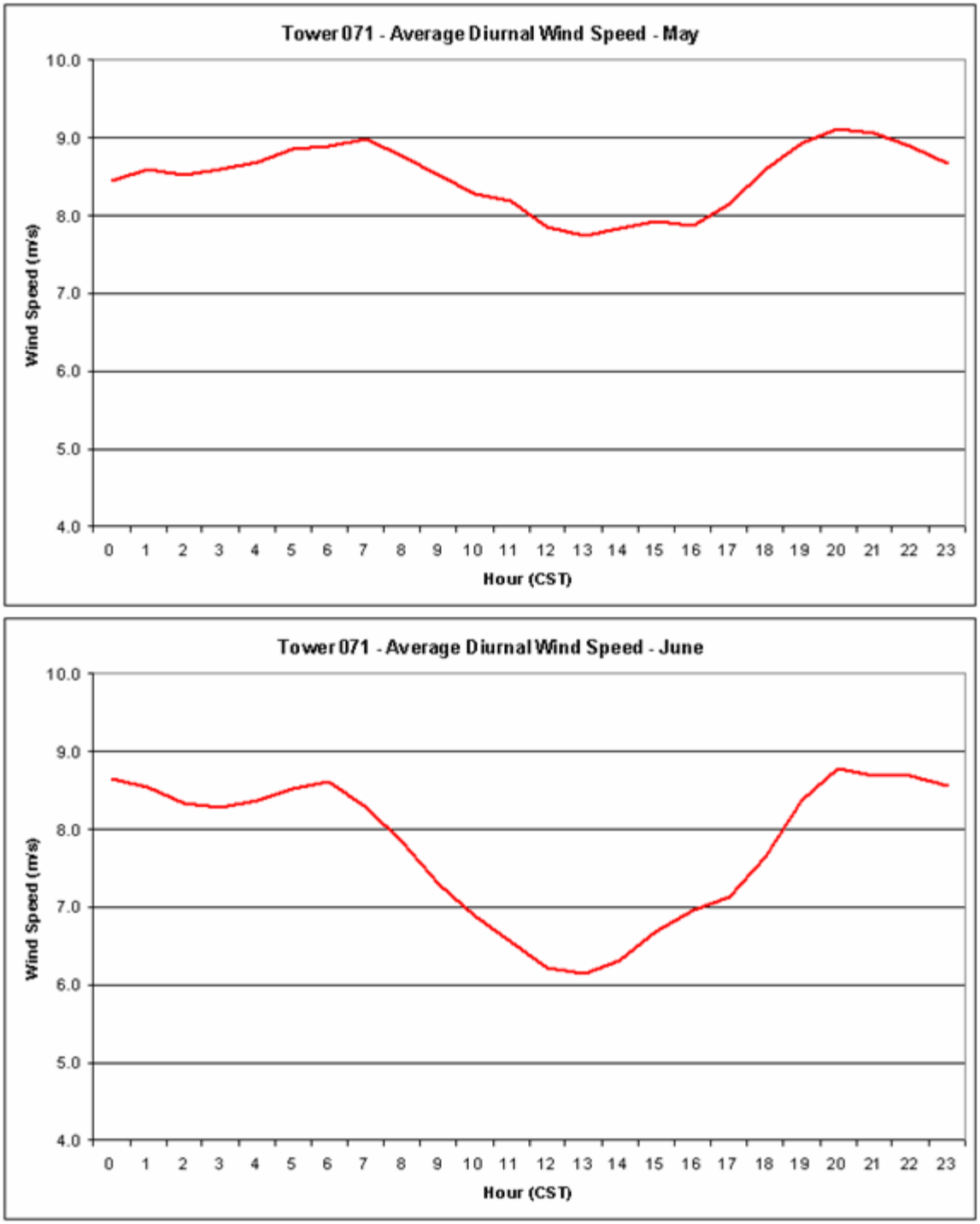

Figure 64: Average May and June 80 m diurnal wind speed at Tower 71 in m/s.

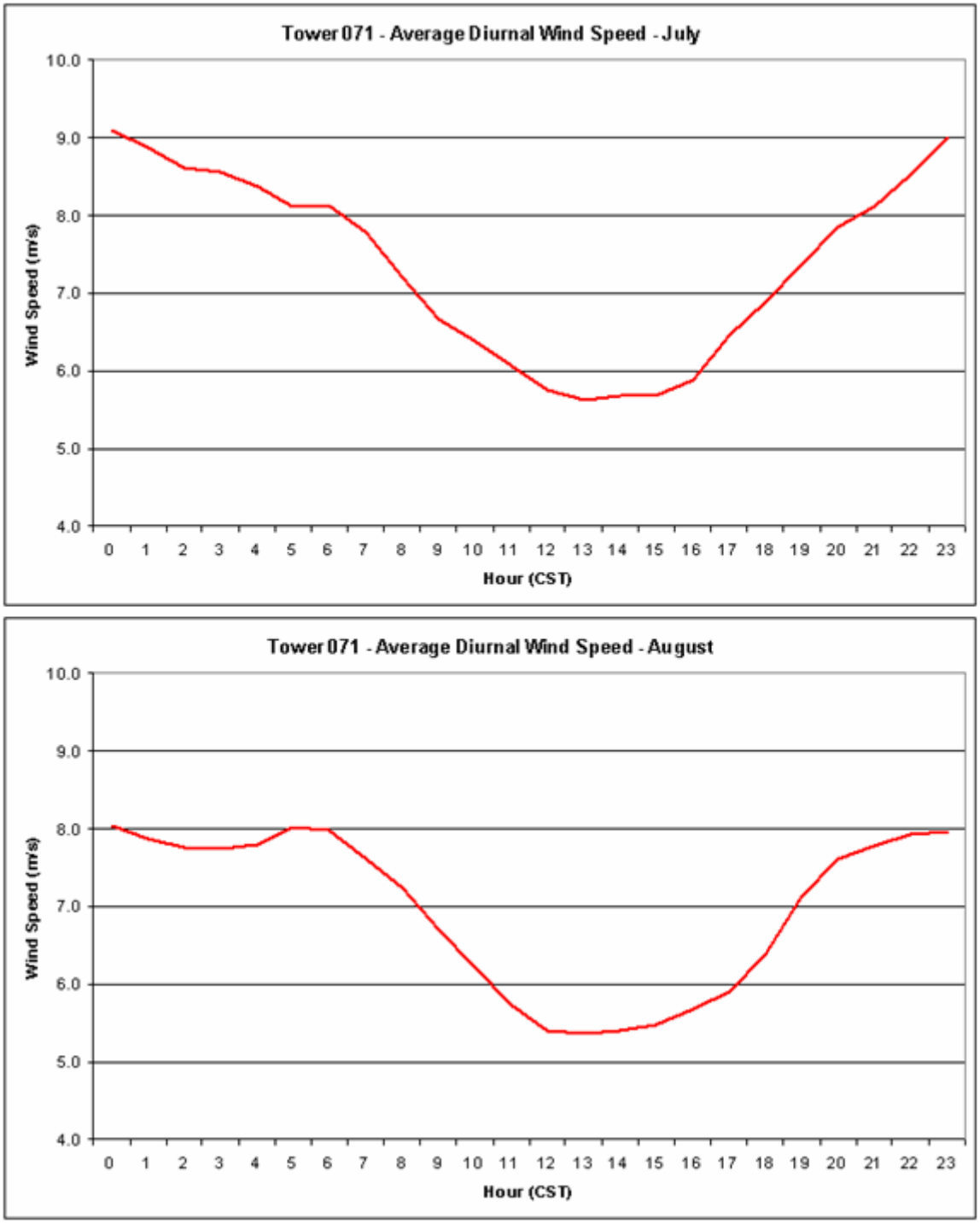

Figure 65: Average July and August 80 m diurnal wind speed at Tower 71 in m/s.

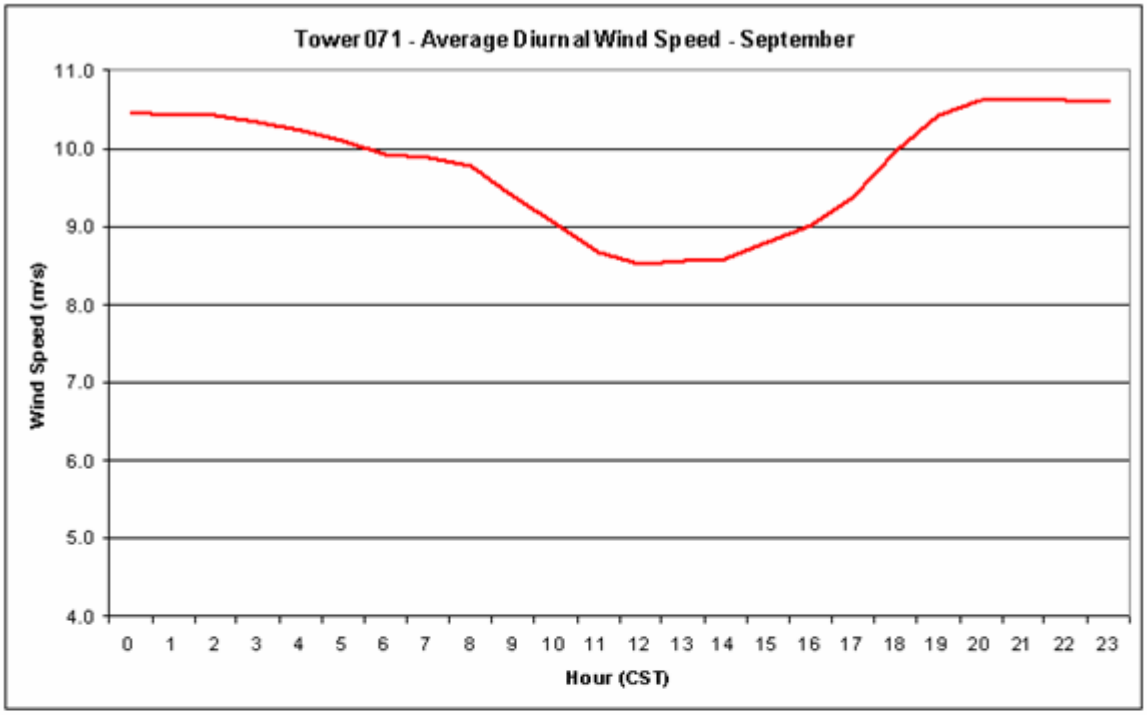

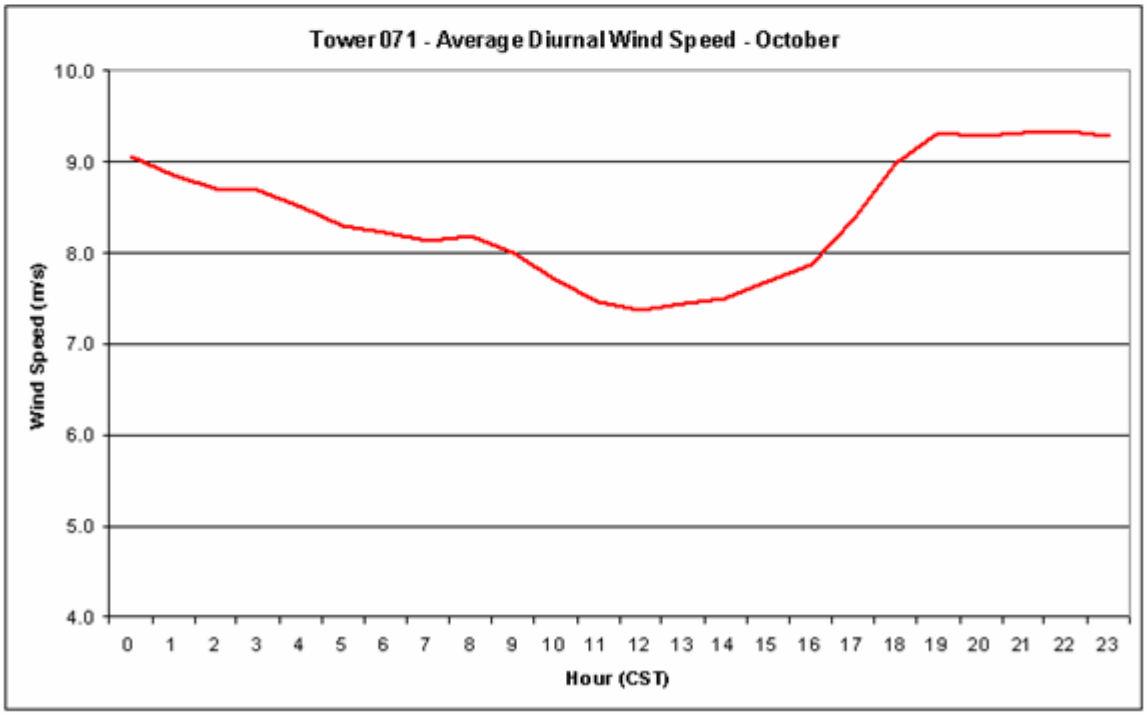

Figure 66: Average September and October 80 m diurnal wind speed at Tower 71 in m/s.

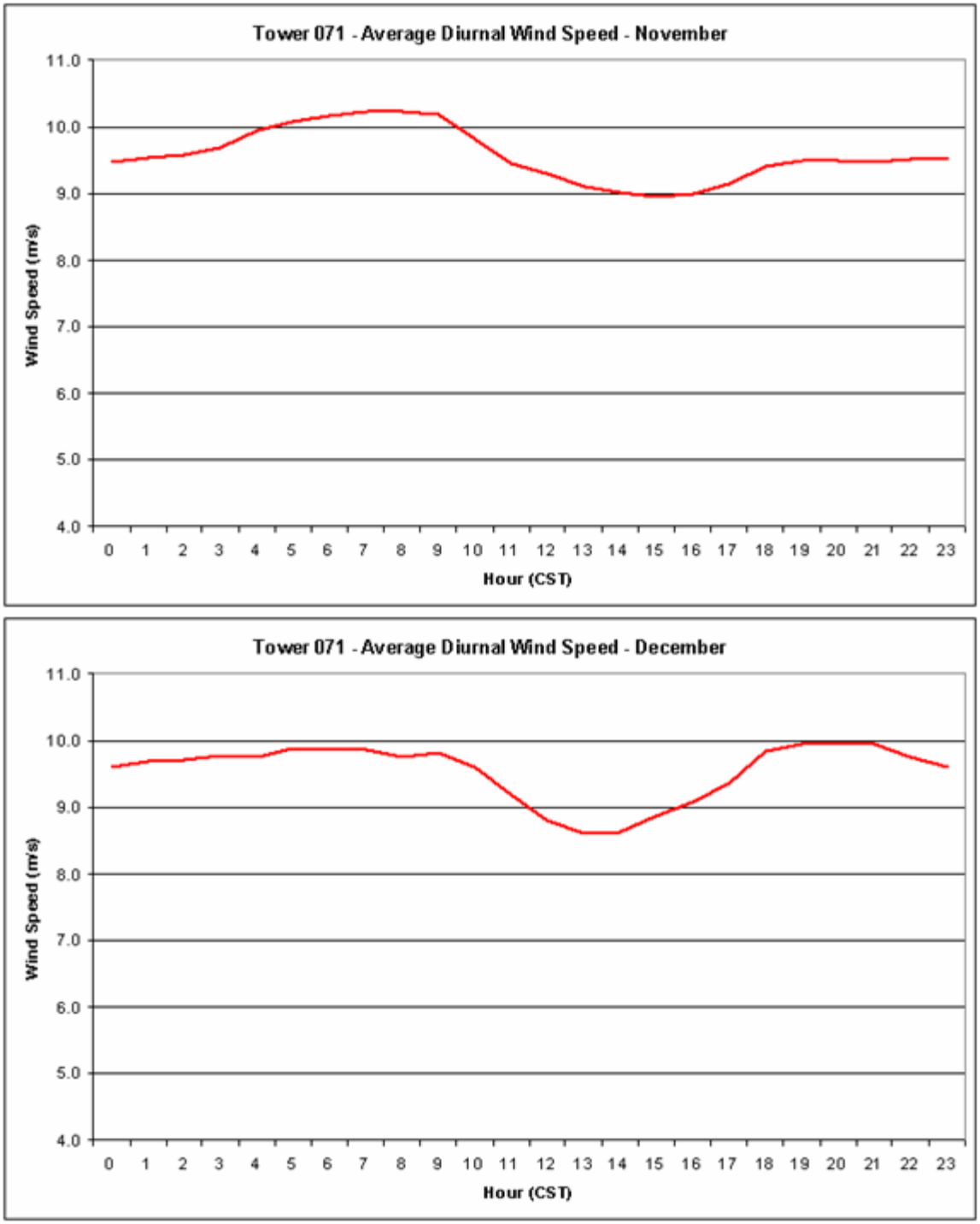

Figure 67: Average November and December 80 m diurnal wind speed at Tower 71 in m/s.

Proxy Tower 41 – Minnesota Southeast

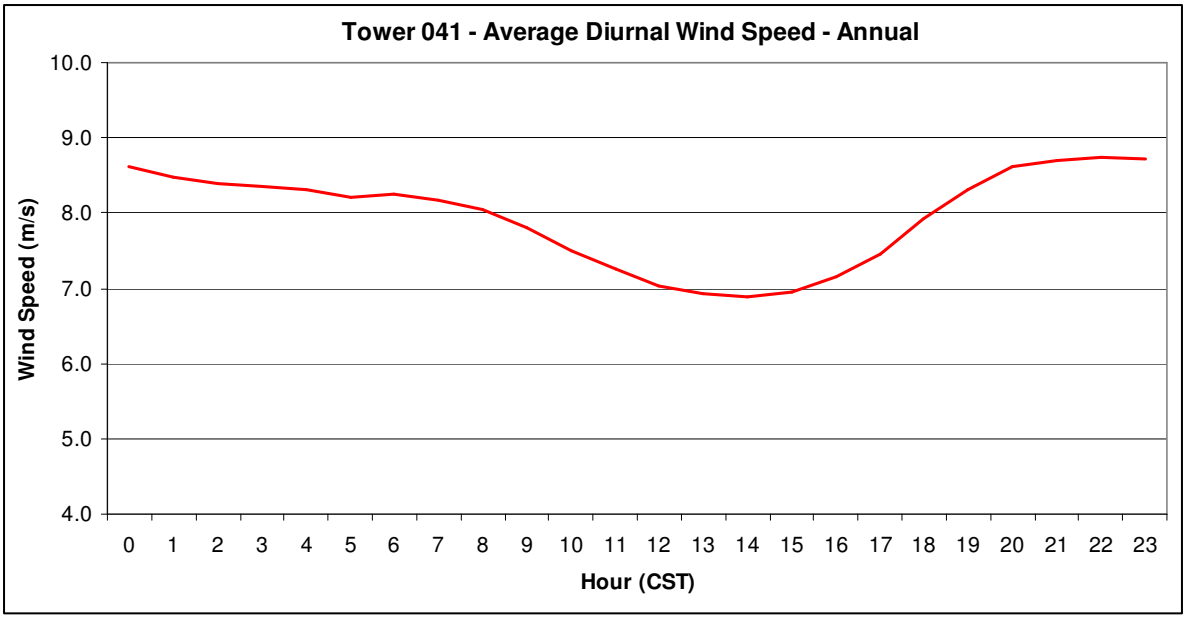

Figure 68: Average annual 80 m diurnal wind speed at Tower 41 in m/s.

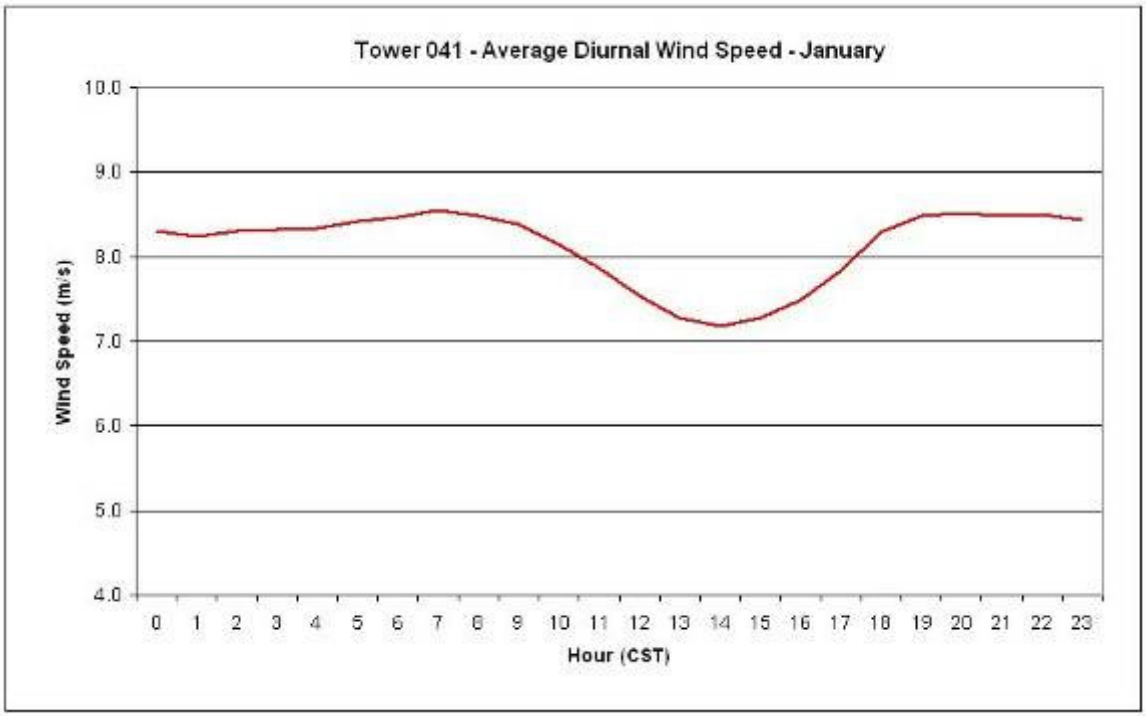

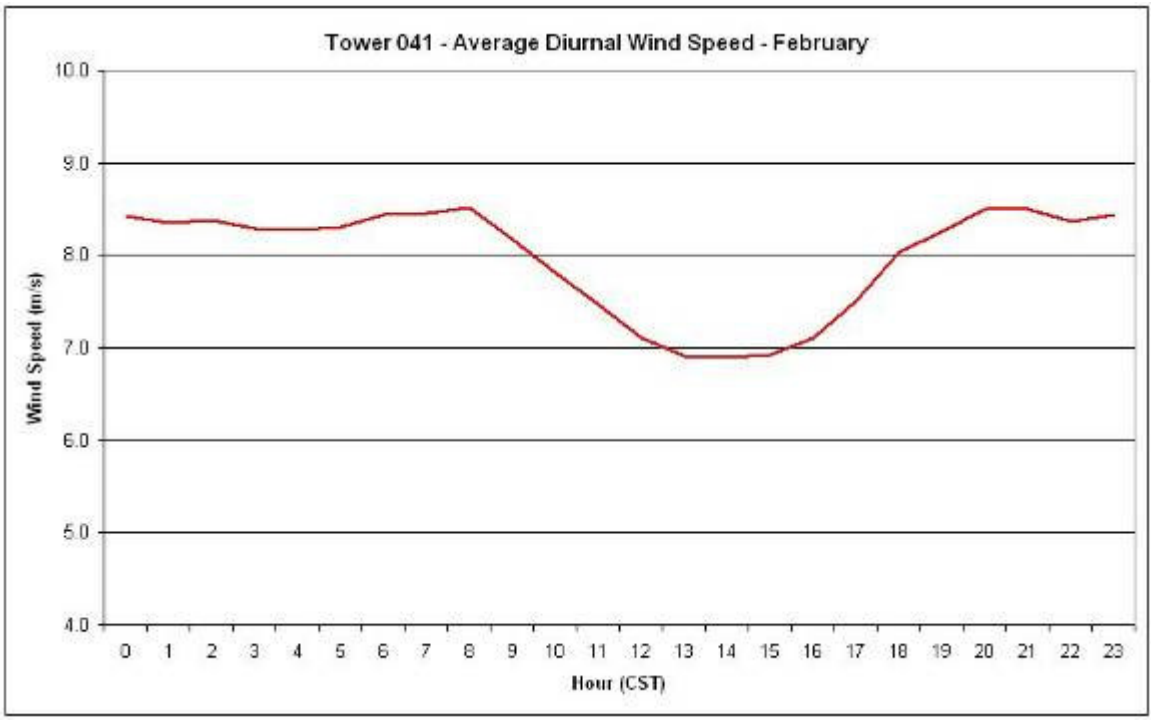

Figure 69: Average January and February 80 m diurnal wind speed at Tower 41 in m/s.

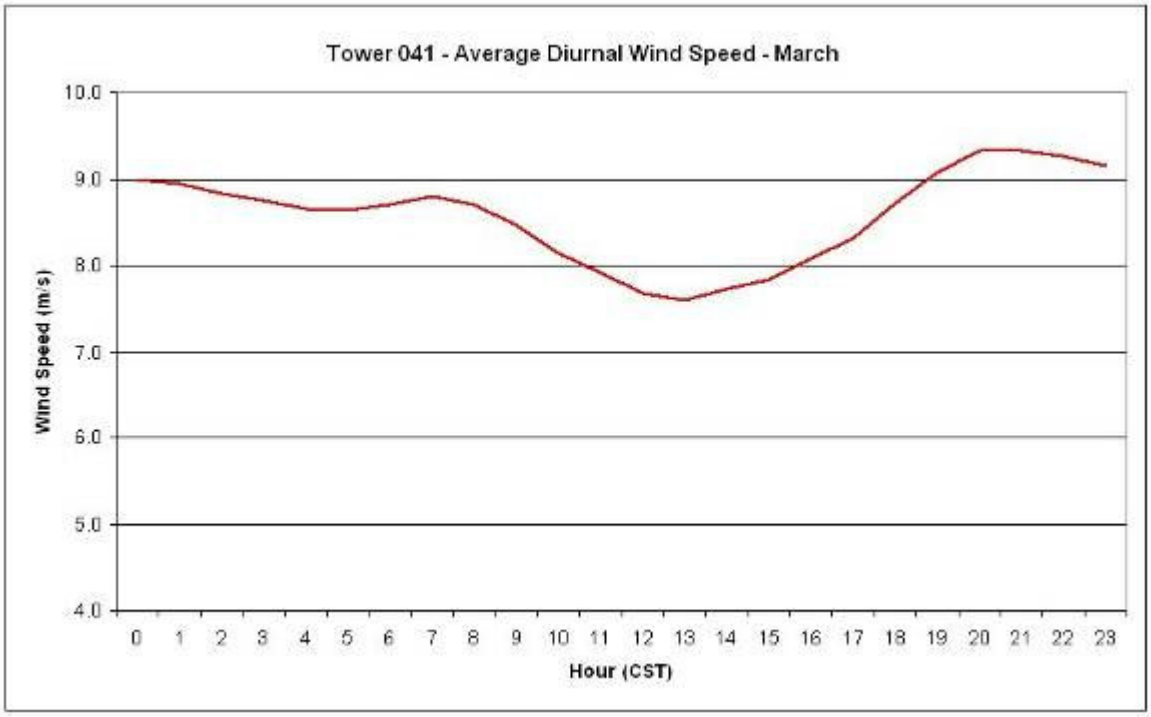

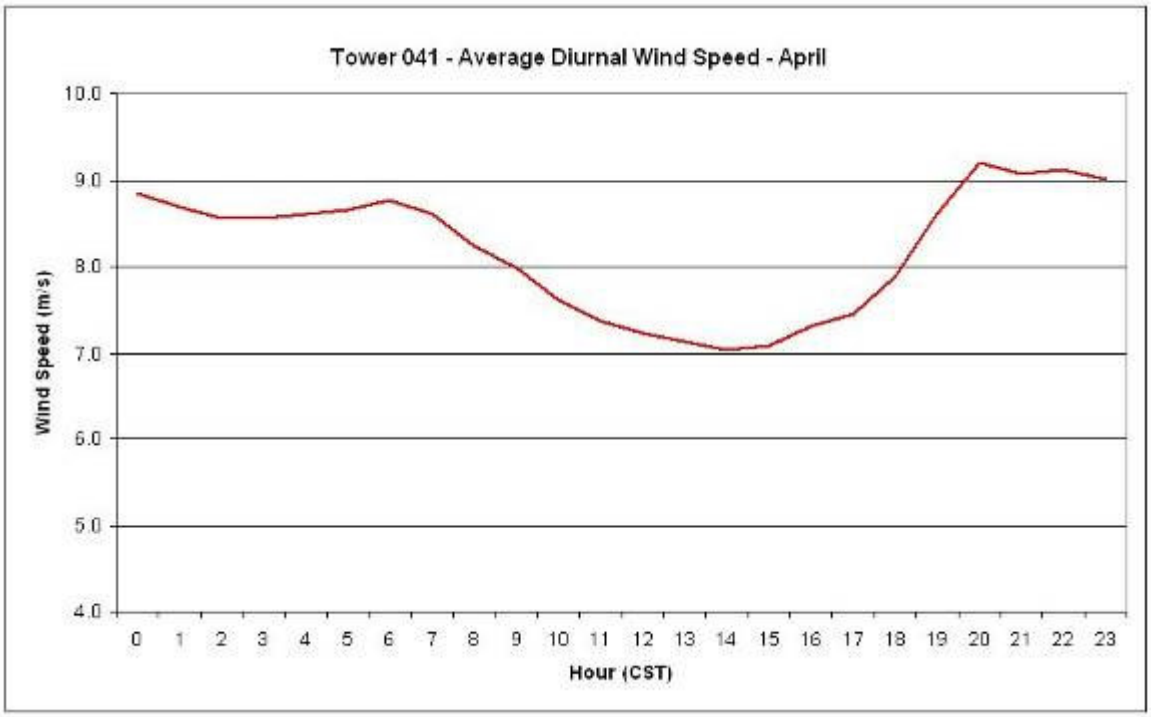

Figure 70: Average March and April 80 m diurnal wind speed at Tower 41 in m/s.

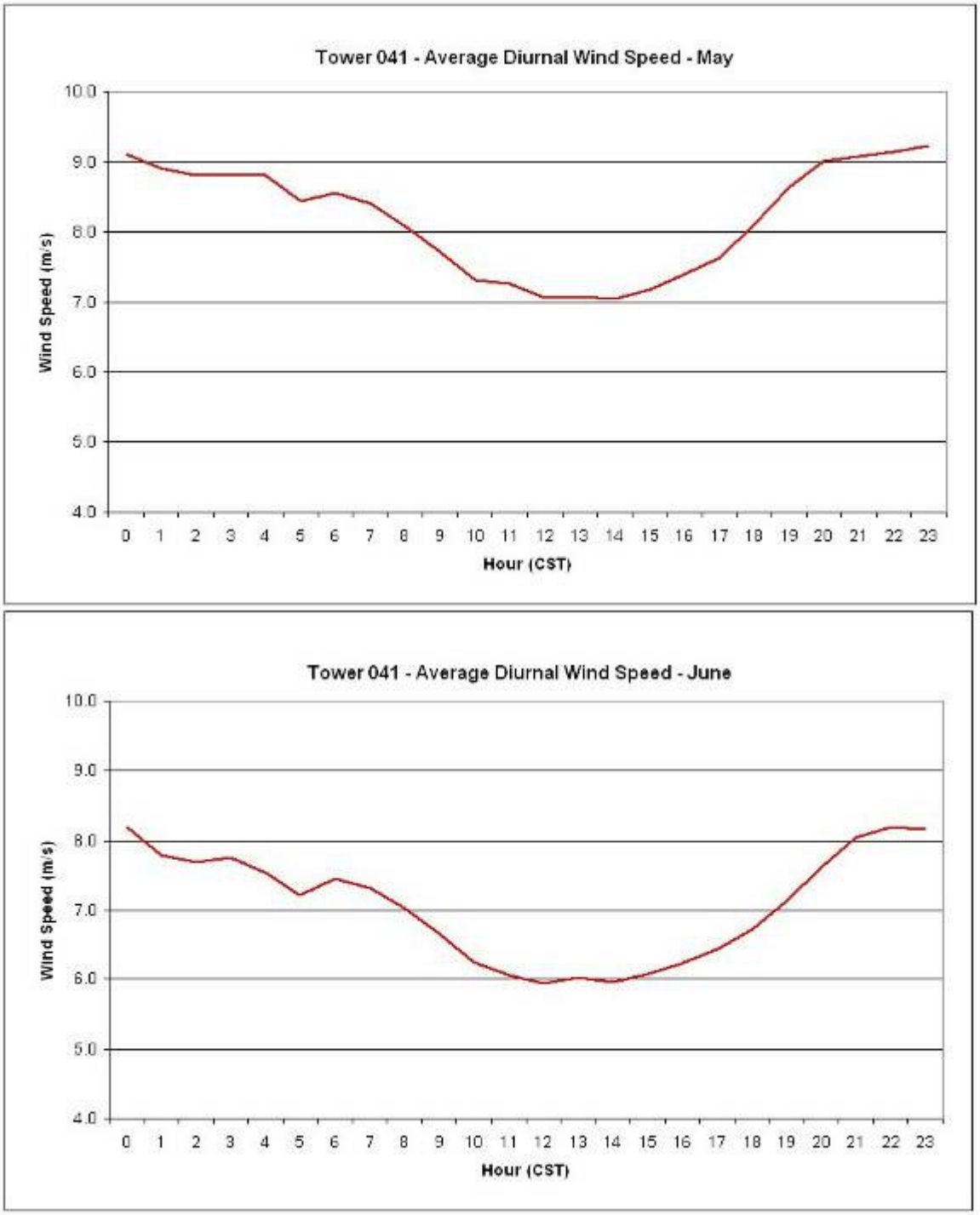

Figure 71: Average May and June 80 m diurnal wind speed at Tower 41 in m/s.

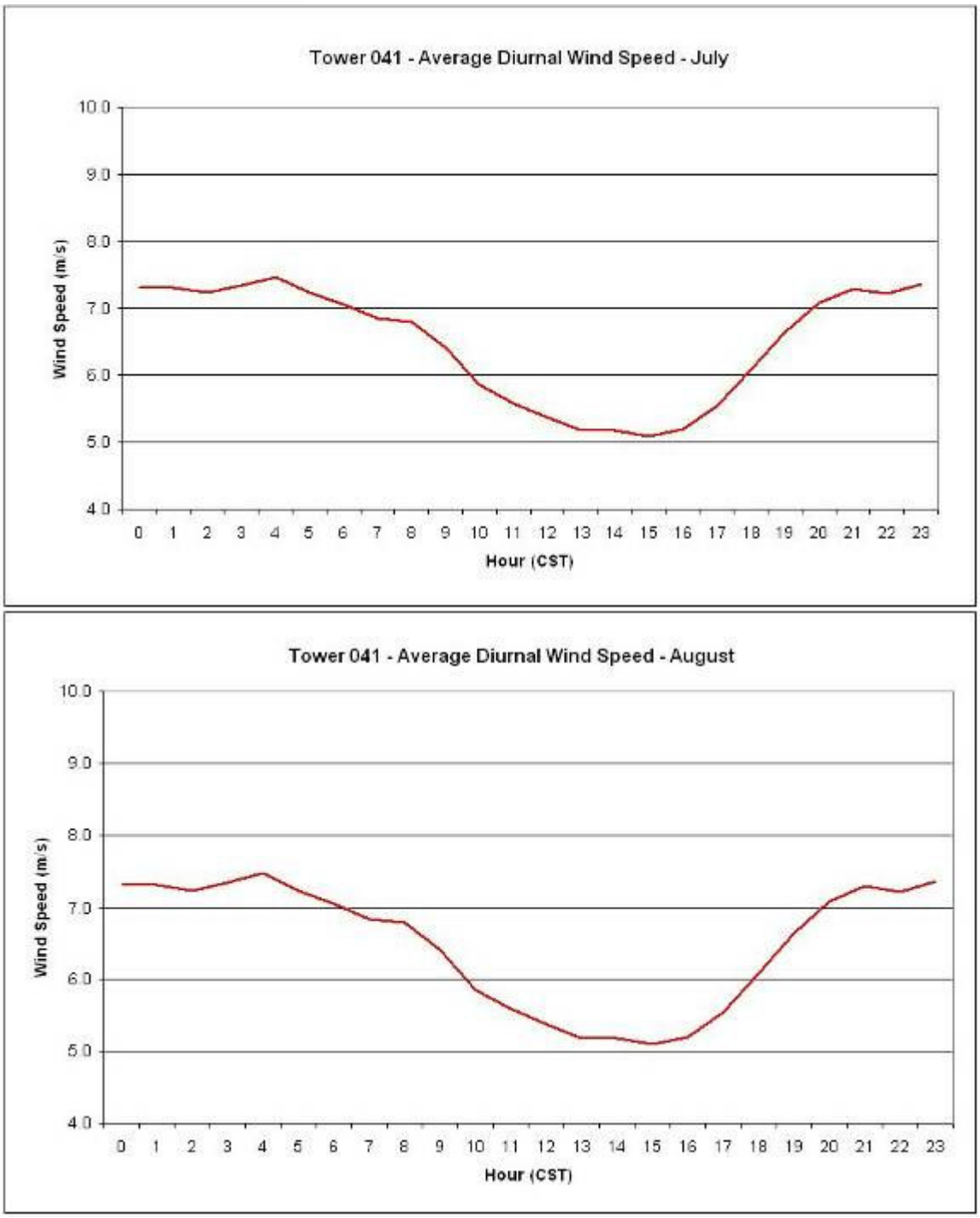

Figure 72: Average July and August 80 m diurnal wind speed at Tower 41 in m/s.

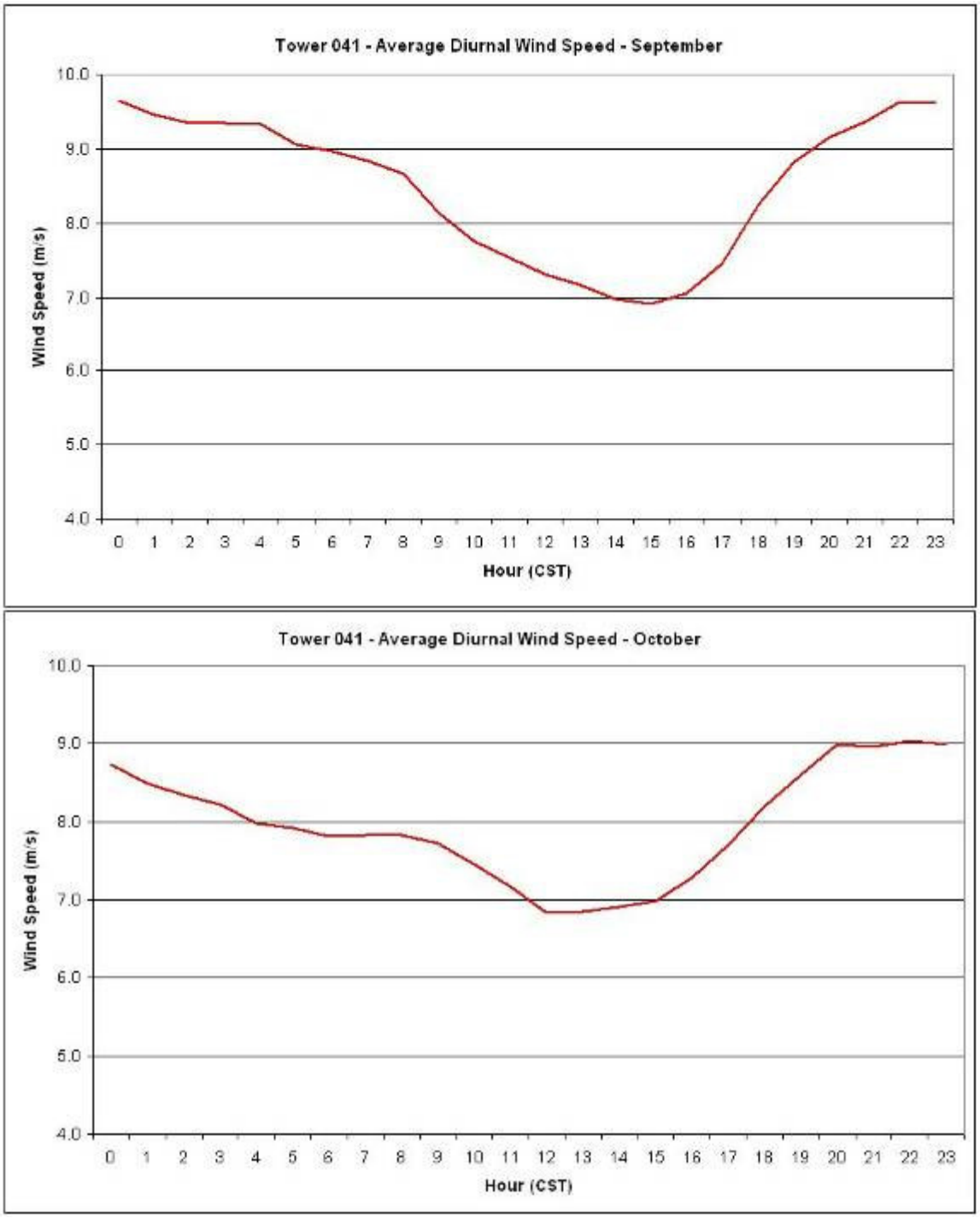

Figure 73: Average September and October 80 m diurnal wind speed at Tower 41 in m/s.

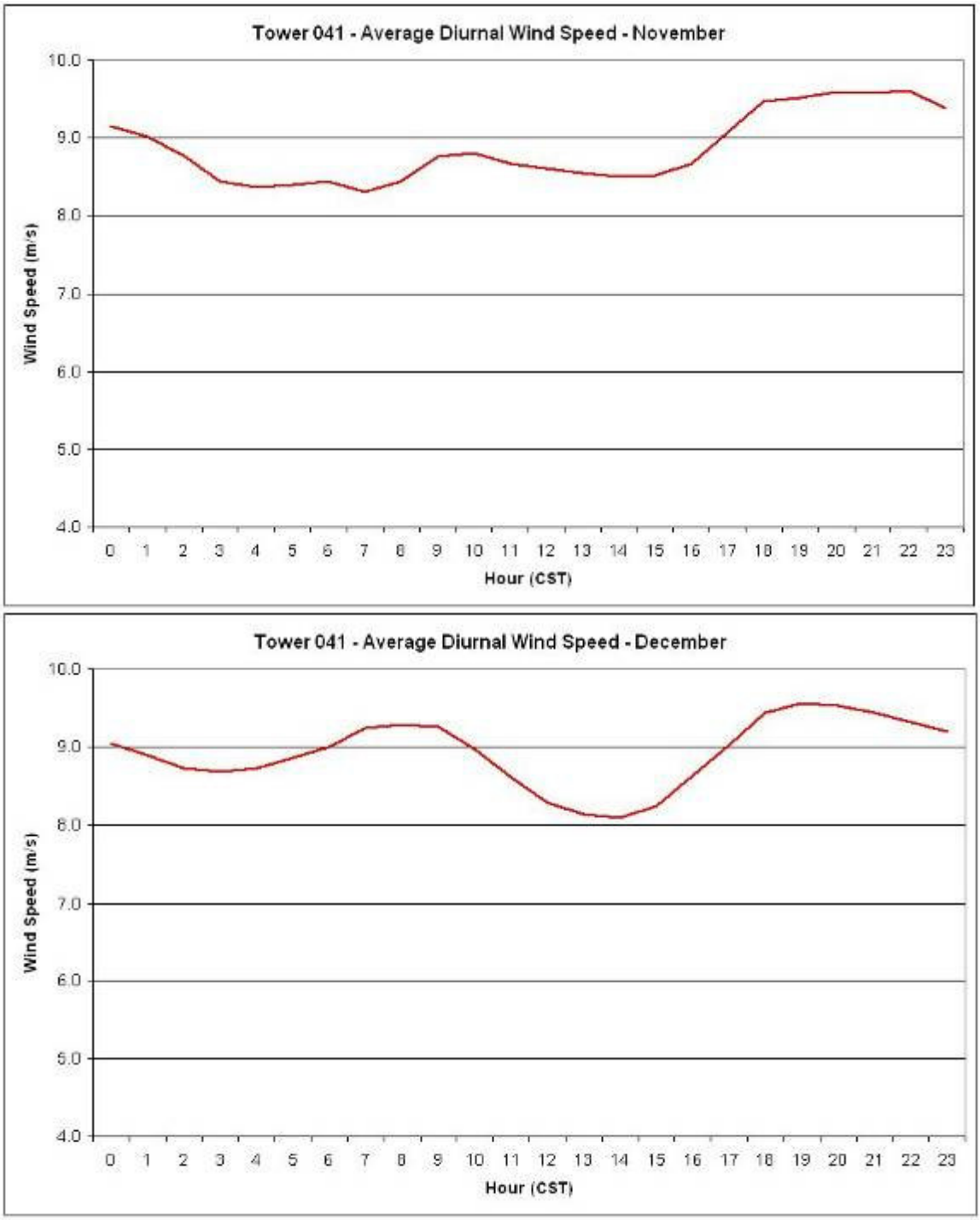

Figure 74: Average November and December 80 m diurnal wind speed at Tower 41 in m/s.

Proxy Tower 82 – Minnesota-Northeast

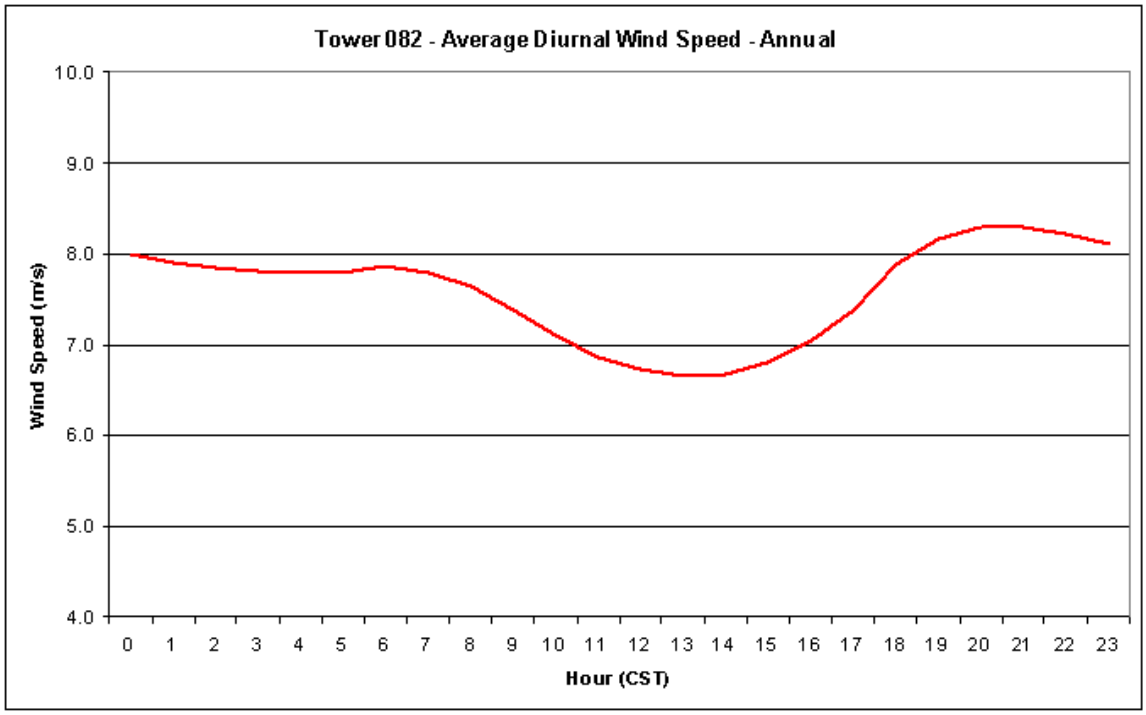

Figure 75: Average annual 80 m diurnal wind speed at Tower 82 in m/s.

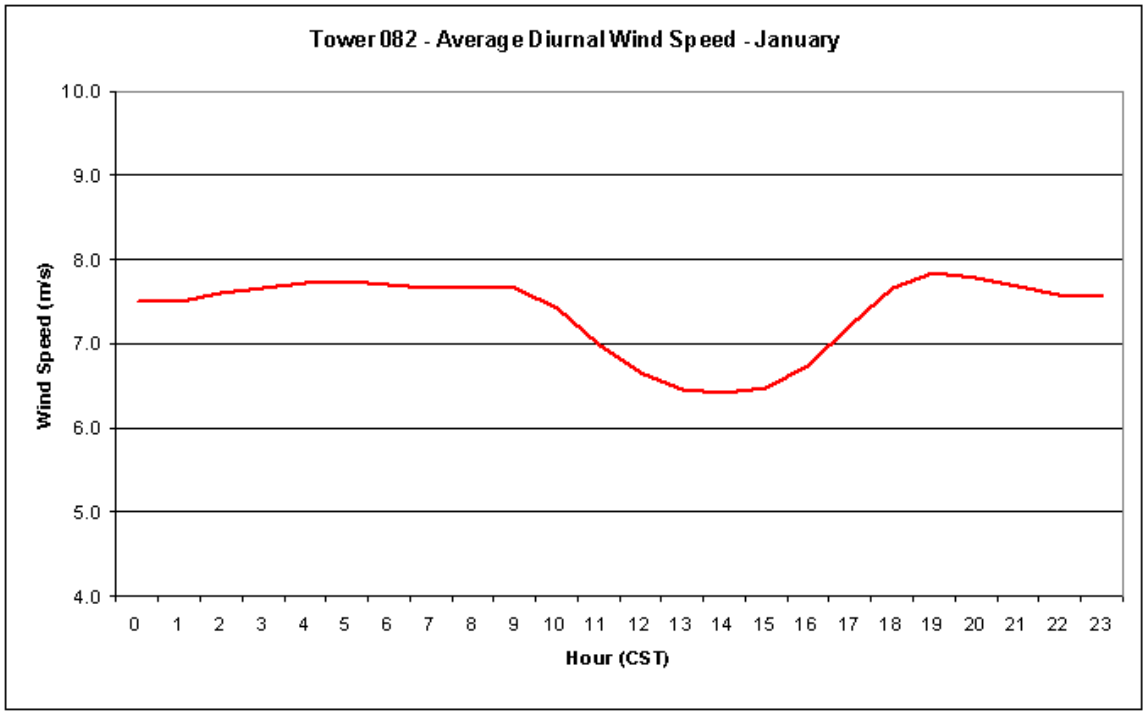

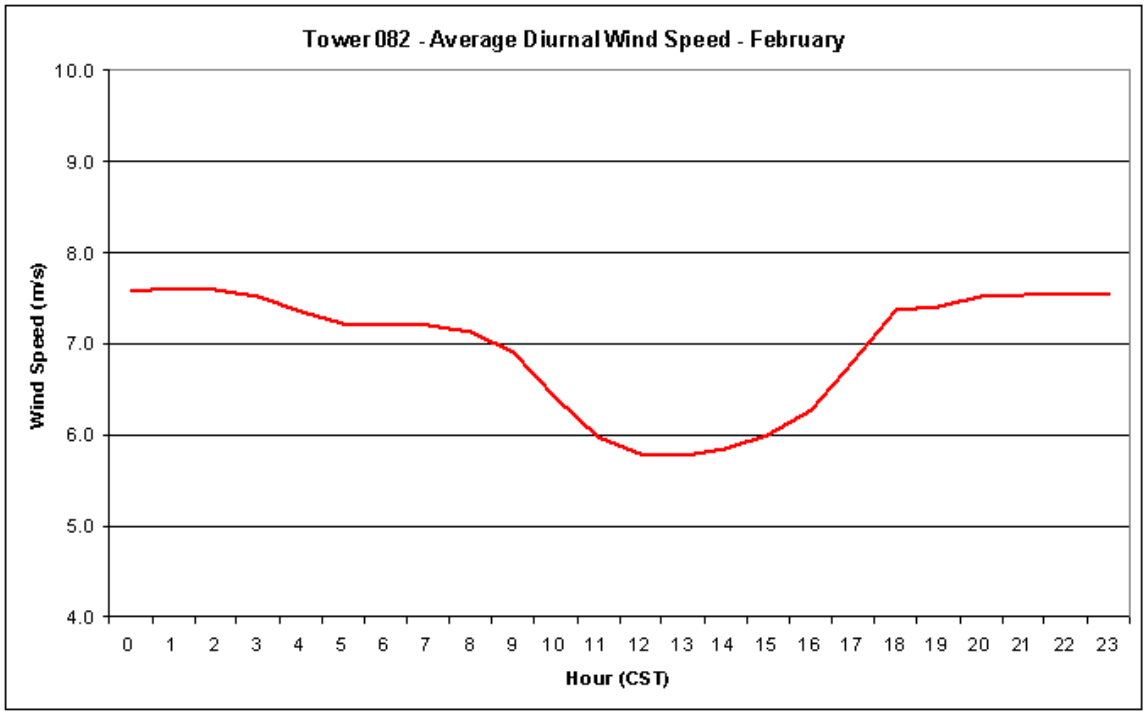

Figure 76: Average January and February 80 m diurnal wind speed at Tower 82 in m/s.

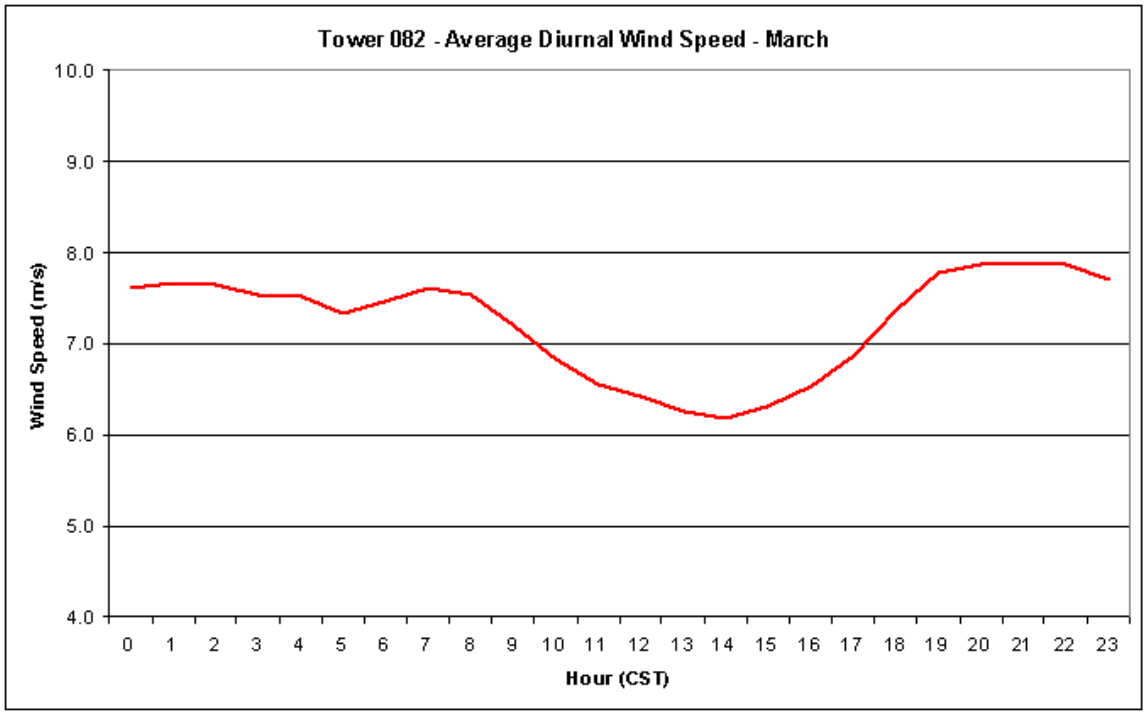

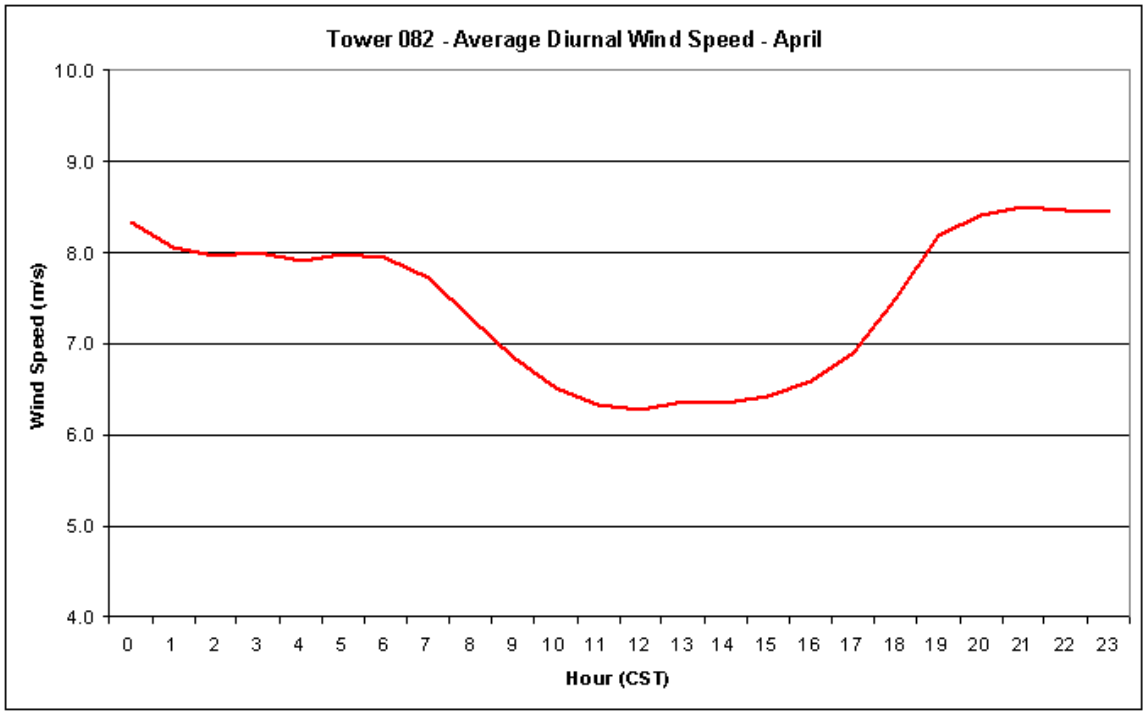

Figure 77: Average March and April 80 m diurnal wind speed at Tower 82 in m/s.

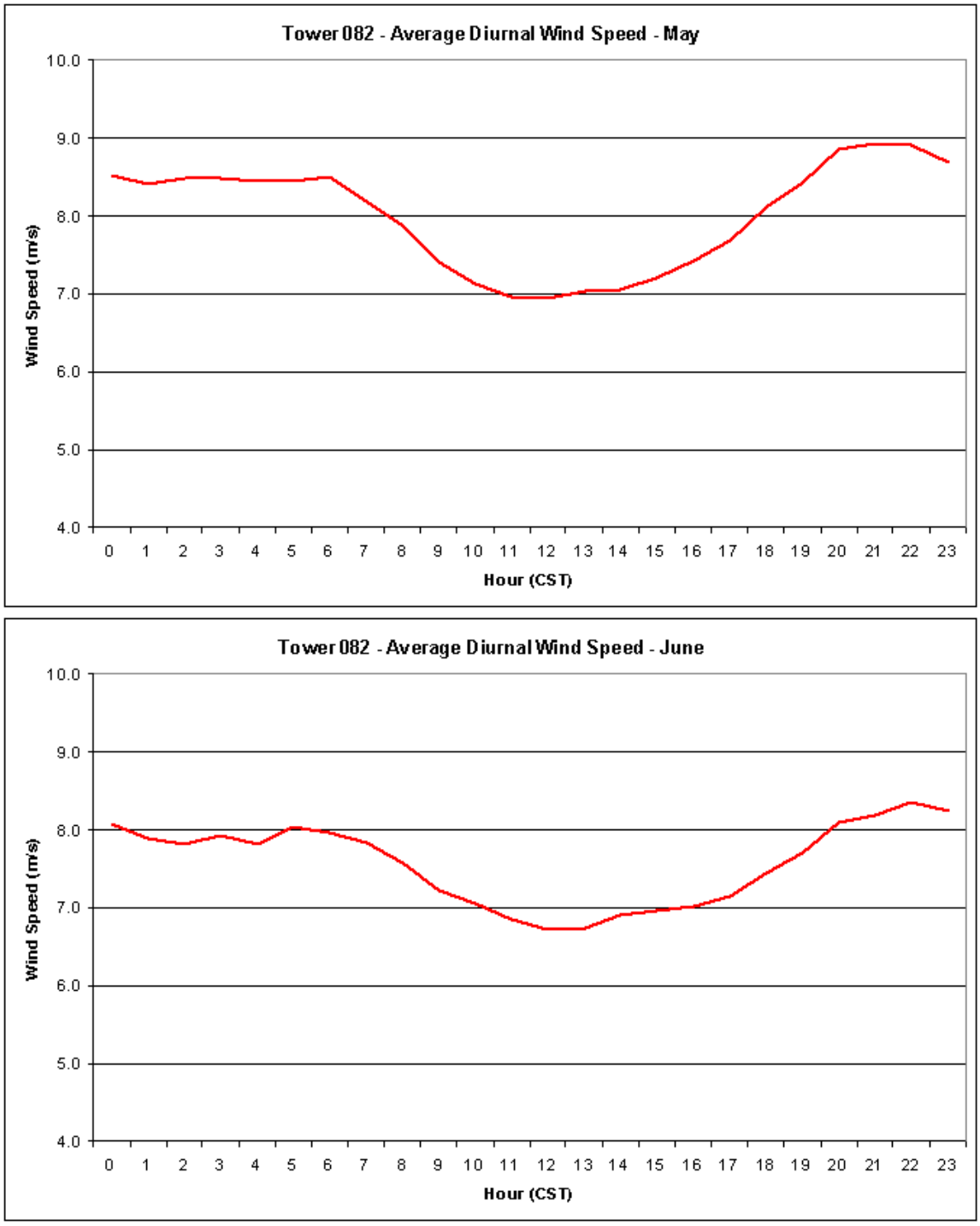

Figure 78: Average May and June 80 m diurnal wind speed at Tower 82 in m/s.

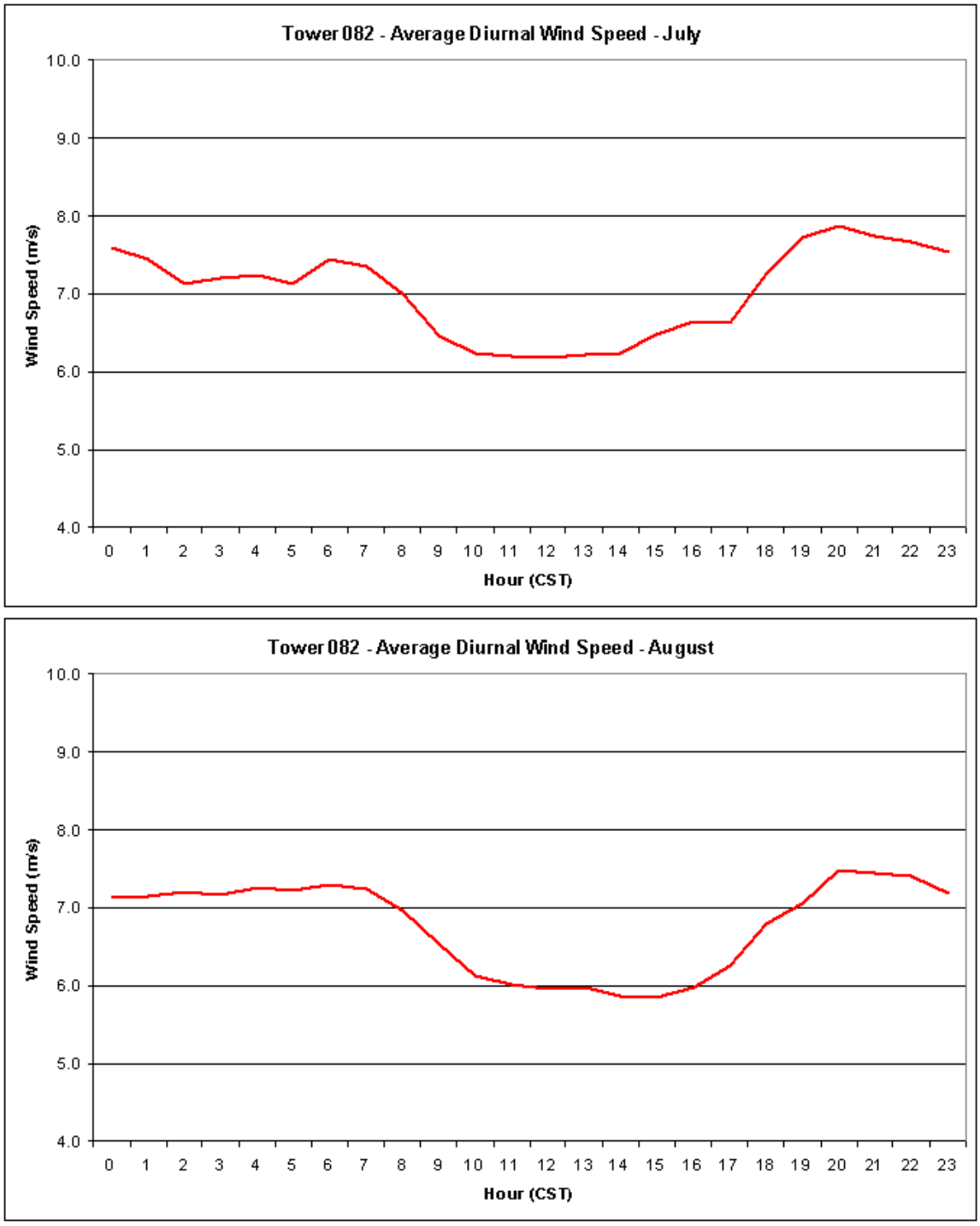

Figure 79: Average July and August 80 m diurnal wind speed at Tower 82 in m/s.

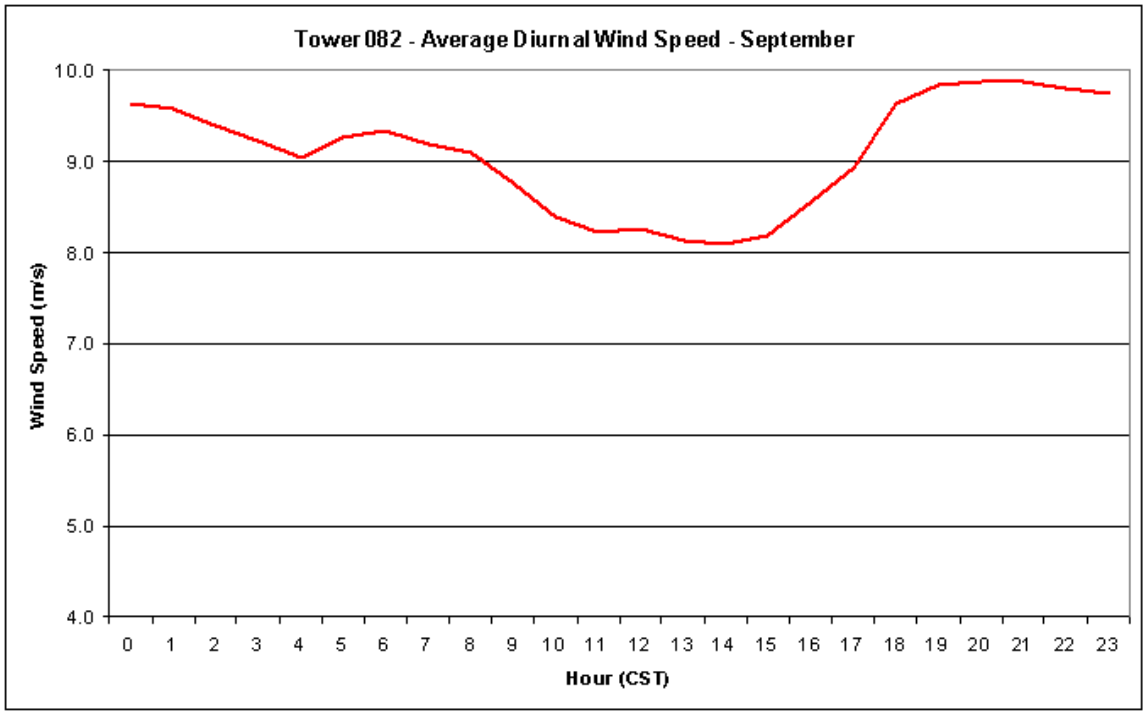

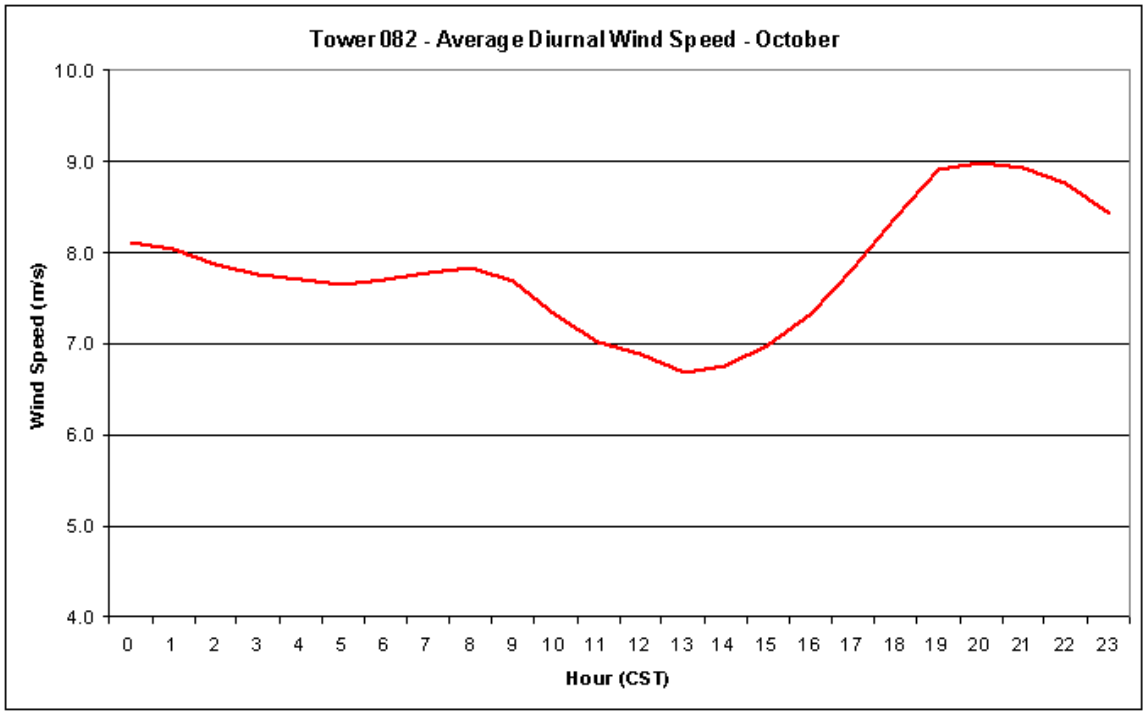

Figure 80: Average September and October 80 m diurnal wind speed at Tower 82 in m/s.

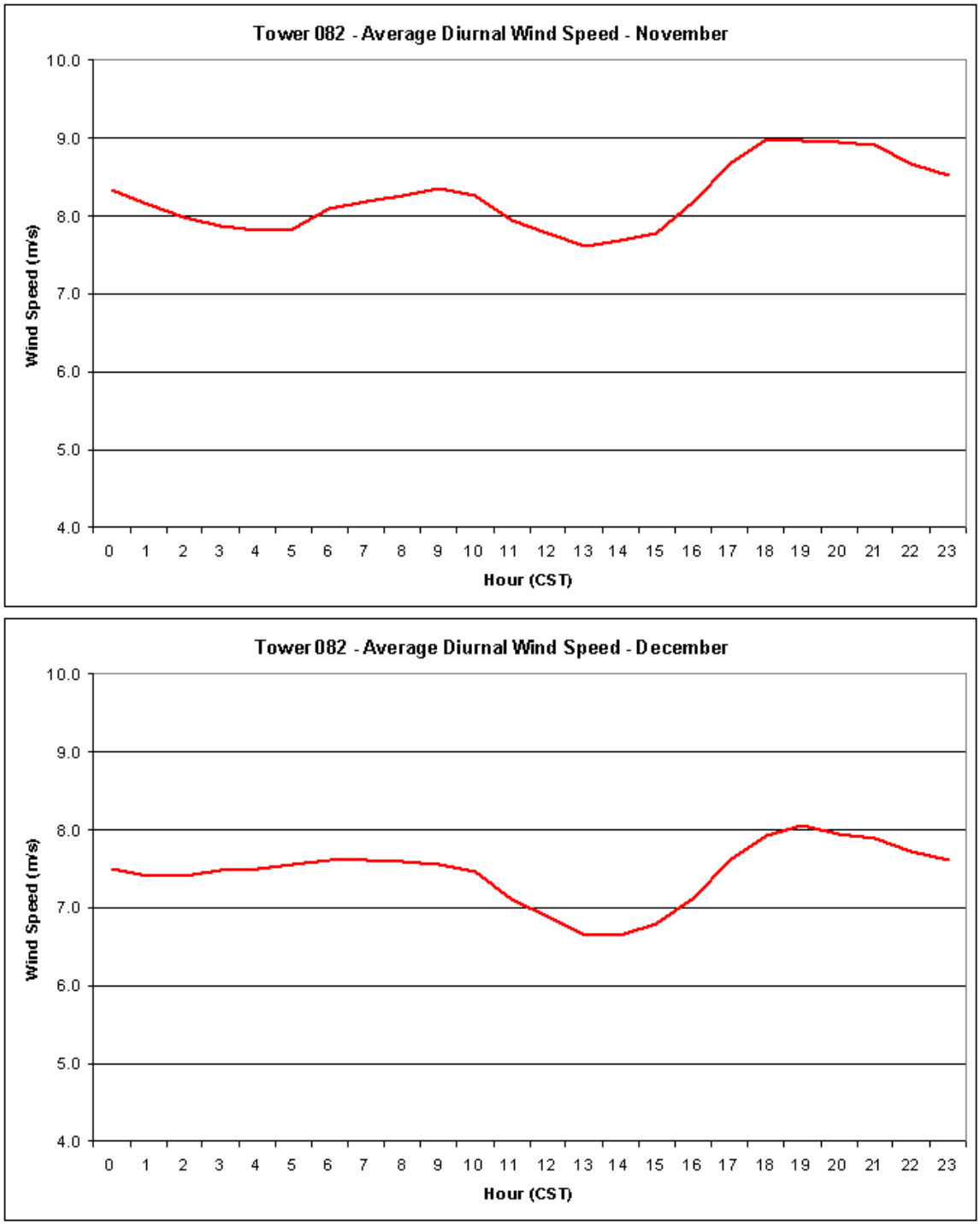

Figure 81: Average November and December 80 m diurnal wind speed at Tower 82 in m/s.

Proxy Tower 115 – North Dakota Central

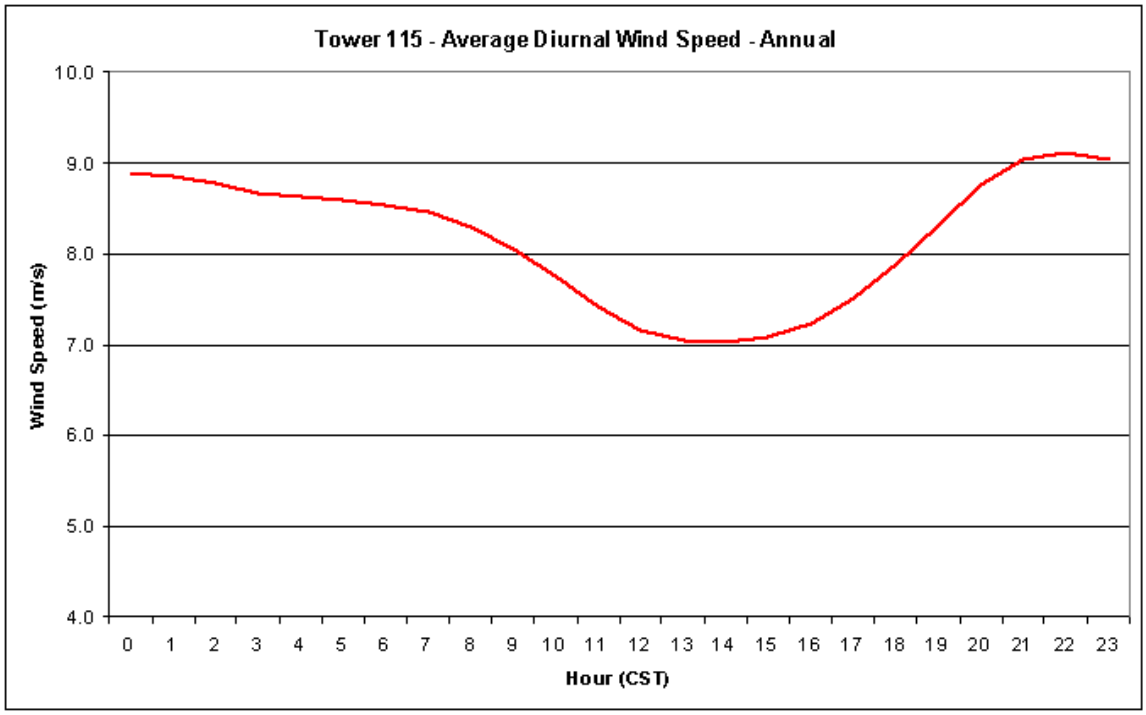

Figure 82: Average annual 80 m diurnal wind speed at Tower 115 in m/s.

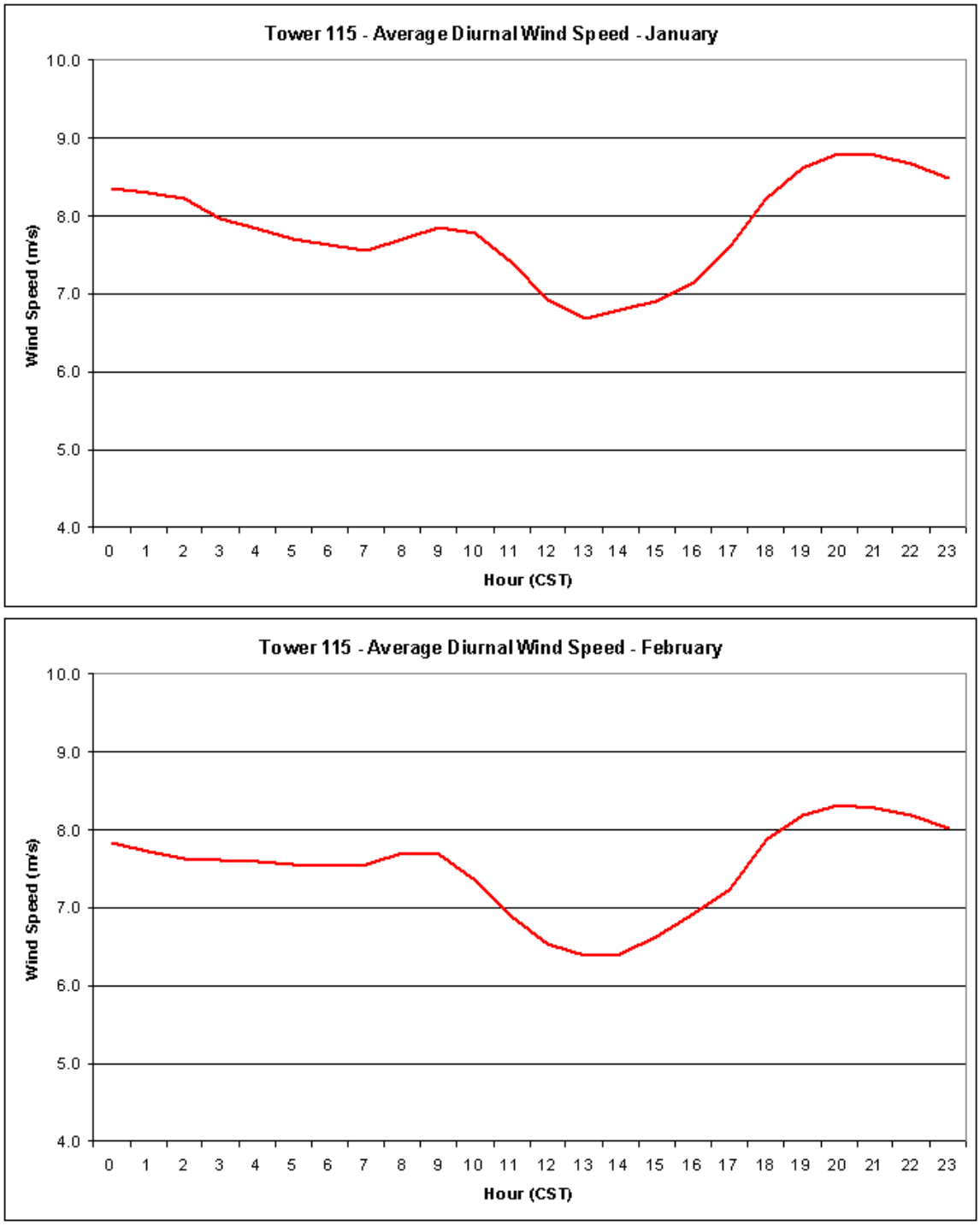

Figure 83: Average January and February 80 m diurnal wind speed at Tower 115 in m/s.

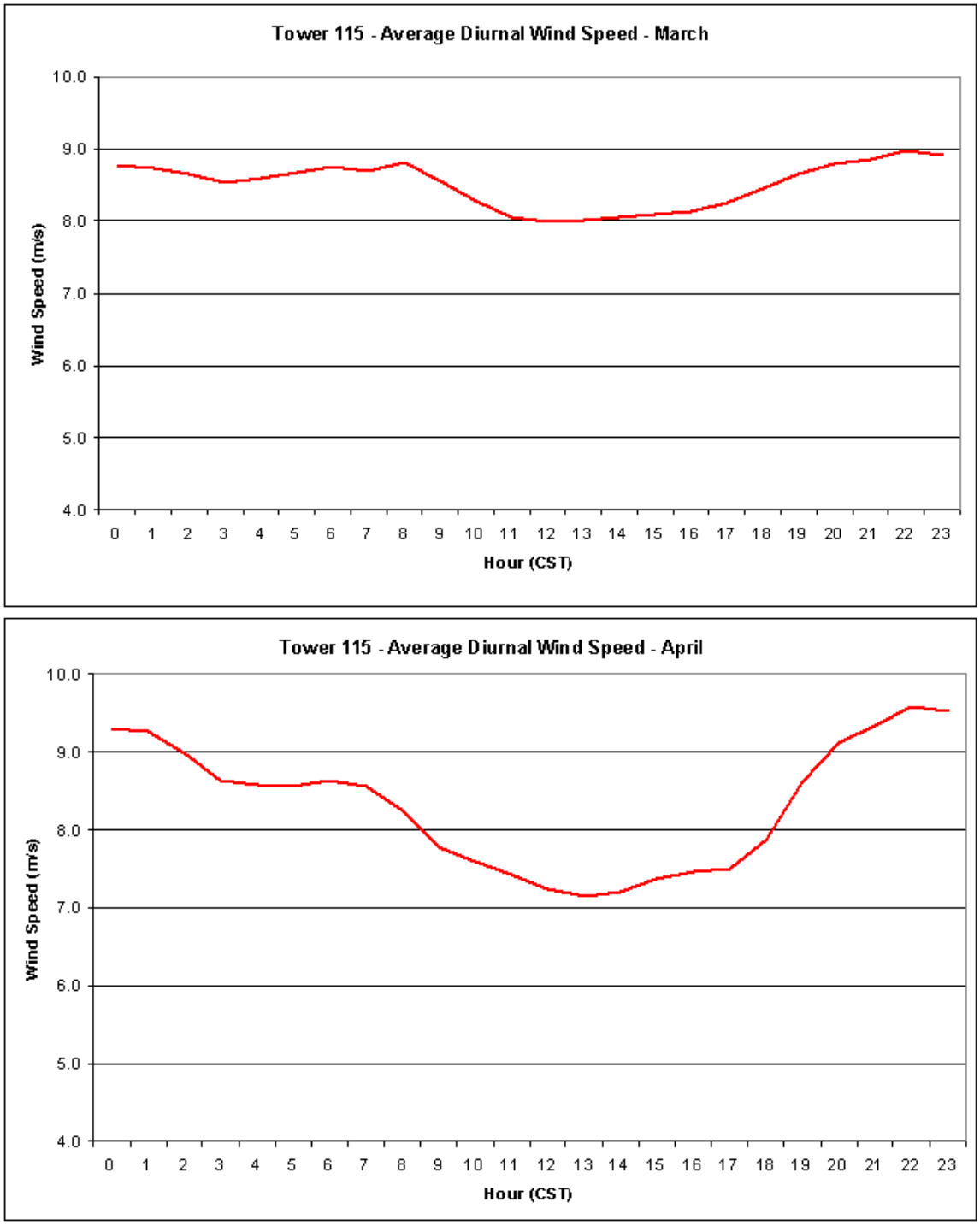

Figure 84: Average March and April 80 m diurnal wind speed at Tower 115 in m/s.

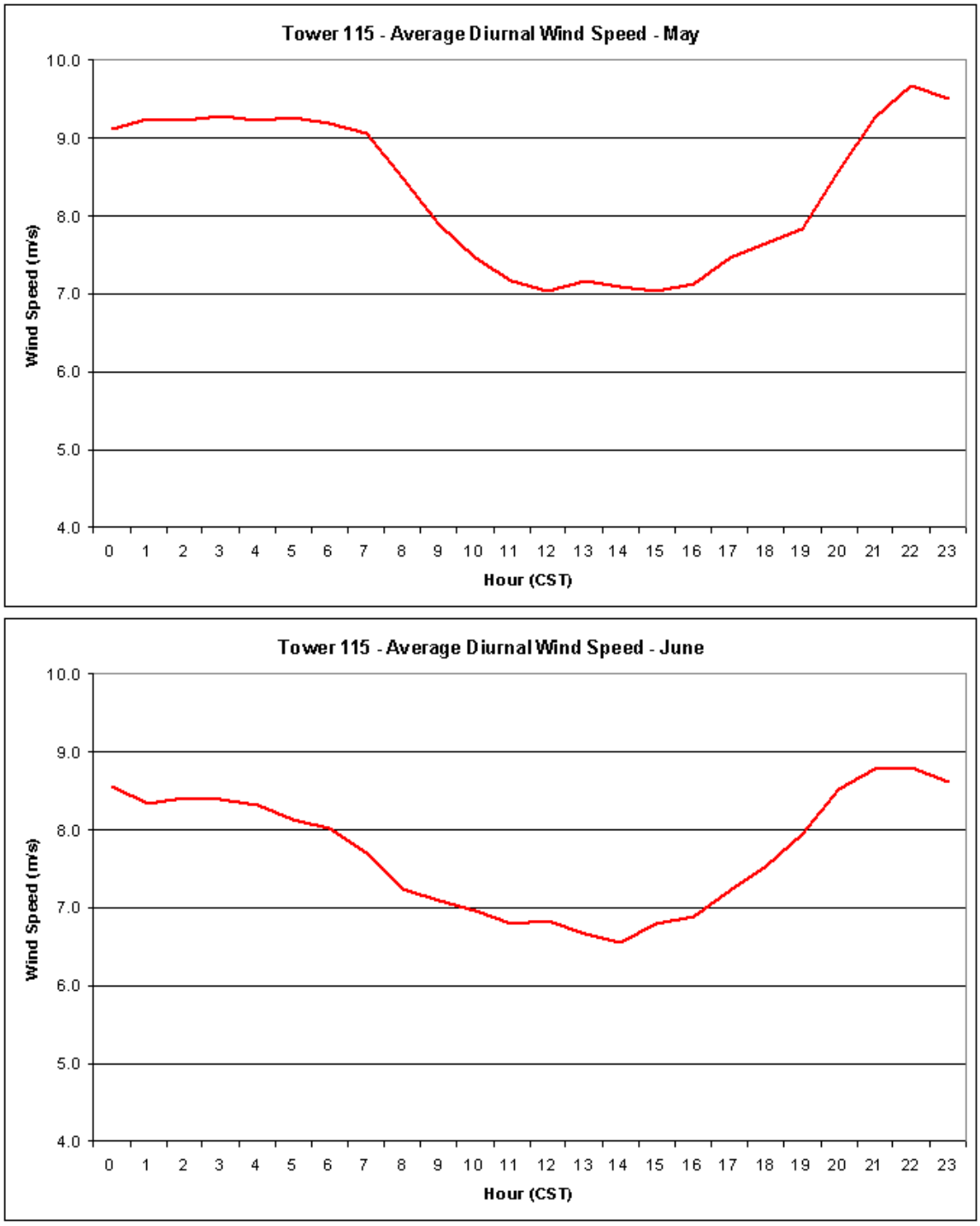

Figure 85: Average May and June 80 m diurnal wind speed at Tower 115 in m/s.

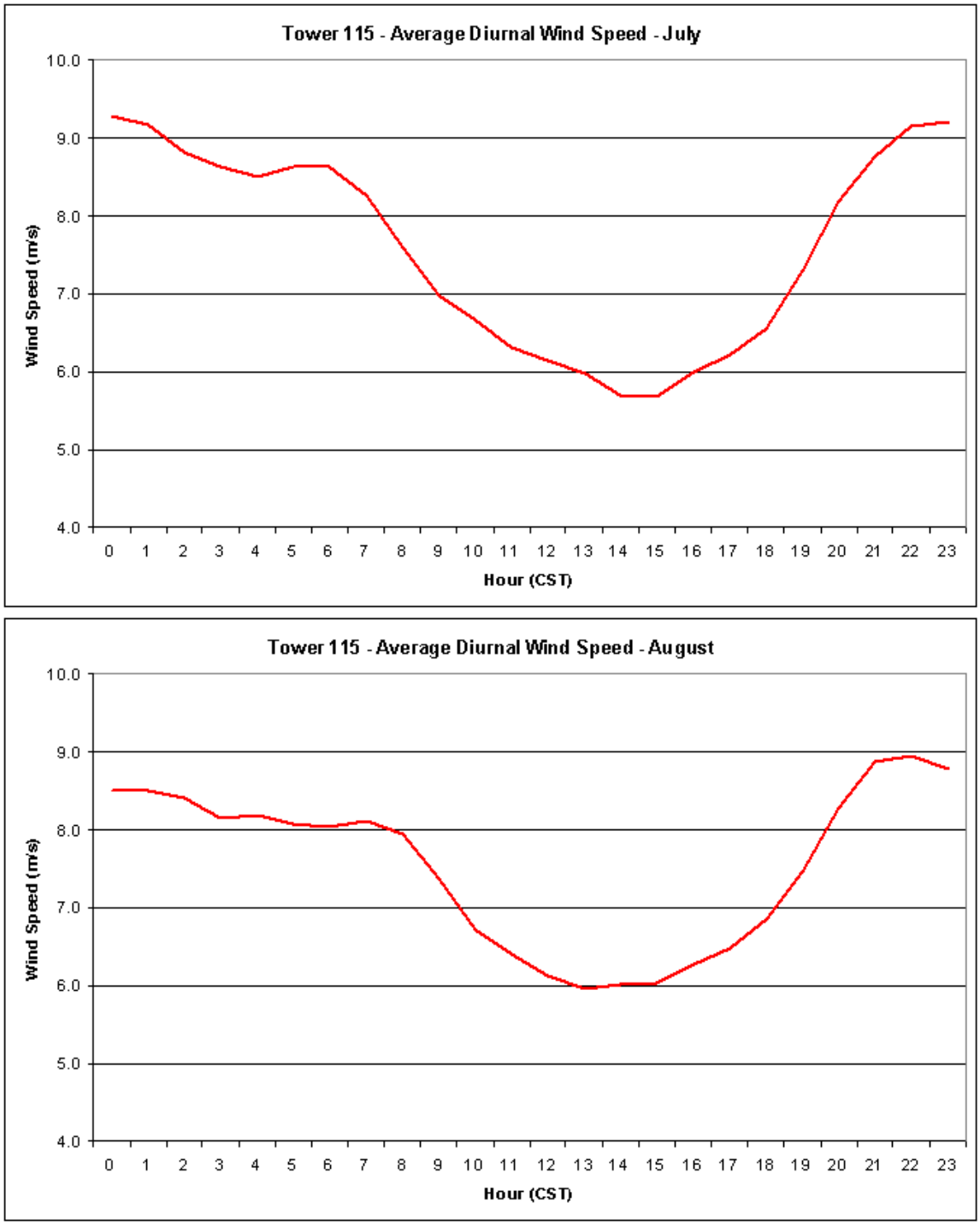

Figure 86: Average July and August 80 m diurnal wind speed at Tower 115 in m/s.

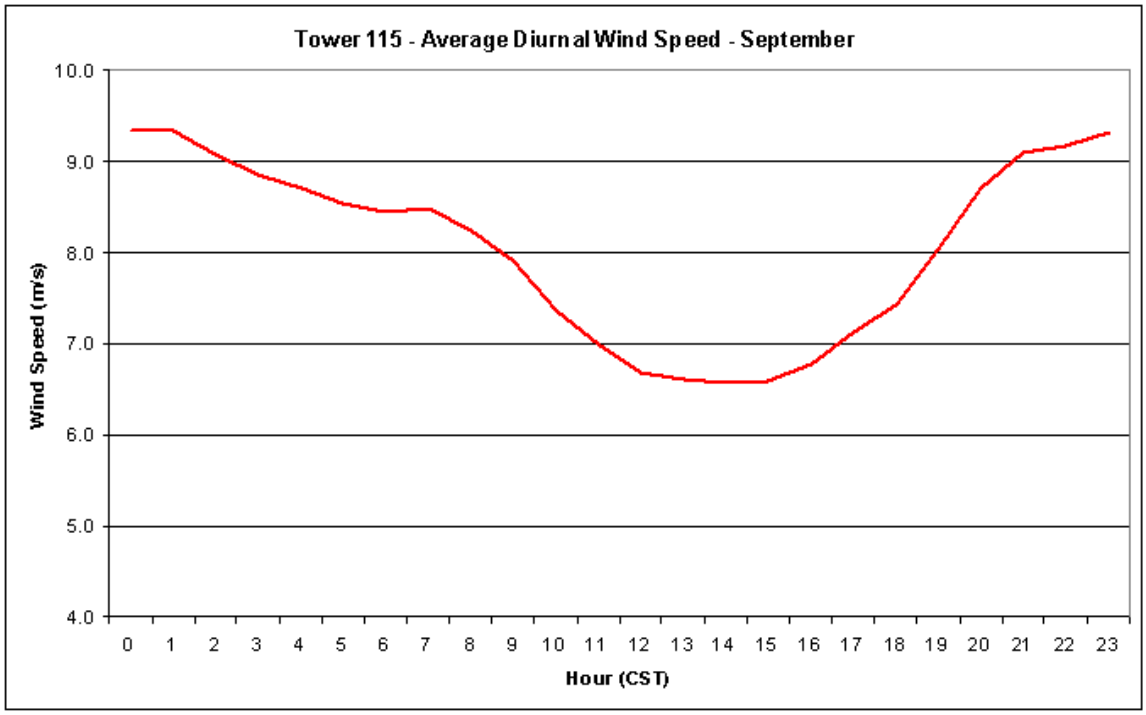

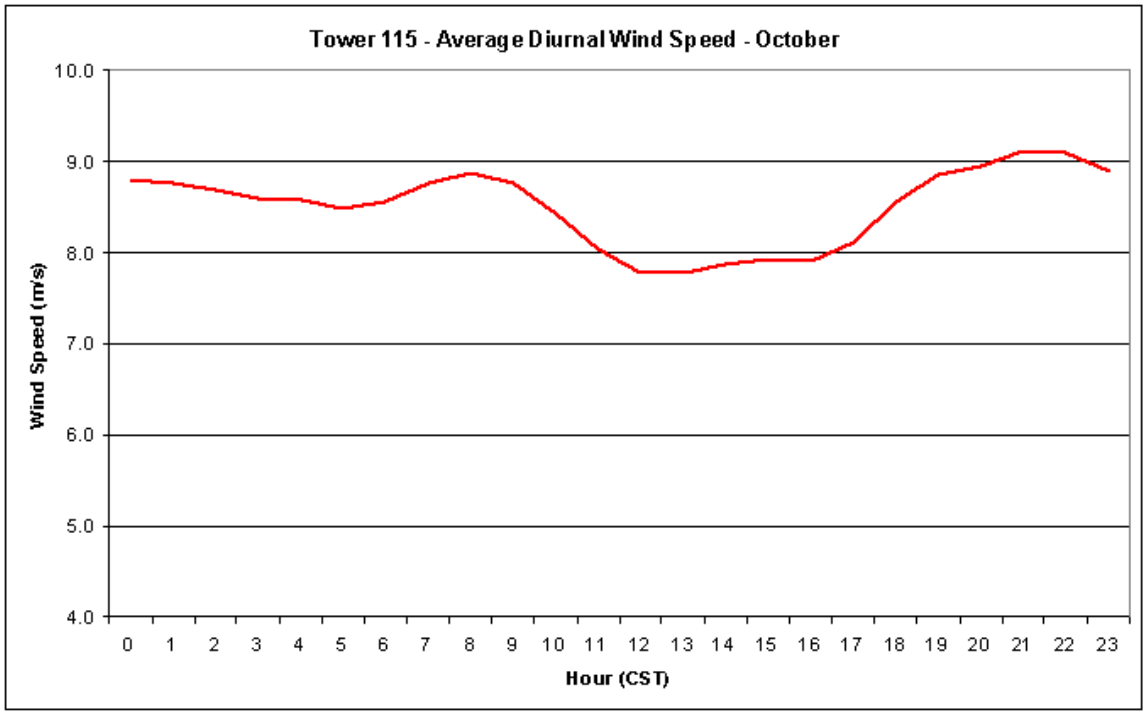

Figure 87: Average September and October 80 m diurnal wind speed at Tower 115 in m/s.

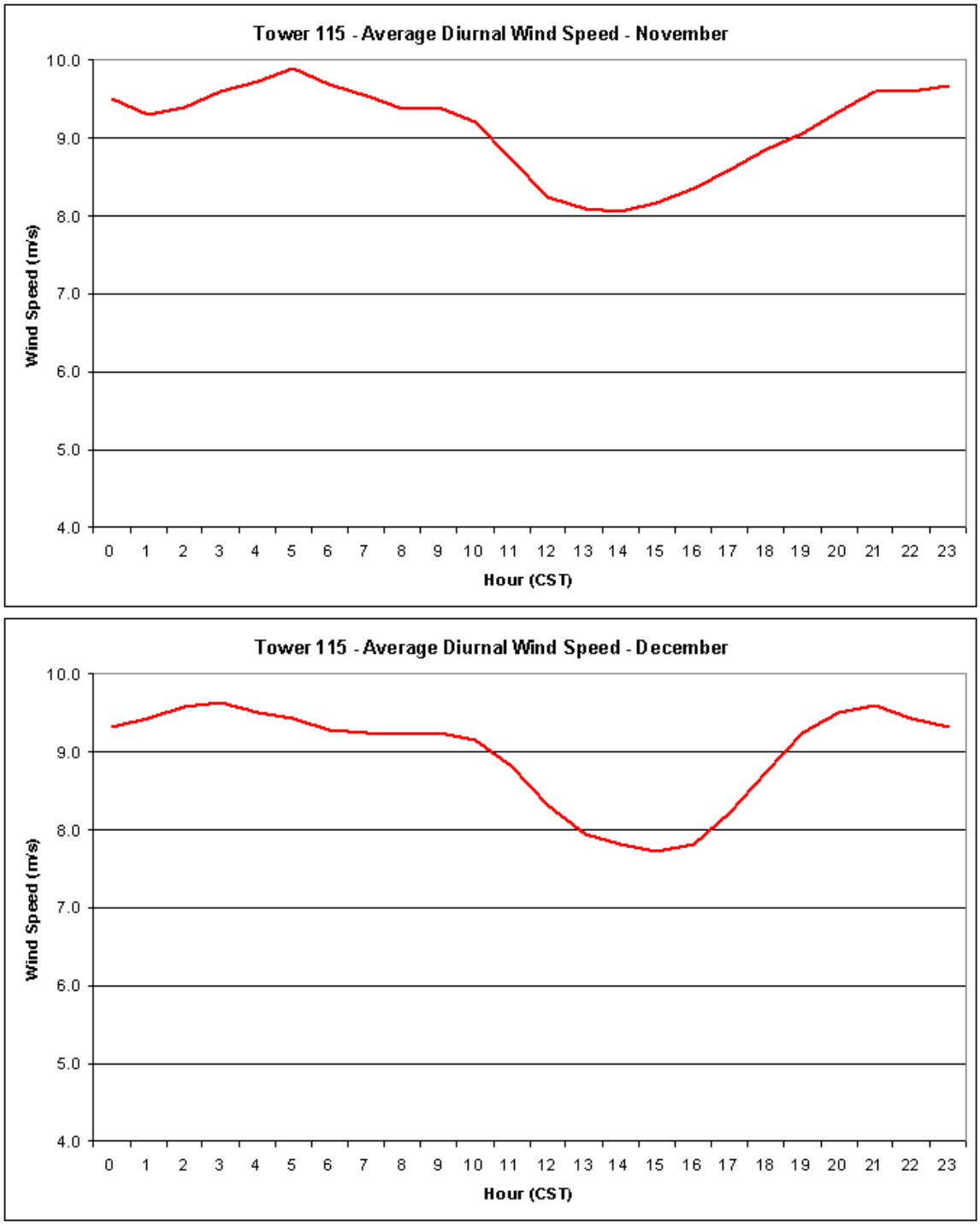

Figure 88: Average November and December 80 m diurnal wind speed at Tower 115 in m/s.

Analysis of diurnal wind patterns and spatial variability

The annual diurnal wind speed patterns for all sites reflect distinct daytime and nighttime wind regimes. The nocturnal decoupling of the surface layer and the associated reduction in vertical transport of near-surface momentum leads to higher nighttime wind speeds at hub height (80 m) than during daytime hours. Not surprisingly, the diurnal range is the largest at Tower 115 (North Dakota Central) as seen in Figure 82, due in part to the more frequent occurrence of low-level jet episodes. Additionally, the region of Tower 115 has generally drier surface conditions, less dense vegetative cover (influencing evapotranspiration) and climatologically less cloud cover than sites farther east. These characteristics result in a larger diurnal temperature range and more rapid development of a marked nocturnal boundary layer, which in turn is conducive to the development of enhanced hub-height nighttime winds. In contrast, Tower 82 (Minnesota Northeast) has the smallest diurnal range in wind speed (Figure 75), due in part to its greater distance from the climatologic location of the low-level jet. Additionally, Tower 82's small diurnal wind speed range is directly related to a more slowly evolving diurnal boundary layer that is associated with a smaller diurnal temperature range. The Minnesota Northeast region experiences a higher frequency of cloud cover and has surface characteristics (lush vegetation with a substantial percentage of water surface area) conducive to a smaller diurnal temperature range. The respective surface moisture/vegetative properties have their largest contribution to the annual diurnal wind speed pattern during the growing season months. In terms of diurnal pattern and diurnal wind speed magnitudes, the annual time series for Towers 71 and 115 (Figs. 61 and 82) are the most similar for the physical reasons mentioned above. Note again that the diurnal plots display average hourly values for the monthly or annual time periods. Any particular day's diurnal wind speed could deviate substantially from the average diurnal pattern as shown in Fig. 89.

The largest monthly diurnal wind speed range occurs in the summer season when the forcing of the flow from transient synoptic systems is the weakest. With the exception of Tower 82, the other sites (especially Towers 71 and 115) show a clear tendency in the warm season for the monthly diurnal range to be larger than during winter and transition seasons. A comparison of the July/August wind speed diurnal range for Towers 115 (Figure 86) and 82 (Figure 79) clearly shows the summer season spatial variability with diurnal speed ranges approximately twice as large for the North Dakota site. Based on the annual and monthly data, the fastest daily wind speeds generally occur in or near the 20-00 CST (8 PM to midnight) time period and the weakest diurnal winds occur in or near the 11-15 CST (11 AM to 3 PM) time period.

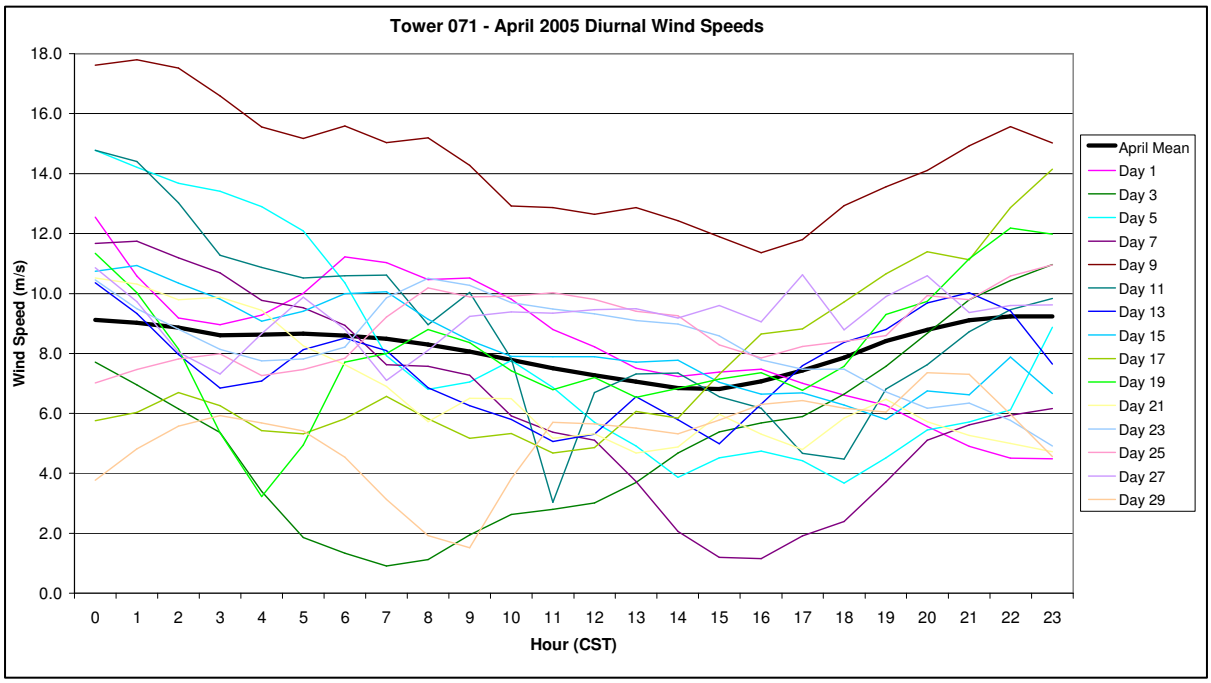

Fig. 89. April 2005 diurnal wind speeds at 80 m for alternating days for Tower 71 in m/s. The heavy black line represents the mean diurnal wind speed for April.

Wind Generation Forecast Accuracy

WindLogics evaluated the accuracy of hourly and day-ahead wind generation forecasts for region-specific wind plants for 2005. This was based on both the NCEP RUC-20 km (for periods 1-6 hours ahead) and NCEP NAM-12 km/NAM-20 km (for periods up to one day-ahead) forecast model data from the WindLogics archives and proxy tower MM5 hourly time series data produced for 2005. The NAM model data and proxy tower time series were used as “training data” for a Support Vector Machine (SVM) based computational learning system. This system “learns” to identify error patterns between the NAM-based source data and the on-site data, and applies optimal corrections to the NAM forecast. SVM is the newest generation of artificial intelligence computational learning system techniques, and has several advantages over earlier neural net systems. The result gives a forecast that is an optimal combination of the raw model outputs and persistence. Forecast error time series will be used by EnerNex in system modeling activities of Task 2 and 3. Additionally, WindLogics investigated potential improvements in forecast accuracy by considering a geographically

diverse wind generation scenario and compared it to the forecast accuracy for a single wind plant.

Deliverables will include graphs showing average forecast accuracy as a function of forecast hour for wind speed, energy production or power.

- Mean absolute error (MAE) for wind speed as a function of forecast hour
- MAE for hourly energy production as a function of forecast hour
- MAE for run-accumulated energy production as a function of forecast hour
- MAE of energy production as a percent of nominal plant output.
- Histogram of forecast speed and energy errors for several forecast intervals and varying levels of geographic dispersion in the forecast quantities

The Day-ahead Forecast Model

The physics-based weather forecast model used in this study for the day-ahead forecast is the NCEP NAM model. The NAM model is one in a suite of numerical forecast models that is routinely used by the National Weather Service for making 1-3 day forecasts. The model calculates wind, temperature, pressure, humidity, and precipitation along with a host of other meteorological parameters at various heights in the atmosphere ranging from 10 m to 20 km above the surface. The model utilizes a horizontal grid spacing of 12 km. New 84-hour forecasts are made every 6 hours. These forecasts are being archived by WindLogics for use in forecasting studies. The archived data used in this study had a grid spacing of 20 km.

The Hour-ahead Forecast Model

The physics-based weather forecast model used in this study for the hour-ahead forecast is the RUC model. 'RUC' model stands for Rapid Update Cycle and is routinely used by the National Weather Service for making short-term (3-12 hour) forecasts. The model calculates wind, temperature, pressure, humidity, and precipitation along with a host of other meteorological parameters at various heights in the atmosphere ranging from 10 m to 20 km above the surface. The model utilizes a horizontal grid spacing of 20 km. New forecasts are generated every hour by taking the previous hour's forecast as a starting point, and then assimilating all of the most recent meteorological observations into the model initial fields before the start of the new forecast. 12-hour forecasts made every three hours (00Z, 03Z, 06Z, etc.) and 3-hour forecasts made at the 'in-between' hours (01Z, 02Z, 04Z, etc.). These forecasts are being archived by WindLogics for use in forecasting studies.

Computational Learning System (CLS) and) and Methodology

While it is possible to make wind (and power) forecasts for a particular site directly from the NAM or RUC model output, further refinements to the site-specific power forecast are made by using the ETA\RUC model output and MM5-generated proxy tower data to train a Computational Learning System at four different locations throughout the Midwest. Recently developed Computational Learning System methods such as Support Vector Machine (SVM) relate complex patterns in forecast model outputs (such as wind, density, etc.) to wind facility target variables (such as power production). While earlier artificial intelligence approaches such as neural nets have been applied, the SVM-based approach offers distinct advantages, such as simplified optimization of training schemes, and estimation of output probability distributions. In this study, data (such as wind speed and direction, density, temperature, etc.) is extracted from the NAM or RUC model output at several heights and 9-12 horizontal grid points surrounding a MM5 proxy tower. The model winds are utilized to calculate power production using the power curve for the Vestas V82 1.65 MW turbine. The NAM or RUC model output and the MM5 proxy tower winds are then used to train the Computational Learning System to make more accurate power production forecasts than those derived by using the NAM or RUC model alone. This improvement in forecasting can be expected on a site-specific basis given the interplay of synoptic, mesoscale, local geographic and diurnal influences on the three-dimensional wind field. One strength of the CLS is in mitigating systematic errors inherent in the model forecast. Forecast accuracy was calculated based on a round-robin CLS training approach in which for each month forecast, the actual MM5 proxy tower data for that month was excluded from the training. The MM5 proxy tower data was then used to evaluate the accuracy of the forecast for that month.

There is a caveat to the forecast accuracy results that follow involving the MM5 proxy tower dataset used for training the CLS. While the MM5 model is an excellent tool for generating characteristic wind time series at a given location, the MM5 proxy tower wind will not always agree with the observed wind at a given point in time and location. Since the observed wind fields are used to initialize the NAM/RUC forecast models, any disagreement between the MM5 wind field and the observed wind field will lead to some inherent error in the forecast from the very start of the forecast period. Thus the forecast errors presented in this report are likely somewhat higher than if the CLS was trained using observed wind or power data.

For this study, the CLS was trained using data from four different proxy towers: Tower 71 (Buffalo Ridge in southwest MN), Tower 41 (Murray Co. in southeast MN), Tower 82 (Iron Range in northeast MN) and Tower 115 (central ND). Both day-ahead and hour-ahead forecasts were generated for each of these sites,

which also allows for consideration of the effects of geographic dispersion on forecast errors.

Day-ahead Forecast Methodology

The day-ahead forecast in this study was issued once per day assuming a needed forecast delivery time of 8am CST (14Z). Because the NAM forecasts are generally not available until ~2.5-3 hours after the forecast start time, the 06Z NAM forecast was used for the day-ahead forecast in order to meet the required delivery time. (The most recent NAM forecast, started at 12Z, would not be available until ~15Z or 9am CST.) *This means that the day-ahead forecasts are based on a NAM forecast that is 8 hours old at the time the forecast is issued, which also has implications for day-ahead forecast accuracy.* To help mitigate some of the forecast errors early in the forecast period, the CLS was used to blend the most current observations (13Z or 7am CST) into the forecast shortly before the forecast was issued. The day-ahead forecast extends out to 60 hours from the 06Z start time.

Hour-ahead Forecast Methodology

The hour-ahead forecasts are issued every hour assuming a needed forecast delivery time 20 minutes before the top of the hour. Because the RUC forecasts are generally not available until ~1-1.5 hours after the forecast start time, the 12Z RUC forecast would be used for the hour-ahead forecast in order to meet a required delivery time of 7:40 am CST (13:40Z). The CLS is used to blend the most current observations into the forecast shortly before the forecast is issued.

Forecast Accuracy Results

Day-Ahead Forecasts

To evaluate the benefits of utilizing the CLS for wind farm power and energy forecasting, plots have been created for both annual and seasonal forecasting performance. For comparison, the error performance for power and energy for forecasts based on climatology and persistence are also plotted for Towers 71 (Buffalo Ridge) and 82 (Iron Range). The results from Towers 41 (Murray Co.) and 115 (central North Dakota) are similar (not shown). As can be seen in Figures 90-95, the CLS forecast demonstrates a far superior ability to prognosticate the power production and energy than either persistence or climatology. In terms of power production, the CLS forecasts MAEs climb about 5% 5-15 hours into the forecast period to ~20% for Tower 71 (~17% for Tower 82), with MAEs in the 20-22 percent range for Tower 71 (17-19% range for Tower 82) thereafter to 32 hours. It is notable that even at the 48-hour point, the CLS forecast has considerable value over climatology. The waves in the power plots are due to inadequacies in the forecast methodologies to accurately

represent (climatology and persistence) or forecast the timing (NAM and CLS) of transitional diurnal boundary layers. In terms of energy forecast accuracy, the system demonstrates energy MAEs in the 20 – 23 percent range (as a percent of actual energy) for the 8 – 48 hour period for Tower 71, and 23 – 26 percent range for Tower 82. Note that although the power errors were larger for Tower 71 than Tower 82, the MAEs as a percent of actual energy are smaller because the total energy production is larger. It is not surprising that the CLS forecast for power and energy is far superior to climatology throughout the 48-hour period, especially in the 0-6 hr time frame, but a striking facet of the CLS forecast involves its ability to outperform persistence within just a few hours into the forecast period. In fact, by the 1-hour forecast point (relative to when the forecast is actually delivered and used), the CLS forecast outperforms the persistence power forecast at all tower locations by 2-3% of rated capacity. In terms of the accuracy of forecasted energy, the CLS system shows an error reduction at the 1-hour point of ~3 percent of actual energy production. The relative forecast percent improvement of the CLS power forecast over persistence and climatology is large from this 1-hour point through the end of the forecast.

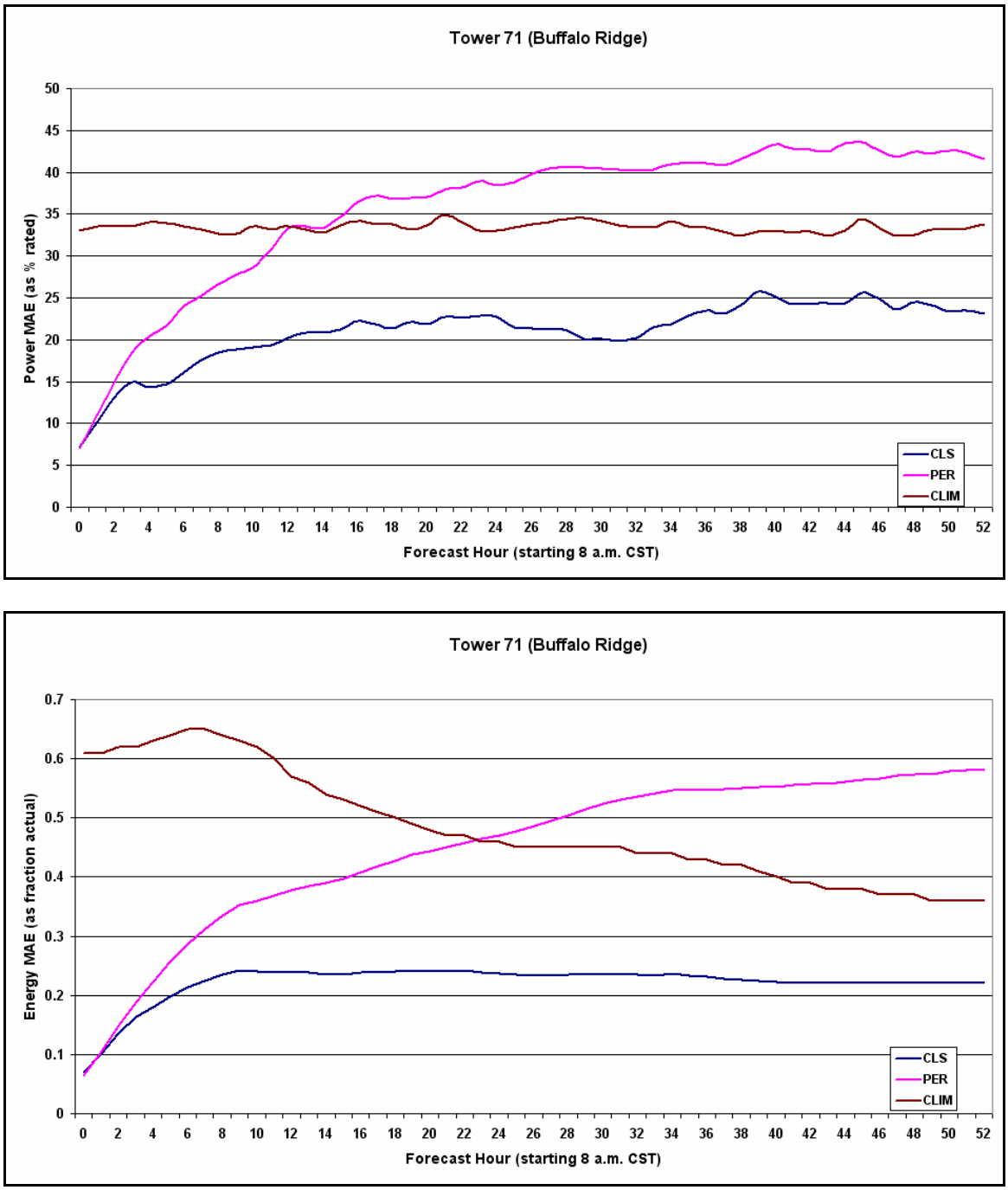

Figure 90: Power mean absolute error (top) and energy mean absolute error as a fraction of actual production (bottom) as a function of forecast hour for all months for the CLS, climatology (CLIM), and persistence (PER) forecasts for Tower 71 (Buffalo Ridge).

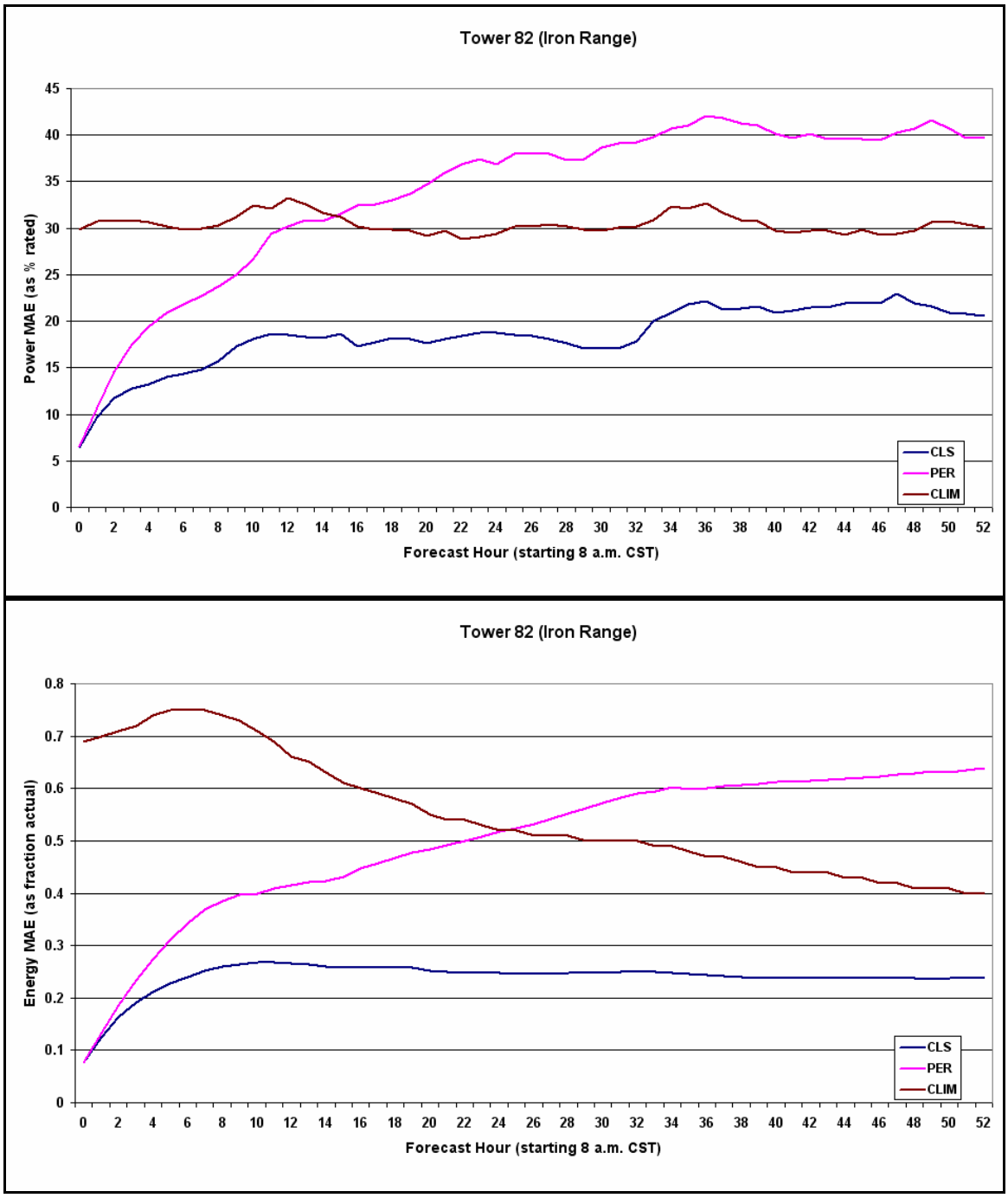

Figure 91: Power mean absolute error (top) and energy mean absolute error as a fraction of actual production (bottom) as a function of forecast hour for all months for the CLS, climatology (CLIM), and persistence (PER) forecasts for Tower 82 (Iron Range).

The seasonality of forecast power and energy errors is shown in Figures 92-95 for the CLS, persistence and climatology at the Tower 71 and 82 locations. As shown in Figures 92-95, the power MAE profiles are similar to the annual profile shown in Figures 90 and 91, but with differing magnitudes.

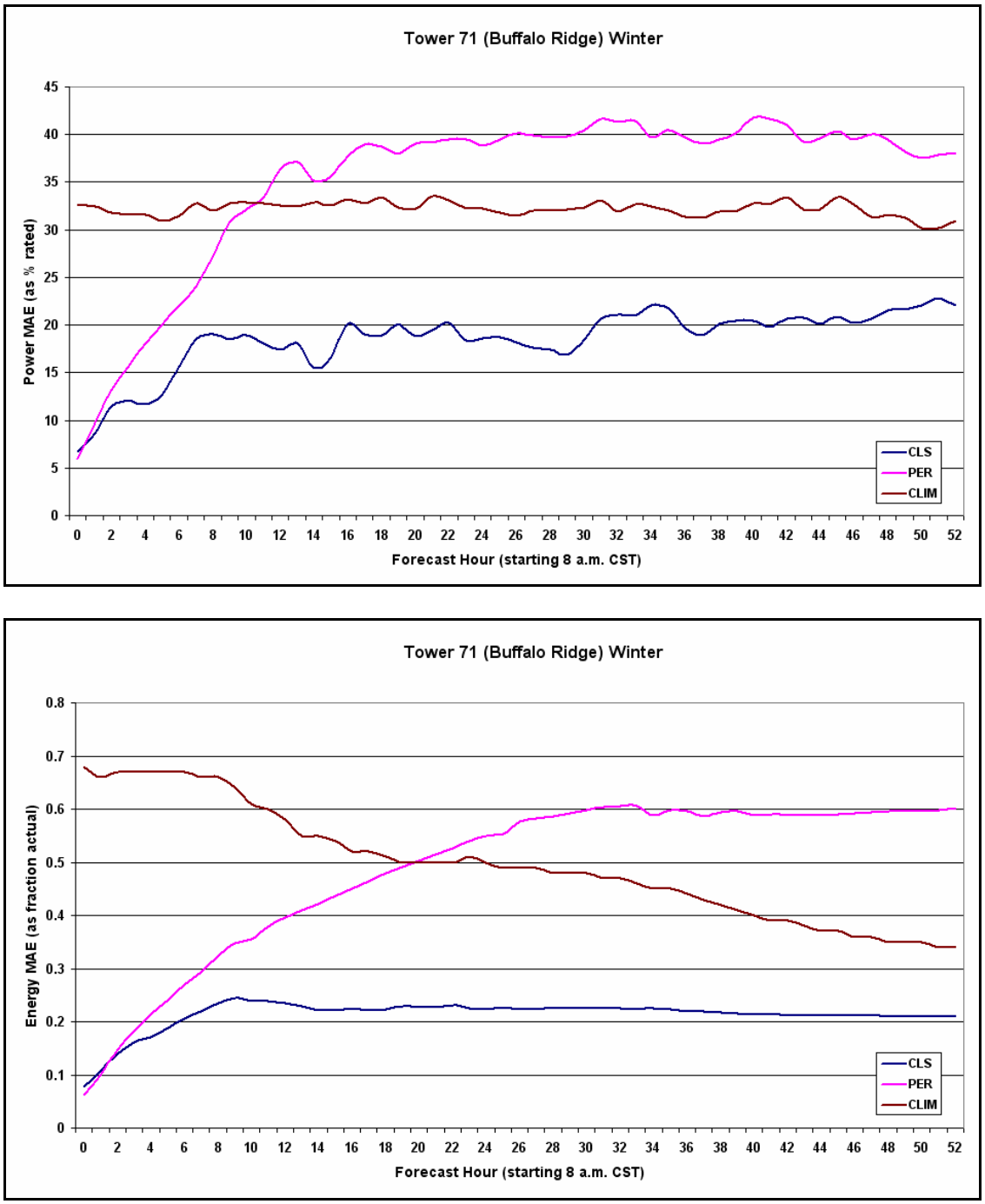

Figure 92: Power mean absolute error (top) and energy mean absolute error as a fraction of actual production (bottom) as a function of forecast hour for the winter months (Dec., Jan., Feb.) for the CLS, climatology (CLIM), and persistence (PER) forecasts for Tower 71 (Buffalo Ridge).

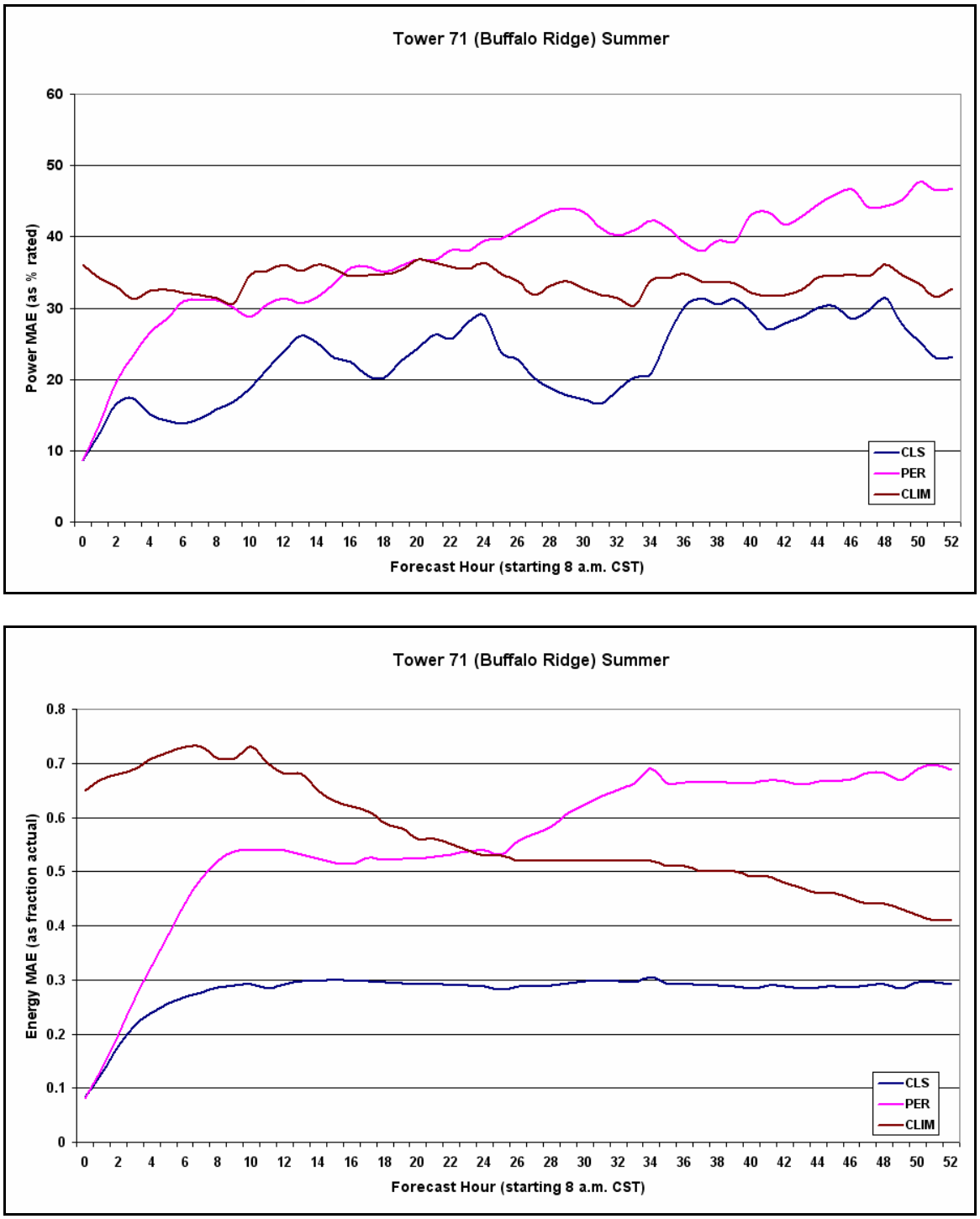

Figure 93: Power mean absolute error (top) and energy mean absolute error as a fraction of actual production (bottom) as a function of forecast hour for the summer months (June, July, Aug.) for the CLS, climatology (CLIM), and persistence (PER) forecasts for Tower 71 (Buffalo Ridge).

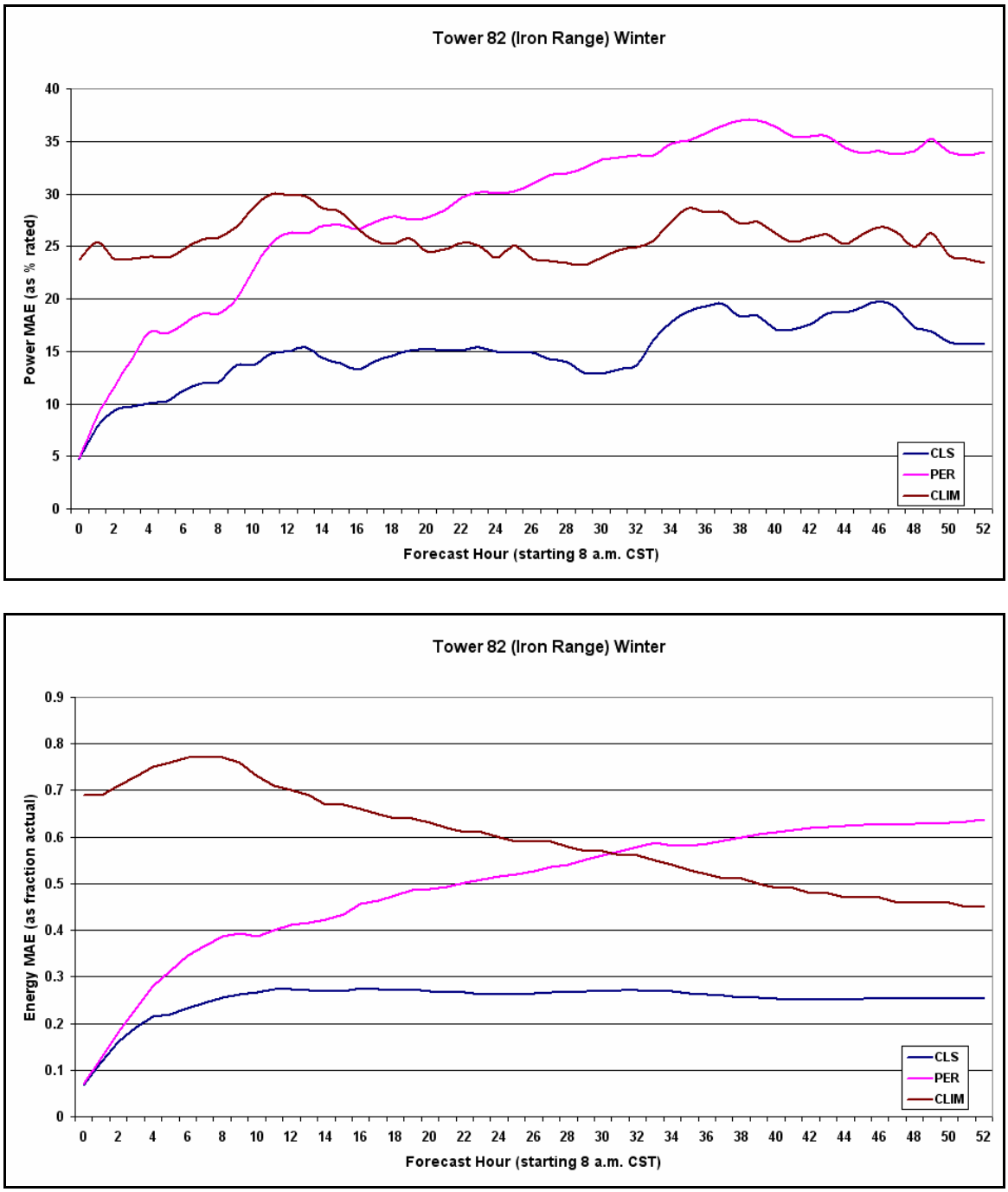

Figure 94: Power mean absolute error (top) and energy mean absolute error as a fraction of actual production (bottom) as a function of forecast hour for the winter months (Dec., Jan., Feb.) for the CLS, climatology (CLIM), and persistence (PER) forecasts for Tower 82 (Iron Range).

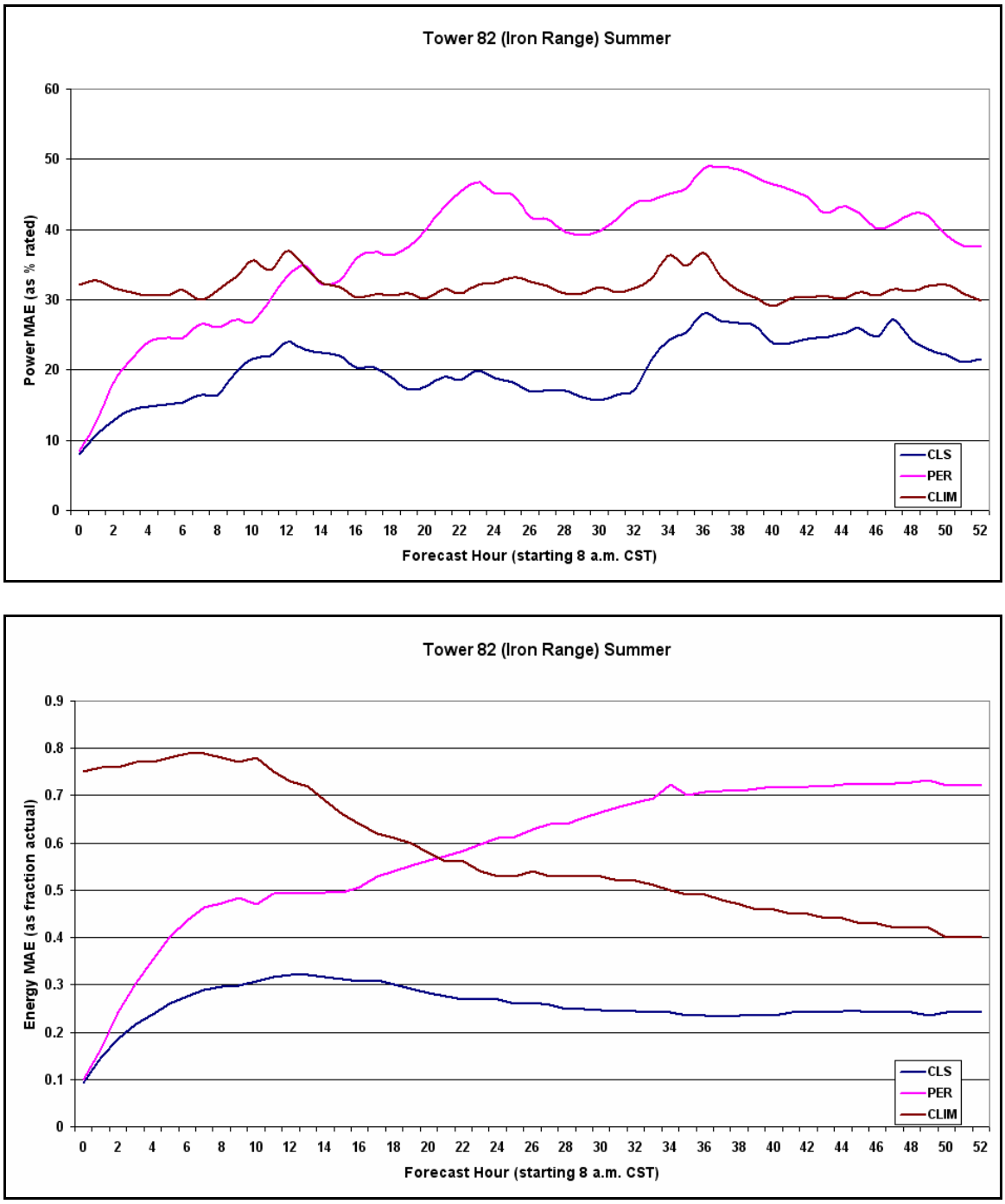

Figure 95: Power mean absolute error (top) and energy mean absolute error as a fraction of actual production (bottom) as a function of forecast hour for the summer months (June, July, Aug.) for the CLS, climatology (CLIM), and persistence (PER) forecasts for Tower 82 (Iron Range).

The definitive advantage of utilizing the CLS forecast over persistence and climatology is present in both summer and winter seasons. Examining both forecast energy error as a fraction of actual energy produced and MAEs as a percentage of rated capacity reveals that, on a season-relative basis, the winter season CLS forecasts are superior to the summer season CLS forecasts. To understand these season-relative forecasting differences, the time and space scales of the controlling meteorology of the Upper Midwest must be addressed. The winter season wind forcing is dominated by synoptic-scale weather systems that tend to be more accurately forecast by weather prediction models because they are large in dimension (up to several thousand km in horizontal scale) and have 3-7 day life spans. Thus, these synoptic systems are well resolved in the numerical model forecasts. In contrast, summer season weather and regional winds are often influenced by mesoscale systems that, due to their size, life span, and transient nature (like individual thunderstorms and mesoscale convective systems) are more difficult to accurately simulate. Thunderstorms often produce very strong, gusty winds, which are very difficult to forecast. Synoptic forcing is weaker in summer, leading to generally weaker winds. This combination can lead to both potentially large power and energy forecast errors during summer.

Hour-Ahead Forecasts

As was the case with the day-ahead forecasts, the CLS forecast demonstrates superior ability to prognosticate the power production and energy than either persistence or climatology in the short-term forecast. This can be seen in Figure 96 which shows results from an example hour-ahead forecast issued for use at 8 a.m. CST at the Tower 82 location. While persistence is often the forecast of choice for the hour-ahead time frame, these results show the importance of combining persistence with a physics-based forecast model because ‘hour-ahead’ forecasts often must be issued as much as half an hour before the top of the hour for which the forecast is to be used -- at which point ‘persistence’ can be as much as 1 hour old.

The CLS forecast begins to outperform persistence at the 1-hour mark, and by 3 hours into the forecast the CLS provides a 5% reduction in error as compared to persistence in the power MAE (as a percent of rated), and 4% reduction in the energy forecast error (as compared to actually energy produced). By the 6-hour mark, the CLS provides a 7-8% reduction in the power MAE, and nearly a 10% reduction in the energy MAEs as compared to persistence.

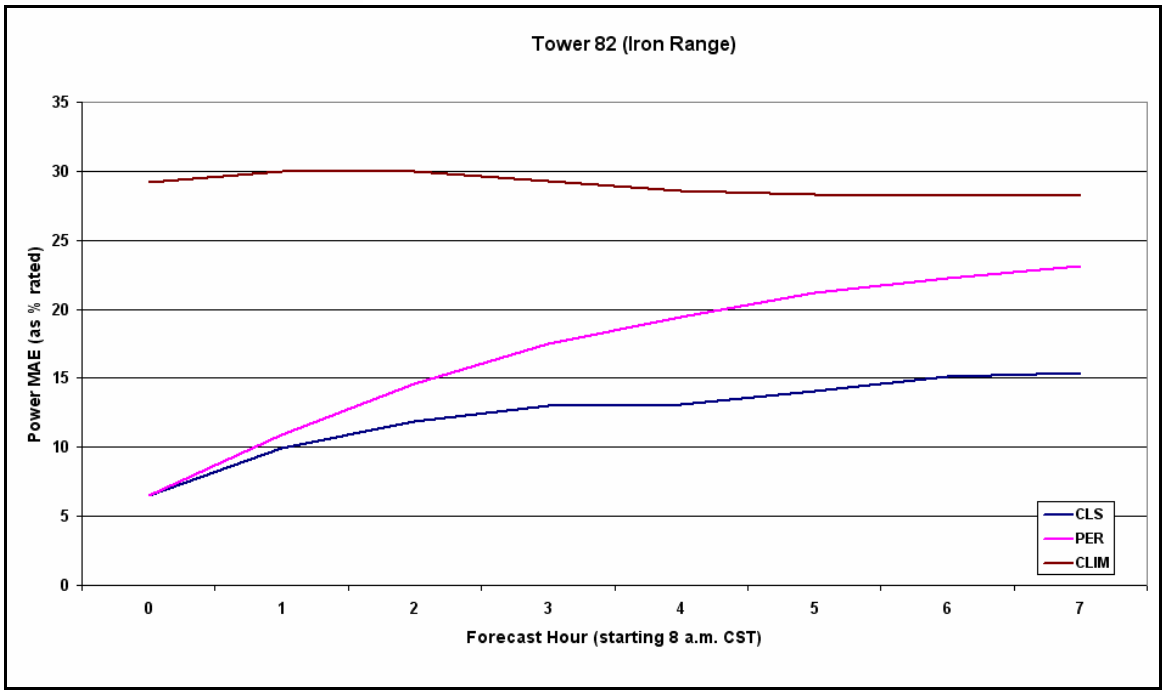

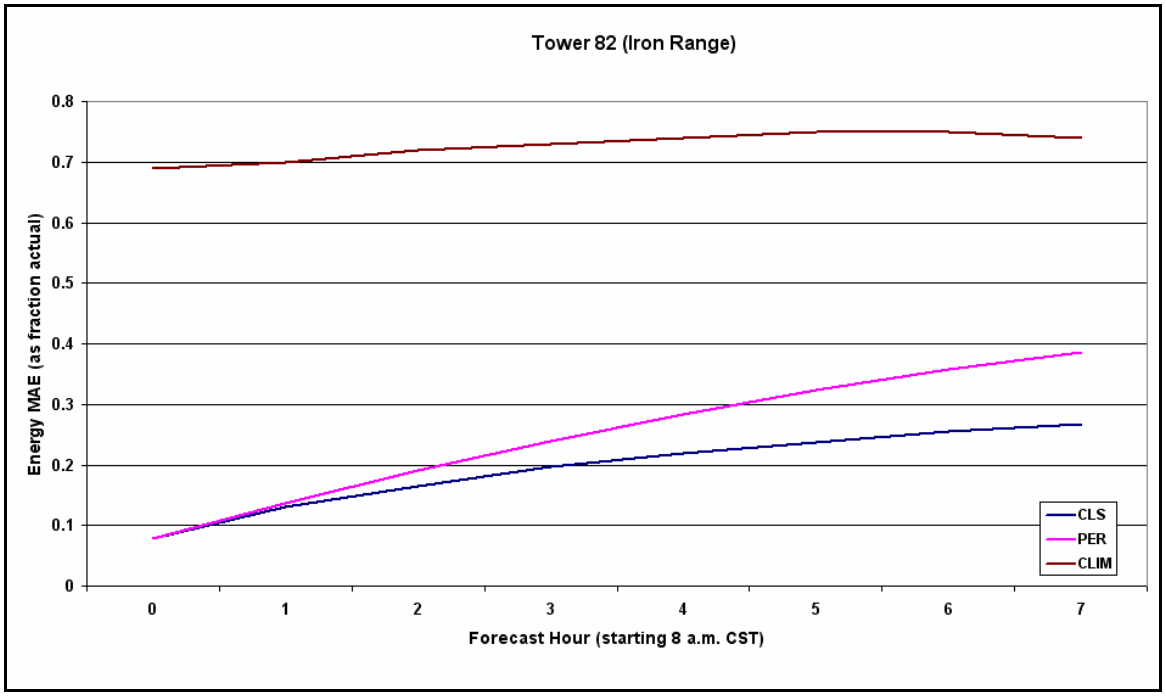

Figure 96: Power mean absolute error (top) and energy mean absolute error as a fraction of actual production (bottom) as a function of forecast hour for all months for the CLS, climatology (CLIM), and persistence (PER) forecasts for Tower 82 (Iron Range).

Effects of Geographic Dispersion on Forecast Accuracy

We have considered the forecast accuracy for individual locations above. However, when wind generation facilities are spread out over an area, it raises the possibility that power and energy production will be over-forecast at some locations and under-forecast at others. As a result, forecasts for the aggregate of several locations should theoretically be more accurate than any individual location alone.

We investigated this idea by first taking the forecast at one location (Tower 71 – Buffalo Ridge), and then adding the three other proxy tower locations to the forecast one-by-one to evaluate the impact geographic dispersion has on the forecast accuracy. The results for the day-ahead forecast are shown in Figure 97, and results for the hour-ahead forecast are shown in Figure 98. In all cases, adding more geographically dispersed wind generation facilities decreased the overall forecast error. The largest error decrease occurred by adding the first additional location, although this effect is much more evident in the day-ahead forecast than in the hour-ahead forecast. The addition of each successive location decreased the power MAEs, but the error decrease was less than its predecessor. At the 24-hour mark, the power MAE is reduced by 43% going from a single site to a composite of 4 sites. The energy MAE is likewise reduced by ~30%. The hour-ahead forecasts also show marked improvement with additional geographic dispersion. The power MAEs are reduced by ~38% going from one site to four by 3 hours into the forecast, and the energy MAEs are reduced by ~35%.

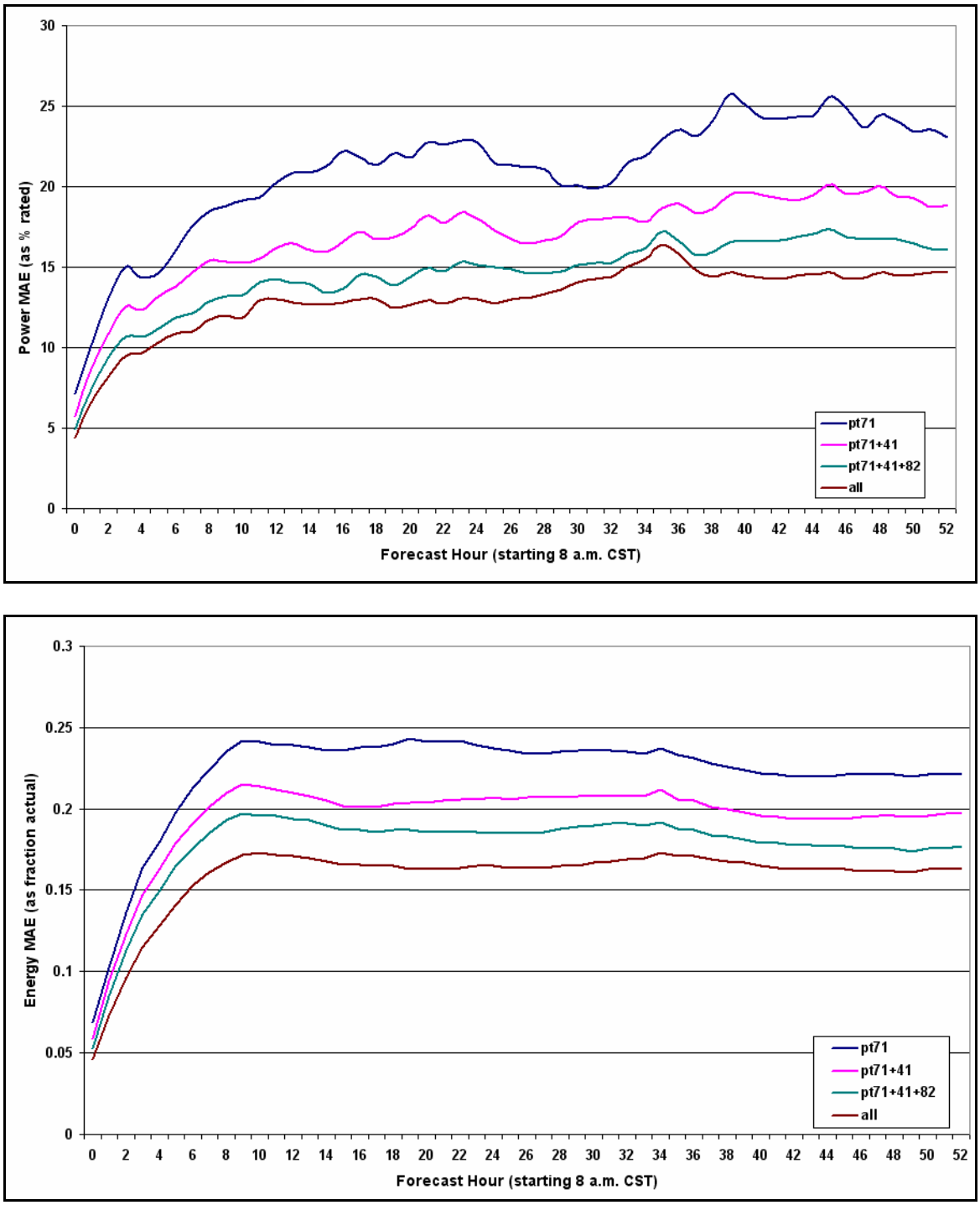

Figure 97: Power mean absolute error (top) and energy mean absolute error as a fraction of actual production (bottom) as a function of forecast hour for all months for the CLS day-ahead forecast with 1 to 4 locations included in the forecast.

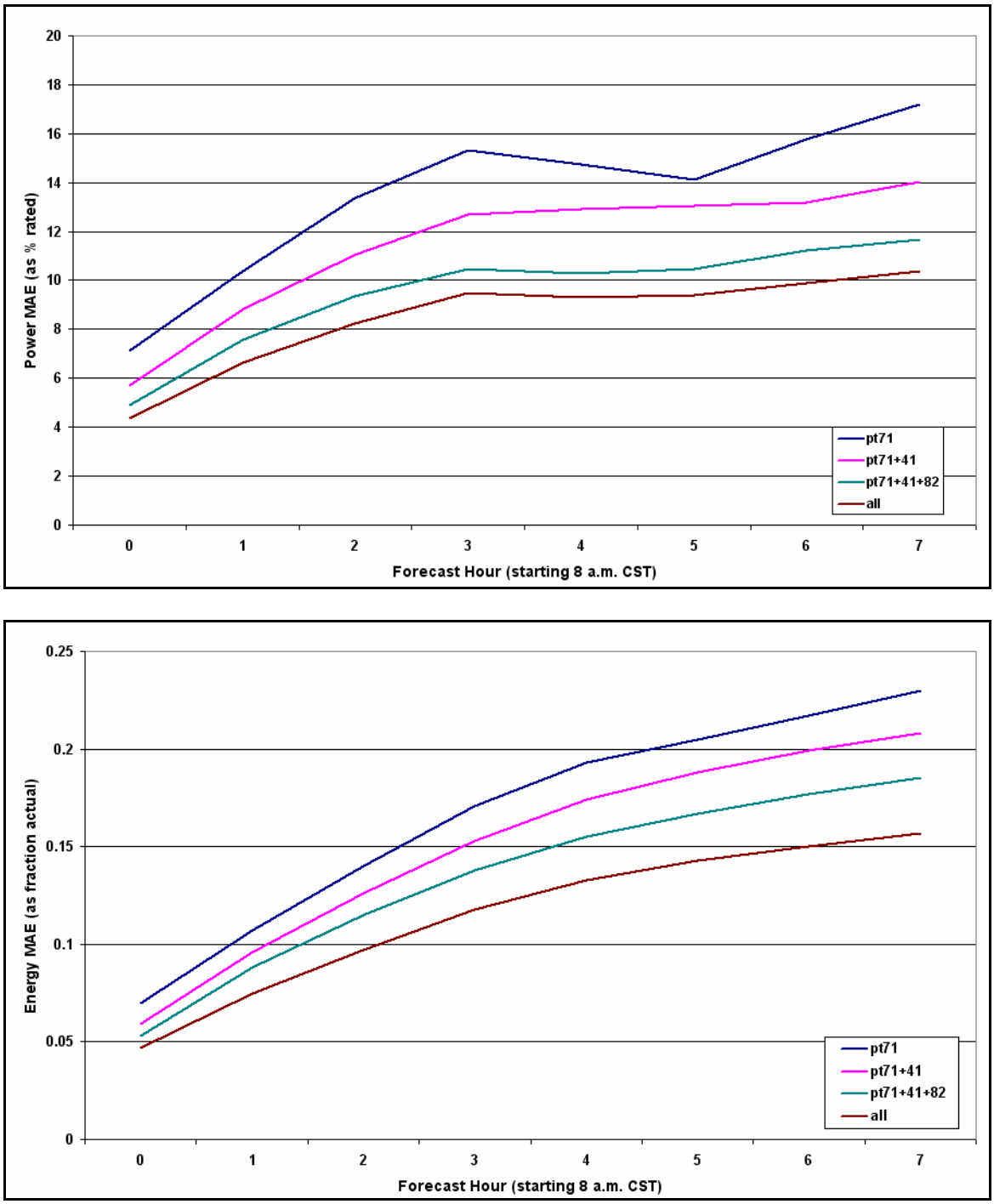

Figure 98: Power mean absolute error (top) and energy mean absolute error as a fraction of actual production (bottom) as a function of forecast hour for all months for the CLS hour-ahead forecast with 1 to 4 locations included in the forecast.

References

Bonner, W. D., 1968: Climatology of the low level jet. *Mon. Wea. Rev.,* **96**, 833-850.

Grell, G. A., J. Dudhia, and D. R. Stauffer, 1995: A description of the fifth-generation Penn State/NCAR Mesoscale Model (MM5). NCAR Technical Note TN-398+STR, 122 pp.

Minnesota Department of Commerce, 2004: Characterization of the wind resource in the Upper Midwest: Wind integration study Task I. Xcel Energy and the Minnesota Department of Commerce. 75 pp.